

**Lancaster Environment Centre**

**Lancaster University**

**The GREAT-ER model as a tool for chemical risk assessment  
and management for Chinese river catchments**

**Benjamin Jackson**

B. Sc. (Hons.) Geography

Msc. Catchment dynamics and management

This thesis is submitted in partial fulfilment of the requirements for the Degree of

Doctor of Philosophy

**May 2018**

## DECLARATION

I declare that this thesis is my own work and contains no material which has been submitted in substantially the same form for the award of a higher degree elsewhere. Any sections of this thesis containing material published and or written by other persons have been referenced.

Benjamin Jackson

## ABSTRACT

The Chinese government has introduced a range of policies with the aim to improve freshwater quality to safe levels for both humans and ecosystem function. These policies form an important part of sustainable economic development. An important component of the improvement in surface water quality is to assess and reduce the risk from organic chemicals. The development of reliable predictive tools is therefore required which can be used for the purpose of chemical risk assessment and catchment management. The catchment scale Geo-referenced Regional Exposure Assessment Tool for European Rivers (GREAT-ER) model was developed for this purpose. Its application in China would represent a valuable water quality management tool. However, the data requirements for the parameterization of GREAT-ER are difficult to meet, especially in countries with limited data accessibility such as China.

A methodology has been developed to facilitate the use of the GREAT-ER model in any catchment in China. Key methodological contributions include an approach to locate sewage treatment works (STW), estimate population served and to estimate the distribution and magnitude of untreated emissions. Low-flow statistics were estimated by means of regional regression. The GREAT-ER model was applied to the East river catchment for the chemicals Triclosan (TCS), Triclocarban (TCC), Estrone (E1) and 17 $\beta$ -estradiol (E2). As part of the study, a sampling campaign was conducted in January 2016 to collect water samples from sites within the East river catchment; samples were subsequently analysed to determine the concentration of target chemicals. These data, along with data obtained from collaborators collected in December 2008, were used to estimate the accuracy of the model. Overall, the model performed well for E1 and E2. However, there were some significant errors in the model's estimation for the concentration of TCC and TCS. This included a number of remote rural subcatchments, which may be a reflection of the affordability of personal care products

to the rural population. These, and other factors, were explored during validation of the model. A risk assessment was performed for the four chemicals for the years 2016 and 2020. In 2016, the model estimated that TCC would not exceed the predicted no effect concentration (PNEC) anywhere in the catchment, however, in 2020 the PNEC was exceeded for 3 stretches, each downstream of major STWs. The model estimated that the concentrations of E1 and E2 in 2016 would exceed PNEC values in stretches largely confined to the heavily urbanised Shenzhen catchment, but also isolated minor stretches located downstream of population centres. In 2020, the number of stretches exceeding the PNEC threshold reduced for areas with improved wastewater treatment infrastructure, but overall, the area that exceeded the PNEC for E1 and E2 was estimated to expand. TCS posed a high risk to the catchment in 2016, with the model predicting the PNEC to be exceeded throughout much of the catchment. In 2020, it was estimated that the same stretches would exceed the PNEC for TCS, but concentrations would be considerably higher overall. A series of catchment management scenarios were then utilised, such as increasing STW removal efficiency and the expansion of STW connectivity. These infrastructure developments were found to be effective for E1 and E2, but not so for TCS.



## ACKNOWLEDGEMENTS

Throughout my PhD I have been supported by a group of kind, intelligent and interesting individuals who I will never be able to forget. I feel enriched by meeting such a diverse group of friends and colleagues.

Firstly, I'd like to thank my two supervisors: Dr Andy Sweetman and Prof Kevin Jones. My supervisors have provided the encouragement, guidance, and friendship that allowed me to push through all the problems I encountered throughout my PhD, and allowed me to produce this thesis. I am grateful for their guidance and for having confidence in me, especially when I lacked it myself. I would also like to thank Unilever for partial sponsorship of my PhD, in particular Dr Oliver Price, who provided valuable guidance, data and support for my PhD.

I would like to thank Dr Chang'er Chen for assistance with fieldwork and laboratory work in China. I would also like to thank Prof Guang-Gou Ying and Dr You-sheng Liu of the Guangzhou institute of Geochemistry, for access to their laboratory, provision of transportation for fieldwork and general assistance with fieldwork in China.

I'd also like to thank both Dr Wei Chen and Dr Andy Young for essential contributions to my PhD. Using a methodology he developed during his PhD, Wei analysed my samples following extraction. This included operation of the mass spectrometer and interpretation of chromatograms. Andy provided guidance towards the estimation of low-flow statistics for the East river catchment.

I'm thankful to all my officemates and colleagues who have supported me over these many years. There is great value in being able to share: complaints, tea, coffee, trials, tribulations, failure and success. I have the wonderful problem of having simply far too many names to list here, but hopefully you know who you all are.

Finally I'd like to thank my parents, who have done an incredible job of putting up with me for all these years. My parents have always been supportive, kind and eager to help. However, sadly in the 2<sup>nd</sup> year of my PhD my mother tragically died of cancer. After the initial sadness of her death, came great strength and determination, I could not give up. I treasure the important values that both my parents have passed on to me and I hope I will take these further, onwards and upwards.

## TABLE OF CONTENTS

<b>DECLARATION .....</b>	<b>II</b>
<b>ABSTRACT .....</b>	<b>III</b>
<b>ACKNOWLEDGEMENTS.....</b>	<b>V</b>
<b>TABLE OF CONTENTS.....</b>	<b>VII</b>
<b>LIST OF FIGURES.....</b>	<b>XI</b>
<b>LIST OF TABLES.....</b>	<b>XVI</b>
<b>LIST OF ABBREVIATIONS.....</b>	<b>XVII</b>
<b>CHAPTER 1 - INTRODUCTION .....</b>	<b>1</b>
<b>1.1. Threats to water quality in China.....</b>	<b>1</b>
<b>1.2. Environmental management .....</b>	<b>3</b>
1.2.1. Chemical management.....	3
1.2.2. Catchment management and wastewater treatment.....	5
<b>1.3. Holistic approach .....</b>	<b>11</b>
<b>1.4. Monitoring to quantify chemical exposure .....</b>	<b>12</b>
<b>1.5. Modelling as a complimentary tool .....</b>	<b>13</b>
<b>1.6. Combining both techniques .....</b>	<b>13</b>
<b>1.7. Model scenarios .....</b>	<b>14</b>
<b>1.8. Modelling challenges .....</b>	<b>15</b>
<b>1.9. Model selection .....</b>	<b>16</b>
<b>1.10. Catchment scale water quality models .....</b>	<b>18</b>
1.10.1. The SWAT model .....	18
1.10.2. The GWAVA model .....	19
1.10.3. SIMCAT .....	21
1.10.4. TOMCAT.....	23
1.10.5. The GREAT-ER model.....	25
1.10.6. Conclusion .....	29
<b>1.11. Barriers to overcome for Chinese catchments .....</b>	<b>30</b>

<b>1.12. Chemicals selected for study .....</b>	<b>31</b>
1.12.1. Triclosan and Triclocarban .....	33
1.12.2. Natural estrogens .....	35
<b>1.13. Primary thesis aim .....</b>	<b>37</b>
1.13.1. Thesis objectives .....	38
<b>1.14 Thesis structure .....</b>	<b>38</b>
<b>CHAPTER 2 – THE GREAT-ER MODEL IN CHINA.....</b>	<b>40</b>
<b>2.1. Data to request.....</b>	<b>40</b>
<b>2.2. Physio-chemical and environmental properties.....</b>	<b>43</b>
2.2.1. Basic removal by biodegradation, volatilization and sedimentation .....	44
2.2.2. Extended five process removal.....	45
2.2.3. Sediment exposure module.....	52
<b>2.3. Simulation procedure .....</b>	<b>53</b>
<b>2.4. Watershed delineation .....</b>	<b>54</b>
2.4.1. DEM availability .....	54
2.4.2. The HydroSHEDS DEM .....	56
2.4.3. Correcting DEMs to enforce flow direction in flat areas .....	58
<b>2.5. Low-flow estimation.....</b>	<b>61</b>
2.5.1. Low-flow hydrology .....	62
2.5.2. Regional regression .....	70
2.5.3. Regional mapping .....	75
2.5.4. Rainfall-runoff modelling.....	75
2.5.5. Artificial influences .....	79
2.5.6. Approaches taken to flow estimation by previous GREAT-ER studies .....	80
<b>2.6. Chemical emission .....</b>	<b>81</b>
2.6.1. Estimating chemical usage .....	82
2.6.2. Estimating the spatial distribution of wastewater discharge .....	83
<b>2.7. Locating and identifying STWs .....</b>	<b>85</b>
<b>2.8. Wastewatershed delineation.....</b>	<b>88</b>
<b>2.9. Identifying STWs.....</b>	<b>95</b>
<b>2.10. Emissions from untreated wastewater sources .....</b>	<b>98</b>
<b>CHAPTER 3 - THE EAST RIVER CATCHMENT .....</b>	<b>99</b>
<b>3.1. An introduction to the East river catchment.....</b>	<b>99</b>
3.1.1. Socio-economic history of the Pearl river delta .....	99
3.1.2. Water supply .....	101
3.1.3. Water quality.....	102

3.1.4.	East river seasonality .....	103
3.1.5.	Objective.....	109
3.1.6.	Study region.....	110
<b>3.2.</b>	<b>Subcatchment delineation .....</b>	<b>111</b>
<b>3.3.</b>	<b>Flow calculation.....</b>	<b>112</b>
3.3.1.	Estimation of catchment descriptors.....	118
3.3.2.	Catchment descriptors .....	120
3.3.3.	Candidate catchment characteristics .....	121
3.3.4.	Artificial influences to flow .....	125
<b>3.4</b>	<b>E2 to E1 conversion.....</b>	<b>133</b>
<b>3.5</b>	<b>Parameterisation .....</b>	<b>134</b>
<b>3.4.1</b>	<b>Sensitivity analysis.....</b>	<b>141</b>
<b>3.5</b>	<b>Wastewatershed delineation.....</b>	<b>142</b>
<b>3.6</b>	<b>Population .....</b>	<b>142</b>
<b>3.7</b>	<b>Delineating upgraded STWs.....</b>	<b>148</b>
<b>3.8</b>	<b>Sampling.....</b>	<b>150</b>
<b>3.9</b>	<b>Analytical method .....</b>	<b>154</b>
3.9.1	Extraction .....	154
3.9.2	Elution and reconstitution .....	154
3.9.3	Analysis .....	155
<b>3.10</b>	<b>Scenario based assessment .....</b>	<b>159</b>
<b>CHAPTER 4 – EAST RIVER MODELLING RESULTS AND DISCUSSION .....</b>		<b>161</b>
<b>4.1.</b>	<b>Introduction.....</b>	<b>161</b>
<b>4.2.</b>	<b>Comparison of measured and modelled concentrations.....</b>	<b>161</b>
4.2.1.	The 2008 model .....	162
4.2.1.1.	The 2016 model .....	170
<b>4.3.</b>	<b>Model analysis.....</b>	<b>200</b>
4.3.1.	Sensitivity analysis .....	208
<b>4.4.</b>	<b>Scenario based assessment .....</b>	<b>211</b>
4.4.1	Risk assessment .....	211
4.4.2	Catchment management scenarios .....	213
<b>4.5.</b>	<b>Conclusions.....</b>	<b>226</b>
<b>CHAPTER 5 – EVALUATION .....</b>		<b>228</b>

<b>5.1. Overview .....</b>	<b>228</b>
<b>5.2. Suggested methodological improvements .....</b>	<b>229</b>
5.2.1. Validation of flow and untreated discharge .....	229
5.2.2. Refining estimates of in-stream removal .....	232
5.2.3. Wet season mechanics .....	233
<b>5.3. Addressing data limitations .....</b>	<b>234</b>
5.3.1. Hydrological data .....	234
5.3.2. Locating STWs .....	235
5.3.3. STW data .....	236
5.3.4. Chemical validation data .....	237
5.3.5. Open data .....	238
<b>5.4. Potential for GREATER .....</b>	<b>241</b>
5.4.1. Modelling climate extremes .....	241
<b>5.5. Future modelling approaches .....</b>	<b>247</b>
5.5.1. Modelling at large scales .....	247
5.5.2. Dilution based large-scale models .....	247
5.5.3. Multimedia modelling .....	248
5.5.4. A cascading modelling system .....	249
<b>5.6. More ecological relevance .....</b>	<b>250</b>
5.6.1. Ecological models .....	250
5.2.1. Effects of multiple stressors .....	255
 <b>CHAPTER 6 – CONCLUSIONS .....</b>	 <b>260</b>
 <b>REFERENCE LIST .....</b>	 <b>264</b>
 <b>APPENDIX.....</b>	 <b>286</b>

## LIST OF FIGURES

Figure 1 - GREAT-ER v3 GUI. ....	26
Figure 2 - Chemical structures for studied chemicals, where: A- triclosan, B - triclocarban, C - estrone, D - 17 $\beta$ -estradiol. ....	32
Figure 3 - Schematic overview of GREAT-ER: assumes only basic in-stream removal and no untreated wastewater sources. ....	42
Figure 4 - Stream delineation procedure. A DEM is required (A) however before use, topographic lows, known as pits within the DEM may need to be corrected. These are often filled to the level of the lowest surrounding cell. To determine flow direction, flow is directed from high to low elevation based upon the lowest value within 8 surrounding cells (B). Further, the number of accumulated cells can be calculated, which is the number of cells that flow into the target cell (C). Finally once the number of accumulated cell reaches a threshold, it can be identified as a stream (D). ....	55
Figure 5 - (A) River network delineation using the D8 algorithm of Jenson and Domingue (1988) and (B) delineation using the flow direction algorithm developed by Garbrecht and Martz (1997). ....	60
Figure 6 - South Asia summer monsoonal pattern – from Wang (2006). For China, the summer monsoon originates from: 1) across the equator, from the Australian region, 2) from the tropical West Pacific ocean and 3) from the Bay of Bengal and the Arabian sea (Wang, 2006). Air above the low temperature of the Australia land mass (experiencing winter), Saudi Arabia and the relatively cool oceans, are driven towards the warm Asian land mass, especially the Tibetan Plateau (Wang, 2006; Wu and Zhang, 1998). ....	65
Figure 7 - Mean monthly surface temperature ( $^{\circ}$ C) over Asia for 1948-2000 in: (a) October, (b) November, (c) December, (d) January, (e) February, and (f) March. In October, a mass of cold air lies above the Tibeau Plateau, which expands to the East and North-West in subsequent months, merging with the expanding cold air mass above Siberia and Mongolia to the North. From (Chang, 2004). ....	67
Figure 8 - Mean sea level pressure (mb) over Asia for 1948-2000 in: (a) October, (b) November, (c) December, (d) January, (e) February, and (f) March. The region of high pressure expands from Northern regions: Siberia and Western Mongolia to the South and to the East. From (Chang, 2004). .	68
Figure 9 –Conceptual model of water pathways to stormflow or baseflow (low-flows), including storage and losses. Data is suggested for each element that may be used to estimate low flows, with explanations in Table 6. Adapted from Price (2011) and Holden (2012). ....	70
Figure 10 - Flow chart outlining the procedure of locating a STW. ....	84
Figure 11 - Locating STWs with the aid of population data. Dataset based upon Landscan (Bright et al., 2006). ....	85
Figure 12 - Population visualisation options; for all three approaches, cells with a low population density are filtered out. The value for “low population density” was determined by means of manual calibration. What was considered to be “low population density” varied between the original and modified population datasets, as the population density in the modified datasets increased as a result of the modifications. (A) Population density data smoothed using focal statistics; (B) resampled population density; and (C) original population dataset. Where the original population density has a cell size of 1km <sup>2</sup> and the aggregated population density has a cell size of 2km <sup>2</sup> . ....	87
Figure 13 - Calculation of population (mean and sum) for river stretch catchments using the zonal statistics tool in ArcGIS spatial analysis toolbox. The river stretch catchments drain only to their respective river stretch, and then subsequently, to other downstream stretches. Using the tool “zonal statistics as table”, the population sum and mean are calculated for each river stretch catchment, using a gridded population dataset for this purpose. ....	90
Figure 14 - Map displaying the sum of population contained within each river stretch catchment. Location: Longchuan county, Heyuan city, Guangdong province. ....	91

Figure 15 - Customising the symbology of the river stretch catchments in order to display standard deviations from the mean (for population density, pop/25m <sup>2</sup> ). As shown, the symbology is automatically generated based upon the mean and standard deviations of the population dataset. ArcGIS is used in this example, however other GIS platforms may be used. ....	93
Figure 16 - Final delineation example – Zjin town, Zjin county, Guangdong Province, South-East China. Population density within river stretch catchments are displayed as standard deviations from the mean. The catchments highlighted in blue are those selected to be delineated for the STW wastewatershed. The river stretch catchments between the STW and the main settlement are selected, as are all river stretch catchments that are within the settlement outline that contain a population >0.5 standard deviations above the mean (8 persons/25m <sup>2</sup> ). The cell size of the original population dataset is 25m <sup>2</sup> . ....	94
Figure 17 - Map displays multiple STWs clustered within a single settlement – Shenzhen city, China. This complicates wastewatershed delineation. ....	95
Figure 18 - Example of wastewatershed delineation for an unidentified STW within an area of Shenzhen city served by multiple STWs. Wastewatersheds were delineated for nearby identified STWs and surround the topographic area upstream of the unidentified STW. Therefore, in this example the entire available area upstream was delineated. The area to the East is outside of the topographic area. ....	97
Figure 19 - The East river catchment a tributary of the Pearl river, South-East China. The study catchment's outlet is the Bolou river gauge, which marks the tidal limit. ....	100
Figure 20 - Monthly discharge at Boluo gauging station for 2006-2008. There is strong seasonality, with much greater discharge in the summer, particularly June, in comparison to the rest of the year. ....	104
Figure 21 - Mean monthly flow (as a percentage of mean flow) at a selection of gauges in the East river catchment. ....	105
Figure 22 – Data from a sampling campaign in a rural subcatchment of the East River (downstream of our study site) (Zhang et al., 2015b). S1-S15 denote the sample site ID, for which S1-S12 are rural sites located downstream of a settlement that is known to discharge wastewater directly into the river. S13 is at the outlet to the East river, and S14 and S15 are sites on the East river. D, N and W denote samples taken in the dry (December, 2012), intermediate (March, 2013) and wet season (June, 2013) respectively. BT (columns shaded black on graph) denotes Benzotriazoles, which are chemicals commonly used in dishwasher detergents and anti-icing fluids (Giger et al., 2006). Biocides studied may be used as ingredients within personal care products (Zhang et al., 2015b). ....	105
Figure 23 – Data from sampling campaign in the Zhujiang, Liuxi and Shijing rivers, tributaries of the Pearl river (Zhao et al., 2010). Sampling sites S1-S3 were taken from the Liuxi river sites, S4-S10 were taken from the Zhujiang river, and sites S11-S14 were taken from the Shijing river. Samples were collected in the dry season (December, 2007) and the wet season (September, 2008). Overall Zhao et al. (2010) determined that there was no statistically significant difference between the concentration of chemicals from samples collected in the wet and dry season. ....	106
Figure 24 - Expansion of STWs in the East river catchment between 2008-2016. ....	109
Figure 25 - Location of all river gauges within the East river catchment. Where, Jiuzhou, Lantang, Shuntian, Yuecheng, Shuibe and Shengqian are upstream of the three major reservoirs and are not affected by significant artificial influences. ....	115
Figure 26 – Dry season (December – February) flow duration curves for the East river, where flow is normalised by mean flow (m <sup>3</sup> /s) - for gauges with little or no artificial influences. ....	117
Figure 27 - Dry season (December – February) flow duration curves, where flow is normalised by mean flow (m <sup>3</sup> /s)- for gauges with artificial influences. The curve is relatively shallow, as a result of reservoir containing flood waters and enhancing the flow in low-flow conditions (Su et al., 2011). ....	117
Figure 28 - Scatterplots displaying the relationship between flow indices and bulk density. ....	124



Figure 29 – The calculation of artificial influences to flow in a river network. Circles indicate nodes in the network. Where: $Adjusted_{stretch(s)}$ – estimated flow, taking into account influence from STW and reservoir outflows ( $m^3/s$ ); $Calc_{stretch(s)}$ – flow calculated for stretch(s) ( $m^3/s$ ); $Res_{diff(i)}$ – arithmetic difference between the measured and calculated flow for the outlet of reservoir(i) upstream of stretch(s) ( $m^3/s$ ); $STW_{disch(j)}$ – discharge from STW(j) ( $m^3/s$ ).....	128
Figure 30 - Measured and calculated flow at river gauges; flow is calculated using Equations 39-42 and is subsequently adjusted for the influence of reservoir and STW outflow.....	129
Figure 31 - Example of final adjustments to flow based upon flow gauges and reservoirs for ungauged sites in a hypothetical river network. ....	132
Figure 32 - Boxplots for calculated usage of E1 and E2. Open circle represent possible outliers ( $1.5-3 * interquartile range$ ) and asterisks represent extreme outliers ( $>3 * interquartile range$ ). ....	139
Figure 33 - Estimated spatial distribution of (A) TCS and (B) TCC usage. ....	141
Figure 34 - Comparison of population datasets. The Worldpop dataset (A) boasts a higher resolution in comparison to Landscan (B). However when compared to satellite imagery (C), it is likely that Landscan is a more realistic representation of the underlying population. Sparsely populated areas such as the region to the North-West are poorly represented by Worldpop. The census data used by Landscan is older than the data used by Worldpop, however utilising the GPWv4 dataset, Landscan was adjusted to 2010 population levels (D).....	146
Figure 35 – Population density surface generated from the GPWv4 dataset. ....	147
Figure 36 - Census boundaries derived from GPWv4. As part of the development of GPWv4, the developers assigned cells that lay on the boundary to share the value of all intersecting boundaries. And therefore these cells are unique and when backcalculating census boundaries, these cells grouped only with themselves. These are shown here as boundaries that include only a single cell each. ....	148
Figure 37 - Use of digitised development areas to aid the delineation of downgraded STWs. Developed areas, those plots of land that were developed between 2008 and 2016 were not included in the 2008 wastewatershed. ....	149
Figure 38 - Sampling sites, divided into three zones. Zone A represents Huizhou and Shenzhen, Zone B represents Heyuan City region and Zone C represents Longchuan area. ....	153
Figure 39 - Planned STWs within the East River catchment - the Shiba (A) and Mabei (B) STWs. ....	160
Figure 40 - Legend for measured vs modelled concentration box plots (ng/l). ....	162
Figure 41 – A comparison between the measured and modelled concentrations for Estrone, 17 $\beta$ -estradiol and Triclocarban, for the December 2008 scenario.....	165
Figure 42 – A comparison between the measured and modelled concentrations for Triclosan, parameterised with different in-stream removal constants, for the December 2008 scenario. Where: (A) – $0.0138h^{-1}$ , (B) – $0.061h^{-1}$ , (C) – $0.21h^{-1}$ . ....	166
Figure 43 – Scatterplots displaying measured concentration against estimated concentration of Estrone, 17 $\beta$ -estradiol, Triclocarban and Triclosan for the 2008 model. Triclosan is parameterised with different in-stream removal constants, where: TCS A – removal constant = $0.0138h^{-1}$ , TCS B – removal constant = $0.061h^{-1}$ , TCS C – removal constant = $0.21h^{-1}$ . A line is drawn on all graphs, where: measured = modelled. ....	168
Figure 44 – Median simulated concentration of Triclocarban in 2008. ....	169
Figure 45 – Simulated and measured results for the 9 sampling sites within the Longchuan sampling zone in 2016 – for Estrone, 17 $\beta$ -estradiol and Triclocarban. ....	173
Figure 46 – Simulated and measured results for the 9 sampling sites within the Longchuan sampling zone in 2016 – For Triclosan. Triclosan is parameterised with different in-stream removal constants, where: (TCS A) – removal constant = $0.0138h^{-1}$ , (TCS B) – removal constant = $0.061h^{-1}$ , (TCS C) – removal constant = $0.21h^{-1}$ . ....	174
Figure 47 – Median simulated concentration of TCC in 2016 in the Longchuan sampling zone (ng/l). ....	175
Figure 48 - Rural wastewater discharge at site HT6.....	178

Figure 49 - Satellite imagery of sampling site HT6 in a rural catchment within the Heyuan zone. Arrows indicate direction of flow. Imagery from Google Earth .....	180
Figure 50 - Photo taken from the area near sample site HT6. This small, unstable bridge and a ferry is the only means for accessing the other side of the river. This photo provides an example the level of development in the area.....	181
Figure 51 – Photo taken from the area near sampling site HT6. These residents appear to tend a small amount of crops, and chickens. This is an example of small-scale, subsistence farming observed in the area. ....	182
Figure 52 - Satellite imagery of the catchment of HT7 in a rural area within Heyuan zone. Arrows indicate direction of flow. Imagery from Google Earth. ....	183
Figure 53 -Photo taken at sampling site HT7 - looking upstream. This area is rural with a sparse population, as illustrated here.....	183
Figure 54 - Simulated and measured results for the 13 sampling sites within the Heyuan sampling zone in 2016 - for Estrone, 17 $\beta$ -estradiol and Triclocarban. ....	184
Figure 55 - Simulated and measured results for the 9 sampling sites within the Longchuan sampling zone in 2016 – For Triclosan. Triclosan is parameterised with different in-stream removal constants, where: (TCS A) – removal constant = 0.0138h <sup>-1</sup> , (TCS B) – removal constant = 0.061h <sup>-1</sup> , (TCS C) – removal constant = 0.21h <sup>-1</sup> .....	185
Figure 56 - Median simulated concentration of Triclocarban in 2016 in the Heyuan sampling zone (ng/l).....	186
Figure 57 - Median simulated concentration of Triclosan A in 2016 in the 14 sites within Huizhou sampling zone (ng/l).....	190
Figure 58 - Median simulated concentration of Triclosan B in 2016 for the 14 sites within the Huizhou sampling zone (ng/l).....	191
Figure 59- Median simulated concentration of Triclosan C in 2016 for the 14 sites within the 14 Huizhou sampling zone (ng/l).....	192
Figure 60 - Median simulated concentration of Triclocarban in 2016 for the 14 sites within the Huizhou sampling zone (ng/l).....	193
Figure 61 - Median simulated concentration of Estrone in 2016 for the 14 sites within the Huizhou sampling zone (ng/l).....	195
Figure 62 - Median simulated concentration of 17 $\beta$ -estradiol in 2016 for the 14 sites within the Huizhou sampling zone (ng/l).....	196
Figure 63 - Satellite imagery of sampling site HTZ1, in a rural area of Huizhou zone. Arrows indicate direction of flow. Imagery from Google Earth.....	197
Figure 64 – Scatter graphs displaying measured concentration against estimated concentration of Estrone, 17 $\beta$ -estradiol, Triclocarban and Triclosan for the 2016 model. Triclosan is parameterised with different in-stream removal constants, where: (TCS A) – removal constant = 0.0138h <sup>-1</sup> , (TCS B) – removal constant = 0.061h <sup>-1</sup> , (TCS C) – removal constant = 0.21h <sup>-1</sup> . A line is drawn on all graphs, where: measured = modelled. ....	199
Figure 65 - Scatter graphs for the analysis of Estrone, 17 $\beta$ -estradiol and Triclocarban between the 2008 and 2016 models, where: (A) concentration in 2016 (C2016) against concentration in 2008 (C2008); and (B) ratio of C2016/C2008 against ratio of Q2016/Q2008. Line drawn on graphs is where: C2008 = C2016.....	206
Figure 66 - Scatter graphs for the analysis of Triclosan between the 2008 and 2016 models, where: (A) concentration in 2016 (C2016) against concentration in 2008 (C2008), and (B) ratio of C2016/C2008 against ratio of Q2016/Q2008. Triclosan is parameterised with different in-stream removal constants, where: (TCS A) – removal constant = 0.0138h <sup>-1</sup> , (TCS B) – removal constant = 0.061h <sup>-1</sup> , (TCS C) – removal constant = 0.21h <sup>-1</sup> . Line drawn on graphs is where: C2008 = C2016. ....	207
Figure 67 - Scatter graph illustrating the relationship between in-stream removal and the ratio between the concentration in 2016 (C2016) and 2008 (C2008). ....	208

Figure 69 – Scatter graph displaying measured concentration against estimated concentration for all chemicals, using the 2016 model. A line is drawn on the graph, where: measured = modelled. ....	212
Figure 70 - Assessment of risk, at the 50 <sup>th</sup> percentile concentration, from TCS (left) and TCC (right) for the 2016 model, assuming a PNEC of 4.7 and 146ng/l respectively.....	214
Figure 71 - Assessment of risk at the 90 <sup>th</sup> percentile concentration from TCS (left) and TCC (right) for the 2016 model, assuming a PNEC of 4.7 and 146ng/l respectively.....	215
Figure 72 - Assessment of risk, at the 50 <sup>th</sup> percentile concentration, from E1 (left) and E2 (right) for the 2016 model, assuming a PNEC of 6 and 2ng/l respectively.....	216
Figure 73 - Assessment of risk at the 90 <sup>th</sup> modelling percentile concentration from E1 (left) and E2 (right) for the 2016 model, assuming a PNEC of 6 and 2ng/l respectively. ....	217
Figure 74 - Assessment of risk, at the 50 <sup>th</sup> percentile concentration, from TCS (left) and TCC (right) in the year 2020 base scenario, assuming a PNEC of 4.7 and 146ng/l respectively. ....	220
Figure 75 - Assessment of risk, at the 50 <sup>th</sup> percentile concentration, from E1 (left) and E2 (right) in the year 2020 base scenario, assuming a PNEC of 6 and 2ng/l respectively. ....	221
Figure 76 - Assessment of risk, at the 50 <sup>th</sup> percentile concentration, from TCS (left) and TCC (right) in the year 2020 with high STW removal (95.1-99% and 90.5-97.5% respectively); assuming a PNEC of 4.7 and 146ng/l respectively. ....	223
Figure 77 - Assessment of risk, at the 50 <sup>th</sup> percentile concentration from E1 (left) and E2 (right) in the year 2020 with high STW removal (93.6-99.9% and 93.9-99.4% respectively); assuming a PNEC of 6 and 2ng/l respectively. Circles indicate areas in need of improvement. ....	224
Figure 78 - Risk from E1 (left) and E2 (right), at the 50 <sup>th</sup> percentile concentration, in 2020 following proposed STW management scenario; assuming a PNEC of 6 and 2ng/l respectively.....	225
Figure 79 – Mean annual temperature and mean annual precipitation of China produced based upon data produced by Fick and Hijmans (2017). ....	243
Figure 80 - Population in China, based upon GPWv4 dataset (CIESIN, 2016b). The majority of the population is within South-East China; whilst much of North-West China is uninhabited, or sparsely populated. ....	244

## LIST OF TABLES

<i>Table 1 - Parameters required for all river stretches in TOMCAT, excluding the main river.....</i>	<i>23</i>
<i>Table 2 - Physio-chemical properties for studied chemicals .....</i>	<i>33</i>
<i>Table 3 - Physio-chemical properties required for advanced removal mode. Where pKa is the acid dissociation constant.....</i>	<i>54</i>
<i>Table 4 - Average residence time of water. From Holden (2012). .....</i>	<i>63</i>
<i>Table 5 - Effects of soil texture on soil properties. Presented by Holden (2012), adapted from Brady (1999). .....</i>	<i>69</i>
<i>Table 6 - Examples of catchment descriptors that may relate to low-flows. ....</i>	<i>73</i>
<i>Table 7- Concentrations of PPCPs measured in samples collected from urban streams in the Pearl river delta (Peng et al., 2008). As shown, concentrations in the dry season are significantly higher than those in the wet season. ND denotes: not detected; and NQ denotes: detected, but not quantified. ....</i>	<i>107</i>
<i>Table 8 – Data determined from samples collected from a semi-arid sub catchment of the Yellow river (Liu et al., 2017). Where ND denotes: not detected. The target compounds are known endocrine disrupting chemicals, apart from E1-3S and E2-3S, which are conjugates of E1 and E2 respectively. The concentration of the majority of compounds is greater in the wet season than the dry season. ....</i>	<i>108</i>
<i>Table 9- River gauges, used within the East River catchment. ....</i>	<i>116</i>
<i>Table 10 - Correlation coefficients of significant characteristics and normalised low-flow indices. ....</i>	<i>122</i>
<i>Table 11 - Coefficients of performance for different regression model types, generated using IBM SPSS v22. Bold indicates the selected regression form. Some regression types were not included here as they were deemed unsuitable. ....</i>	<i>125</i>
<i>Table 12 - Difference between estimated and observed flow at the outlets of the three major reservoirs within the East river catchment.....</i>	<i>126</i>
<i>Table 13 - Table detailing the different artificial influences within the catchment in 2008, from Su et al. (2011). ....</i>	<i>133</i>
<i>Table 14 - Parameters used for input into the GREAT-ER model.....</i>	<i>140</i>
<i>Table 15 - Weather conditions during sampling in 2016.....</i>	<i>152</i>
<i>Table 16 – Gradient program used by the HPLC for analysis.....</i>	<i>156</i>
<i>Table 17 - MS transitions and parameters for the target chemicals, including retention time (RT), collision energy (CE), cone voltage (CV), parent ion, daughter ions and internal standard used for each target chemical.....</i>	<i>157</i>
<i>Table 18 –Detection limits for the target chemicals.....</i>	<i>158</i>
<i>Table 19 - Concentration of target chemicals within blank control samples (ng/l).....</i>	<i>158</i>
<i>Table 20- RMSE (ng/l) between the median estimated concentration and the mean measured concentration for samples collected at sampling sites within specified spatial units - for the 2008 model. Triclosan is parameterised with different in-stream removal constants, where: (TCS A) – 0.0138h<sup>-1</sup>, (TCS B) – 0.061h<sup>-1</sup>, (TCS C) – 0.21h<sup>-1</sup>. ....</i>	<i>163</i>
<i>Table 21- RMSE (ng/l) between the median estimated concentration and the mean measured concentration for samples collected at sampling sites within specified spatial units - for the Longchuan sampling zone, 2016 model. Triclosan is parameterised with different in-stream removal constants, where: (A) – 0.0138h<sup>-1</sup>, (B) – 0.061h<sup>-1</sup>, (C) – 0.21h<sup>-1</sup>. ....</i>	<i>171</i>
<i>Table 22- RMSE (ng/l) between the median estimated concentration and the mean measured concentration for samples collected at sampling sites within specified spatial units - for the Heyuan sampling zone, 2016 model. Triclosan is parameterised with different in-stream removal constants, where: (A) – 0.0138h<sup>-1</sup>, (B) – 0.061h<sup>-1</sup>, (C) – 0.21h<sup>-1</sup>. ....</i>	<i>177</i>
<i>Table 23 - Mean flow estimated at tributary sites in the Heyuan sampling zone. ....</i>	<i>179</i>
<i>Table 24- RMSE (ng/l) between the median estimated concentration and the mean measured concentration for samples collected at sampling sites within specified spatial units - for the Huizhou</i>	

<i>sampling zone, 2016 model. Triclosan is parameterised with different in-stream removal constants, where: (A) – 0.0138 h<sup>-1</sup>, (B) – 0.061 h<sup>-1</sup>, (C) – 0.21 h<sup>-1</sup>.....</i>	<i>187</i>
<i>Table 25- RMSE (ng/l) between the median estimated concentration and the mean measured concentration for samples collected at sampling sites within the East river catchment as a whole, for the 2016 model. Triclosan is parameterised with different in-stream removal constants, where: (A) – 0.0138h<sup>-1</sup>, (B) – 0.061h<sup>-1</sup>, (C) – 0.21h<sup>-1</sup>.....</i>	<i>198</i>
<i>Table 26 - Ratio of modelled concentration between the 2008 and 2016 models. ....</i>	<i>201</i>
<i>Table 27 – Parameter set for TCC used for the purpose of sensitivity analysis of the 2016 East river model. The base state is the default state and the sensitivity state is the value 20% above/below the base state, used to test the sensitivity of the model to changes in this parameter. ....</i>	<i>209</i>
<i>Table 28 - Sensitivity of the model to changes of each parameter by +/- 20%. Sensitivity is the percentage change in concentration normalised by the percentage change in the parameter (20%).</i>	<i>209</i>
<i>Table 29 - The fraction removed by STWs defined for use within a management scenario assuming increased STW efficiency. ....</i>	<i>218</i>

## LIST OF ABBREVIATIONS

AS – Activated sludge

BOD - Biological oxygen demand

CA – Concentration addition

COD – Chemical oxygen demand

COMMPS - Combined monitoring-based and modelling-based priority setting

CSO – Combined sewer overflow

CSTRS - continually stirred tank reactors in series

CV – Cone voltage

DEM - Digital elevation model

DER – Diffuse emission ratio

DGT – Diffusive gradients in thin films

DO – Dissolved oxygen

DTED - digital terrain elevation data

E1 – Estrone

E2 - 17 $\beta$ -estradiol

EQS – Environmental quality standard

ERA – Ecological risk assessment

EU – European Union

EUSES - European Union System for the Evaluation of Substances

GIS – Geographic information system

GLS - Generalized least squares

GPWv4 - Gridded Population of the World version 4

GREAT-ER - Geo-referenced Regional Exposure Assessment Tool for European Rivers

GUI - Graphical user interface

GRDC – Global runoff database

GUTS – General unified threshold of survival

GWAVA - Global water availability assessment

HOST - Hydrology of soil types

HPLC - High performance liquid chromatography

HRU - Hydrological response unit

HWSD - Harmonised water soil database

IA – Independent action

IBM – Individual based model

IDL – Instrument detection limit

$K_d$  - Solids/liquid partitioning coefficient in water

$K_{oc}$  - Organic carbon/water partition coefficient

$K_{ow}$  – Octanol/water partition coefficient

L/EC50 – Median lethal/effect concentration

LAS - Linear Alkylbenzenesulfonate

LC-MS - Liquid chromatography–mass spectrometry

MAM10 – Mean annual 10-day minimum flow

MDL – Method detection limit

MEP - Ministry of environmental protection

MQL – Method quantification limit

MODIS - Moderate resolution spectroradiometer imagery

NAFTA – North American trade agreement

NOEC - No Observed Effect Concentration

OLD - Ordinary least squares

OSM – Openstreetmap

PCA - Principle component analysis

PCPs – Personal care products

PDB - Probability Distributed Moisture

pe - Population equivalents

PEC – Predicted exposure concentration

pKa - Acid dissociation constant

PNEC - Predicted no effect concentration

PPCP - Pharmaceuticals and personal care product

PSBI - Physiographic space based interpolation

Q95 - 95% exceedance flow

REACH - Registration, evaluation, and authorization of chemicals

RMSE – Root mean square error

RT – Retention time

SIMCAT – Simulation of catchments model

SPE – Solid phase extraction

SRTM - shuttle radar topography

SSD – Species sensitivity distribution

STW – Sewage treatment works

SWAT – Soil water assessment tool



SWBD - SRTM water body data

TCC – Triclocarban

TCS – Triclosan

TD - Toxicodynamics

TF – Trickling filter

TK – Toxicokinetics

TOMCAT - Temporal/Overall Model for catchment

TPWP - 10-point water pollution action plan

UK – United Kingdom

UWWT- urban wastewater treatment directive

WFD - Water framework directive

XFJ – Xinfengjiang reservoir

## Chapter 1 - Introduction

### 1.1. Threats to water quality in China

The effects of industrialisation and population growth within China have been poorly constrained by its environmental policy. Economic growth has led to the increased availability of chemicals within China. China's share of the global chemical market has increased from 11.6% in 2005 to 39.9% in 2015 (CEFIC, 2016). In 2015, the sale of chemicals in China was greater than the total sales in the European Union (EU) and the North America Trade Agreement (NAFTA) countries combined (CEFIC, 2016).

This has led to concerns regarding the environmental impact of chemicals, particularly the release of so called "down-the-drain chemicals" to the environment in China.

Down-the-drain chemicals are those which are primarily released with domestic wastewater. Examples of down-the-drain chemicals include ingredients within personal care products (PCPs), pharmaceuticals, caffeine and estrogens.

Within the EU and other developed regions, these chemicals will likely pass through a sewage treatment works (STW). Chemicals are treated by physical, chemical and biological processes. Physical processes primarily involve the use of grids and meshes to filter out solids from wastewater (Stuetz and Stephenson, 2009). Chemical processes include flocculation, which aggregates fine particulars, enabling removal via settlement. Chemical removal may also include disinfection processes, such as ultraviolet disinfection, which aims to significantly reduce the population of micro-organisms (Stuetz and Stephenson, 2009). Biological processes involve the use of micro-organisms to degrade organic matter under aerobic and anaerobic conditions (Stuetz and Stephenson, 2009). Furthermore, chemical residues will be released to the river network or the ocean. These chemicals may have a detrimental effect upon the wildlife within the stream.

China's wastewater system is far less effective than the system just described. Many of its

settlements lack a STW or are only partially served by a STW. In the case of rural settlements, collection of wastewater is difficult; rural population density is low and population within villages are scattered (Yu et al., 2015). Due to a lack of sewer piping, toilets often discharge directly to water bodies without treatment (Bei et al., 2009). The release of untreated wastewater has significant implications for the environment and human health. However, diffuse sources may be most significant for some rivers as a result of the release of pesticide and fertiliser to water bodies via runoff (Yu et al., 2015).

In China, drinking water may be taken directly from water bodies in rural areas, and in general, drinking water quality is provided significantly greater protection in urban areas in comparison to rural areas (Zhang et al., 2015c). During the 11<sup>th</sup> Five-Year Plan (2006–2010), it was estimated that ~34% of the rural population drank from unsafe drinking water (National Development and Reform Commission et al., 2007).

Poor water quality also has significant implications for biodiversity. For example, severe algae blooms occurred in 2007 at Taihu Lake in Jiangsu Province, likely as a result of fertiliser, pesticides and detergents (Yu et al., 2015); in which ~25% Total Nitrogen and ~60% of Total Phosphorous detected within Taihu Lake were estimated to be a result of domestic sewage (Su et al., 2005).

The Chinese government has attempted to ease the pressure on China's water quality with significant investment towards upgrading sewage treatment facilities. The initial focus has been placed upon sewage treatment within large urban areas, although increasing priority has been given to towns. In the "12<sup>th</sup> Five Year plan", the Chinese government announced that sewage treatment rates reached 77.5% in cities but less than 30% in towns in 2010 (The State Council, 2012). In the "13<sup>th</sup> Five Year plan" it was announced that sewage treatment rates in 2020 must reach 95% in cities, >85% in counties, 50% in central and western towns and 70% for all other towns (National Development and Reform Commission, 2016).

## 1.2. Environmental management

There are two approaches used in tandem which may reduce the environmental impact from down-the-drain chemicals in China. Firstly, chemical substances that are used within products that may enter the environment can be managed. The risk of many of these substances to the Chinese environment is unknown. Chemical risk assessment is required in order to determine how best to manage chemicals that are manufactured or used in China. Secondly, catchments can be better managed by deploying mitigation mechanisms (e.g. STW construction) and stakeholder engagement.

### 1.2.1. Chemical management

Examples of such legislation include the EU's Registration, Evaluation, and Authorization of Chemicals (REACH) regulation which was introduced with the aim to protect human and environmental health whilst maintaining the integrity of the chemical industry within the EU (European Commission, 2006b). REACH requires manufacturers and importers to register information about a relevant substance. This includes a tiered risk assessment which first identifies if the substance is potentially persistent, has a high potential to bioaccumulate or is toxic (denoted PBT/vPvB substances) (European Commission, 2006b). If the substance is identified as PBT/vPvB, an exposure scenario is required which describes how the substance is manufactured and/or used during its life cycle and how this substance is or should be controlled to ensure that the risk to humans and the environment are minimised (European Commission, 2006b). In the case of down-the-drain chemicals this may include the amount of substance used, removal by a sewage treatment plant and the capacity of the environment (e.g. river or lake volume). The scenario is used to generate a predicted environmental concentration (PEC). This is compared to the predicted no effect concentration (PNEC), the concentration deemed to be most likely to not lead to adverse effects in organisms living in the receiving environment. This is derived based upon the

toxicity of the chemical of interest to organisms that may inhabit the aquatic ecosystem (European Chemical Agency, 2011). The aquatic toxicity of the substance of interest is determined through laboratory based tests. Either the acute or the chronic toxicity may be estimated (European Chemical Agency, 2011). Acute toxicity is estimated based upon relatively short duration testing, for which toxicity is expressed as the median lethal or effect concentrations (L/EC50), which is the concentration at which 50% of organisms are affected or when a 50% effect level is measured for a specified endpoint (European Chemical Agency, 2011). Chronic toxicity is measured using tests that are relatively long in comparison to the lifespan of the target organism. Chronic toxicity is expressed as the highest tested concentration at which no effect was observed, the No Observed Effect Concentration (NOEC) (European Chemical Agency, 2011). Typically toxicity data will be available for a relatively small number of species in comparison to the biodiversity of the target ecosystem, and therefore the toxicity data is conservatively adjusted to determine a value for PNEC (European Chemical Agency, 2011). This can be achieved by one of two approaches. Firstly, aquatic toxicity data may be adjusted to environmental conditions using a conservative assessment factor. The assessment factor depends upon the type, quantity and quality of effect based data provided, which accounts for the level of confidence of the protecting capabilities of the derived PNEC (European Chemical Agency, 2011). Alternatively, when sufficient chronic toxicity data is available, it may be possible to estimate the lowest protective environmental concentration based upon the distribution of the sensitivities of species observed (European Chemical Agency, 2011); a species sensitivity distribution (SSD) (Posthuma et al., 2001; Kooijman, 1987). This is achieved by describing this distribution mathematically, using a minimum of 10 tests on a minimum of 8 different taxonomic groups (European Chemical Agency, 2011).

For cases when the PEC/PNEC ratio is  $>1$ , further assessment is required (European Chemical

Agency, 2011). Initially, a highly conservative but simplistic model may be used to create and simulate an exposure scenario, such as the European Union System for the Evaluation of Substances (EUSES) model. If the substance fails this assessment, it can be repeated using a higher-tier, more complex but more environmentally realistic model. Alternatively, more data can be acquired to provide a new PNEC (European Chemical Agency, 2011).

In 2010, MEP Order 7 was implemented in China, which many consider to be the Chinese equivalent of REACH. This legislation requires the registration of chemicals by manufacturers and importers with the purpose of controlling environmental pollution. Chemicals are classified by risk and hazardous chemicals which are persistent, bioaccumulative or toxic are identified (Wang et al., 2012). Exposure needs to be assessed, in the context of risk control measures. However, chemical risk assessment has been regarded as somewhat lacking in China, with particular reference to a lack of chemical hazard and exposure assessment tools (Wang et al., 2012).

#### 1.2.2. Catchment management and wastewater treatment

An example of legislation aiming to improve catchment management is the EU's water framework directive (WFD). The WFD focuses upon the wider picture, aiming to ensure good ecological and chemical status for all water within the EU. 'Good ecological status' is defined by individual EU member states based upon the biological community, hydromorphological characteristics and physio-chemical characteristics (European Commission, 2000). An acceptable biological community should be that which would be expected from conditions of minimal anthropogenic impact (European Commission, 2000). Hydromorphological elements do not directly contribute to the ecological status of the water body other than to qualify for 'high ecological status'. However, hydromorphological elements should be improved or preserved to sustain a habitat suitable for a 'good' biological community; where

hydromorphological elements include: variation in river depth and width, structure and substrate of the river bed and structure of the riparian zone (European Commission, 2000). Physio-chemical characteristics include temperature, dissolved oxygen concentration, pH, acid neutralising capacity, salinity and nutrients; which must be within a range that may sustain a good biological community (European Commission, 2000). Many of these parameters are likely to be more or less important for different water bodies with different biological communities, which is why the WFD allows member states to define what is 'good' for the native biological community (European Commission, 2000). Annex VIII of the WFD lists types of pollutants that may be of concern (European Commission, 2000):

1. Organohalogen compounds and substances which may form such compounds in the aquatic environment.
2. Organophosphorus compounds.
3. Organotin compounds.
4. Substances and preparations, or the breakdown products of such, which have been proved to possess carcinogenic or mutagenic properties or properties which may affect steroidogenic, thyroid, reproduction or other endocrine-related functions in or via the aquatic environment.
5. Persistent hydrocarbons and persistent and bioaccumulable organic toxic substances.
6. Cyanides.
7. Metals and their compounds.
8. Arsenic and its compounds.
9. Biocides and plant protection products.
10. Materials in suspension.
11. Substances which contribute to eutrophication (in particular, nitrate and phosphate).
12. Substances which have an unfavourable influence on the oxygen balance (and can be measured using parameters such as biological oxygen demand (BOD), chemical oxygen

demand (COD), etc.).

The WFD requires member states to identify pollutants from this list that are discharged in significant quantities and derive environmental quality standards (EQS) for these substances for the purpose of achieving good ecological status (European Commission, 2000). EQS are similar to PNEC values. They are thresholds at which when exceeded, may harm the biological community of the water body. Potential substances of concern are first identified then ranked in a prioritisation process. Substances are prioritised based upon the potential exposure and their hazardous nature (European Commission, 2000). Substances that are prioritised are then assessed to determine the EQS for each substance. Results from effect tests are adjusted by a correction factor, which provides an initial EQS value. This is then compared to field data and is subject to peer review and public consultation (European Commission, 2000).

'Good chemical status', however, is more specific, with European Union wide quality standards to meet, based upon a list of priority substances (European Commission, 2000).

The WFD is also complimented by other directives such as the bathing waters directive (European Commission, 2006a), the drinking water directive (European Commission, 1998), the nitrates directive (European Commission, 1991a) and the urban waste water treatment directive (UWWT) (European Commission, 1991b); all of which require either EU wide or member state defined water quality standards.

To achieve 'good chemical status', priority substances were initially identified using a similar approach to REACH. The WFD also requires that these standards are updated when required.

In addition, a subset of priority substances were identified as priority hazardous substances which are those substances of particular concern (European Commission, 2000). Priority substances must be controlled to within acceptable levels, whilst priority hazardous substances must not be discharged at all after 2020.



Priority chemicals were initially determined using a combined monitoring-based and modelling-based priority setting (COMMPS) approach (European Commission, 1999). A set of 820,000 monitoring data samples were used alongside modelling approaches for substances with insufficient monitoring data. In summary the process can be described in 5 steps (European Commission, 1999):-

- Selection of candidate substances based upon various official lists and monitoring data.
- Estimation of exposure based upon monitoring data and the Mackay level I fugacity box model (Mackay et al., 1992). This is a simple model that estimates the equilibrium partitioning of chemicals between homogenous media; the model operates within a closed system, and does not consider degradation of chemical substances.
- Calculation of effects scores based upon laboratory tests.
- Computation of risk based upon exposure and effects.
- Determination of priority substances based upon risk-ranking and expert judgement. Substances determined by modelling means are only selected if additional data is provided such as monitoring data.

These priority substances must be controlled to levels below the substance's EQS, which are defined for the whole of the EU (European Commission, 2000).

Many pollutants identified as a result of the WFD are somewhat challenging to manage at source. These include naturally occurring estrogens, which may interfere with the hormonal systems of organisms (Green et al., 2013). Other substances such as metals, sediment and organophosphates are also included as substances that must be controlled. The directive requires all relevant substances to be reduced to levels considered manageable by the ecosystem (European Commission, 2000). To assess whether progress is being made, monitoring is required.

The WFD requires river basins, including those that cross international borders, to be managed by a designated authority. Each authority must produce river basin management plans with the aim of moving toward “good” status (European Commission, 2000).

In addition, the EU enforces the UWWT, which requires EU member states to collect and treat all wastewater from all agglomerations of >2000 population equivalents (pe) (European Commission, 1991b). For populations less than 1000 pe, secondary treatment is required (e.g. activated sludge or trickling filter treatment), whereas more advanced treatment is required for populations above 10000 pe and for areas that are designated to be sensitive. In addition the directive enforces member states to pre-authorise all discharges of urban wastewater, discharges from the food processing industry and industrial discharges into urban wastewater collection systems (European Commission, 1991b). Sewage treatment plants and receiving waters must be monitored for compliance to water quality standards, with reports of compliance released to the public.

In 2015, China announced the 10-point water pollution action plan (TPWP). This plan describes the steps it will take in order to significantly improve the quality of water by 2050 (State council, 2015). The 10 action points are as follows:

“1) The discharge of pollutants will be controlled and emission reduction measures will aim to tackle pollution caused by industries, urban living, agriculture and the rural sector, and ships and ports.

2) Economic restructuring and upgrading will be further boosted. Industrial water and reclaimed water and seawater will be used to promote cyclic development.

3) Measures will aim to continue saving and protecting water resources. A strict management system of water resources will be implemented so as to control the overall use of water, improve water-use efficiency, and protect the ecological flows of key rivers.

4) Scientific and technological support will be further improved. Advanced technologies will

be promoted and fundamental research is set to be strengthened. The environmental protection industry will be regulated and the authorities will accelerate the development of the environmental protection service industry.

5) Market will play a bigger role. The authorities will make efforts to step up water price reform, improve taxation policies, facilitate diversified investment and establish an incentive mechanism that promotes water environment treatment.

6) Relevant law enforcement and supervision will be more strict, and environmental violations and illegal construction projects will be severely punished.

7) The management of water environment will be further strengthened. The authorities will strictly control the amount of pollutants and various environmental risks, and give authorization, whenever appropriate, to discharge pollutants.

8) The authorities will also make efforts to ensure the safety of aquatic ecosystem, including ensuring the safety of drinking water sources, treating underground water pollution and pollution in major river basins, and strengthening the protection of water bodies and the ocean environment. By the end of 2017, foul water in urban built-up areas will be basically eliminated.

9) The duties of all parties will be clarified and implemented. Local governments should be more responsible for the protection of the water environment and pollutant discharge units should be made accountable. The central government will check the implementation of the action plan in different basins, regions and sea areas every year.

10) Public participation and community supervision will be improved, and the government will regularly publish a list of cities and provinces that have the best and worst water environment. ” (State council, 2015).

The plan institutes water quality targets for 2020 and 2030. By 2020, 70% of water within China’s 7 major catchments should reach an acceptable standard (water classes I-III) and this figure reaches 75% in 2030 (Han et al., 2016).

Measures to achieve the goals of the TPWP include requirements for regions that fail to meet water quality standards to produce specific catchment plans including deadlines for improvement. This must be subsequently published and made available to the public (Li, 2015). This can be considered to be analogous to the WFD river basin catchment plans.

### **1.3. Holistic approach**

With reliable monitoring and modelling, effective decisions are enabled with the intention of improving the ecological status of water. With regards to China, tailored solutions are required to meet the challenges of China's complex, dynamic and uncertain nature. Chemical substances may be released from both treated and untreated sources. Most untreated sources are of an unknown location, and therefore could be considered diffuse rather than point sources. There is therefore uncertainty surrounding the relative contribution of untreated sources to chemical exposure. There is also a need to determine how exposure may change in the future. Sewage treatment capabilities are improving rapidly in China, increasing the removal of chemical substances before release to the environment. This is a counter to continued population change in China and increasing availability of products containing chemicals of potential concern.

A holistic solution is required to effectively address this issue which has the capability to assess and manage risk at the river catchment scale. Water quality is likely to vary significantly within each catchment; factors such as the locations of point sources and the spatial variation of dilution strongly influence the spatial distribution of water quality (Fewtrell and Bartram, 2001). An appreciation of the locations and possible causes of water quality "hotspots" open up opportunities for improved catchment management. Therefore, an approach which is able to provide a spatially explicit account of chemical risk within river catchments will be used. In addition, environmental conditions such as river discharge and

sewage treatment are likely to vary significantly over time. In order to fully appreciate chemical risk within a catchment, it is important to take into account this variability.

#### **1.4. Monitoring to quantify chemical exposure**

The use of monitoring data is essential, since it provides a snapshot of a chemical's exposure within a river. However, there are limitations to sampling. Each sample will only represent a single point in space and time (Johnson et al., 2008b). Chemical concentrations could fluctuate significantly within space and time due to factors such as the variation of flow or wastewater discharge. Careful planning regarding where to take a sample is necessary. For example, wastewater that enters a river will not become well mixed immediately downstream of a discharge point (Johnson et al., 2008b), and therefore sampling should be considered further downstream. It is also important to consider when to sample. For example, there is significant diurnal variation in domestic water demand, and hence variation in the release of wastewater (Almeida et al., 1999). Seasonal variation must also be considered, particularly in lake systems. Seasonality has a significant influence upon water mixing and thermal stratification in lake systems, which in turn, influences the vertical distribution of water quality (Martin and McCutcheon, 1998). For instance, the concentration of a range of pharmaceuticals was reported for a vertical concentration profile in Lake Greifensee, Switzerland (Tixier et al., 2003). The measurements suggested significant variation between the concentration and variability within the hypolimnion (the lower layer of a stratified lake), and the epilimnion (the upper layer of a stratified lake).

There are also limitations related to the chemical analysis. Firstly, it is important to note that these measurements aren't necessarily accurate, since errors in sampling, extraction and analysis are not uncommon (Johnson et al., 2008b). Sub-samples, analysed by different laboratories have, in some cases, reported significantly different concentrations. For

example, in an interlaboratory comparison reported by van Leeuwen et al. (2006), a sample containing canal water was assigned 19.4 ng/l and further, was divided and sent to 38 different laboratories for analysis. Measurements varied between 3.4-190 ng/l, a significant deviation. Most samples were quantified using liquid chromatography–mass spectrometry (LC–MS).

Secondly, chemicals may be present within waters at levels below the method detection limit, which may be critical if the relevant chemical's PNEC/EQS is low (Johnson et al., 2008b).

### **1.5. Modelling as a complimentary tool**

When using an appropriate model structure many of the issues addressed above can be avoided. Models can make predictions in time and space, and detection limits are non-existent (Johnson et al., 2008b). In addition, one of the greatest strengths of a model is its ability to perform 'What if?' scenarios. This may include an assessment of the benefits of upgrading a STW or to estimate the effect of population change upon future emissions. However modelling also has its limitations. It may be impractical to model certain systems, perhaps due to a lack of data or when the system is poorly understood or too complicated to represent (Wainwright and Mulligan, 2013; Johnson et al., 2008b). In addition, detailed information regarding the sources of the modelled chemical and how it may act within the environment must be made available (Johnson et al., 2008b). Modelling emerging contaminants, chemicals that have recently appeared (Sauvé and Desrosiers, 2014), may be extremely challenging, as there may be little information available to describe the properties of these chemicals and how they act within the environment.

### **1.6. Combining both techniques**

Both modelling and monitoring have limitations. However they often can be used to complement the other. Whereas modelling requires a sound understanding of the system (Johnson et al., 2008b), successful monitoring does not normally require detailed information about the system. Whilst sampling's limitations can be acknowledged, it is effectively a "ground truth". If modelling and monitoring are used side-by-side it is possible to gain a better understanding of the current state of the system.

Traditionally, monitoring data can be used to "validate" a model. It is important to appreciate this is not the true definition of validation (Oreskes et al., 1994), but instead the validation process is used to provide some indication of the model's reliability. A model is a simplified representation of the modeller's knowledge of the system. Attempting to emulate monitoring results with a model is, therefore, an attempt to try and assess his/her knowledge of the system and/or the quality of the data used.

In addition to validation, monitoring data can be used to provide additional data to either input directly into the model or to provide information that may allow the modeller to better understand the system or other datasets. For example the presence of caffeine may be an indicator of wastewater input (Buerge et al., 2003), this information may aid the modeller to improve his/her model or as an aid during the validation process.

Furthermore, a combined approach will be used. A model can be used to generate exposure scenarios, and provide an estimation of the chemical concentration within a given catchment. This may be supported by measured concentrations from a catchment wide sampling campaign.

### **1.7. Model scenarios**

Once a model has been calibrated and validated using monitoring data, scenarios can be

designed which represent future conditions or to simulate the effect of different management strategies. An evaluation of future conditions is useful, as it enables an assessment of potential risks in the future. This may be used for the purpose of decision making, for example, for a chemical which is deemed to be of no significant risk in the present, may pose a risk in the future (e.g. as a result of increased usage), it may be reasonable to consider restrictions upon that chemical. Also, for specific regions/catchments that are at risk from an array of different chemicals, mitigation options such as improved sewage treatment may be suggested as potential solutions. These may be tested by including these conditions as model scenarios, with the aim of reducing chemical risk to acceptable levels.

### **1.8. Modelling challenges**

A model capable of simulating a realistic chemical exposure scenario for chemicals released to water will require a considerable amount of data. This may include: chemical emission rates, physio-chemical properties, population data and river topology. This requirement for data is inversely related to scale, with more detail required about elements and processes within the catchment at the small-scale such as hydrological data and STW locations and properties. However, in comparison to the EU, data availability is relatively poor in China. Despite development, China lacks the same level of resources to acquire and store data. Data availability is also partially hindered by the nature of data administration in China (Shen et al., 2015; Hsu et al., 2012; Chen et al., 2015; Mackay et al., 1992). Data is often held by many different organisations, all with different data policies and there are many who are unwilling to share data.

China hosts some of the largest rivers in the world and has very large, dense and heterogeneous urban areas. This presents the difficulty of environmental complexity.



Modelling these environments requires additional information about the environments in question, which compounds the issue with data availability. The primary concern is that of untreated discharges.. As previously discussed, a significant fraction of the Chinese population is not served by a STW, and of this untreated wastewater, an unknown fraction will be released to the waterways. There is uncertainty regarding the location of untreated discharge points, and the quantity of wastewater that is released from each point. It is therefore important that a model structure is selected that can address the challenge of poor data availability yet can also represent the complexity of a Chinese catchment.

Furthermore, there are two main elements that need to be addressed: 1) accounting for untreated discharges and 2) addressing lack of data availability. There is also the need for some degree of efficiency in model development and operation. A methodology that is overly time consuming presents barriers to transferability and adoption. A degree of pragmatism is required to move towards an approach where it is possible to parametrise a catchment model for any catchment in China without great difficulty. Otherwise, the use of higher-tier risk assessment models are likely to be of limited use within China.

### **1.9. Model selection**

The primary goal for model selection here is to choose a model that is capable of realistic estimation of the PEC for down-the-drain-chemicals at the catchment scale. This requires the removal of a chemical within a STW and in-stream, which is important for all but the most persistent chemicals (Keller, 2006). The model should also be able to account for spatial and temporal variation. Chemical input, chemical load and dilution varies significantly, spatially and temporally, within a catchment and therefore should be considered in order to provide a realistic estimate (Keller, 2006). Finally, model selection must also consider the data

requirements of the model, which should be balanced against the ability to preserve realism and to provide reliable outputs.

There are a variety of different model structures that could be used. For chemical risk assessment, multimedia models are most commonly used. These models consider the fate and partitioning of chemicals between different media such as soil, water, air, sediment and biota. Simple multimedia models are available with basic data requirements, with the capability to model chemicals up to the global extent. Many multimedia models are based upon the Mackay fugacity models (Mackay et al., 1992; Mackay et al., 1996). These models increase in complexity between model levels I to IV. Level I is a closed system at steady state. The system is assumed to be at equilibrium and does not consider chemical losses. Fugacity and fugacity capacity govern chemical partitioning (Mackay et al., 1992). Fugacity describes the potential of a chemical to escape from one media and move to another, whilst fugacity capacity describes the ability of a phase to receive the chemical. Fugacity is determined below by (Mackay et al., 1992; Mackay et al., 1996):

$$F = \frac{M}{\sum V(i) * Z(I)} \quad (1)$$

where:

F – fugacity (Pa)

M – total amount of chemical (mol)

V(i) – volume of medium i (m<sup>3</sup>)

Z(i) – fugacity capacity for the chemical in medium i (mol/m<sup>3</sup> Pa).

This can also be rewritten to describe the molar concentration, C (mol/m<sup>3</sup>) as shown by

Equation 2:

$$C = Z * F \quad (2)$$

At level II, there is consideration of losses as a result of advection and degradation reactions. The system is considered to be an open system at steady state. Degradation is determined based upon experimental studies, whilst default values are available for advection. At level III, the system is considered not to be at equilibrium. Fugacity rates may differ between media and further, intermedia transportation rates are calculated (Mackay et al., 1996; Mackay et al., 1992). Finally, at level IV the model assumes the same conditions as a level III

model, but differs in that it is at an unsteady state (Mackay et al., 1996). The Mackay models form the basis of North American models: Chem-CAN (Webster et al., 2004; Woodfine et al., 2002) and BETR North America (MacLeod et al., 2008).

The most commonly used model for EU risk assessment is EUSES, a framework consisting of multiple models for the purpose of assessing chemical exposure in multiple medias (European Commission, 2003). Within EUSES, estimation of the environmental distribution of a chemical takes into consideration: chemical partitioning, chemical degradation, removal in STWs, regional/continental distribution and local environmental distribution. The local scale considers the risk of one large point source (European Commission, 2003).

However, these multimedia models are generic tools, with no consideration for site specific information. These tools are viable as a screening tool, but cannot be used for site-specific assessment, with limited use as a catchment management tool (Keller, 2006).

A more appropriate choice would be a catchment scale, water quality model which may be used to provide an estimate of flow and to route the relevant chemical through the river network. The designed use and complexity of these models varies significantly. Models were reviewed below, with regards to the modelling selection aims.

## **1.10. Catchment scale water quality models**

### **1.10.1. The SWAT model**

The Soil and Water Assessment Tool (SWAT) is a semi-distributed rainfall-runoff model (Neitsch et al., 2011), designed as a complete water management tool with the capabilities of simulating a wide scope of different management scenarios. This includes agricultural practices such as crop rotation, different tillage and rearing farm animals. SWAT may also be used to simulate the effect of best management practices upon flow and water quality. The

model can also account for point sources such as STWs, for which the user must provide the daily loadings. Watershed processes are described in detail, requiring a large number of input parameters (Arnold et al., 2012). The model may require hundreds if not thousands of parameters, depending upon the functions used. The model can potentially be used in ungauged catchments due it being “Physically-based”, and databases with default parameters are available to provide an initial estimate (Beven, 2012b). However, these values may not be appropriate for the place or working scale. Therefore, most SWAT applications require some degree of calibration, usually calibrating against observed flow data. Automatic calibration is possible but there is a danger of overparameterisation and overfitting of the hydrograph due to the great number of parameters available to calibrate (Beven, 2012b). Over-parameterisation, from a hydrological perspective, concerns situations when the amount of information available from observations (e.g. a hydrograph) is insufficient in order to calibrate the required number of parameters (Jakeman and Hornberger, 1993). Overfitting relates to models which include more parameters than are necessary and/or use a more complicated approach than necessary (Hawkins, 2004). This added complexity may lead to a similar or worse performance in comparison to a more simplistic model; the use of unnecessary predictors may add random noise to the predicted values. In addition, measurement of unnecessary parameters is inefficient and increases the risk of additional errors (Hawkins, 2004). Manual calibration can take place by changing a few sensitive variables (Beven, 2012b). However, again this may be challenging when faced with hundreds of parameters. Furthermore, it is uncertain whether a calibrated model will have any meaningful predictions (Beven, 2012b).

#### 1.10.2. The GWAVA model

The Global Water Availability Assessment (GWAVA) model is primarily used to determine the availability of water resources at the regional to continental scale. The model is grid based which can be scaled depending upon the spatial extent and data availability. Flow is calculated based upon the Probability Distributed Moisture (PDM) model (Moore, 1985). Each model defines the distribution of different storage capacities. These storage elements fill during storm events and are released as runoff when the storage capacity is breached. Between storms the stores will slowly release, representing the recession period and baseflow. This model type is simple and is designed to be easily calibrated using automatic routines (Beven, 2012b). The PDM model has shown to provide realistic estimates of flows in a variety of different regions (Meigh et al., 1999).

The GWAVA model contains a PDM model in every grid cell. It uses physical characteristics such as soil type and land cover, which correlate well with the limited set of parameters required by PDM (Meigh et al., 1999). Each cell generates runoff which routes to the next downstream cell. This is then refined to incorporate artificial influences such as water abstraction and reservoirs (Meigh et al., 1999). The model has been extended to include a water quality module capable of modelling standard water quality indicators such as biological oxygen demand (BOD) (Dumont et al., 2012), but also organic chemicals such as estrogens (Liu et al., 2015). Point sources such as wastewater inputs can be included, but the emissions must be pre-determined and assigned to a grid square. Therefore if multiple emissions are within one grid square, they must be lumped (Liu et al., 2015). Removal may occur both in-stream and via abstraction. The model is significantly less complex than SWAT and most of the input parameters are readily available. The model has been used to simulate estrone (E1) and 17 $\beta$ -estradiol (E2) within the Yellow River catchment (Liu et al., 2015). The modelled annual hydrograph was comparable with observed data and estimated E1 concentrations were similar to monitoring data (The simulation of E2 was not discussed).

However, it was not possible to simulate monthly flow as there was insufficient information regarding the seasonal effects of reservoirs on flow.

### 1.10.3. SIMCAT

The SIMulation of CATchments model (SIMCAT) was originally developed by the UK water company, Anglian water (Warn, 1986). The model was developed for the purpose of determining costed, appropriate measures in order to improve water quality to acceptable standards within English catchments (Warn, 2010; Warn, 1986). The model has since been adopted by the Environment Agency (Cox, 2003) and has received numerous updates. The model has now been developed for all river basin districts in England and Wales (Crabtree et al., 2009), and is now primarily used for the purpose of complying with the WFD (Hankin et al., 2016).

SIMCAT is a one-dimensional, steady-state stochastic-deterministic model (Cox, 2003). The model is composed of river reaches (maximum of 600) and features such as STWs and abstraction points (maximum of 1400). A mass balance Monte-Carlo approach (Warn and Brew, 1980) is used to model flow and contaminants, and outputs are provided as distributions (Cox, 2003); with a maximum of 2400 “shots”. The model may be defined as a Continually Stirred Tank Reactors In Series (CSTRS) model, which assumes perfect and instantaneous mixing of contaminants (Cox, 2003). Contaminants are transported at the same velocity as the water. Flow and contaminant mass balances are described below:

$$Q_o = Q_i + Q_t + Q_e - Q_a \quad (3)$$

$$C_o = \frac{(Q_i C_i + Q_t C_t + Q_e C_e)}{Q_r + Q_t + Q_e} \quad (4)$$

where:

Q – flow (m<sup>3</sup>/s)

C – contaminant concentration (mg/L)

Subscripts – *o*, *i*, *t*, *e* and *a* refer to: input, tributary, effluent discharge and abstraction respectively.

Contaminants may be degraded by first-order decay, which is described by Equation 5 and 6:

$$\frac{dC}{dt} = -kC, dt = \frac{dx}{v} \quad (5)$$

$$C_x = C_o * e^{-k \frac{x}{v}} \quad (6)$$

where:

C<sub>x</sub> – contaminant concentration at the end of the stretch (mg/l)

k – decay constant (h<sup>-1</sup>)

x – distance (m)

v – velocity (m/s).

Velocity is calculated based upon an empirical relationship between velocity and discharge described by Equation 7 below (Cox, 2003):

$$v = aQ^b \quad (7)$$

where:

Q – flow (m<sup>3</sup>/s)

a and b – Constants determined by calibration.

Flow and water quality data must be provided for the reaches of the main river, tributaries, wastewater discharges and abstraction points (Cox, 2003). These may be input as

distributions, and data regarding the seasonal distribution of flow may also be included (monthly means and standard deviations). Flow and quality observations may be used to calibrate the model manually, or the data may be used to auto-calibrate flow and water quality (Cox, 2003). Auto-calibration of river discharge is achieved by applying additional flows as a function of river length until simulated flows match observations. During water quality auto-calibration, required adjustments are made to water quality parameters and velocity in order to result in an agreement between measured and modelled data (Cox, 2003; Kannel et al., 2011).

As a case study, the SIMCAT model created for the river Ribble catchment (UK) is discussed here (Crabtree et al., 2009). The purpose of the study was to try to estimate the proportion of pollutant loads from point and diffuse sources within the catchment, with a focus on phosphate, BOD and ammonia. To achieve this, the following data were estimated: agricultural diffuse loads, urban runoff loads, wastewater intermittent discharge data and STW data. However, no agricultural diffuse load estimates were available for BOD and ammonia (Crabtree et al., 2009). Following calibration it was estimated that STWs contributed 88%, 29% and 67% of the phosphate, BOD and ammonia load respectively. For phosphate, management scenarios targeting improved wastewater infrastructure were applied to the model (Crabtree et al., 2009). Results from these scenarios suggested that 157.1 km of the river would still fail to comply with the WFD when all STWs operate under the UK Environment Agency's best available technology (BAT) policy, with consents limited to 1mg/l for STWs with PE > 1000 and 2mg/l for STWs with PE < 1000 (Crabtree et al., 2009). However, the model did not undergo validation and therefore it is difficult to determine how viable the model's estimates were.

#### 1.10.4. TOMCAT



The model Temporal/Overall Model for CATchment (TOMCAT), was developed by the UK water company, Thames Water for the purpose of reviewing effluent quality standards at Thames Water sites in order to meet water quality objectives for receiving rivers (Bowden and Brown, 1984). TOMCAT is conceptually similar to SIMCAT (Cox, 2003), with a few significant differences. TOMCAT is temporally more complex than SIMCAT. A number of seasons may be defined, each with a user-defined number of months (Keller, 2006). Data may also be input to TOMCAT for each season (Cox, 2003), whilst SIMCAT only allows for monthly data to be input.

TOMCAT defines two temporal indices: a monthly index and an hour-of-day index (Cox, 2003). This defines the seasonal and diurnal effects for inclusion in each Monte Carlo shot. During the simulation, temporal indices are allocated in turn until all 12 months – 24 hour combinations have been simulated.

This allow model outputs to be provided for user defined “time windows” (Cox, 2003). However, TOMCAT does not include a post-processor to visualise results (Keller, 2006); instead results are presented as text files.

Flow in the main river is defined to accumulate downstream as a function of river length (Cox, 2003). Velocity is calculated based upon the mean cross-sectional area for the stretch. Data relating to flow and water quality are defined in the first reach of the main river. Excluding the main river, data described in Table 1 must be defined for every stretch (Keller, 2006), although flow in these stretches may also be correlated with flow in the main river or other elements with the catchment (e.g. a STW discharge).

<b>Data required</b>	<b>Unit</b>
Reach length	km
Reach mean cross-sectional area	m <sup>2</sup>
Reach mean depth	m
BOD decay parameter	day <sup>-1</sup>
Ultimate BOD concentration (minimum)	mg/l

Ammonia decay parameter	day <sup>-1</sup>
Ultimate ammonia concentration (minimum)	mg/l
Oxygen exchange parameter	day <sup>-1</sup>
Catchment ID (used for estimating the diffuse catchment runoff)	-
Scale factor for runoff (proportion of the total runoff for the catchment which is received by the reach, per km)	-

Table 1 - Parameters required for all river stretches in TOMCAT, excluding the main river

Point sources may be assigned to reaches, however there is no consideration for STW removal (Keller, 2006), and therefore the concentration within effluent must be pre-calculated. TOMCAT may also be able to simulate the effects of storm water overflow events. When flow exceeds a given threshold, effluent is diverted to an alternative outlet (Cox, 2003).

TOMCAT is incorporated into WaterWare (Fedra and Jamieson, 1996; Jamieson and Fedra, 1996a; Jamieson and Fedra, 1996b). WaterWare is a decision support system for integrated river catchment management. The model utilises TOMCAT for its surface-water quality element (Fedra and Jamieson, 1996). WaterWare has been utilised in catchments such as the river Thames (UK), and the Rio Lerma catchment (Mexico) (Jamieson and Fedra, 1996b).

#### 1.10.5. The GREAT-ER model

The Geo-referenced Regional Exposure Assessment Tool for European Rivers (GREAT-ER) model is a catchment-scale GIS model, initially published by Feijtel et al. (1997). The model estimates the exposure to a chosen chemical within the vector river network.

The model was originally designed as a higher-tier chemical risk assessment tool for EU risk assessments, prior to REACH (Feijtel et al., 1997). Higher-tier risk assessment tools were required to provide more realistic exposure scenarios. Without such, chemical risk assessment relied upon highly conservative generic models.

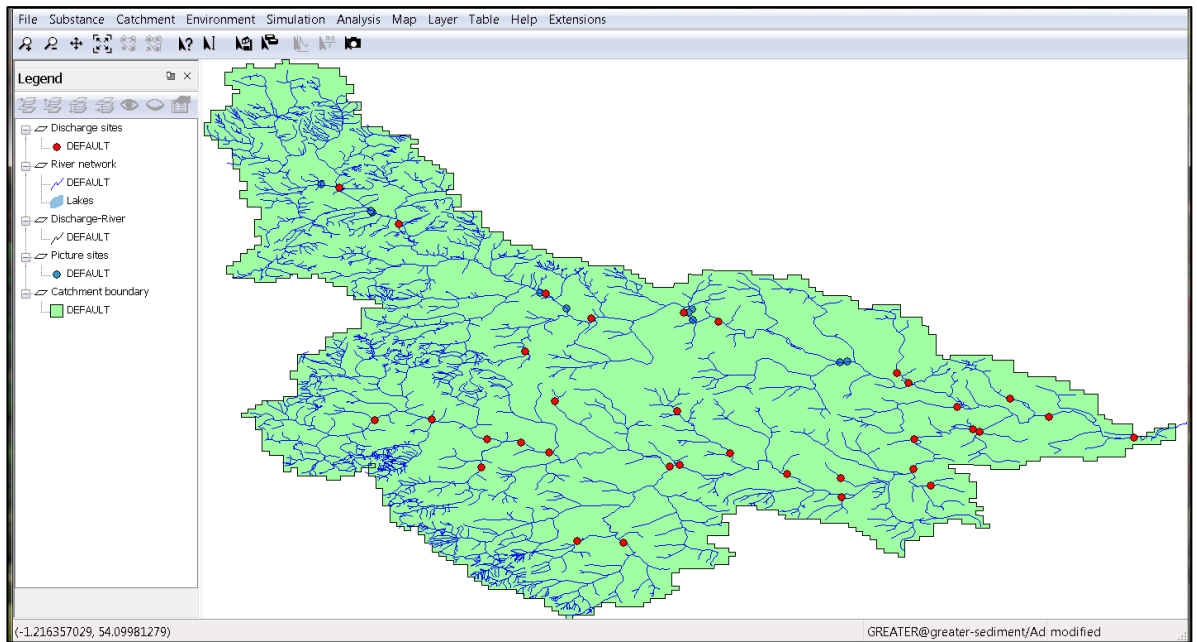


Figure 1 - GREAT-ER v3 GUI.

The model is designed to be used by those with a less technical background. GREAT-ER v3 is operated using a graphical user interface (GUI) within the GIS framework, Thuban (Figure 1). Catchments are generated outside of the model, and are then imported. Once imported, the task of running a simulation is simple and minimum data requirements are relatively low. GREAT-ER therefore provides value for catchment managers and chemical risk assessors.

Chemical emissions may be from point or diffuse sources (using the GREAT-ER v3 sediment extension) and are calculated on a per capita emission basis (Wagner and Koormann, 2011). Removal of the contaminant can take place prior to emission and in-stream. The complexity of the method used to calculate removal may be adjusted depending upon data availability. The lowest tier methodology applies a simple 1st-order removal rate for in-stream removal and a static or distributed removal ratio for sewage treatment removal. When applying simple removal options to an existing catchment model, in the absence of diffuse pollution, data required is limited to per capita consumption of the substance of interest and an estimation of the sewage treatment and in-stream removal rates. Removal rates can be calculated using data from the literature. In the absence of data within the literature,

chemical consumption may need to be estimated based upon market sales data (e.g. Zhu et al., 2016), or by back-calculation based upon measured concentrations within STW influent/effluent (e.g. Liu et al., 2015).

The GREAT-ER model determines concentrations using a stochastic-deterministic approach, and uses a Monte-Carlo method during simulation (Wagner and Koormann, 2011), which uses a method of combining distributions (Warn and Brew, 1980). All outputs and a significant number of inputs are distributions rather than single values (Wagner and Koormann, 2011). This can be used to account for uncertainty and natural variation in the data. This may also enable the worse-case scenario to be determined in addition to the concentration under average conditions.

To model a catchment not currently available for GREAT-ER, this must be first developed outside of the software. Riverlines are required, or when not available may be generated from a digital elevation model (DEM) or digitised from satellite imagery. Riverlines should be composed of multiple lines, known as stretches. Each stretch must contain information regarding the mean flow and the flow exceeded 95% of the time. Flow statistics may be achieved by various means (see section 2.5). The model also requires the location of all STWs within the catchment, with details of the population served and the type of sewage treatment.

#### *Examples of previous usage*

The GREAT-ER model has been used for a number of different substances and purposes. The model's use has been largely restricted to European catchments. However, the conceptual nature of GREAT-ER does not limit its use to Europe and there is considerable potential to use it elsewhere. The model has been used in many different catchments of varying size and nature.

The model is not limited to the boundaries of a single catchment. The LF2000-WQ model employs the lower-tier GREAT-ER model structure with additional functionality, most crucially the utilisation of UK low flow and STW data. This has allowed for the creation of a UK-wide model which was used to estimate the concentration of estrogens (Williams et al., 2009).

The initial iterations of the model estimated the exposure of household cleaning product ingredients such as Boron and Linear Alkylbenzenesulfonate (LAS) (Schröder et al., 2002; Schulze and Matthies, 2001; Price et al., 2009). GREAT-ER (and its iterative products) has also been used to investigate the fate of pharmaceuticals (Johnson et al., 2008a; Schowanek and Webb, 2002), personal care products ingredients (Wind et al., 2004; Price et al., 2010) and estrogens (Sumpter et al., 2006; Williams et al., 2012).

The model can also be used outside of its original scope. For instance, in a study described by Hüffmeyer et al. (2009) who successfully modelled the concentration of Zinc from both point and urban non-point sources, with similarity between observed and modelled concentrations. Removal in STWs was determined based upon influent and effluent data from all STWs within the catchment (Ruhrverband, 2005). In-stream removal was assumed to be entirely due to sedimentation, using a soil-water partition coefficient ( $K_d$ ) of  $84000 \text{ L kg}^{-1}$ . The GREAT-ER model is also viable to model any standard water quality parameters which can be reasonably removed by 1st-order processes such as BOD.

The GREAT-ER model has been successfully parameterised to simulate nonylphenol and nonylphenol ethoxylates within the Wenyu catchment, an urban catchment in North-East Beijing (Zhang et al., 2015a). The catchment was well developed, with an effective sewage collection system. The authors assumed that the majority of wastewater was treated by the 11 STWs within the catchment and, therefore, did not consider untreated discharge. Data availability for the catchment was reasonable; including results of a SWAT model, providing

estimates of flow for the catchment. The study suggested that the GREAT-ER model may be used in China. However, the authors stated that the catchment was chosen due to the relatively high data availability and the near complete STW service for the catchment. It is important to be able to model catchments that are more complex and with limited data availability in order to provide a more realistic representation of the average Chinese river environment.

#### 1.10.6. Conclusion

The SWAT model is far too complicated for the application required and the number of parameters is of some concern. The data required would likely be accessible. However, parameterisation and calibration is likely to be complex, with dangers of over-parameterisation.

The GWAVA model is a more appropriate model structure, with significantly less complexity. The model has already been demonstrated to be capable of modelling large Chinese catchments, such as the Yellow River.

SIMCAT is a simple but functional model. However, the model's simplicity is relatively restrictive. The model allows for chemical removal by first-order reaction rate only, and there is no consideration for more complex processes or sediment partitioning. Furthermore, the model is limited in the number of stretches and features, which may be restrictive for large catchments.

TOMCAT, as described earlier, is conceptually similar to SIMCAT. One significant advantage over SIMCAT is its temporal complexity, which allows the model to account for seasonality within the catchment. However, its approach to estimating velocity is overly simplistic, which is based upon the cross-sectional area of the river. In addition, it has a significant

disadvantage in that the model does not take into account removal within STWs, which must be pre-calculated.

The GREAT-ER model has the key advantages of flexibility regarding: 1) data requirements, allowing for more complexity when data allows and 2) the methodology, with the freedom to utilise the best method to determine removal rates and flow statistics. This flexibility is important. For example, it is possible to simulate flow in a model such as GWAVA and SWAT, for use in GREAT-ER (Zhang et al., 2015a); whereas the water quality modules of SWAT and GWAVA are inseparable from their flow modules. It also provides a stochastic shell that takes into account the uncertainty and variability that surrounds many of the datasets. Finally, it has been shown to provide reliable results in comparison to monitoring data, with success within Europe and China. As a result, the GREAT-ER model was selected for this project.

#### **1.11. Barriers to overcome for Chinese catchments**

GREAT-ER is designed for use in European catchments. Furthermore, there are a number of problems that must be overcome in order to model Chinese catchments. Largely, this is an issue of the construction of the catchment prior to upload to GREAT-ER. Data availability for riverlines, flow, STW location and attributes, and diffuse emissions is limited and/or of poor quality.

Riverlines may be generated from a DEM which is readily available. However, at the small scale, the positional accuracy of the riverlines is critical as this will affect all other elements of catchment construction.

Flow may be calculated based upon a flow duration curve, which may be determined for individual flow gauging stations with long-term flow records. This may be estimated for the entire catchment by using spatially explicit environmental data that may describe the natural

variability of flow (e.g. geological data, topography, land cover data etc.) and relate this to relevant flow indices using an appropriate model. This is discussed in more detail in section 2.5. Long-term flow data is difficult to obtain and/or may only be available at the monthly or annual resolution. Data on artificial influences is desirable, although this is challenging to obtain. Most critical is the availability of data that may describe the influence of medium and large reservoirs, which may have a large impact upon flow. However, the exact method used for flow calculation is up to the user's discretion.

STW data is perhaps the most challenging to obtain. A list of STWs in China up to 2014 is available from the Chinese Ministry of Environmental Protection, although this may not explicitly define the locations of each STW and is not completely exhaustive. This does not include data on population served and this therefore must be obtained by other means. Finally, untreated wastewater emissions must be calculated. These data must be estimated, based largely upon population density distribution.

#### 1.12. Chemicals selected for study

Chemicals were selected based primarily upon data availability. Two chemicals found in personal care products were selected: Triclosan (TCS) and Triclocarban (TCC). In addition, two natural estrogens were selected: Estrone (E1) and 17 $\beta$ -estradiol (E2). Chemical properties are displayed in Table 2, whilst chemical structures are presented below in Figure 2.



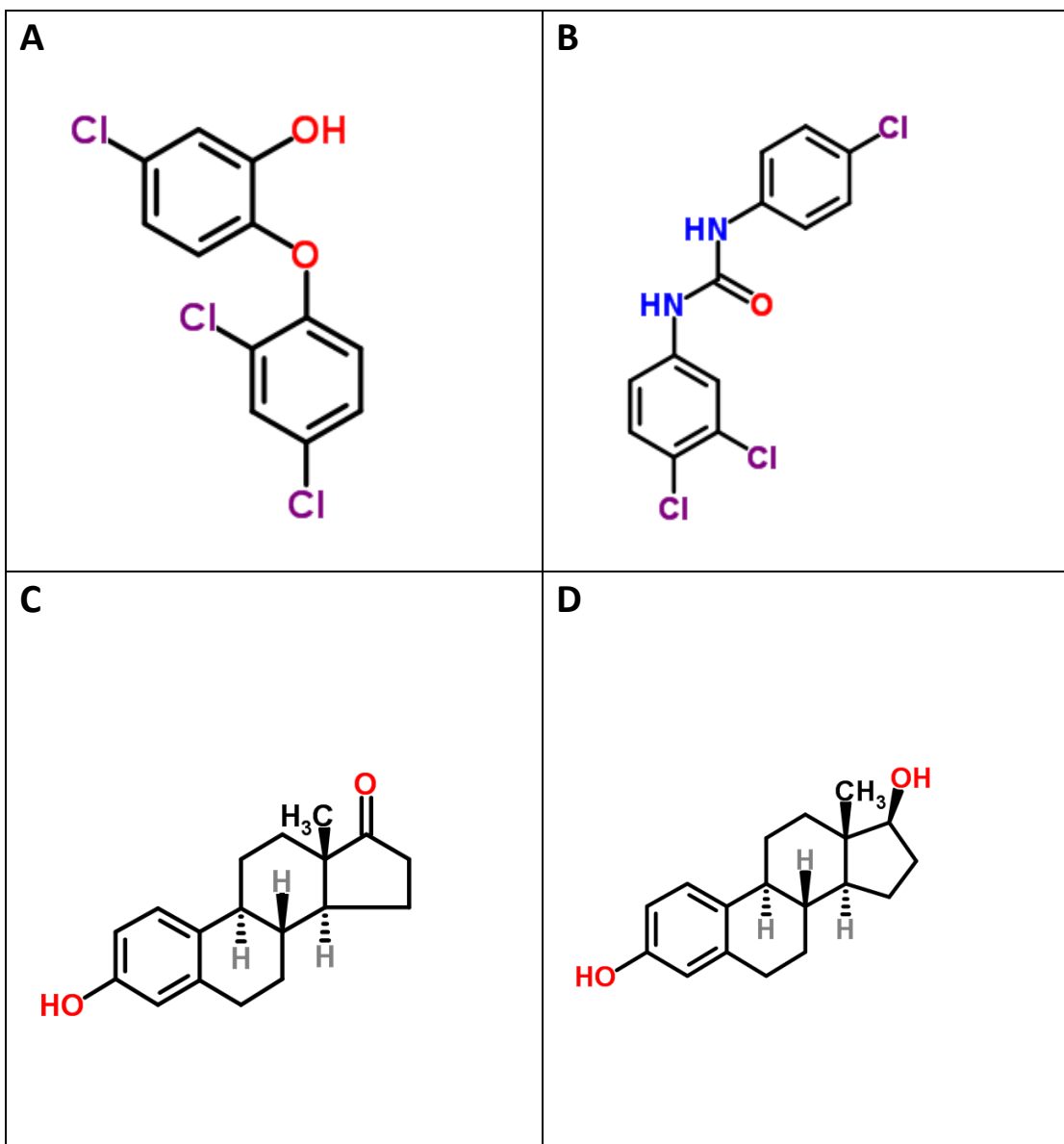


Figure 2 - Chemical structures for studied chemicals, where: A- triclosan, B - triclocarban, C - estrone, D - 17 $\beta$ -estradiol.

All chemicals studied are primarily from domestic use or human excretion, and are released down-the-drain. However, these two groups are likely to have significantly different spatial release patterns. Natural estrogens will be released wherever there is population. However, personal care products may not be used in rural areas to the same extent as in urban areas. There is a large socio-economic gap between rural and urban areas, with implications for chemical emissions (Hodges et al., 2012; Xie and Zhou, 2014).

	TCS	TCC	E1	E2
CAS number	3380-34-5	101-20-2	53-16-7	50-28-2
Chemical formula	C <sub>12</sub> H <sub>7</sub> Cl <sub>3</sub> O <sub>2</sub>	C <sub>13</sub> H <sub>9</sub> Cl <sub>3</sub> N <sub>2</sub> O	C <sub>18</sub> H <sub>22</sub> O <sub>2</sub>	C <sub>18</sub> H <sub>24</sub> O <sub>2</sub>
Molar mass (g mol <sup>-1</sup> )	289.536	315.578	270.372	272.388
Boiling point (°C)	373.62 <sup>c</sup>	434.57 <sup>c</sup>	391.87 <sup>c</sup>	395.47 <sup>c</sup>
Melting point (°C)	136.79 <sup>c</sup>	182.04 <sup>c</sup>	153.08 <sup>c</sup>	152.43 <sup>c</sup>
Vapor pressure (Pa)	1.15 × 10 <sup>-3c</sup>	1.57 × 10 <sup>-4c</sup>	253 <sup>c</sup>	3.35 × 10 <sup>-5c</sup>
Henry's law constant (Pa m <sup>3</sup> mol <sup>-1</sup> )	2.1 × 10 <sup>-8d</sup>	4.5 × 10 <sup>-11d</sup>	3.8 × 10 <sup>-10e</sup>	3.6 × 10 <sup>-11e</sup>
Koc (L kg <sup>-1</sup> )	3467-15892 <sup>f</sup>	12022-71687 <sup>f</sup>	212-13183 <sup>h</sup>	457-7244 <sup>g</sup>
Kow*	57544 <sup>c</sup>	79433 <sup>c</sup>	1349 <sup>c</sup>	10233 <sup>c</sup>
Water solubility (mg L <sup>-1</sup> at 25°C)	12 <sup>b</sup>	2.37 × 10 <sup>-3c</sup>	1.30 <sup>a</sup>	1.51 <sup>a</sup>

Table 2 - Physio-chemical properties for studied chemicals

\* octanol/water partition coefficient

a - Shareef et al. (2006)

b - Pointurier and Volz (1990)

c - US EPA (2011)

d - Meylan and Howard (1991)

e - Mansell and Drewes (2004)

f - Wu et al. (2009); Barron et al. (2009)

g - Khanal et al. (2006); Yu et al. (2004)

h - Holthaus et al. (2002); Yu et al. (2004)

### 1.12.1. Triclosan and Triclocarban

#### *Uses*

TCS and TCC have similar uses and physiochemical properties. They are primarily used to kill or hinder the growth of microorganisms (Halden, 2014; Bhargava and Leonard, 1996). Both are most commonly found in personal care products such as cosmetics, soaps, hand gels and shampoo; with TCC most commonly used within bar soap (Halden, 2014). TCS is also used in a number of other applications including clinical applications (Jones et al., 2000; Bhargava

and Leonard, 1996), plastics and textiles (Angle et al., 2008; Halden, 2014). A detailed list of applications for Triclosan can be found within Angle et al. (2008).

#### *Detection in environment and chemical fate*

Both TCS (Kolpin et al., 2002; von der Ohe et al., 2012; Halden, 2014; Halden and Paull, 2005; Guerra et al., 2014; Sabaliunas et al., 2003; Schatowitz, 1999; Ying and Kookana, 2007) and TCC (Halden, 2014; Halden and Paull, 2005; Heidler et al., 2006; Lozano et al., 2013; Ryu et al., 2014; Yu et al., 2011; Lv et al., 2014; Zhao et al., 2010) are widely detected in water and wastewater. TCS and TCC both have the tendency to sorb to organic carbon with organic carbon/water partition coefficients ( $K_{oc}$ ) between 3467-15892 and 12022-71687 L kg<sup>-1</sup> measured for TCS and TCC respectively (Wu et al., 2009; Barron et al., 2009). Volatilisation is not expected to be significant with a Henry's law constant of  $2.1 \times 10^{-8}$  Pa m<sup>3</sup> mol<sup>-1</sup> and  $4.5 \times 10^{-11}$  Pa m<sup>3</sup> mol<sup>-1</sup> for TCS and TCC respectively (Meylan and Howard, 1991). Both TCS (Lv et al., 2014; Yu et al., 2006; McAvoy et al., 2002; Lozano et al., 2013; Latch et al., 2005) and TCC (Lv et al., 2014; Lozano et al., 2013; Ding et al., 2013; Guerard et al., 2009; TCC Consortium, 2002) have been shown to degrade by means of photodegradation and biodegradation.

#### *Effects in the water environment*

As biocides, the primary threat from TCS and TCC is toxicity. However, there have also been observations that indicate bioaccumulation and bio-concentration of TCS and TCC is possible (Halden, 2014) with implications for species higher in the food web. Chronic ecotoxicology studies suggest that invertebrates may be the most sensitive taxa to TCC (*Ceriodaphnia dubia* - survival and reproduction endpoints (US EPA, 2002)), with chronic PNECs varying from 146-190 ng/l (Tamura et al., 2013; TCC Consortium, 2002). For TCS, toxicology studies

suggest that algae are the most sensitive taxa, for which chronic PNECs range from 4.7-1550 ng/l (Capdevielle et al., 2008; von der Ohe et al., 2012). Calculation of PNEC values varied significantly between studies. The highest PNEC value (1550 ng/l) was estimated from a SSD, generated using effects data (chronic NOEC and EC10–25 values) for 14 species including aquatic plants, invertebrates and fish (Capdevielle et al., 2008). The 5<sup>th</sup> percentile of the SSD (50% confidence interval - HC5,50) was selected for calculation of the chronic PNEC.

The lowest PNEC value (4.7 ng/l) was estimated by taking the NOEC of 4.7 µg/l derived from a *Selenastrum capricornutum* growth inhibition test, and applying a 1000 assessment factor (von der Ohe et al., 2012).

TCS is ionisable with a *pKa* of 7.9 to 8.1. However, it will largely exist in its neutral form at pH 7 and in its ionised form at pH 8.5 and therefore is likely to be at least partially ionised within river water (Orvos et al., 2002). It is believed that molecules in an ionised state may be less likely to cross lipid membranes (Lipnick, 1995). This is reflected by experiments by Orvos et al. (2002), which suggest a significant reduction in toxicity as a result of increasing pH from 7 to 8.5.

Endocrine disruption has been noted for TCC (Chen et al., 2008) and TCS (Crofton et al., 2007; Veldhoen et al., 2006). There is also concern regarding the possibility of TCS (Levy, 2001; Yazdankhah et al., 2006; Veldhoen et al., 2006) and TCC provoking antibiotic drug resistance due to their antimicrobial nature (Halden, 2014).

#### 1.12.2. Natural estrogens

##### *Emissions and detection in the environment*

Natural estrogens, E1 and E2 are excreted from both the male and female population. Approximately half as much naturally occurring estrogen is excreted by males compared with menstruating females (Johnson et al., 2000). However, estrogens may also be excreted from other animals especially from farm animals (Liu et al., 2015). The presence of estrogens is widespread; E1 and E2 have been detected in the influent and effluent of a wide selection of STWs in China (Liu et al., 2015; Zhou et al., 2012a; Zhang et al., 2011; Ye et al., 2012), North America (Ternes et al., 1999; Lee and Peart, 1998; Snyder et al., 1999) the EU (Williams et al., 2012; Desbrow et al., 1998; Körner et al., 2000; Ternes et al., 1999) and Japan (Matsui et al., 2000; Komori et al., 2004).

#### *Chemical fate*

Laboratory experiments by Lin and Reinhard (2005) and Jürgens et al. (2002) observed significantly different biodegradation and photodegradation half-lives for E2 in river water under laboratory conditions. The photodegradation half-life of E2 within river water varied between 1.98 hours and 10 days (Jürgens et al., 2002; Lin and Reinhard, 2005). Laboratory biodegradation experiments reported by Lin and Reinhard (2005) resulted in 80% of E2 converted to E1 within 20 minutes. In contrast, Jürgens et al. (2002) noted a mean biodegradation half-life for E2 of approximately 28 hours.

E1 has been shown to degrade rapidly under controlled photolysis experiments which may be an effective degradation mechanism for E1; controlled experiments using solar simulators reported photolysis half-lives of 7.9 hours (under a simulated sunlight intensity of  $250 \text{ W m}^{-2}$ ) (Caupos et al., 2011) and 0.875 hours (under a simulated sunlight intensity of  $1000 \text{ W m}^{-2}$ ) (Chowdhury et al., 2010) in purified water. Biodegradation is also likely to be an effective mechanism, with a mean half-life of 23.4 hours observed in river water (Jürgens et al., 2002).

Henry's law constant of  $1.33 \times 10^{-12} \text{ Pa m}^3 \text{ mol}^{-1}$  and  $3.64 \times 10^{-11} \text{ Pa m}^3 \text{ mol}^{-1}$  were measured for E1 and E2 respectively (Mansell and Drewes, 2004), suggesting volatilisation is not significant for these two substances. Measurements for Koc ranges between 457 – 7244 (Khanal et al., 2006; Yu et al., 2004) and 212 – 13183  $\text{L kg}^{-1}$  (Holthaus et al., 2002; Yu et al., 2004) for E2 and E1 respectively, suggesting some affinity towards solids.

### *Effects*

Steroidal estrogens are significantly more potent than other endocrine disruptors (Desbrow et al., 1998; Sumpter and Jobling, 1995) and E1 and E2 are amongst the most potent (Liu et al., 2015). In China, male fish have been observed to have undergone some degree of feminisation, likely as a result of exposure to estrogenic compounds (Lu et al., 2010; Yan et al., 2012). In addition, there are suggestions that chronic exposure may cause greater effects in fish than other organisms (Tyler and Jobling, 2008). Therefore, an indication of potential exposure is important. For E2, a PNEC of 2 ng/l was suggested by Caldwell et al. (2012), who utilised consolidated NOEC data from ecotoxicology studies using a SSD methodology, generated from NOEC data for 9 fish species; the 5<sup>th</sup> percentile of the SSD (50% confidence interval - HC5,50) was selected for calculation of the chronic PNEC. In addition to E2, EE2 was also estimated by Caldwell et al. (2012), using the same methodology as E2. However, for E1, there was insufficient data to estimate a PNEC using the same methodology as E2 and therefore a different approach was required. It was noted by Caldwell et al. (2012) that the ratio of PNECs of E2 to EE2 was similar to the relative potency for vivo vitellogenin induction of E2 to EE2, as determined from literature gathered by the authors. It was thus suggested that the relative potency for vivo vitellogenin induction of E1 to E2 should equal that of the ratio of the PNECs of E1 to E2. This approach was used to derive a PNEC of 6 ng/l for E1.

### **1.13. Primary thesis aim**

The aim of this thesis was to develop a methodology to set up the GREAT-ER model in China. To be deemed successful, it was proposed that this methodology should provide reliable results whilst minimising the requirements for data and model complexity. This included a methodology to locate sewage treatment plants, to estimate the population served by sewage treatment plants and to estimate untreated discharge.

#### 1.13.1. Thesis objectives

1. To develop a complete methodology that allows one to reasonably setup a catchment model in China using the GREAT-ER model. This requires:
  - a. A methodology to locate STWs and further, to predict STW population served.
  - b. To account for untreated discharge
2. To be able to predict reliably the in-stream concentration of down-the-drain chemicals Triclosan, Triclocarban, Estrone and 17 $\beta$ -estradiol
3. To demonstrate the potential of GREAT-ER for both risk assessment and catchment management purposes, based upon the present and year 2020 scenario.

#### 1.14 Thesis structure

Chapter 2 is a methodological chapter which focuses on the first thesis objective and contains a description of a methodology to setup the GREAT-ER model in any catchment in China. Firstly, data required and the operation of the model is outlined. Further, different options are provided for watershed delineation and low-flow estimation. Finally, a flexible approach to address the problem of chemical emission estimation is described.

Chapter 3 describes the application of the methodology discussed in Chapter 2 to the East river catchment. Whilst Chapter 2 describes a more generic methodology, Chapter 3 describes specific measures taken to model the East river catchment. This includes low-flow estimation, parameterisation, chemical usage estimation, sampling methodology, estimation of chemical emissions and modelled scenarios.

Chapter 4 describes the outputs of the East river study. Sampling and simulation results are described and compared, in an attempt to estimate the accuracy of the model. Further, each element of the model is evaluated, in the context of the simulation results. Finally, simulation results for a number of risk assessment and catchment management scenarios are described.

Chapter 5 is a discussion regarding the potential for the GREAT-ER model to be used within China. Limitations are described, with possible strategies to overcome these limitations in future studies. Future studies are proposed for use of the GREAT-ER model, or others when appropriate, with a focus on catchments that are both interesting and important to study. Finally, a modelling focused approach is discussed to address the challenge of water pollution in China.

Chapter 6 concludes the thesis, including a summary of the findings of this thesis and suggested future research



## Chapter 2 – The GREAT-ER model in China

This section outlines the proposed methodology used to setup the GREAT-ER model in any catchment within China. The model was designed for catchments within Europe and the challenges presented by such environments. Utilising the model in China provides unique challenges that must be overcome. Each element will be discussed in turn, with mention of possible data sources for each. An overview of the GREAT-ER model is shown in Figure 3.

### 2.1. Data to request

When setting up the GREAT-ER model for a new catchment, it is useful to assess the overall data requirements for the model and to make requests for data from the appropriate authorities. Data may take a significant amount of time to acquire, and therefore it is suggested that data should be requested as soon as possible. However, the methodology described in this section will provide different approaches depending upon the data available to the user.

Data requirements are listed below with comments about general availability and possible data sources. The data is listed in the order of importance, based upon the experience gained during this research project. Items of higher importance should be prioritised, as they often take longer to obtain. If the researcher is not native to the study area, locating a 3<sup>rd</sup> party contact may significantly increase the chances of receiving high quality data in a timely manner.

- Flow data – This is the highest priority for data request. Daily or sub-daily data (in units of m<sup>3</sup>/s) is highly preferable, however often only monthly or annual data are available. Flow data may be difficult to obtain from authorities, especially if the user is not a Chinese national. The official route is to request data from the Ministry of

Water Resources. However, the most plausible option available is to request this data from a 3<sup>rd</sup> party. This may be available electronically, or it may be only available in hard copy. If the latter, this must be carefully copied into a spreadsheet.

Alternatively, flow data is available from the Global Runoff Data Centre (<http://www.bafg.de/GRDC>) which provides hydrological data for stations around the globe. However, much of the data is relatively old and only a limited selection of gauging stations is available. It may still be possible to use old hydrological data, however if the catchment has changed significantly as a result of anthropogenic activity (e.g. deforestation or construction of reservoirs), the old data may not be representative of current hydrological conditions (Rees, 2009).

- Artificial influences upon hydrology – Data that describes the artificial influences upon flow may be critical to calculating flow throughout the catchment. This includes elements that may reduce flow such as abstraction, those that may increase flow such as STW discharges or elements with more complex influences such as reservoirs (Gustard and Young, 2009). It is particularly important to obtain data for large reservoirs, ideally at a similar temporal resolution to the available flow data. In addition, data on the level of abstraction and return flows in the area is useful, with actual locations of abstraction points being especially useful yet challenging to obtain.
- STW data – The location of all STWs and other relevant emission points within the area is required. A later section describes a procedure for when this not available, however it is best to request this early. The required data includes: geographic coordinates, population served and treatment type. It is also useful to obtain mean effluent discharge, which may be useful to further describe artificial influences to flow.

- Riverlines – The river network is required in a vector (polyline) format. Global and continental datasets are available, although these are often poor quality or at an inappropriate scale. Therefore locally derived datasets are more appropriate, although difficult to obtain.
- Digital elevation model (DEM) – A DEM is a representation of the elevation surface, and may be used for applications such as defining the river catchment area and the river topology. A DEM is readily available from global datasets (e.g. the Shuttle Radar Topography (SRTM) dataset (Farr et al., 2007)). However if locally derived, high resolution datasets are available, they should be obtained when possible. This is discussed in more detail in section 2.4.

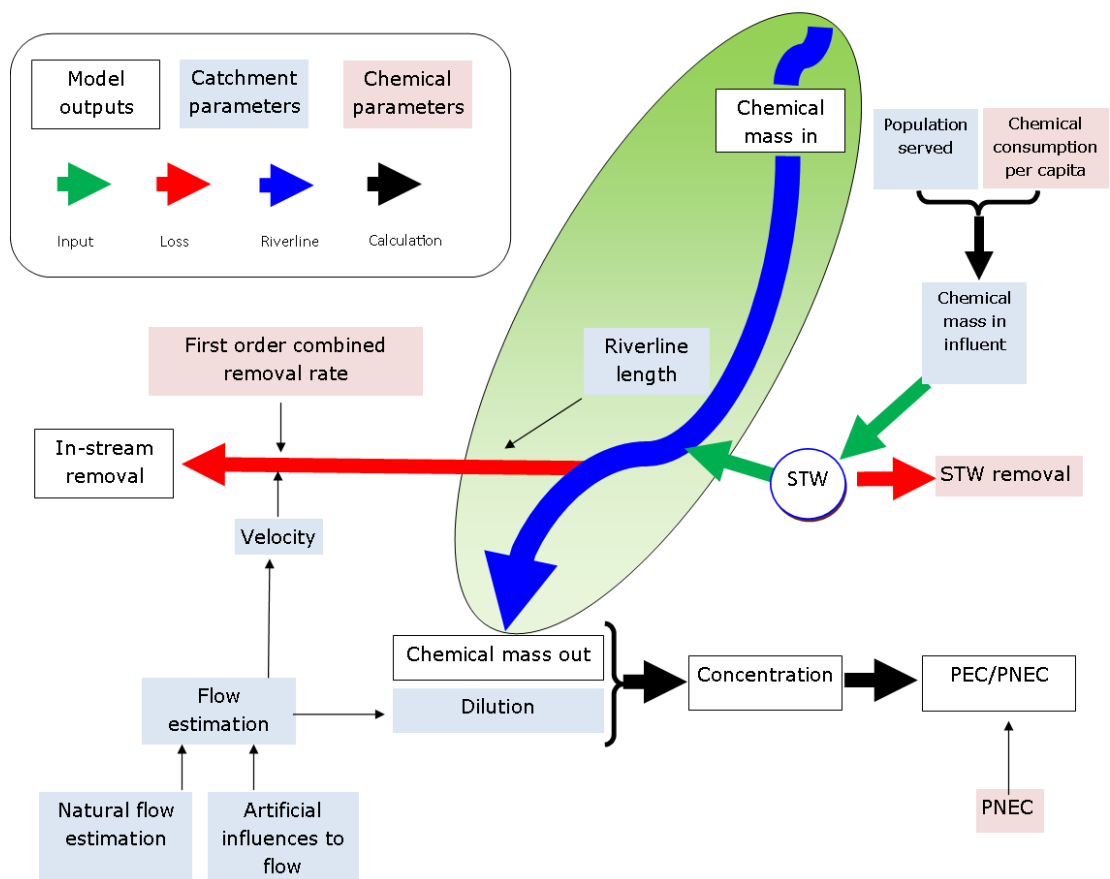


Figure 3 - Schematic overview of GREAT-ER: assumes only basic in-stream removal and no untreated wastewater sources.

## 2.2. Physio-chemical and environmental properties

The model allows the user to simulate in-stream removal at three levels of complexity: 1) a basic combined first-order rate, 2) basic removal by biodegradation, volatilization and sedimentation, 3) advanced removal by up to five different processes. All three levels of complexity are based upon first-order kinetics.

Basic removal is calculated based upon combined removal rate and travel time. This is described by Equation 8, whilst travel time is described by Equation 9 for lakes and Equation 10 for river stretches (Boeije, 1999):

$$R_{\text{end}(i)} = R_{\text{start}(i)} * -e^{-\text{HRT}*k} \quad (8)$$

For Lakes:

$$\text{HRT} = \frac{v}{Q * 3600} \quad (9)$$

For rivers:

$$\text{HRT} = \frac{L}{v * 3600} \quad (10)$$

where:

$R_{\text{end}(i)}$  – chemical mass at the downstream end of stretch  $i$  (kg)

$R_{\text{start}(i)}$  – chemical mass at the upstream end of stretch  $i$  (kg)

HRT – travel time (h)

$k$  – combined in-stream removal rate ( $\text{h}^{-1}$ )

$v$  – river velocity (m/s)

$L$  – river stretch length (m)

$Q$  – river discharge ( $\text{m}^3/\text{s}$ ).

In addition to removal in stream, the removal rate in primary, trickling filter and activated sludge treatment plants is required. This can be provided as a single value, a normal, log-normal or uniform distribution. If the removal rate for individual sewage treatment plants is known it can be applied to each, although only as a single value. Finally the per capita emission rate is required for each chemical. This is the mass of chemical used and released to the environment each year on a per capita basis. The calculation of emissions is described later in this chapter.

The two advanced removal modes are explained below including the data requirements for each.

#### 2.2.1. Basic removal by biodegradation, volatilization and sedimentation

First-order removal rates are required for biodegradation, volatilization and sedimentation; where sedimentation represents the net suspended sediment settling rate. There is also an element to estimate the fraction chemical partitioned to suspended solids, described below. The fraction of organic carbon in suspended solids within the catchment is defined, along with the concentration of suspended solids and the correlation between flow and suspended solids concentration. The concentration of suspended solids may be defined as a single value, or a normal/log-normal/uniform distribution. The fraction sorbed to suspended solids may then be estimated; the fraction dissolved ( $F_d$ ) and fraction sorbed ( $F_s$ ) are estimated by Equation 11, 12, and 13 (Wagner and Koormann, 2011):

$$F_d = \frac{1}{1 + 10^{-6} * K_d * SSC} \quad (11)$$

$$K_d = K_{oc} * F_{oc} \quad (12)$$

$$F_s = 1 - F_d \quad (13)$$

where:

$K_d$  - solids/liquids partitioning coefficient in the river (L/kg)

SSC - suspended solids concentration (mg/L)

$K_{oc}$  - organic carbon/water partition coefficient (L/kg)

$F_{oc}$  - fraction organic carbon in suspended solids (kg/kg)

In-stream removal is calculated using Equation 8, and the in-stream removal rate,  $k$  ( $h^{-1}$ ), is calculated using Equation 14:

$$k = k_{deg} + F_s k_{sed} + F_d k_{vol} \quad (14)$$

where:

$k_{deg}$  – chemical degradation rate ( $h^{-1}$ )

$k_{sed}$  – net suspended sediment settling rate ( $h^{-1}$ )

$k_{vol}$  – chemical volatilisation rate ( $h^{-1}$ ).

### 2.2.2. Extended five process removal

The five processes considered by the model are: hydrolysis, photodegradation, volatilization, sedimentation and biodegradation. If this mode is selected, the user may then select which processes they wish to include. The number of parameters required is quite extensive and is summarised in Table 3. The approach used by the GREAT-ER model for individual processes are described here (Boeije, 1999). Firstly, the model corrects for solubility as described by Equation 15 and 16:

$$C_{0(i)} < S_w * MM \Rightarrow C_{start(i)} = C_{0(i)} \quad (15)$$

$$C_{0(i)} > S_w * MM \Rightarrow C_{start(i)} = S_w * MM \quad (16)$$

where:

$C_{0(i)}$  – estimated concentration at the start of the stretch i (g/m<sup>3</sup>)

$C_{start(i)}$  – actual concentration at the start of stretch i (g/m<sup>3</sup>)

$S_w$  – chemical water solubility (mol/m<sup>3</sup>)

$MM$  – chemical molecular mass (g/mol).

The concentration at the end of stretch i,  $C_{end(i)}$ , is then estimated using Equation 17 below:

$$C_{end(i)} = C_{start(i)} * e^{-k*HRT} \quad (17)$$

the in-stream removal rate (k) is calculated by using Equation 14, but  $k_{deg}$  is estimated by Equation 18 below:

$$k_{deg} = k_{hydrolysis} + k_{photolysis} + k_{biodeg} \quad (18)$$

where:

$k_{hydrolysis}$  – 1<sup>st</sup> order chemical hydrolysis rate (h<sup>-1</sup>)

$k_{photolysis}$  – 1<sup>st</sup> order chemical photolysis rate (h<sup>-1</sup>)

$k_{biodeg}$  – 1<sup>st</sup> order chemical biodegradation rate (h<sup>-1</sup>)

HRT – hydraulic residence time (h).

The representation of hydrolysis is taken from the SMPTOX4 model (US EPA, 1995), mode 3.

The model differentiates between neutral, acid and basic hydrolysis as described by Equation 19 below:

$$k_{\text{hydrolysis}} = K_b * 10^{\text{pH}-14} + K_n + K_a * 10^{-\text{pH}} \quad (19)$$

where:

$K_a$  – acid hydrolysis rate ( $\text{h}^{-1}$ )

$K_b$  – base hydrolysis rate ( $\text{h}^{-1}$ )

$K_n$  – neutral hydrolysis rate ( $\text{h}^{-1}$ )

pH – acidity- potential of hydrogen.

The model for photolysis was taken from SMPTOX4 mode 3 (US EPA, 1995). The model takes into account light extinction in water, based upon water depth and a 1<sup>st</sup> order extinction rate. This is described by Equation 20:

$$k_{\text{photolysis}} = k_{\text{ph},0} * \frac{1 - e^{-k_z * d}}{k_z * d} \quad (20)$$

where:

$k_{\text{ph},0}$  - near-surface photolysis rate ( $\text{h}^{-1}$ )

$k_z$  - light extinction coefficient ( $\text{m}^{-1}$ )

$d$  – river depth (m).

For biodegradation, the model requires several specific parameters that describe how the properties of the river modify the biodegradation rate (Boeijs, 1999). The model's



representation of biodegradation considers degradation rates to differ for the chemical fraction within the sorbed and dissolved phase, using the approach used by the ROUT model (Cowan et al., 1993). Chemical and biomass concentrations are assumed to degrade by first-order kinetics (Boeije, 1999). A pseudo-first-order rate is derived by multiplying the biomass level by the double first-order degradation rate, which represents the combined biological and non-biological degradation in the dissolved phase (Boeije, 1999). The model's representation of biodegradation is described by Equations 21, 22 and 23:

$$k_{\text{biodeg}} = k_{\text{stdbiodeg}} * B * (F_d + F_s * \alpha_s) * \alpha_{\text{DO}} * \alpha_{\text{temp}} \quad (21)$$

$$\alpha_{\text{DO}} = \frac{\text{DO}}{k_{\text{DO}} + \text{DO}} + \frac{k_{\text{DO}}}{k_{\text{DO}} + \text{DO}} * \alpha_{\text{anaerobic}} \quad (22)$$

$$\alpha_{\text{temp}} = Q_{10} \frac{t_{\text{water}} - 20}{10} \quad (23)$$

where:

$k_{\text{stdbiodeg}}$  – double 1<sup>st</sup> order biodegradation rate under standard conditions ( $\text{L mg}^{-1} \text{h}^{-1}$ )

$B$  – lumped river biomass level, suspended and in biofilms ( $\text{mg/l}$ )

$\alpha_{\text{DO}}$  – biodegradation rate correction for dissolved oxygen

$\alpha_{\text{temp}}$  – biodegradation rate correction for temperature

$\alpha_{\text{anaerobic}}$  – rate correction for anaerobic biodegradation

$k_{\text{DO}}$  – oxygen saturation constant for aerobic biodegradation ( $\text{mg/l}$ )

$\text{DO}$  – dissolved oxygen concentration ( $\text{mg/l}$ )

$Q_{10}$  – biodegradation Q10 factor (rate change factor per 10°C)

$t_{\text{water}}$  – water temperature (°C).

Sedimentation describes the settling of chemical sorbed to suspended sediment. This is described by Equation 24 and 25 (Boeije, 1999):

$$k_{\text{sed}} = \frac{v_{\text{sed}}}{d} \quad (24)$$

$$v_{\text{sed}} = \frac{(v_{\text{sedgrowth}} * 3.171 * 10^{-11}) * (10^6 * \rho_{\text{SS}}) * (1 - \epsilon_{\text{sed}})}{\text{SSC}} \quad (25)$$

where:

$k_{\text{sed}}$  – 1<sup>st</sup> order net suspended sediment settling rate ( $\text{h}^{-1}$ )

$v_{\text{sed}}$  – suspended sediment settling velocity (m/s)

$v_{\text{sedgrowth}}$  – sediment growth velocity (mm/year)

$\rho_{\text{SS}}$  – sediment particle density ( $\text{kg/m}^3$ )

SSC - suspended solids concentration (mg/L)

$\epsilon_{\text{sed}}$  – sediment porosity.

Finally, volatilization is modelled based on the two film theory (Whitman, 1923). Complete mixing of both the water and atmospheric compartments is assumed, and that the boundary layers of the gas-liquid interface are laminar. The exchange rate between these two compartments is calculated using Henry's law constant, the conductance of the gaseous and

liquid films, and water depth (Boeije, 1999). This approach is described by Equation 26 and 27:

$$k_{vol} = \frac{1}{d} * \frac{1}{\left(\frac{1}{k_L} + \frac{1}{K_H * k_g}\right)} \quad (26)$$

$$K_H = \frac{H}{R * (t_{air} + 273)} \quad (27)$$

where:

$k_{vol}$  – 1<sup>st</sup> order chemical volatilisation rate ( $h^{-1}$ )

$k_L$  – conductance of liquid film (m/s)

$k_g$  – conductance of gaseous film (m/s)

$K_H$  – air-water exchange coefficient (dimensionless Henry coefficient)

$H$  – Henry's law constant ( $Pa \text{ m}^3 \text{ mol}^{-1}$ )

$t_{air}$  – air temperature ( $^{\circ}C$ ).

Conductance is calculated using the approach of Southworth (1979) for rivers, as described by Equation 28 - 31:

$$k_g = 3.16 * 10^{-3} * (v + v_{fr}) * \sqrt{\frac{18}{MM}} \quad (28)$$

$$k_l = 65.31 * 10^{-6} * F * \frac{v^{0.969}}{d^{0.673}} * \sqrt{\frac{32}{MM}} \quad (29)$$

$$F = \begin{cases} v_{fr} < 1.9 \text{ m/s} : F = 1 \\ 5 > v_{fr} \geq 1.9 \text{ m/s} : F = e^{0.526 \cdot (v_{wind} - 1.9)} \end{cases} \quad (30)$$

$$v_{fr} = v_{wind} * \left( \frac{\log \frac{0.1}{z_0}}{\log \frac{10}{z_0}} \right) \quad (31)$$

where:

$v_{fr}$  – friction velocity - wind speed at 10 cm height (m/s)

F – correction factor for high wind speeds

$v_{wind}$  – wind speed at 10m height (m/s)

$z_0$  – roughness height (m) – describes the height of which wind is theoretically zero; this is assumed to be  $10^{-3}$  above rivers.

Conductance is estimated for lakes using the approach of Mackay and Yeun (1983) for lakes, as described in Equation 32 - 36:

$$k_l = 10^{-6} + \alpha * v_{shear}^\beta \quad (32)$$

$$* \frac{\beta}{\sqrt{SC_l}} \begin{cases} v_{shear} < 0.3 \text{ m/s} \Rightarrow \alpha = 14.4 * 10^{-3}, \beta = 2.2 \\ 0.3 \text{ m/s} \leq v_{shear} \leq 1 \text{ m/s} \Rightarrow \alpha = 3.4 * 10^{-3}, \beta = 1 \end{cases}$$

$$v_{shear} = 0.0359 * v_{wind}^{0.93} \quad (33)$$

$$k_g = 10^{-3} + 46.2 * 10^{-3} * v_{shear} * \frac{1}{\sqrt[3]{SC_g^2}} \quad (34)$$

$$SC_g = \frac{\eta_g}{D_g} = 1.4 * \frac{10^{-6}}{2.22 * \sqrt{\frac{18}{MM}}} \quad (35)$$

$$SC_l = \frac{\eta_l}{D_l} = 1 * \frac{10^{-6}}{172.8 * 10^{-6} * \sqrt{\frac{32}{MM}}} \quad (36)$$

where:

$v_{\text{shear}}$  – shear wind velocity (m/s)

$SC_g$  – Schmidt number in air

$SC_l$  – Schmidt number in liquid

$\eta_g$  - kinematic viscosity coefficient for air ( $\text{m}^2/\text{s}$ )

$\eta_l$  - kinematic viscosity coefficient for water ( $\text{m}^2/\text{s}$ )

$D_g$  - diffusion coefficient in air ( $\text{m}^2/\text{s}$ )

$D_l$  - diffusion coefficient in water ( $\text{m}^2/\text{s}$ )

$\alpha$  and  $\beta$  are constants.

### 2.2.3. Sediment exposure module

The GREAT-ER sediment extension allows the user to increase the complexity of the sediment component within the model. Without the extension, the concentration in the dissolved and sorbed phase may be estimated using the two more advanced removal modes, modes 2 and 3, however this information is used solely for the calculation of removal, and is not made available to the user. The primary feature of the sediment module is, following simulation, to allow the user to display estimates for the concentration of the chemical of interest within the sorbed and dissolved fractions, but also provides estimates for the concentration within the sediment phase. The user may also specify the concentration of suspended solids and diffuse chemical emissions for each stretch.

### 2.3. Simulation procedure

The procedure to start a simulation is simple. Firstly, select a catchment and the chemical of interest. Next, specify the environmental and physio-chemical properties, removal mode and sediment exposure settings, which are described above. Finally, provide the number of iterations to be performed by the Monte Carlo simulation.

Hydrolysis	Photodegradation	Volatilization	Sedimentation	Biodegradation
Correlation coefficient between suspended solids and flow	Correlation coefficient between suspended solids and flow	Air temperature (°C)	Correlation coefficient between suspended solids and flow	Temperature (River) (°C)
Molar mass (g/mol)	Molar mass (g/mol)	Wind speed (River) (m/s)	Molar mass (g/mol)	Correlation coefficient between temperature and flow
Koc (L/kg)	Koc (L/kg)	Correlation coefficient between temperature and flow	Koc (L/kg)	Correlation coefficient between suspended solids and flow
Water solubility (mol/m <sup>3</sup> )	Water solubility (mol/m <sup>3</sup> )	Correlation coefficient between wind speed and flow	Water solubility (mol/m <sup>3</sup> )	Correlation coefficient between dissolved oxygen and flow
Solids/liquid partitioning coefficient in river (L/kg)	Solids/liquid partitioning coefficient in river (L/kg)	Correlation coefficient between suspended solids and flow	Solids/liquid partitioning coefficient in river (L/kg)	Molar mass (g/mol)
Default hydrolysis rate - acid (h <sup>-1</sup> )	Photolysis rate - near surface (h <sup>-1</sup> )	Molar mass (g/mol)		Koc (L/kg)
Default hydrolysis rate - base (h <sup>-1</sup> )		Koc (L/kg)		Water solubility (mol/m <sup>3</sup> )
Default hydrolysis rate - neutral (h <sup>-1</sup> )		Vapour pressure (Pa)		Solids/liquid partitioning coefficient in river (L/kg)
		Water solubility (mol/m <sup>3</sup> )		Standard aerobic biodegradation rate (double

				first-order) (L mg <sup>-1</sup> h <sup>-1</sup> )
		pKa - chemical acid / base dissociation constant		Affinity constant for transition from aerobic to anaerobic processes
		Solids/liquid partitioning coefficient in river (L/kg)		Temperature correction for biodegradation
		Henry's law coefficient (Pa m <sup>3</sup> mol <sup>-1</sup> )		Reduction of biodegradation rate under anaerobic conditions
				Reduction of biodegradation rate under adsorbed conditions
				Increase or reduction of biodegradation rate under river conditions

Table 3 - Physio-chemical properties required for advanced removal mode.

## 2.4. Watershed delineation

### 2.4.1. DEM availability

A DEM) provides the basis of the river network, subcatchments and catchment area. These elements are subsequently required to calculate flow and to provide an estimation of chemical emission. Consequently, a poor representation of the underlying topography may impact upon the accuracy of the model output. Selection of a suitable DEM and the methodology used to process the DEM are important.

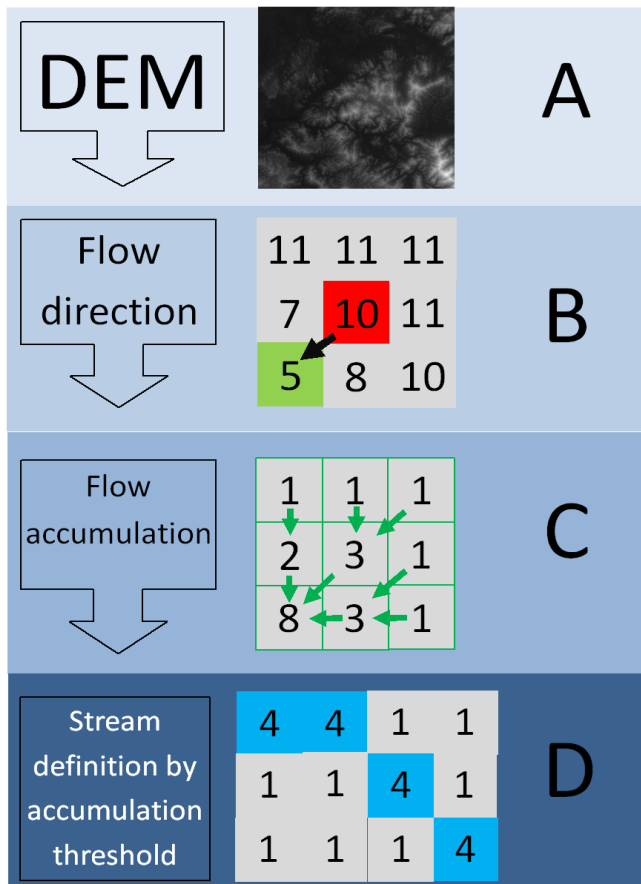


Figure 4 - Stream delineation procedure. A DEM is required (A) however before use, topographic lows, known as pits within the DEM may need to be corrected. These are often filled to the level of the lowest surrounding cell. To determine flow direction, flow is directed from high to low elevation based upon the lowest value within 8 surrounding cells (B). Further, the number of accumulated cells can be calculated, which is the number of cells that flow into the target cell (C). Finally once the number of accumulated cell reaches a threshold, it can be identified as a stream (D).

A DEM is most commonly obtained from satellite imagery, however for more precise applications aerial or ground surveys may be used, albeit at significant expense.

Satellite-derived DEMs are available with a global coverage. Resolutions of global datasets are often relatively low, however the public release of the SRTM 1 arc-second DEM (~30m at the equator) in 2015 provides a reasonable horizontal resolution for modelling applications (Buis and Cole, 2014). Superior alternative datasets should be obtained if possible, however the availability of elevation data in China is limited. Within the selection of global datasets,



SRTM is a favourable choice, although the SRTM dataset size and processing time may become unacceptably high for very large catchments.

#### 2.4.2. The HydroSHEDS DEM

For medium to large-scale applications, the HydroSHEDS dataset may be suitable (<http://hydrosheds.cr.usgs.gov/>), which is based upon the SRTM dataset. HydroSHEDS offers hydrologically optimised datasets at resolutions between 3 arc-seconds (~90m at the equator) to 5 minutes (~10km at the equator). The methodology used to derive this dataset is described here. The dataset is based upon the SRTM 3-arc second (~90m at the equator) and the Digital Terrain Elevation Data (DTED) 3 arc-second DEMs (Lehner et al., 2006). The DTED dataset is derived from SRTM data, but generated using the data standards required by the National Geospatial-intelligence Agency of the US Department of Defence (NASA, 2003). DTED was upscaled from the 1 arc-second SRTM dataset by selecting the value of the centre pixel within a 3x3 kernel. The 3-arc second SRTM dataset was upscaled from the 1 arc-second SRTM dataset to 3 arc-seconds by taking the mean value of a 3x3 kernel. As a result of upscaling the DTED dataset, on occasion, elevation values on river stretches were assigned an elevation greater than the surrounding floodplain. This has significant implications for hydrological applications, as water may be predicted to spill from a river channel into the floodplain (Lehner et al., 2006). However, the DTED dataset represents shorelines and open-water better than the SRTM 3 arc-second dataset due to corrections made to the DTED dataset; for example, lakes of  $\geq 600\text{m}$  length were flattened to a constant height, and the ocean was set to a constant elevation of 0m (NASA, 2003; Lehner et al., 2006). Therefore, the two datasets were combined by taking the minimum value found in either dataset to provide an initial surface (Lehner et al., 2006). A number of corrections were made to this surface in

order to reduce the number of errors within the surface and to improve the performance for hydrological applications. Firstly, the original SRTM data included large areas of “nodata” (voids). These voids were filled using a combination of two void-filled datasets. The first dataset was that of CIAT (2004), which was generated using the interpolation methodology of TOPOGRID (Hutchinson, 1989; Hutchinson, 1988) available in the GIS, Arc/Info and ArcGIS. This approach uses contours at an interval of 10m, derived from the elevation surface, to interpolate. This approach produces a smooth elevation surface that has been demonstrated to represent macro scale topography well, in comparison to cartographic data (Jarvis et al., 2004). The second dataset was produced using an algorithm designed especially for HydroSHEDS, for the purpose of better representing low-level and flat water surfaces within voids (Lehner et al., 2006). This was achieved through an iterative process. The first step fills the outermost pixel-rim of a no-data void using a combination of a 3x3 minimum and a 5x5 mean filter (the minimum filter dominates the mean filter by a factor of 3:1). Then, the next pixel-rim is filled until the entire no-data void is processed. This is then repeated until the entire void is filled. Finally, the void area is smoothed using a 9x9 filter, selecting the mean value (Lehner et al., 2006). The two datasets were combined by selecting the minimum value of either dataset. However, if the HydroSHEDS algorithm derived cell value was >30m lower than the CIAT algorithm, the CIAT value was used, subtracted by 30m (Lehner et al., 2006). In addition, in cases where mountains were “lost” following interpolation, data from GTOPO30, a global 30 arc-seconds DEM (Gesch et al., 1999), was inserted.

Sinks, defined as depressions within the elevation surface, present a problem for hydrological applications because they interrupt runoff as it moves from high to low elevations (e.g. Figure 4B). These sinks may be naturally occurring but many may be a result of anomalies during the production of the DEM, or as a result of the generalisation of the surface (Lyon, 2003; Mark, 1988). HydroSHEDS used a manual approach to identify sinks that may be natural, and to reject those that were not (Jenson and Domingue, 1988). Sinks that

were deeper than 10m and larger than 10km<sup>2</sup> were marked as being potential natural sinks, all others were rejected and filled to the elevation of its lowest neighbour (Lehner et al., 2006). All potential sinks were examined manually along with auxiliary data such as paper based maps and atlases.

Improvements were made to ocean, lake and river boundaries. The SRTM Water Body Data (SWBD) (NASA, 2003), a dataset defining ocean, lake and river boundaries from the original SRTM 1 arc-second dataset, was used to assign all cells in the ocean to “no data” (Lehner et al., 2006). In addition, within a 0.02 decimal degree wide buffer along the coastline, every random third cell was reduced by 5m. This action was taken because in areas along the coastline with heavy vegetation growth, radar derived DEMs may erroneously detect the elevation to be that of the vegetation height rather than the surface, creating a barrier to flow along the coastline (Lehner et al., 2006).

To conclude, the HydroSHEDS offers an elevation surface which is readily available for hydrological applications, with little or no modifications. However, for applications that may require a DEM with a smaller cell size, other datasets would have to be considered.

#### 2.4.3. Correcting DEMs to enforce flow direction in flat areas

One limitation of the SRTM dataset is the vertical resolution of 1 metre. The vertical resolution defines the precision of elevation data. This has implications for flat areas, such as flood plains. A vital application of a DEM is to estimate the direction of flow. With the flow path known, it is also possible to determine the catchment boundary for any cell in the catchment and to determine the number of cells that contribute to this cell; the latter is determined using a flow accumulation algorithm. The number of contributing cells can then

be used to determine catchment area, and when a threshold is provided, the location of a stream may be estimated. This is shown in Figure 4D. The most commonly used algorithm to calculate flow direction is the D8 method (O'Callaghan and Mark, 1984; Jenson and Domingue, 1988) (see Figure 4B), which estimates flow direction based upon the lowest elevation value from 8 neighbouring cells. However, within a flat region, due to a low vertical resolution, there may be no unique lowest neighbour and thus the assignment of flow direction would be set arbitrarily (Garbrecht and Martz, 1997). As a result, the flow direction may be assigned erroneously. There are two procedures that can be used to mitigate this problem. An alternative flow direction algorithm can be used such as that of Garbrecht and Martz (1997), which assigns direction in flat areas by modifying the surface, based upon the area surrounding the flat area, in order to force flow away from higher elevation and towards lower elevation. The network generated may be significantly more realistic than the output from the default D8 algorithm, as shown by the example in Figure 5. As shown, the default algorithm generates erroneous straight riverlines, which are located in flat areas. This is resolved by using the algorithm of Garbrecht and Martz (1997).

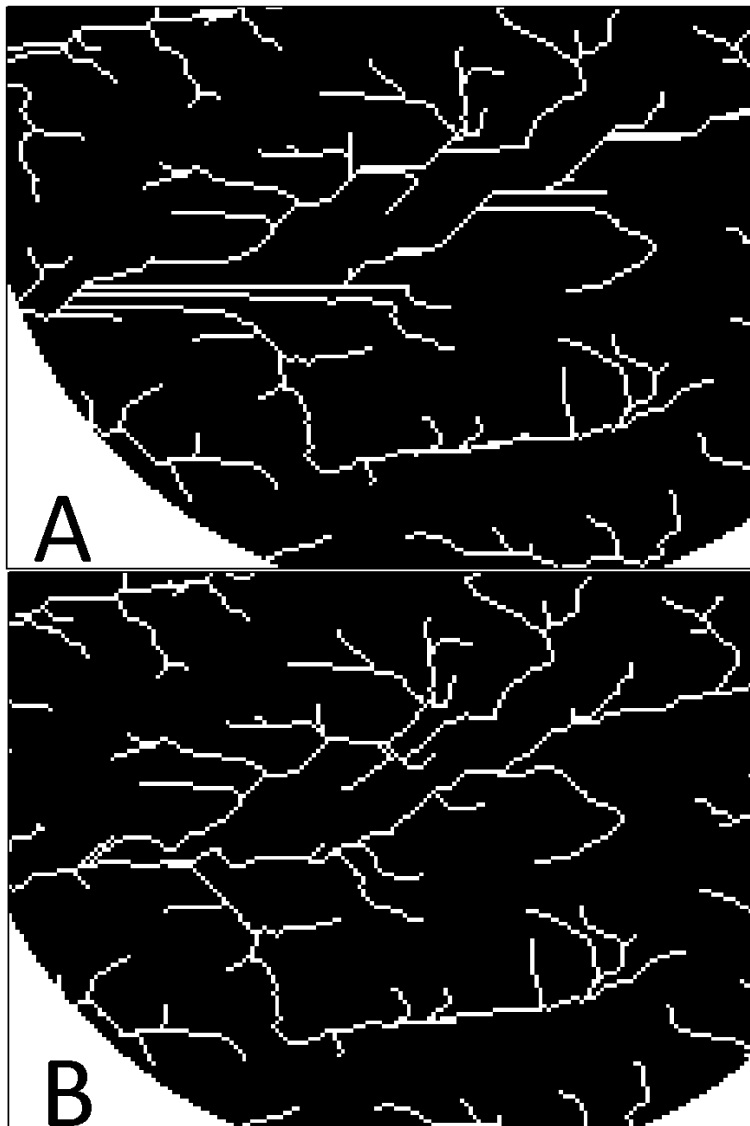


Figure 5 - (A) River network delineation using the D8 algorithm of Jenson and Domingue (1988) and (B) delineation using the flow direction algorithm developed by Garbrecht and Martz (1997).

The second procedure involves a process called “burning in”, such as the AGREE method developed by Hellweger (1997), which is described here. A polyline is required which represents the true position of the river. The algorithm drops elevation within a buffer incrementally to create a smooth path to the vector line from the buffer boundary. Next, the algorithm excavates a deep, sharp trench for cells intersecting the vector line. This algorithm

modifies the DEM in a way that forces the model to propagate runoff towards the river channel and to contain flow within. The buffer smoothing attempts to avoid the occurrence of “parallel streams”, which are usually erroneous low points in the elevation grid. Without correction, riverlines parallel to those produced could be generated (Hellweger, 1997). Calibration may be required to determine the optimum buffer width and smooth/sharp drop distance. Caution is required as there is the potential for boundary (Maidment and Djokic, 2000), stream line (Baker et al., 2006) and other undesirable terrain errors as a result of the riverline buffer.

This process requires accurate polyline data at the desired resolution and detail. This may be already available, either from local or global datasets. However, the accuracy and resolution of the riverline data must be inspected to determine whether it is suitable for use. Global datasets often lack detail and are created at a large-scale, therefore lacking accuracy. Therefore it may be necessary to manually digitise the river channels from satellite imagery. Google Earth is a useful application for this task, which provides high resolution satellite imagery from multiple time points. This is a time consuming task and therefore should only be completed if necessary. Critically, this depends upon the scale of the modelling study, including the extent and the raster resolution.

## **2.5. Low-flow estimation**

The GREAT-ER model represents flow as a log-normal distribution defined by the mean and the 95% exceedance flow (Q95). A UK study investigating the performance of GREAT-ER and the sensitivity of its input parameters concluded that the variability of flow was significant in explaining the difference between modelled and observed concentrations. In contrast, they noted that the form of probability distribution of treatment efficiency and emissions had

little effect upon chemical exposure (Price et al., 2009). An estimate of flow is used to determine dilution and the transportation of the chemical of interest. Transportation is assumed to occur at the same rate of velocity, which is estimated from river discharge using the approach of Round et al. (1998), described in Equation 37:

$$v = 10^{-0.583} Q_{\text{mean}}^{0.283} \left( \frac{Q}{Q_{\text{mean}}} \right)^{0.495} \quad (37)$$

where:

$v$  – river velocity (m/s)

$Q$  – river discharge (m<sup>3</sup>/s)

$Q_{\text{mean}}$  – mean river discharge (m<sup>3</sup>/s).

Flow estimation is important and every effort should be taken towards providing a realistic and reliable estimate of flow. Firstly, an overview of low-flow hydrology is provided, with a discussion regarding the various natural elements and processes that dominate flows in the absence of rainfall. There are three main approaches for calculating low-flow statistics: 1) regional regression, 2) regional mapping and 3) rainfall-runoff modelling. These are discussed within this section, followed by examples of flow estimation approaches used for previous applications of the GREAT-ER model.

### 2.5.1. Low-flow hydrology

After a storm event, water reaches a stream by both fast and slow processes. Fast processes contribute to storm flow, whereas slow processes primarily contribute to baseflow (Holden, 2012). Baseflow may be defined as the flow that occurs in the absence of precipitation, instead reliant upon storage elements throughout the catchment. The potential and actual storage of these elements is important, as is residence time, which will vary significantly

between different elements (Table 4). Water may be stored on the surface (e.g. in lakes), in the soil and within groundwater; the fraction that reaches each storage element may vary significantly in space and time as a result of surface and sub-surface properties (e.g. Table 5) and conditions (e.g. soil saturation).

Water source	Residence time
<b>Atmospheric waters</b>	10 days
<b>Terrestrial waters</b>	
Rivers	2 weeks
Lakes	10 years
Soil moisture	2-50 weeks
Biological waters	A few weeks
Groundwaters	Up to 10,000 years
Polar ice	15,000 years
<b>Oceanic waters</b>	3600 years

Table 4 - Average residence time of water. From Holden (2012).

### *Precipitation and the East Asian Monsoon*

The input to any catchment is through precipitation, with the exception of artificial water transfers. For mid-latitudes, at the catchment scale, the dominant factor influencing precipitation is elevation, with greater precipitation at higher altitudes (Holden, 2012). At larger scales precipitation is controlled by global and continental moisture circulation.

Precipitation patterns across China are heavily influenced by the East Asian Monsoon (Wang, 2006; Sui et al., 2013). The summer is usually characterised as being the wettest period of the year, during which the majority of the annual rainfall occurs, whereas, the winter is



characterised as being a significantly drier and cooler period (Sui et al., 2013; Chang, 2004; Wang, 2006).

The summer monsoon is primarily a result of the contrast in air pressure above the tropical oceans (high pressure) and the Chinese land mass (low pressure) which results in a change in the prevailing wind direction, away from the ocean and towards the land. As the air mass rises and crosses the land, it cools, resulting in precipitation (Rohli and Vega, 2011), which decreases from South-East to North-East, as water is lost by condensation (Figure 6). In the winter, this pattern is reversed as the land loses heat more rapidly than the ocean, forming a zone of a high pressure above the land mass, and a zone of relatively low pressure above the ocean (Rohli and Vega, 2011). As a result, the wind direction reverses and is directed away from the land and towards the ocean. From October to January a cold air mass expands south from the Northern regions of Siberia and Western Mongolia, as shown in Figure 8 (Chang, 2004). This lowers temperatures (Figure 7) and raises air pressure, which leads to strong north-easterlies extending to the South China Sea. This air mass is relatively dry (in comparison to an air mass from the oceans to the South) and results in significantly reduced precipitation during the winter period (Chang, 2004).

The Tibetan Plateau in North West China (Figure 6) also has a significant influence over the monsoon (Ge et al., 2017). The Plateau is an extensive, high altitude landform (mean altitude of 4000m). The Plateau is a significant atmospheric heat source in the summer, especially in May and June (Chang, 2004). Temperature rises in the Plateau region at a greater rate in comparison to the surrounding atmosphere, forming an area of low pressure over the Plateau (Ding, 2013; Keshavamurthy and Rao, 1992); this contrast is greater than the contrast between the land mass and the ocean. It has been suggested by Wu and Zhang (1998) that the Plateau acts as an “air pump” that sucks in air towards it, which may play an important part in the onset of the East Asian Monsoon. Observations suggest that the

formation of an enhanced atmospheric heat source over the Plateau coincides with reduced precipitation over Southeast China and enhanced precipitation in the Yangtze and Huaihe river basins (Wang et al., 2014; Ping and Longxun, 2001). Many of the effects of the Plateau are still not understood (Ding, 2013), but it is likely that the effect of the landform is critical to the East Asian monsoon.

Figure 6 - South Asia summer monsoonal pattern – from Wang (2006). For China, the summer monsoon originates from: 1) across the equator, from the Australian region, 2) from the tropical West Pacific ocean and 3) from the Bay of Bengal and the Arabian sea (Wang, 2006). Air above the low temperature of the Australia land mass (experiencing winter), Saudi Arabia and the relatively cool oceans, are driven towards the warm Asian land mass, especially the Tibetan Plateau (Wang, 2006; Wu and Zhang, 1998).

#### *Water pathways and storage*

Factors that control the movement of water are of great significance. The main water pathways are described by Table 5.

As water falls as precipitation, a fraction will be intercepted by vegetation, which will either be lost via evaporation or travel to the ground by stemflow (Holden, 2012). Water that

reaches the ground will infiltrate into the soil or runoff as overland flow. Overland flow may enter waterways and contribute directly to stormflow, or enter lakes. In winter, water may freeze and be stored as snow and ice, this is especially important in cold climates (see section 5.4.1).

Soil and groundwater storage is likely to be the most important water source for rivers outside of storm events (Holden, 2012). The rate of infiltration depends upon soil moisture content, the soil grain size (soil texture), the soil condition (crusting, cracks, compaction), vegetation cover and topography. Soil texture is of particular importance, which relates to various properties that are useful when attempting to interpret flow and water quality within a catchment (e.g. Table 5).

Figure 7 - Mean monthly surface temperature (°C) over Asia for 1948-2000 in: (a) October, (b) November, (c) December, (d) January, (e) February, and (f) March. In October, a mass of cold air lies above the Tibetan Plateau, which expands to the East and North-West in subsequent months, merging with the expanding cold air mass above Siberia and Mongolia to the North. From (Chang, 2004).

Figure 8 - Mean sea level pressure (mb) over Asia for 1948-2000 in: (a) October, (b) November, (c) December, (d) January, (e) February, and (f) March. The region of high pressure expands from Northern regions: Siberia and Western Mongolia to the South and to the East. From (Chang, 2004).

Property/behaviour	Sand	Silt	Clay
Water holding capacity	Low	Medium	High
Aeration	Good	Medium	Poor
Drainage rate	High	Slow to medium	Slow
Organic matter decomposition	Rapid	Medium	Slow
Compaction	Resists	Easily compacted	Easily compacted
Susceptibility to water erosion	Low	High	Low
Ability to hold nutrients	Poor	Medium to high	High
Leaching of pollutants	Allows	Moderately retards	Retards

Table 5 - Effects of soil texture on soil properties. Presented by Holden (2012), adapted from Brady (1999).

Water that infiltrates may continue to move deeper into the soil until it reaches a confining layer that is resistant to percolation, such as impermeable bedrock (Price, 2011). A fraction of water may continue to infiltrate, which largely depends upon the permeability of the confining layer, whilst the other fraction will move parallel to the confining layer via the process of throughflow. Throughflow is heavily influenced by the sub-surface topography of the confining layer, however this is very difficult to determine (Price, 2011). The rate of throughflow influences residence time within shallow groundwater storage, which is of importance for more extended periods of low-flow (Holden, 2012). Throughflow varies depending upon the porosity of the soil and the structure of the soil pores. Water may travel through the smaller pores via matrix flow, by larger pores called macropores or through large holes called soil pipes (Holden, 2012). Water passes quickly through the larger voids, which are often connected, allowing for relatively rapid travel. Therefore, the structure of

soil significantly influences residence time. Soil pipes are more common in arid and semi-arid areas, which form as a result of soil shrinkage and crusting (Holden, 2012).

Groundwater within bedrock (deep groundwater) may have long residence times (Table 5), as water usually travels very slowly through the rock. Like soil, rock may have small pores, but also larger voids such as cracks and fissures which water may travel rapidly (Holden, 2012).

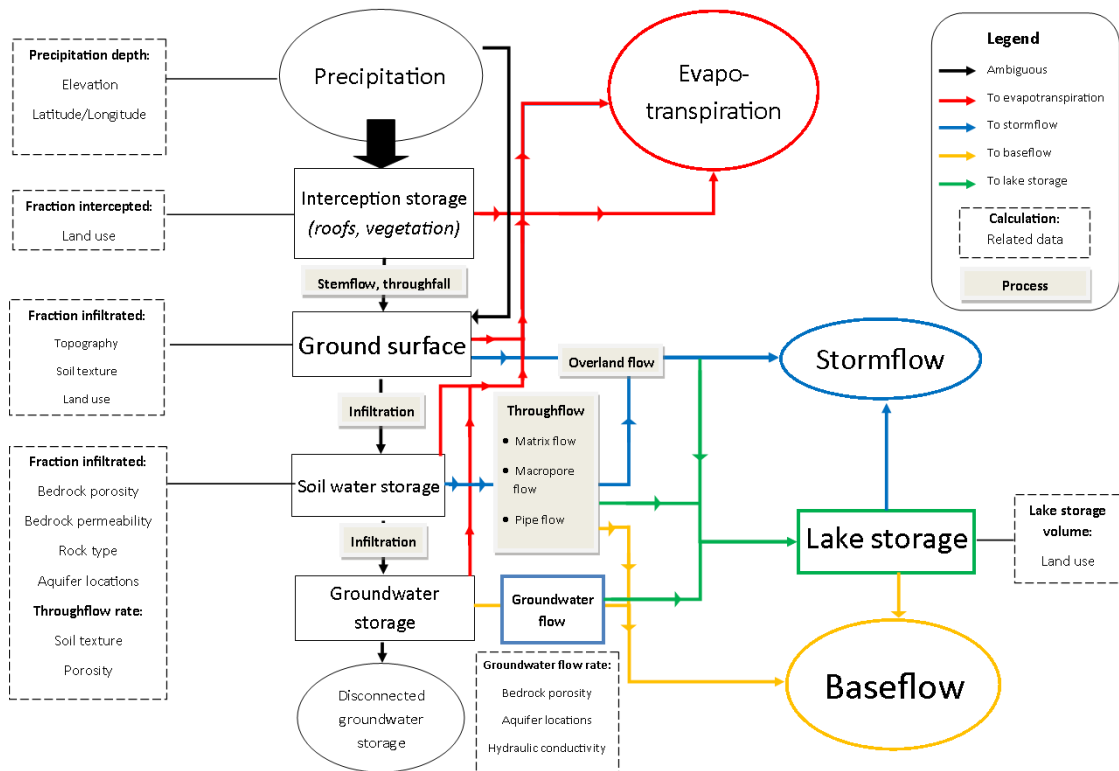


Figure 9 –Conceptual model of water pathways to stormflow or baseflow (low-flows), including storage and losses. Data is suggested for each element that may be used to estimate low flows, with explanations in Table 6. Adapted from Price (2011) and Holden (2012).

### 2.5.2. Regional regression

Regional regression is an approach that attempts to establish a relationship between catchment characteristics and low-flow indices using a regression model (Smakhtin, 2001). It is perhaps the most commonly used methodology for low-flow estimation.

For large catchments or regions, hydrologically homogenous regions must be delineated.

Regional regression assumes that the region has similar streamflow responses in similar sized catchments. For example, flood peak magnitudes and timing. These catchments may be defined as hydrologically homogenous. Therefore, by delineating the homogenous regions within a large catchment, a separate regression model should be produced for each if possible. However, this is not necessary for anything other than large catchments or catchments with significant physiographic variation. Possible ways of achieving this are outlined in Smakhtin (2001).

Sufficient flow data should be acquired to represent the spatial and temporal variability of the catchment (Rees, 2009). Gauged data should represent catchments with little or no artificial influences upon flow; initially, low flow indices should be estimated for natural conditions .

The regional regression model construction process initially depends upon the selection of the type of regression model and the selection of potential catchment characteristics to describe the spatial variation of low flow indices. Selection of catchment characteristics should be aided by prior knowledge of the catchment. This is often dominated by catchment area, with larger catchments generally experiencing higher flows than smaller catchments (Young et al., 2009). Larger catchments are able to receive more rainfall, which drains to the catchment outlet, but in addition, larger catchments also have longer response times and larger channel storage which contributes to low-flows (Cassie and El-Jabi, 1995). The challenge is therefore to identify the characteristics that differentiate catchments of similar size. To reduce the effects of scale, flow may be normalised by area to better assess the



relationships between flow and other catchment characteristics (Young et al., 2009). Alternatively, flow may be normalised by other flow indices (e.g. mean flow) (Holmes et al., 2002b). This is important, as the effects of scale are usually dominant and therefore the effects of other important characteristics are difficult to identify; once the effects of scale are minimised, other relevant relationships are easier to identify (Young et al., 2009). Common catchment characteristics used to describe low flows are described in Table 6. It may be difficult to identify catchment characteristics that may describe low-flows within a catchment (Smakhtin, 2001), and therefore it is important to gain an understanding of the type of characteristics that are likely to describe low-flows.

Cervione et al. (1993) used regional regression to estimate the 7-day, 10-year flow (7Q10) for a selection of streams in Rhode Island, US. The 7Q10 is the lowest average flow within 7 consecutive days, with an average recurrence interval of 10 years. The 7Q10 was estimated based on the percentage of stratified drift (unconsolidated, stratified sediment) and till (unconsolidated, non-stratified sediment) within a river basin. Schreiber and Demuth (1997) attempted to relate the mean annual 10-day minimum flow (MAM10) to geology, petrography, groundwater capacity and land use, by means of regional regression in Southwest Germany. Rather than calculating the entire catchment area of each gauging station, the area within a 1km buffer of five river stretches directly upstream of each gauging station were sampled, each stretch had a length of 1km (Schreiber and Demuth, 1997). It was noted that geology was the strongest variable, but groundwater capacity and land use were useful for accounting for some of the variance of MAM10. Schreiber and Demuth (1997) suggested this approach would be useful in situations where catchment properties would be difficult to estimate.

To determine the “best” regression model including its form and parameters, both manual and automatic techniques can be used. Automatic techniques such as stepwise-regression

may be used, (Derksen and Keselman, 1992; Babyak, 2004; Altman and Andersen, 1989) and/or a more visual approach such as analysing a correlation matrix and scatter graphs.

<b>Catchment Descriptor</b>	<b>Relation to low-flows</b>
<i>Climate descriptors</i>	Precipitation and evapotranspiration define total streamflow within a catchment, in absence of artificial water transfers. In cold climates, temperature is significant as it relates to snowfall and snowmelt. Storage of precipitation as snow significantly reduces runoff and may therefore lead to a period of low-flow. In contrast, the snow melts, there is likely to be a significant increase in runoff.
<i>Elevation</i>	Catchments at higher altitudes are often exposed to more frequent and heavier precipitation. Elevation is also negatively correlated with temperature and therefore potential evaporation is reduced and precipitation is more likely to fall as snow.
<i>Slope</i>	On steep slopes, rainfall is more likely to travel via overland flow or throughflow processes rather than infiltrate into deep groundwater storage.
<i>Soil type</i>	Soil type influences soil water storage, hydraulic conductivity (ease of travel) and the rate and capacity of infiltration. Soil properties may also relate to the proportion of water that will infiltrate into deep groundwater storage, which is important during low-flow periods.
<i>Geology</i>	Geology primarily relates to deep groundwater storage. Sedimentary rock types are more porous and may have greater storage capabilities than the harder igneous and metamorphic rock type.
<i>Drainage density</i>	Drainage density is defined as the length of all streams per unit area; which relates to the permeability of the basin. Steep and/or impermeable slopes are associated with higher drainage densities and therefore reduced flow during dry periods.
<i>Land-use</i>	Land-use influences runoff processes and interception. Forests intercept rainfall, but provide greater soil stability and infiltration capacity. Urban areas are most associated with impermeability, but may also have other significant influences upon flow, which is discussed in section 2.5.5. Arable land may lead to preferential flow in plough lines. Pasture may be hydrologically similar to grassland, although poaching (destruction of the top soil layer by the movement of large animals) and soil compaction may occur. Lakes and reservoirs are a form of surface storage that may be significant for sustaining flow outside of storm events.
<i>Catchment area</i>	Catchment area is a scaling factor describing the accumulation of runoff to a single point. It therefore has a strong, positive correlation with flow.

Table 6 - Examples of catchment descriptors that may relate to low-flows (Holden, 2012; Rees, 2009).

The number of parameters that may be used depends upon the number of gauges available, otherwise there is danger of overfitting (Babyak, 2004). To illustrate this, consider a regression model that includes 5 predictors but only has 10 observations, in this case this is the equivalent of estimating 5 separate regression models with 1 predictor and 2 observations, which is indicative of a very poor model (Babyak, 2004). The inclusion of a predictor in a regression model reduces the amount of information available (observations) to estimate regression weights for each predictor, and will result in regression weights varying considerably between different samples.

Care must be taken to understand the observed relationships between catchment characteristics and flow indices, as characteristics may be cross-correlated with other characteristics. This is a common problem when interpreting the relative strength of influence for topography and soils, which are often cross-correlated. Soils on steep slopes are generally coarser and thinner than soils on shallow slopes, and the combined effects encourage rapid water runoff and throughflow processes (Price, 2011).

Once the form of a regression model has been determined the parameters must be estimated using the procedure of least squares minimisation. Traditionally, the ordinary least squares (OLS) approach is used, which assumes that the observations of the independent variable (i.e. flow) are equally reliable throughout the dataset. However this assumption is often not the case. Cross-correlation between concurrent flows and different record lengths between flow gauges is commonplace, violating the key assumption of OLS. An alternative procedure should be considered when this is the case. Generalized least squares (GLS) (Stedinger and Tasker, 1986) was developed for this purpose. Studies by Moss and Tasker (1991) and Kroll and Stedinger (1998) discuss the situations where OLS is satisfactory and where GLS should preferably be used.

### 2.5.3. Regional mapping

Various spatial mapping techniques may be used to estimate low-flow indices. The most commonly used methodology is the flow contour map. A flow index can be plotted onto the centroid of its catchment and flow contour lines may be drawn using manual or automatic procedures. This technique is simple, however it relies upon factors such as the quality and spatial density of gauged flow data, catchment variability and contour intervals (Smakhtin, 2001).

Physiographic space based interpolation (PSBI) is a spatial interpolation method, although within a two dimensional space of physiographic and climatic descriptors; described as the physiographic space (Chokmani and Ouarda, 2004). Any subcatchment can be represented as a set of X and Y co-ordinates within this physiographic space. These co-ordinates may be derived using techniques such as principle component analysis (PCA). The index of interest may be represented as the 3rd dimension and thus, may be interpolated, using kriging techniques (Chokmani and Ouarda, 2004). PSBI has been used successfully to estimate low-flow indices (Castiglioni et al., 2009; Castiglioni et al., 2011); and to regionalise flow duration curves (Castellarin, 2014), using a PSBI methodology that was determined to be more representative of low-flows (in terms of relative error) than a regional regression approach.

### 2.5.4. Rainfall-runoff modelling

A rainfall-runoff model can be used to create a synthetic time series using rainfall data, from which low-flow statistics can be extracted. Rainfall-runoff models may be categorised in many different ways. But, generally, they may vary in complexity, time-step and spatial distribution.

*Temporal and spatial resolution*

Rainfall-runoff models operate at different temporal and spatial resolutions. The temporal resolution largely depends upon the resolution of available data, but commonly varies between the sub-hourly to annual time step.

Spatial resolution can generally be categorised as lumped, semi-distributed and distributed models. Lumped models do not account for spatial variation and, therefore, attempt to describe the modelled region as one unit. These are generally quite simple models that focus upon the relationship between rainfall and runoff response, often with little or no attempt to explain this relationship (Beven, 2012d).

One different approach is to attempt to group elements within the catchment based upon the similarity of characteristics. This may be accomplished by grouping sub-regions of the catchment by similar properties such as soil, geology and land use. A common approach is based upon the idea of hydrological response units (HRUs), popularised by the SWAT model (Arnold et al., 1993). HRUs attempt to classify areas of the catchment by a combination of different properties by overlaying maps of these different properties in order to identify areas which can be described as similar (Beven, 2012b). These models are spatially distributed to some extent, although they involve some degree of spatial lumping too. These are therefore known as semi-distributed models.

Finally, models may be fully-distributed, applying a grid based system. Each grid cell stores parameters for the model, which are used to determine the distributed runoff response from rainfall (Beven, 2012c). For example, the Penn State Integrated Hydrologic Model (Qu and Duffy, 2007), the Systeme Hydrologique Europeen (Abbott et al., 1986), the KINEROS model (Smith et al., 1995), and the Institute of Hydrology Distributed Model (Calver and Wood, 1995).

### *Complexity*

Complexity varies significantly between different rainfall-runoff models. This often relates to the spatial resolution, but also upon the extent the model can be considered to be empirical or process based. These could be categorised as:

- Simplistic mathematical models, with little or no consideration of processes within the catchment. These are generally lumped models, with only a few select parameters often determined through calibration (Beven, 2012d).
- Conceptual models, which try and consider the different storage elements and the fluxes between them. They are often catchment specific, attempting to determine the runoff response to rainfall which is specific to the catchment in question. Model parameters representing hydrological processes at the spatial and temporal scale are chosen for modelling the specific catchment (Young et al., 2009).
- Physical models, which utilise parameters which are measurable and are generally spatially distributed in nature. Relationships between these parameters are commonly generated from sets of laboratory or field experiments (Young et al., 2009). For these physically based models it is especially important to have an appropriate model structure and parameter set for the catchment and operating scale. These models have the advantage of theoretically being able to model flows without the need for calibration and to be able to utilise scenarios; for example, simulating the effects of land use change within the catchment (Smakhtin, 2001).

### *Parameterisation*

When attempting to estimate flows in an ungauged basin, some degree of parameter estimation is required, for which there is often a great deal of uncertainty. For simple and conceptual models this is often achieved by relating measurable properties to parameters,

(e.g. Midgley et al., 1995). This requires a sufficient number of representative gauged sites to quantify this relationship.

Relationships between parameters and measurable watershed properties may be determined using techniques such as regional regression. However, for conceptual models, care must be taken when constructing such relationships, as there is often interaction between parameters. Techniques are available to alleviate this problem such as sequential regression (Lamb et al., 2000) and region of influence (Young, 2006).

In contrast, physical models often require high detail, high resolution data (Young et al., 2009). Success using this model type depends upon the availability and quality of data within the catchment.

### *Calibration*

Most rainfall-runoff models require calibration to some degree in order to compensate for model structure and parameter errors. Mathematical models with few parameters are relatively simple to calibrate using automatic techniques. However, as the model complexity and number of parameters increases, automatic calibration becomes more difficult. This is a result of a greater number of possible parameter set combinations and interrelationships between parameters (Young et al., 2009). Therefore, these are often calibrated manually when possible. In such cases a sensitivity analysis may be used to determine which parameters are most important to adjust (Beven, 2012b).

Calibrating a large number of parameters exposes the model to the threat of equifinality. First described by von Bertalanffy (1968), but with its roots in the work of Driesch (1908), equifinality describes the phenomenon of which different starting conditions may reach the same result. In the modelling context, this suggests that for a group of observations, there may be multiple feasible parameter sets (Beven, 2006). Following calibration, a set of

parameters may be chosen to be “optimum”; however, there may be a huge number of alternative parameter sets that will also provide an adequate solution. This is therefore a problem, as it is difficult to determine whether the parameter set chosen is representative.

As parameters have a physical basis and are inherently measurable, physical models may theoretically be modelled without calibration. However, there is uncertainty as to how well a physical model describes the catchment it means to represent. All forms of distributed models involve some sort of lumping of data. In the case of grid based models, data is lumped within each grid cell at a scale greater than the scale of variation (Beven, 2012a). There is uncertainty as to how well data is measured and then approximated at the element level (grid or semi-distributed unit) (Young et al., 2009). Secondly, physically based equations are often derived from laboratory studies and there is uncertainty as to what extent these equations can be used at the working scale of the model. Therefore to compensate for these sources of uncertainty and error within the model structure, calibration is needed in the majority of cases (Beven, 2012a).

For all model types, a low-flow calibration and validation approach is needed, such as measures proposed by Smakhtin et al. (1998). Models calibrated with the objective of simulating the timing and/or magnitude of flood peaks may not be appropriate to generate reliable low-flow statistics.

#### 2.5.5. Artificial influences

Human activity has a profound effect upon water within river catchments. It is impounded by reservoirs, it is abstracted, weirs and levees are built, and water is released from sewage treatment plants (Smakhtin, 2001; Gustard and Young, 2009). With only a consideration of flow under natural conditions, flow estimation lacks realism. The challenge is to obtain



information about artificial influences in the catchment, to quantify their effect and thus apply this to the estimate of natural low-flow (Gustard and Young, 2009).

#### 2.5.6. Approaches taken to flow estimation by previous GREAT-ER studies

For the majority of GREAT-ER applications outside of the UK, the estimation of low-flows has been simplistic, with the stream network approach most favoured. For example, the study of the river Glatt utilised simple interpolation between gauges for the mean and Q95 low-flow statistics (Alder et al., 2010). This approach assumes that flow is entirely dependent on the accumulated length from the upstream gauge, and lumps elements that may increase (e.g. tributaries, STW outflow) or reduce flow (e.g. water abstraction), this lacks realism.

Low-flow statistics were estimated for the river Rur and the river Lambro using non-linear regression, with the accumulated river length as the predictor variable (Schulze and Matthies, 2001; Schowanek and Webb, 2002). This was then corrected using adjustment factors based upon the differences between gauged and estimated flow at gauging stations. In addition, further adjustments were made if the level of dilution within the receiving waters for large sewage treatment plants was too low. Dummy gauging stations were created in both the receiving stretch and the upstream stretch, applying the mean effluent flow as the difference in flow between these two gauges. Finally, in a study by Zhang et al. (2015a), a SWAT model was used to estimate low flows for a catchment within the Beijing region. However, the model was originally validated with the purpose of simulating monthly mean flow and loadings of sediment and nutrients, for which correctly estimating low-flows was of less importance. As described in section 2.5.4, rainfall-runoff models should be calibrated for the purpose of low-flow estimation and therefore it is unlikely to perform optimally for the task of low flow estimation. It is also uncertain as to whether artificial influences were included within this model. Although there are limitations with the approach

used by Zhang et al. (2015a), the ease of estimating low-flow statistics from a pre-existing model is advantageous, and therefore this form of approach, in general, may be considered to be pragmatic.

The approaches described above provided little consideration of artificial influences to flow, which may be significant. One exception is a study by Aldekoa et al. (2013), when a more detailed approach was applied that took artificial influences into account (i.e. reservoirs, abstractions and STW discharges). Their model also considered chemical removal from the main stream via water abstractions, accomplished by creating artificial bifurcations at abstraction points.

Studies within the UK have taken perhaps the most complex approach towards the calculation of low flows for the GREAT-ER model. The methodology used by Young et al. (2000a) and Young et al. (2000b) is summarised here. Mean flow was calculated using a simple water balance model based upon gridded annual precipitation, potential evaporation and catchment area. The Q95 statistic was determined by relating Q95 normalised by mean flow (to reduce climatic control over the statistic) to soil and geology type. A UK soil classification system, the hydrology of soil types (HOST), relates soils and geology to their hydrological properties. A regional regression model was derived based upon the normalised Q95 statistic and the fractional extent of each HOST class (Young et al., 2000b).

## **2.6. Chemical emission**

This section outlines the approach developed to provide a spatially explicit estimate of chemical emission throughout a catchment, from both treated and untreated wastewater discharge.

### 2.6.1. Estimating chemical usage

Chemical emissions are calculated based upon two factors: population and the mass of chemical released to wastewater per capita (hence denoted as chemical usage). Chemical usage may be calculated based upon: 1) sales data for the chemical of interest or 2) by back-calculating based upon STW influent or effluent data.

Sales data for products containing the chemical of interest may be available (Hodges et al., 2014). If then the mass of the chemical of interest can be determined for each product, the total mass per annum can be calculated. The chemical usage can therefore be determined by dividing the total mass of chemical sold per annum by the population of the given year. However wealth generated from China's economic development is not uniformly distributed. The South-East is the wealthiest region of China. At the provincial scale, per capita wealth is significantly higher in urban areas. It is, therefore, likely that the affordability and general availability of products containing the chemical of interest is not uniformly distributed in China. By estimating the affordability of each product based upon GDP, it is possible to estimate the spatial distribution of chemical usage based upon GDP and population density. This is fully explained in Hodges et al. (2014).

Alternatively, chemical usage may be back-calculated. Samples taken at the influent or effluent of a STW within China may be collected with the intention of measuring the concentration of the chemical of interest (Liu et al., 2015). If the population served and mean discharge for the STW is known, the chemical usage may be estimated. Due to the uncertainty and variability surrounding the data (Johnson et al., 2008b), measurements from multiple STWs is required for an accurate estimate.

### 2.6.2. Estimating the spatial distribution of wastewater discharge

The discharge element of GREAT-ER requires a significant amount of data about STWs and untreated discharges. Firstly, STWs must be located and population served by a STW must be acquired or estimated in order to estimate the mass of chemicals to be treated (Wagner and Koormann, 2011). Once obtained, the treatment type (e.g. activated sludge technology) is required to determine how much of that mass is removed by the STW. Removal may vary significantly depending upon the treatment type, for example chemical removal occurs as a result of biological processes in trickling filter plants, whilst activated sludge plants rely upon both biodegradation and sorption for chemical removal (Stuetz and Stephenson, 2009). Therefore, chemicals that are more effectively removed by sorption will likely be removed to a greater extent in activated sludge plants than trickling filter plants. Finally, information about the spatial distribution and magnitude of untreated discharges is required.

A list of STWs operational in China is made available annually by the MEP (<http://www.mep.gov.cn>). This provides the STW mean and capacity daily discharge, STW treatment type and construction date. However, the population served and the STW locations are not provided. STWs constructed in the last or current year will not appear on the list.

Consequently, STWs must be located with the assistance of alternative sources and then populated with the necessary attributes of each STW. Finally the distribution of untreated discharges throughout the catchment must be estimated using limited data. Figure 10 provides an overview of the approach used to acquire this information. It is important to note the acquisition of each data element is not independent of others. The key is to

estimate the STW wastewatershed, where a wastewatershed is the area served by a STW, represented as a vector polygon. Gridded population is utilised, each grid cell representing the sum of population within each cell. Using the wastewatershed polygon, the population sum for the area served by the STW can be determined. The untreated discharge can be estimated from the population outside of wastewatersheds.

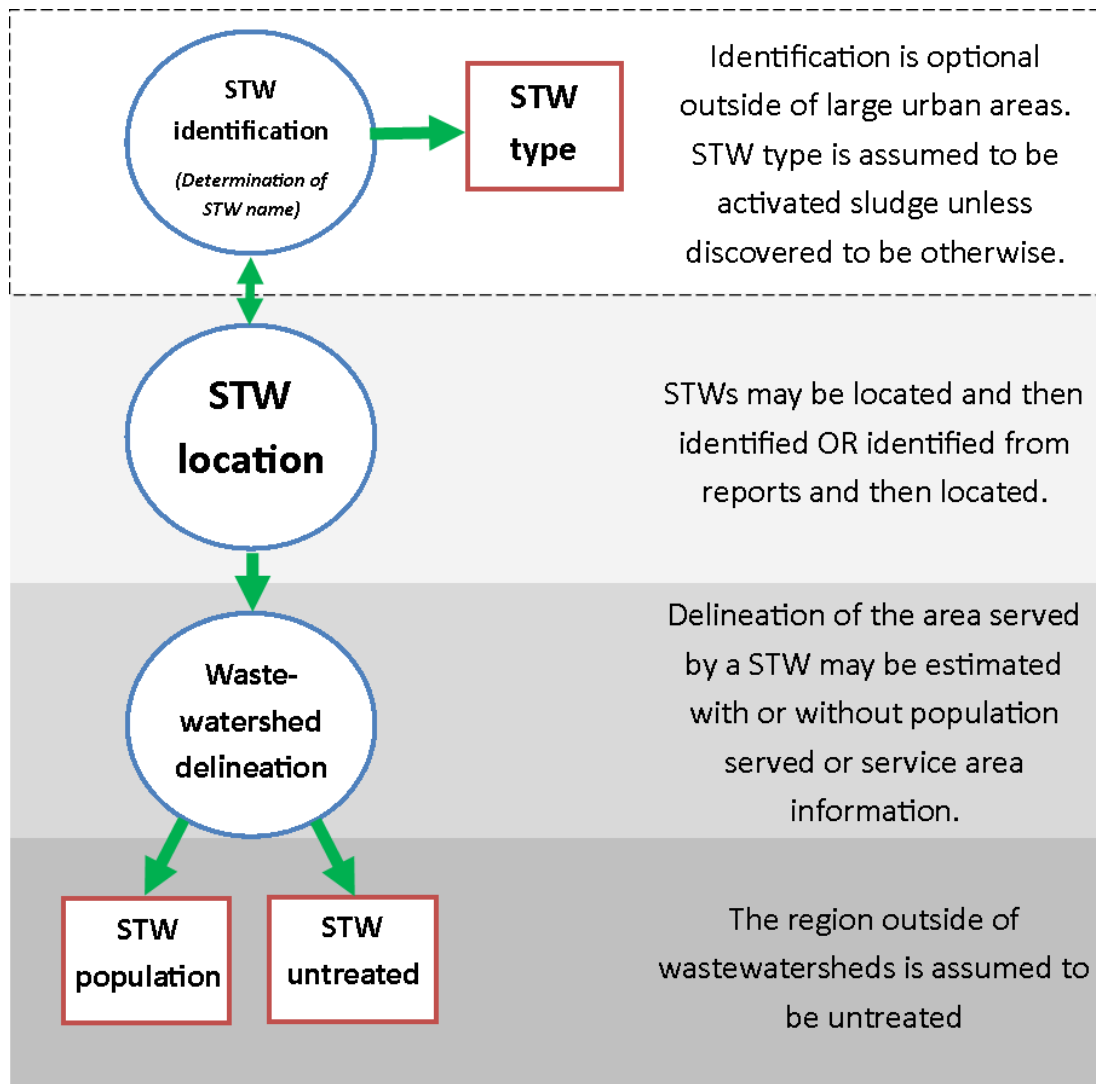


Figure 10 - Flow chart outlining the procedure of locating a STW.

Each of these elements will be discussed in further detail.

The contents of this section are as follows:

- 1) Approach used to locate and identify STWs
- 2) Methodology used to delineate a STW wastewatershed
- 3) Estimation of untreated discharge spatial distribution

## 2.7. Locating and identifying STWs

STWs were located manually using Google Earth. To aid this search a dataset was developed to highlight population centres and settlement extents; areas that are likely to contain a STW.

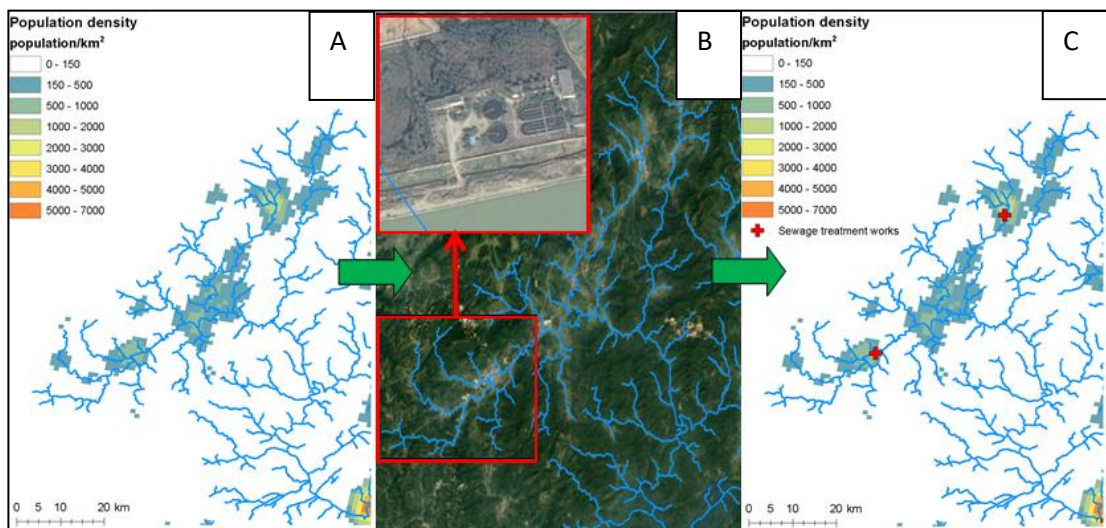


Figure 11 - Locating STWs with the aid of population data. Dataset based upon Landsat (Bright et al., 2006).

A gridded population dataset may be used to assist this process. A gridded population dataset is an estimation of the population distribution, usually based on census data (e.g. Gridded Population of the World, Version 4 (GPWv4) (CIESIN, 2016a)). More detail is provided about available population datasets in section 3.6. These datasets are used to identify the location of settlements. This is made more efficient by modifying these population datasets, by filtering out isolated cells with high population (that we are not interested in) and to emphasise the area occupied by a settlement. To accomplish this, the population dataset is smoothed using the focal statistics tool within ArcGIS's toolbox. For

each cell, the sum of the surrounding cells is calculated. As a result, the relative population of low population cells in town centres is increased, as these cells are usually surrounded by cells with high population. Moreover, the population of isolated high population cells are reduced significantly, as they are usually surrounded by cells with very low population. The resulting dataset is categorised and the category representing the lowest population density is made invisible, filtering out areas with low population. The lowest population density category is determined by means of calibration. This result can be achieved without the first step that smooths the dataset, however, isolated cells would still be displayed, and there would be “holes” within the settlements’ extent (Figure 12B). By smoothing the population dataset using focal statistics, the location and extent of settlements is clearer (A). Figure 11 shows the result of this visual modification and further how this may aid the identification of a STW. Figure 11-B displays a satellite image, if compared to Figure 11-A the areas of interest are immediately apparent and thus can be examined for STWs such as those identified in Figure 11-C. Alternatively, the population dataset could be aggregated into a larger cell size and/or simply use an effective categorisation system for visualisation. However, whilst reducing the cell size has a similar effect, it sacrifices some of the shape of the population centres. A categorisation system alone will lack clarity provided by the smoothing effect of focal statistics. Figure 12 provides an example of these alternative approaches. This process is not essential, but it may significantly increase the efficiency of locating STWs, and assists with a more systematic search. In addition, if riverlines are digitised as discussed in section 2.4.3, many STWs may be noted alongside the river during the digitisation process, although, this is not sufficient alone.

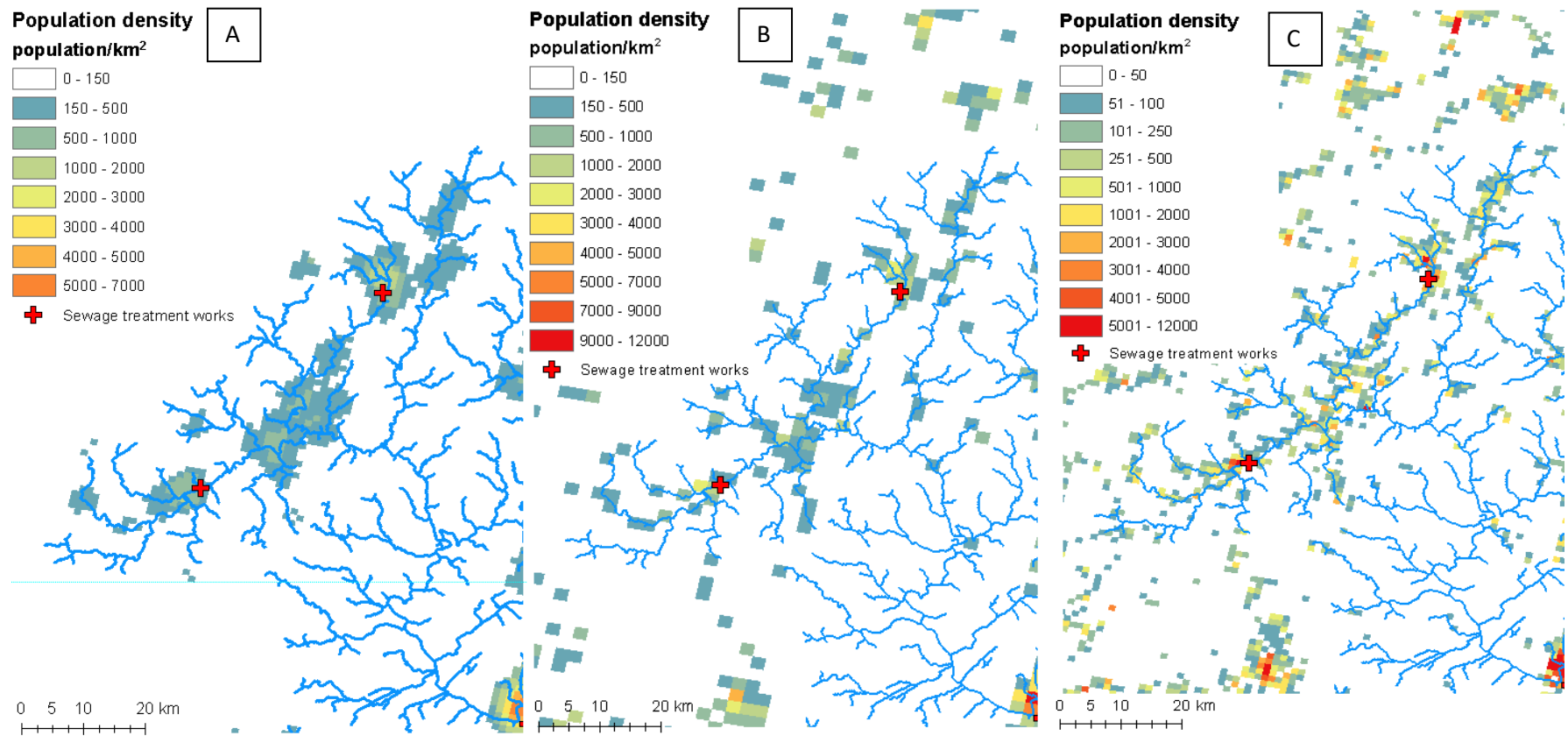


Figure 12 - Population visualisation options; for all three approaches, cells with a low population density are filtered out. The value for “low population density” was determined by means of manual calibration. What was considered to be “low population density” varied between the original and modified population datasets, as the population density in the modified datasets increased as a result of the modifications. (A) Population density data smoothed using focal statistics; (B) resampled population density; and (C) original population dataset. Where the original population density has a cell size of 1km<sup>2</sup> and the aggregated population density has a cell size of 2km<sup>2</sup>.



## 2.8. Wastewatershed delineation

As discussed earlier, the wastewatershed is the boundary for the area served by a STW. This allows the population served to be estimated by using the boundary to extract the sum of population from a population grid. The area outside the wastewatersheds is assumed to be untreated.

It is difficult to know the exact boundary for a STW's wastewatershed. However, the principle factor that is considered when constructing a sewer network is cost (Federation, 2009). The maximum possible volume of sewage is collected per meter of pipe. Therefore, densely populated areas and/or areas with industry are likely to be prioritised. Pipes are usually built so that wastewater flows to the STW by gravity (Brière, 2007). If an area is topographically situated so that water must travel uphill, a pumping station is required. This is a significantly more expensive approach than gravity based sewers, and will therefore be avoided unless it is considered to be worth the expense.

Delineation of STW wastewatersheds relies upon an underlying population grid and the DEM. The principle assumptions when delineating a wastewatershed are that:

- 1) Areas of high population are more likely to be served than areas of low population density.
- 2) Wastewatersheds do not cross the STW's topographic watershed. Primarily sewers will be gravity based and not pumped unless absolutely necessary. STW's may serve an area a short distance upstream, within the stream's topographic boundary.
  - a. However, if a population centre is served by a single STW it may be acceptable to serve areas of high population that are slightly outside of the boundary.

In order to achieve this, subcatchments are generated for each river stretch (described hereafter as river stretch catchments). The catchment area for each river stretch excludes the area drained by upstream river stretch catchments (e.g. Figure 14). This was achieved by using the stream reach and watershed tool within the TauDEM GIS toolbox (<http://hydrology.usu.edu/taudem/taudem5>) for ArcGIS. Using the DEM, flow direction grid, flow accumulation grid and the river stretch grid (see Figure 4) as inputs, polyline river stretches and polygon river stretch catchments are generated. Each river stretch and associated river stretch catchment is assigned a stretch ID (shared by the river stretch and the river stretch catchment). The mean and total population for each river stretch catchment are then calculated using the “zonal statistics as table” tool within ArcGIS’s Spatial Analysis toolbox (<http://desktop.arcgis.com/en/arcmap/10.3/tools/spatial-analyst-toolbox/zonal-statistics-as-table.htm>) using data from the underlying population dataset. This is then stored as a table (e.g. Figure 14), with each river stretch catchment identified by its stretch ID. The river stretch catchments are then linked to the table output using the stretch ID as the key/foreign field. This enables the population within each river stretch catchment to be displayed on a map (e.g. Figure 14).

The population density of each river stretch catchment is displayed visually, which aids the delineation of the wastewatersheds. The delineation procedure varies depending upon the size of the settlement; initially the focus will be on towns and small cities.

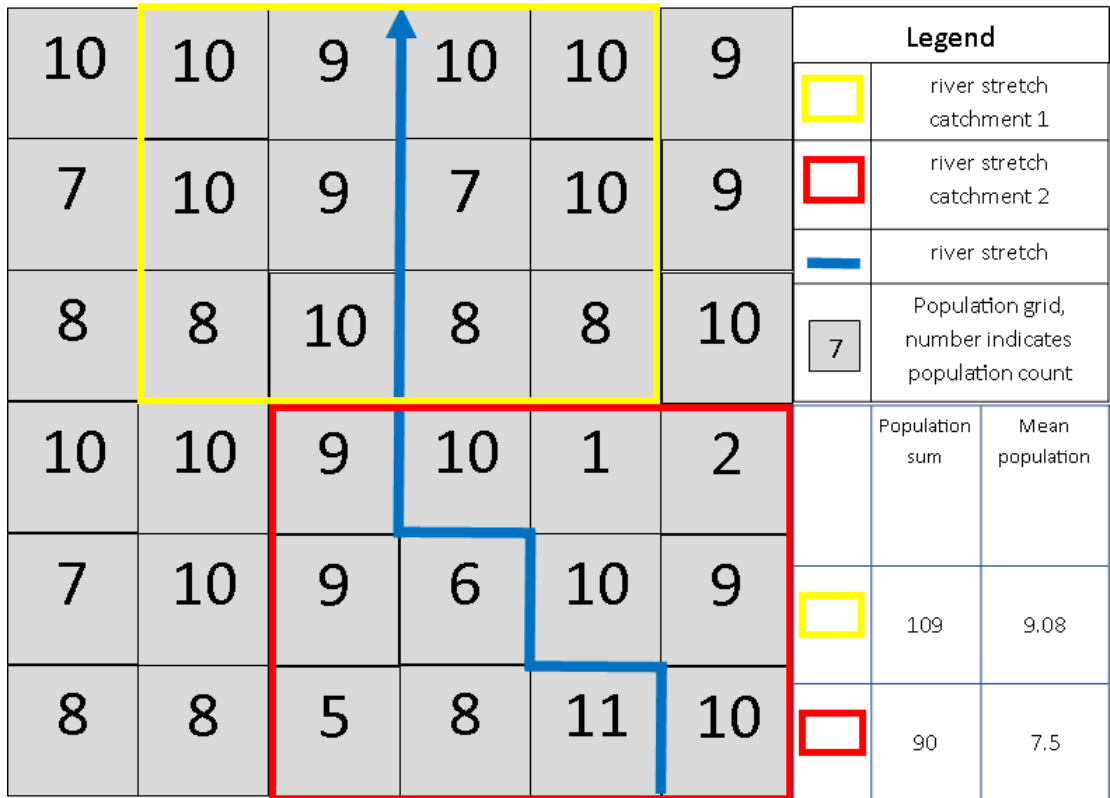


Figure 13 - Calculation of population (mean and sum) for river stretch catchments using the zonal statistics tool in ArcGIS spatial analysis toolbox. The river stretch catchments drain only to their respective river stretch, and then subsequently, to other downstream stretches. Using the tool “zonal statistics as table”, the population sum and mean are calculated for each river stretch catchment, using a gridded population dataset for this purpose.

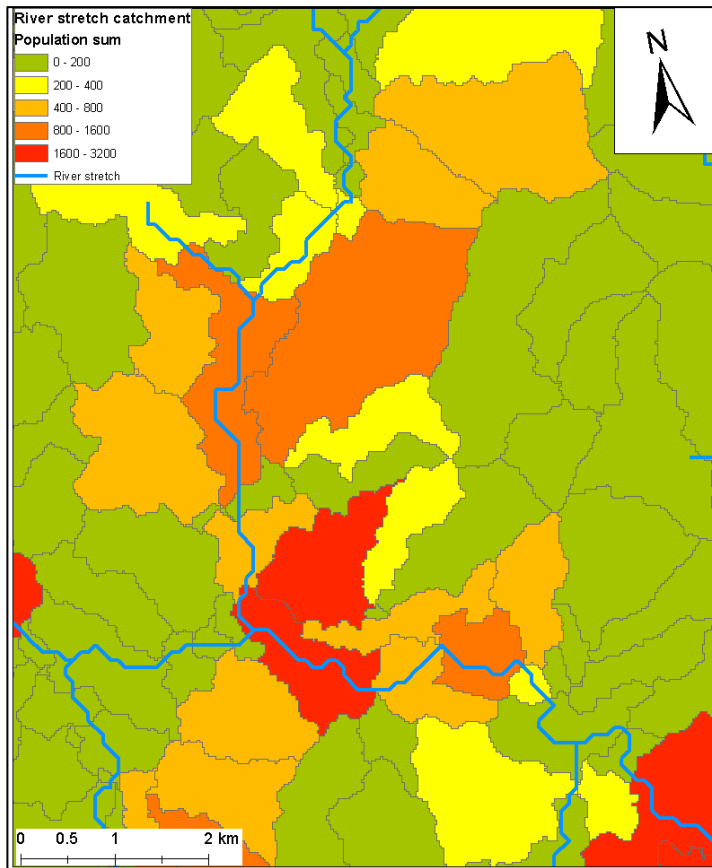


Figure 14 - Map displaying the sum of population contained within each river stretch catchment. Location: Longchuan county, Heyuan city, Guangdong province.

The main concern with this methodology is its inconsistency. A methodology that multiple users could use to produce similar results is desirable. This proves to be difficult due to the somewhat arbitrary nature of digitisation decisions. Furthermore, a procedure was produced which provided greater consistency, this is described below.

The symbology is redefined for the delineation of every STW, as it is important to display the relative population for the region. Defining a symbology that represents the variability of population within the area makes it significantly easier to determine which areas are more likely to be served by a STW. This is achieved using a manual but relatively consistent approach. In most GIS platforms, the symbology classes (e.g. Figure 15) may be generated

semi-automatically based on the statistical distribution of the dataset. The approach found to be most effective was to classify the data based on the standard deviation from the mean of the dataset (e.g. Figure 15 and Figure 16). This approach is most effective when generated from a subset of the dataset; where the symbology is generated from population data within the same region as the STW only. River stretch catchments were selected from the region, at a scale of approximately 1:250,000.

In Google Earth, the outline of the nearby/adjacent settlement is digitised and imported to the GIS. In the next step, the population symbology is defined, using standard deviations from the mean as symbology categories. Using the digitised settlement outline, river stretch catchments with a population  $> 0.5$  standard deviations above the mean are selected, which includes the main areas of the settlement and excludes the sparsely populated areas, as shown by Figure 16. In addition, river stretch catchments for river stretches that connect the STW with the town or city should be selected. Wastewatershed digitisation, in the majority of cases, is similar to the situation illustrated by Figure 16, where the outline of the settlement can be clearly seen. In the example given, digitisation follows the outline polygon created in Google Earth, selecting subcatchments along the river from the STW to the settlement and all river stretch catchments with a population density above and including 0.5 standard deviations above the mean. This category was selected as a result of calibration.

Wastewatershed delineation within large cities may require more precision and additional data. For example, Figure 17 illustrates a scenario where multiple STWs share a catchment; it is challenging to determine where the limit of one wastewatershed ends and another starts. In addition, large sections of these cities may be untreated. In order to tackle this problem it is crucial to acquire additional data regarding population served or the service area of STWs within the area.

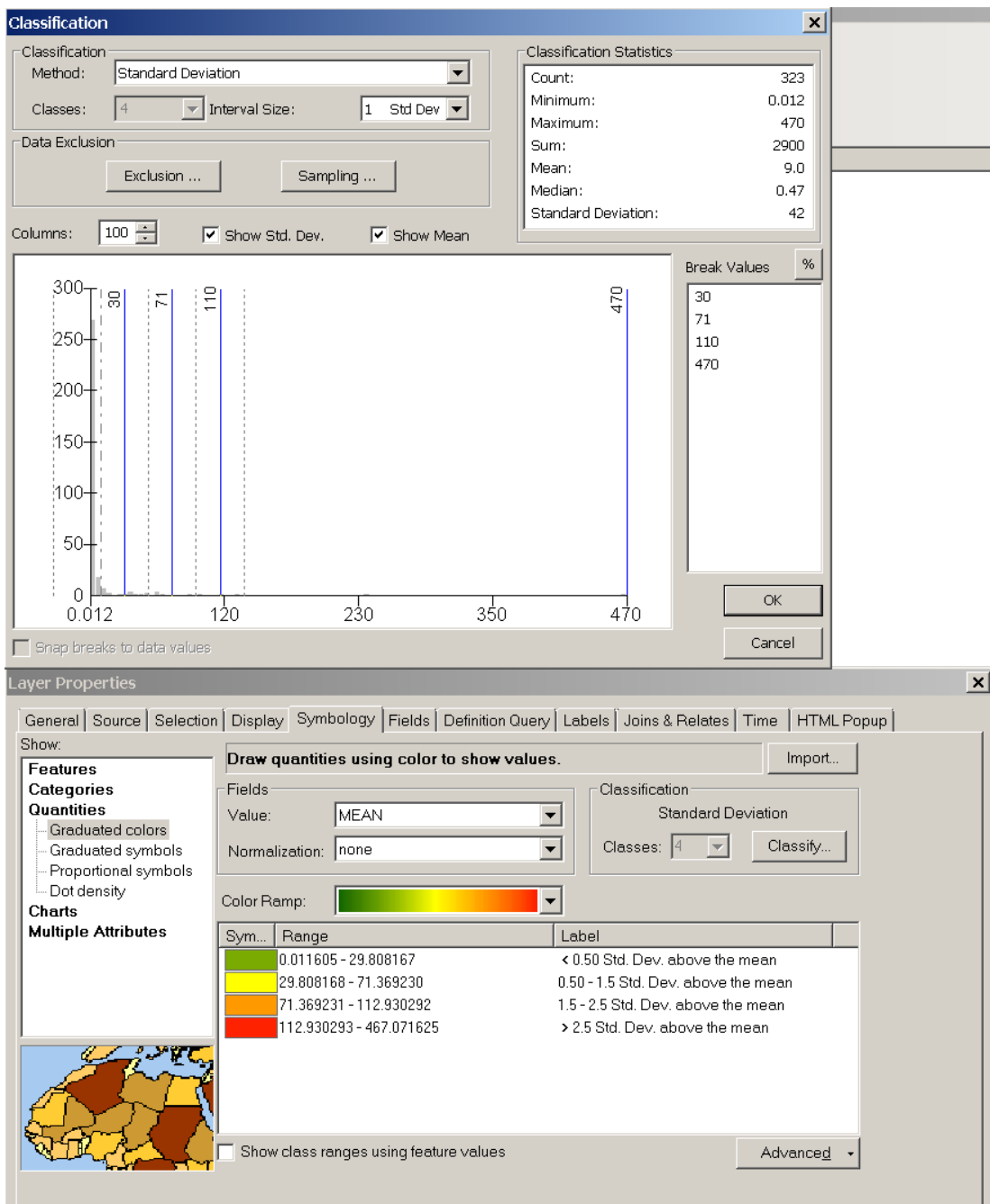


Figure 15 - Customising the symbology of the river stretch catchments in order to display standard deviations from the mean (for population density, pop/25m<sup>2</sup>). As shown, the symbology is automatically generated based upon the mean and standard deviations of the population dataset. ArcGIS is used in this example, however other GIS platforms may be used.

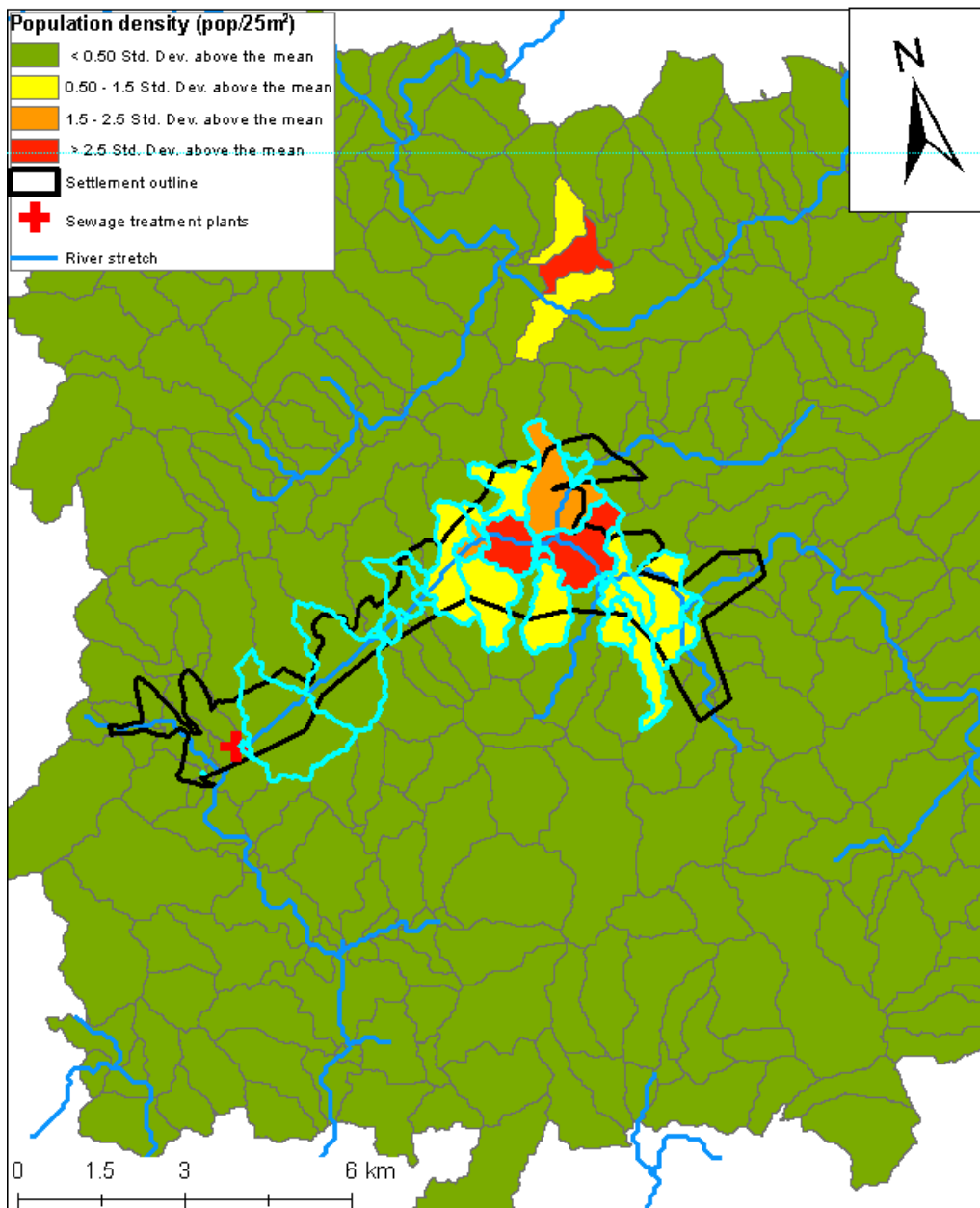


Figure 16 - Final delineation example – Zjin town, Zjin county, Guangdong Province, South-East China. Population density within river stretch catchments are displayed as standard deviations from the mean. The catchments highlighted in blue are those selected to be delineated for the STW wastewatershed. The river stretch catchments between the STW and the main settlement are selected, as are all river stretch catchments that are within the settlement outline that contain a population >0.5 standard deviations above the mean (8 persons/25m<sup>2</sup>). The cell size of the original population dataset is 25m<sup>2</sup>.

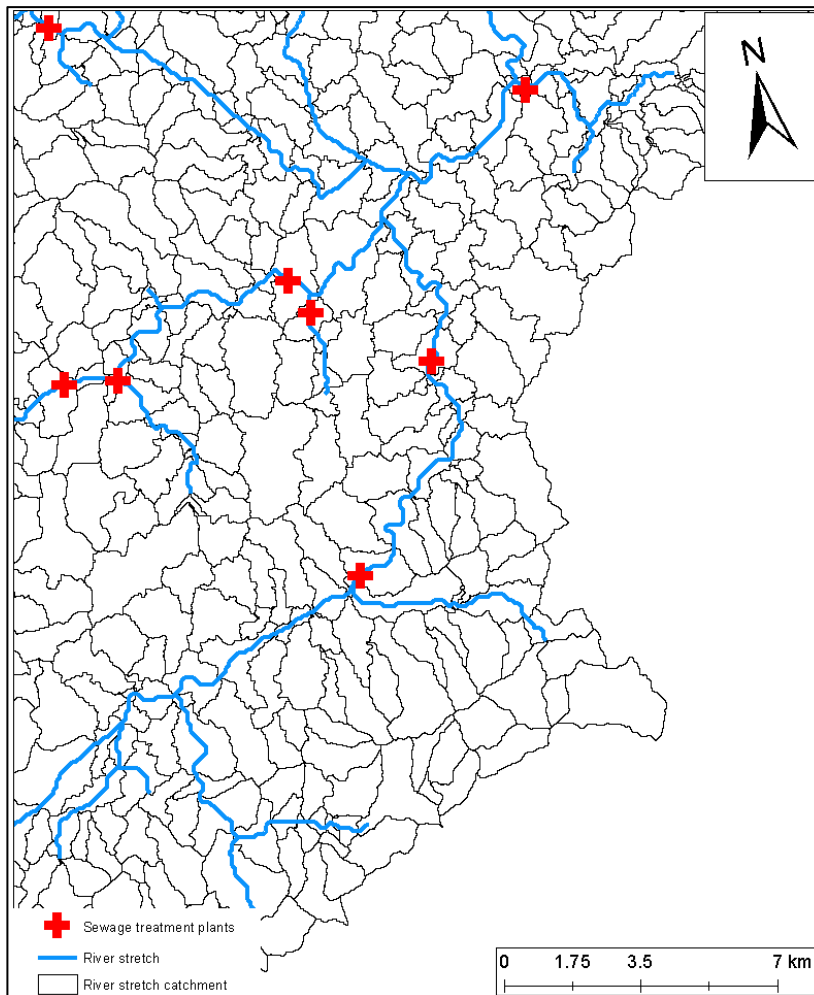


Figure 17 - Map displays multiple STWs clustered within a single settlement – Shenzhen city, China. This complicates wastewater delineation.

## 2.9. Identifying STWs

STWs that are located require identification in order to acquire required attributes. Firstly, the STWs may be checked against the list of STWs in China provided by the MEP. The list provides a construction date and an approximate indicator of location from its name and given city-region. A range of construction dates for located STWs can be determined using Google Earth's historic imagery by identifying which images contain or identify the presence of the STW, and those that do not. Therefore with an idea of construction date and location, some, but not all STWs can be identified. For those remaining, other data sources can be



used. The website [www.lpe.org.cn](http://www.lpe.org.cn) provides a web-based map displaying and naming a significant number of STWs. However, a small number of errors were noted and, therefore, it is important to be critical of this data source. Utilising both above methods provides improved confidence.

Additional information such as population served may be identified using reports and articles on the web. Unidentified STWs may also be identified by reports about any STWs in that given area, although this is a somewhat time consuming step. Owing to the Chinese government's eagerness to display progress towards tackling water pollution, a large number of news outlets often announce the construction of a STW in great detail. This may include treatment type, population, service area and discharge rate. Therefore, reports were located online using either the name or location of the STW as a search term. This approach required an acceptance that many of these sources are likely to be biased, which is unfortunately unavoidable. As this is particularly time consuming, this task should be restricted to STWs in highly populated areas.

For identified STWs, subcatchments should be selected with the intent of reaching the population and service area specified, if available. Several wastewatershed delineation iterations may be required for areas with multiple STWs, to avoid an overlap of boundaries. Once STWs within an urban area are delineated, those without population or service area data may potentially be delineated using the space that remains between already delineated wastewatersheds and the topographic boundary, such as that shown by Figure 18.

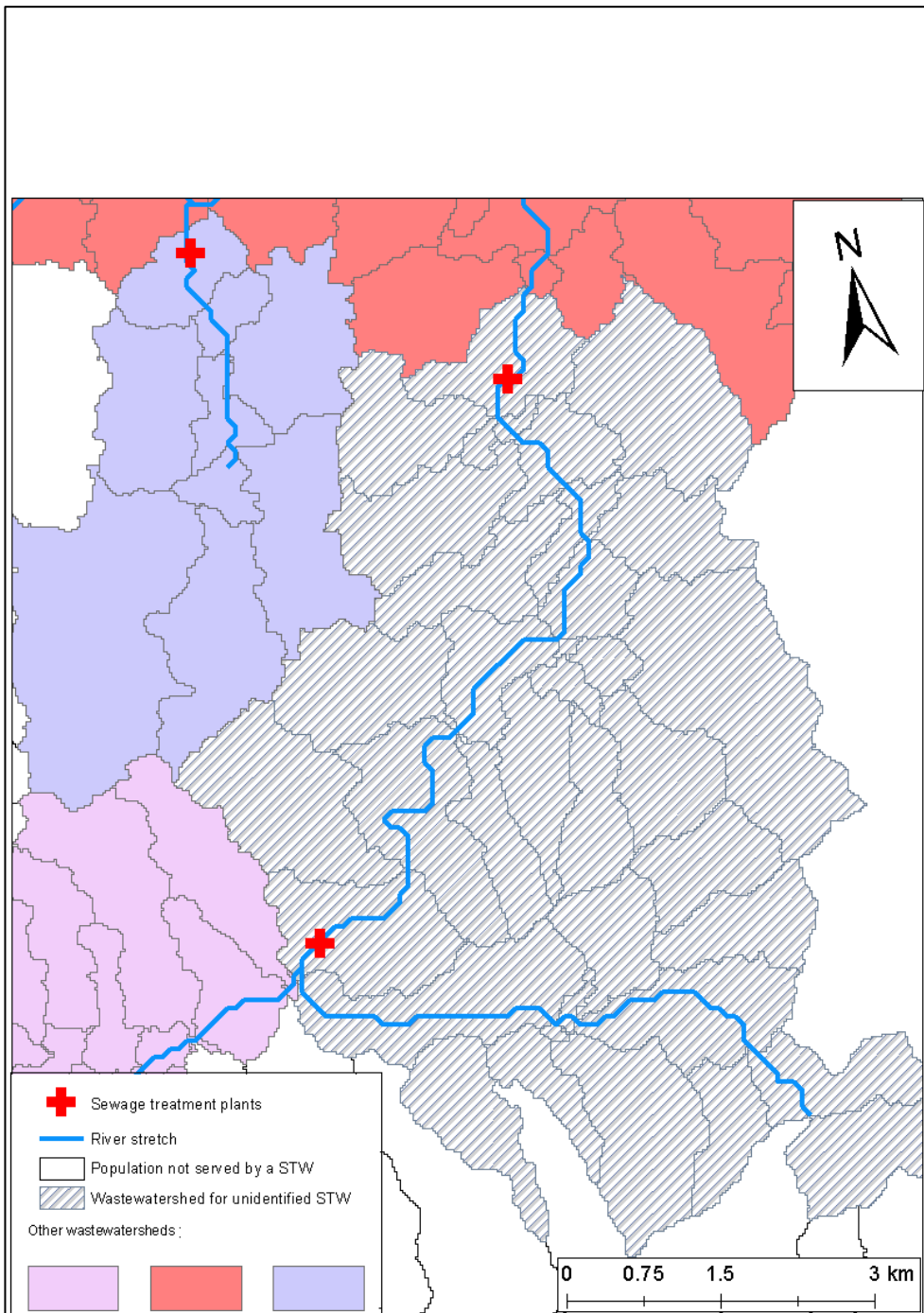


Figure 18 - Example of wastewaterhed delineation for an unidentified STW within an area of Shenzhen city served by multiple STWs. Wastewaterheds were delineated for nearby identified STWs and surround the topographic area upstream of the unidentified STW. Therefore, in this example the entire available area upstream was delineated. The area to the East is outside of the topographic area.

## 2.10. Emissions from untreated wastewater sources

It is assumed that a fraction of a given chemical substance will not be released to the river network. The diffuse emission rate (DER) describes the fraction of a chemical substance that is retained and released to the waterways. Reducing the DER therefore increases the rate of removal for a given chemical substance in subcatchments not served by a STW. Emissions are determined for every untreated subcatchment, where:

$$\text{Untreated chemical emission} = \text{Population} * \text{Per capita chemical usage} * \text{DER} \quad (38)$$

It is assumed that a fraction of untreated wastewater will not reach the waterways as a result of poor drainage; chemical substances within the wastewater that does not reach the waterways are assumed to be lost.

Rural areas are less likely to be treated in comparison to urban areas, and therefore the majority of untreated subcatchments will likely be rural (National Development and Reform Commission, 2016).

Subcatchments that are assumed to be untreated were identified by the method outlined in this section. DER is calculated using a stochastic approach; as DER is unknown, it is assumed to vary from 0-1 in a uniform distribution. This is incorporated into GREAT-ER by assigning a “dummy” STW to every stretch which may receive untreated wastewater; these dummy STWs were assigned a separate distribution to real STWs.

## Chapter 3 - The East river catchment

### 3.1. An introduction to the East river catchment

The East river is a major tributary of the Pearl river, South China (Figure 19). The catchment area is 25,325 km<sup>2</sup> (above Bolou gauging station), of which approximately 90% resides in Guangdong Province. The source of the East river is in the North-East of the catchment, in Xunwu county of Jiangxi province; the river then flows south-westerly to the Pearl river delta, where it discharges into the South China sea. The East river's mean annual discharge is 763 m<sup>3</sup>/s, which peaks in July with a mean monthly discharge of 1758 m<sup>3</sup>/s and drops to an annual low in January with a mean monthly flow of 377 m<sup>3</sup>/s. More details regarding the seasonality of the catchment is provided in section 3.1.4.

#### 3.1.1. Socio-economic history of the Pearl river delta

The East river's downstream region is well developed and relatively prosperous; home to cities such as Guangzhou, Dongguan and Shenzhen. The region has attracted wealth and migrants from other regions and is now home to ~24 million people. Wealth generated within the region is largely a result of trade; the Pearl river delta itself an important region for international trade. Historically, international trade was disproportionately focused upon the Pearl river delta region within China. In the 17<sup>th</sup> Century, trade between China and the rest of the world was largely restricted to Canton City, now known as Guangzhou, Guangdong province's capital. Initially, the majority of trade came from Britain, with the trade of tea, silk and porcelain in exchange for cotton, wool and opium (Nield, 2015).

From 1979, four special economic zones were established within China, allowing some degree of autonomy to establish policies which were attractive to foreign and domestic

trade. Three of these zones were established in Guangdong province: Shenzhen, Zhuhai and Shantou. This greatly opened up the area to foreign investment. The number of special economic zones later expanded to other coastal regions (Zheng, 2014).

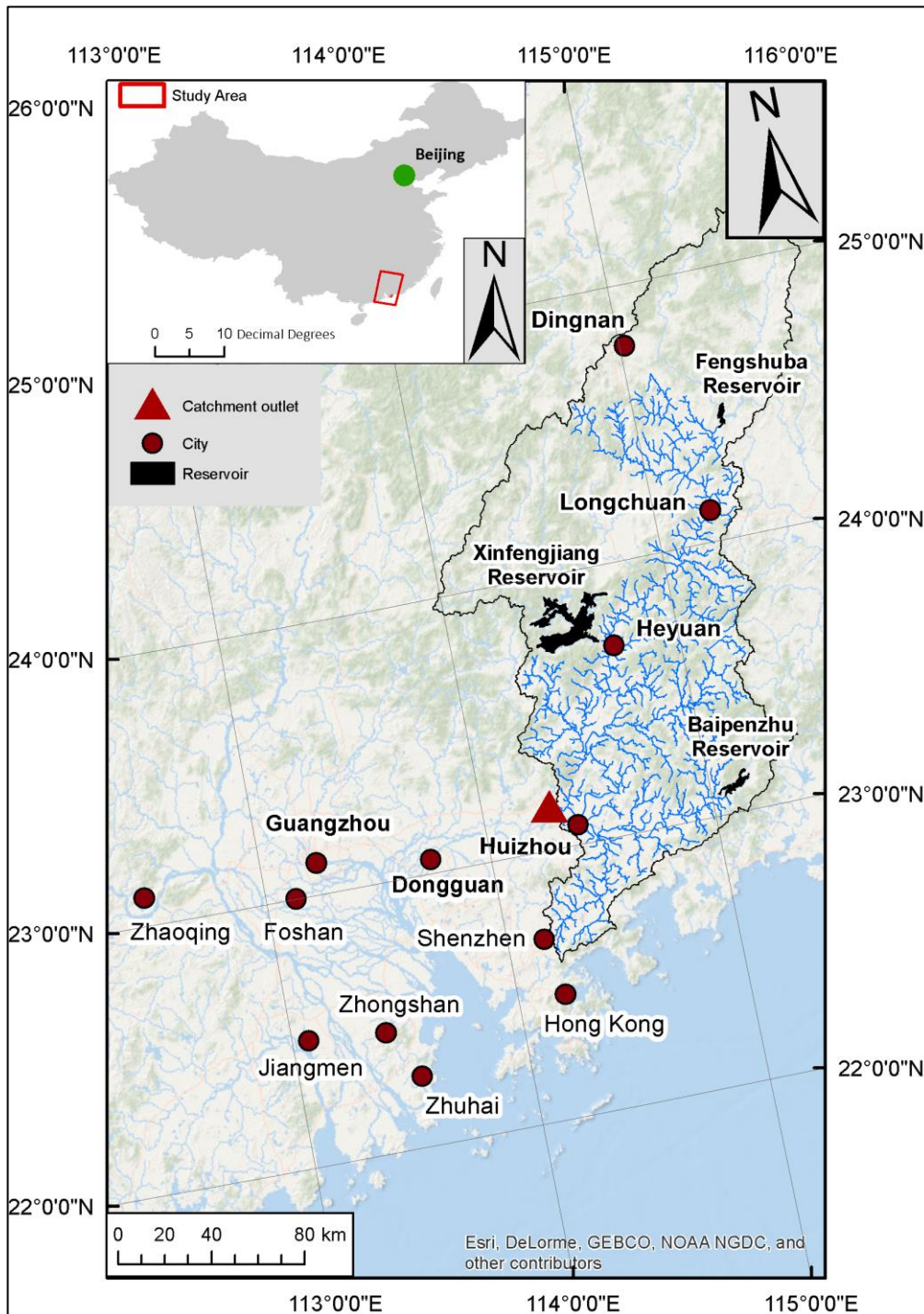


Figure 19 - The East river catchment a tributary of the Pearl river, South-East China. The study catchment's outlet is the Bolou river gauge, which marks the tidal limit.

China's economic reforms led to strong growth, initially focused upon the special economic zones and later extending along China's coastline. The Shenzhen special economic zone attracted large internal migration from other regions; its population increasing from 60,000 in 1980 to 6.07 million in 2000 (Oizumi, 2011). In 1985 the Pearl river delta open economic zone was established (Zheng, 2014). This includes the prefecture-level cities: Guangzhou, Shenzhen, Zhuhai, Foshan, Jiangmen, Zhaoqing, Huizhou, Dongguan and Zhongshan (Figure 19). The zone has demonstrated significant development, however the three peripheral cities: Huizhou, Jiangmen and Zhaoqing have performed less favourably with income levels below the mean for Guangdong province in 2009. This illustrates that although as a whole the region is of great importance, there is great disparity in wealth in China, even at the sub-provincial scale.

### 3.1.2. Water supply

The catchment is politically significant, as the source of the majority of the region's water supply, including perhaps most significantly, Hong Kong. Between 2004-2014, Hong Kong sourced ~64-89% of its water from the East river as a result of the Guangdong-Hong Kong Water Supply Agreement, which in 2015 was extended, guaranteeing 820- 1100 million m<sup>3</sup>/year (Hong Kong Legislative council research office, 2015).

The estimated total water resources (surface water and groundwater) of the East river in 2008 were 32.7 billion m<sup>3</sup>. From this, 10.7 billion m<sup>3</sup> was allocated to 8 different cities/regions. The cities: Hong Kong, Dongguan, Shenzhen, Heyuan and Huizhou heavily rely upon (~>70% reliance) the East river for water resources and are therefore vulnerable to further changes that may threaten water availability. In 2010 allocations for Heyuan, Dongguan and Shenzhen were exceeded; and forecasts for 2020 estimate that Huizhou,

Dongguan and Heyuan will exceed their allocations by 32%, 41% and 58% respectively (Su et al., 2011).

### 3.1.3. Water quality

Monitoring data between 2008-2010 shows a steady reduction in the area of the river basin which meets national water quality standards (Su et al., 2011). With increasing wastewater discharge, there are suggestions that by 2020, even with 100% of wastewater treated in the catchment to national wastewater treatment standards, water would still fail to reach national quality standards (Su et al., 2011).

As part of Guangdong socio-economic policy, industry has been encouraged to relocate from the more prosperous delta region to cities upstream such as Huizhou and Heyuan. Rapid development of industrial parks has been observed in these regions, which is likely to have environmental implications. But there are also concerns that this may expand further upstream into more ecologically sensitive regions (Su and Dao, 2012).

Various measures have been taken to ensure that clean water is provided for Hong Kong. Firstly, the water abstraction point on the East river was moved upstream in 1999, to a position with superior water quality (Hong Kong Water Supplies Department, 2015). The water is then stored within multiple reservoirs, with water within Shenzhen reservoir treated by a bio-nitrification plant and finally pumped to Hong Kong for final water treatment before consumption (Hong Kong Water Supplies Department, 2009).

Measures have also been taken to improve the water quality within the East river, including significant expansion of wastewater treatment facilities (Figure 24) and increased compensation flows from all major reservoirs in the dry season (Dongjiang River Basin

Authority, 2010; Dongjiang River Basin Authority, 2014). This has led to reports of improved water quality (Hong Kong Information Services Department, 2013; Kao, 2013). Further improvements are planned for the catchment which is likely to improve pre-emission contaminant removal throughout the catchment.

Effective management of the catchment is critical to avoid or mitigate these current and future threats. The East river catchment is therefore an ideal study area which will test the GREAT-ER model's capabilities as a management tool.

#### 3.1.4. East river seasonality

The catchment is subject to a sub-tropical climate which is dominated by a highly seasonal pattern of rainfall and flows (Figure 20 and Figure 21). Approximately 78% of rainfall falls between April-September, with frontal rainfall during April-June and monsoonal rainfall June-September (Chen et al., 2007). A long flow recession period follows the wet season, which ends with the dry season between December and February.

The GREAT-ER model accounts for the variability of flow based on the flow duration curve, which plots discharge against the percentage of time that flow will be equalled or exceeded. The flow duration curve may be considered a frequency curve if it is assumed that each data point within a time series for a catchment is independent of one another (Vogel and Fennessey, 1994; Tallaksen and van Lanen, 2004; Telis, 1991). This is an approximation, as the time series from one year will, to some extent, affect the next due to its serial nature and adjacent data points within a time series will also show strong correlation. The approximation of assuming elements within a time series are independent is less appropriate in both groundwater dominated catchments and catchments which experience a strong



seasonal variation in rainfall, for example monsoonal catchments. A catchment with a strong seasonality that is significant when compared with inter year variability will also show a strong trend and hence serial correlation within a year that will tend to repeat itself every year. Calculating low-flow statistics for each month separately, it can be argued, is more appropriate than calculating annual statistics as the influence of within year correlation is reduced within the analysis.

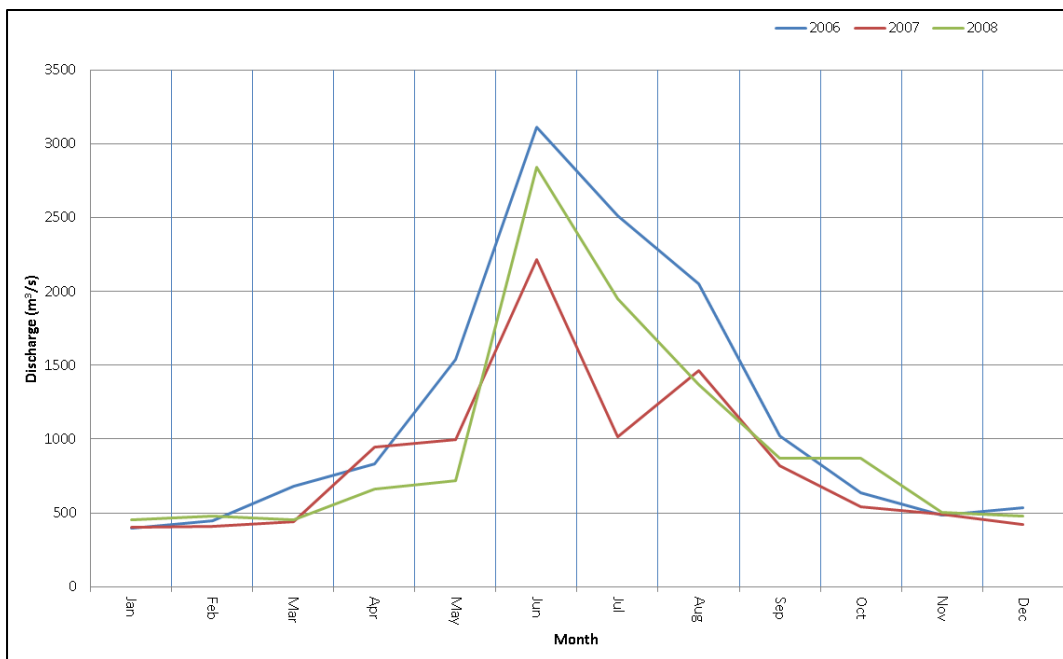


Figure 20 - Monthly discharge at Boluo gauging station for 2006-2008. There is strong seasonality, with much greater discharge in the summer, particularly June, in comparison to the rest of the year.

The difference in flow between the dry and wet season is approximately a factor of between 2 and 4 (Figure 21). However sampling campaigns within the region have presented conflicting data that suggests that the wet season may possibly produce conditions that lead to: higher concentrations (e.g. Figure 22), no significant difference in concentrations (e.g. Figure 23) or lower concentrations (e.g. Table 7) in comparison to the dry season for pharmaceuticals and personal care product (PPCP) ingredients such as TCS, TCC and

ibuprofen. This has also been noted in a semi-arid subcatchment of the Yellow river for estrogens and bisphenol A (Table 8), which was attributed to runoff driven diffuse sources (Liu et al., 2017).

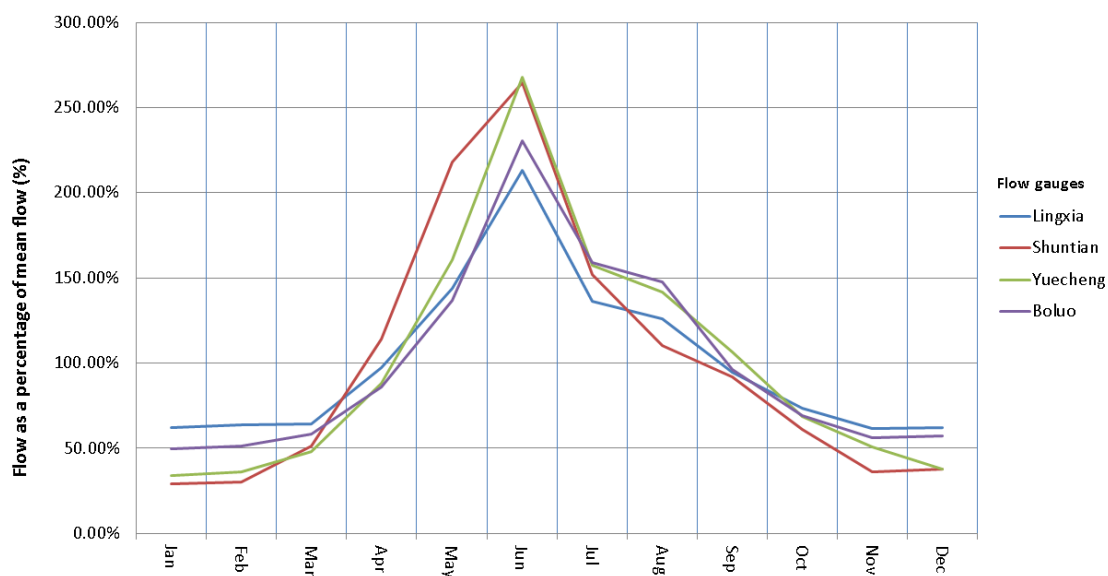


Figure 21 - Mean monthly flow (as a percentage of mean flow) at a selection of gauges in the East river catchment.

Figure 22 – Data from a sampling campaign in a rural subcatchment of the East River (downstream of our study site) (Zhang et al., 2015b). S1-S15 denote the sample site ID, for which S1-S12 are rural sites located downstream of a settlement that is known to discharge wastewater directly into the river. S13 is at the outlet to the East river, and S14 and S15 are sites on the East river. D, N and W denote samples taken in the dry (December, 2012), intermediate (March, 2013) and wet season (June, 2013) respectively. BT (columns shaded black on graph) denotes Benzotriazoles, which are chemicals commonly used in dishwasher detergents and anti-icing fluids (Giger et al., 2006). Biocides studied may be used as ingredients within personal care products (Zhang et al., 2015b).

Figure 23 – Data from sampling campaign in the Zhujiang, Liuxi and Shijing rivers, tributaries of the Pearl river (Zhao et al., 2010). Sampling sites S1-S3 were taken from the Liuxi river sites, S4-S10 were taken from the Zhujiang river, and sites S11-S14 were taken from the Shijing river. Samples were collected in the dry season (December, 2007) and the wet season (September, 2008). Overall Zhao et al. (2010) determined that there was no statistically significant difference between the concentration of chemicals from samples collected in the wet and dry season.

The difference in emissions and chemical removal between seasons is likely to be relatively small in comparison to dilution. Regarding emissions, certain products are likely to be used more often in the wet season, for example it is possible that residents may take more frequent showers in the hot and humid summer, therefore the use of soaps will likely to be greater. Although it is not likely this increase in usage will be large.

In regards to degradation, greater solar radiation will likely increase photodegradation, and increased water temperatures may increase biodegradation. It is generally accepted that increased temperatures enhance biological activity and processes. This will lead to lower exposure levels for chemicals for which these processes are significant.

Compound	Low-flow season		High-flow season	
	Concentration		Concentration	
	Range	Median	Range	Median
Estrone	8–65	34	ND-32	9
17 $\alpha$ -Estradiol	ND-2	1	ND-1	0
17 $\beta$ -Estradiol	ND-2	1	NQ	NQ
Estriol	ND-1	0	ND	ND
17 $\alpha$ -ethynylestradiol	ND-1	0	ND	ND
Mestranol	ND	ND	ND	ND
Diethylstilbestrol	ND-1	0	ND	ND
Methylparaben	NQ-1062	82	NQ-213	12
Propylparaben	8–2142	631	NQ-480	34
Butylparaben	ND	ND	ND	ND
Nonylphenol	36–33,231	2516	484–30,548	1284
Bisphenol A	6–481	106	13–881	36
Triclosan	48–1023	405	35–217	77
2-Phenylphenol	8–2506	112	NQ-400	30
Salicylic acid	9–2098	132	18–1440	52
Clofibric acid	NQ-248	46	22–59	35
Ibuprofen	ND-1417	360	ND-535	59
Naproxen	ND-328	181	ND-22	11
Gemfibrozil	ND	ND	ND	ND
5 $\beta$ -Coprostanol	10–2717	99	11–345	66

Table 7- Concentrations of PPCPs measured in samples collected from urban streams in the Pearl river delta (Peng et al., 2008). As shown, concentrations in the dry season are significantly higher than those in the wet season. ND denotes: not detected; and NQ denotes: detected, but not quantified.

Compounds	Wet season (ng/l)		Dry season (ng/l)	
	Range	Mean	Range	Mean
Estrone	ND-16	2.51	ND-4.46	0.85
17 $\beta$ -estradiol	ND-5.79	0.32	ND-2.52	0.24
Estriol	ND-10.5	0.86	ND-8.3	1.59
17 $\alpha$ -ethinylestradiol	ND	-	ND-0.86	0.03
E1-3S	0.06-14	1.48	0.05-1.7	0.51
E2-3S	ND-26.3	2.69	ND-5.8	0.98
Bisphenol A	1.06-1036	86.3	0.63-348	37.7

Table 8 – Data determined from samples collected from a semi-arid sub catchment of the Yellow river (Liu et al., 2017). Where ND denotes: not detected. The target compounds are known endocrine disrupting chemicals, apart from E1-3S and E2-3S, which are conjugates of E1 and E2 respectively. The concentration of the majority of compounds is greater in the wet season than the dry season.

It was noted by Zhao et al. (2010), that concentrations of PPCP ingredients were similar in the dry and wet season in samples taken in Guangzhou, South China (Figure 23). They suggested that there may be untreated water released from the >200 small urban dammed streams in Guangzhou during rainfall events in the wet season, which are normally pumped to STWs in the dry season. It is also possible that the volume of stormwater exceeded the capacity of the sewers, leading to wastewater spilling through combined sewer overflows (CSOs) (Field et al., 2003).

Greater concentrations of PCP ingredients in the wet season was also noted in the study by Zhang et al. (2015b), for which the focus was upon several small rural towns and villages. As shown in Figure 22. It is possible that the nature of rural wastewater treatment (e.g. wastewater storage ponds) in the area leads to the flushing of wastewater during large rainfall events in the wet season. However, there is no substantial evidence in either case.

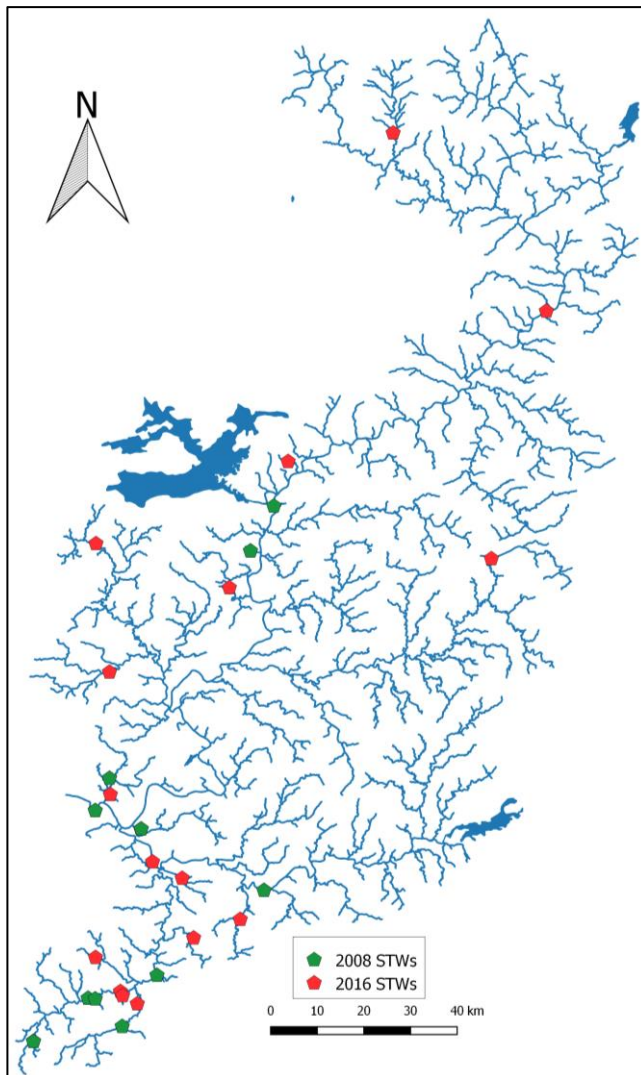


Figure 24 - Expansion of STWs in the East river catchment between 2008-2016.

A model is a representation of the modeller's understanding of system, therefore as this wet season mechanism is not yet understood, it is not possible to create a model for this season.

A model representing the dry season is possible, and in terms of dilution the dry season theoretically poses a greater risk.

### 3.1.5. Objective

The GREAT-ER model was used to simulate the concentration of two personal care product ingredients: TCS and TCC, and two natural estrogens: Estrone and Estradiol in the East river

catchment, South China. The model was used to generate exposure scenarios for the past, present and future. The past scenario was based upon the dry season of 2008/09, and attempts were made to validate the model using sampling data obtained in December 2008 by collaborators from the Guangzhou Institute of Geochemistry. The present scenario was based upon the 2015/16 dry season, with samples taken in January 2016 as part of this current study.

Finally, the model was used to simulate conditions in the dry season of January 2020, for which two scenarios were modelled. The first future scenario examined the effect of increased chemical emissions as a result of population change, mitigated by the development of sewage treatment infrastructure within the catchment.

The second scenario built upon the first, but focused upon catchment management. A hotspot analysis was performed to determine the areas of greatest concern and the main pollution sources. As a result, possible mitigation measures were designed and then incorporated into a catchment management scenario to estimate the effectiveness of each approach. This is described in more detail in section 3.10.

#### 3.1.6. Study region

A sub-catchment within the East river was selected. The outlet to the chosen sub-catchment is the Boluo river gauge (Figure 19), which marks the tidal limit. A simulation of the influence of the tide is unfeasible due to the complexities involved. The upper limit is marked by the three main reservoirs of the catchment, shown in Figure 24. The catchment upstream of these reservoirs is sparsely populated and unlikely to be of great risk from organic contaminants, outside of a few hotspots. It is challenging to sample the entire catchment with limited resources and it is more desirable to have a more focused campaign in a more

restricted area. As a result, the focus of this study was placed upon the catchment downstream of these reservoirs.

### **3.2. Subcatchment delineation**

Sub-catchments and the overall catchment for the East river were generated from the 1 arc-second SRTM DEM. The SRTM DEM was projected to an North Asia Albers equal area conic projection with a cell size of 25m. The Garbrecht and Martz (1997) D8 algorithm was utilised along with the AGREE burning in procedure (Hellweger, 1997). Riverlines were digitised using Google Earth for use of the “burning in” process. Riverline digitisation focused upon major stretches, major urban areas, river stretches that were sampled (see section 3.8) and those riverlines that connect to STWs. All digitised riverlines were connected to the outlet. The algorithm requires the following parameters:

- 1) Smooth drop - the depth that the cells intercepting the river line will drop (or raise), the cells within the buffer zone will then be interpolated in order to create a straight line between the river line and the elevation just outside of the buffer zone. Therefore, a greater value for smooth drop will lead to a steeper slope within the buffer zone
- 2) Sharp drop - the depth of which the DEM that intersects the river line will drop (or raise), which is performed after the smooth drop
- 3) The buffer width - defines the area that will be modified, adjacent to the river line (Hellweger, 1997).

After calibration, the optimum parameters for the AGREE algorithm were 50m sharp drop, 5m smooth drop with a 100m buffer. Riverlines were then generated from the DEM as



described in section 2.4 using a threshold of 1000 accumulating cells. Subcatchments were then generated as described in section 2.8, using the TauDEM GIS toolbox.

### *Evaluation*

Digitisation was focused on the main network and major urban areas. Streams that were not digitised were generated using the DEM alone, and therefore are subject to uncertainty regarding their flow path and catchment area. However, even digitised streams, may be affected by imperfect flow routing. Major urban areas are particularly vulnerable to this problem, for which the main tributaries are digitised and therefore are routed correctly. However, the minor flow paths that route runoff and wastewater from untreated subcatchments may be routed incorrectly. It is important to appreciate that the topographic flow paths and the wastewater flow paths may be significantly different on flat terrain; the similarity of topographic and wastewater flow paths becomes more likely as slope increases. These routing errors may result in the underestimation of chemical load locally on the main stream; this is due to the model routing wastewater to discharge at an outlet downstream of the actual outlet location.

Finally, there are a number of bifurcations and man-made diversions such as canals which are not represented within the model. It was not possible to determine and represent these features using the network generation methodology used.

### **3.3. Flow calculation**

The objective was to calculate the mean and the 95% exceedance flow (Q95) for each stretch in the river network for the months of December and January.

Three large reservoirs are located in the upper reaches of the catchment, all of which have a considerable influence upon flow. The Xinfengjiang (XFJ) reservoir is the largest reservoir at a capacity of 13.98 billion m<sup>3</sup> (Zhou et al., 2012b). This influence is shown within the flow duration curves for gauges downstream (Figure 26) and upstream (Figure 27) of the three reservoirs. In comparison to catchments upstream of the three reservoirs, high flows in catchments downstream of the three reservoirs are reduced, and low flows are enhanced. It is also probable that the river that flows through Heyuan, Huizhou, and Shenzhen city, in the downstream area of the catchment (Figure 19), is significantly influenced due to abstraction and wastewater release. However, these artificial influences, and others present within the catchment, are unquantifiable due to poor data availability. Therefore, the focus was upon the three major reservoirs.

To estimate natural flow, a regional regression approach was used. The principles behind this are described in Chapter 2. As the catchment is moderate in size and with only six gauges available with little or no artificial influences (see Table 9 and Figure 25), delineation of hydrologically homogenous areas was not considered.

Firstly, catchment descriptors that may possibly describe the spatial distribution of low flow were explored. The final selection of descriptors was based upon the correlation coefficient, the coefficient of determination, scatter graphs, and the validity of the conceptual basis between the descriptor and low-flow. Following this, the form of the regression model was chosen and further, parameters were estimated by ordinary least squares.

Further refinement of the natural flow estimate was required to take into account the influence of the three reservoirs. The overall approach chosen was largely dictated by data availability and the expertise of the modeller.

Daily flow data were extracted from physical copies of hydrological yearbooks for 2006-2013 for 11 gauges, 5 of which are downstream of a major reservoir and 6 which are considered to have limited artificial influence. In addition, outflow data for XFJ and Fengshuba reservoir were obtained for this period (Table 9). Additional outflow data for the three major reservoirs were provided by the Dongjiang river basin authority ([www.djriver.cn](http://www.djriver.cn)) for 2011-2016.

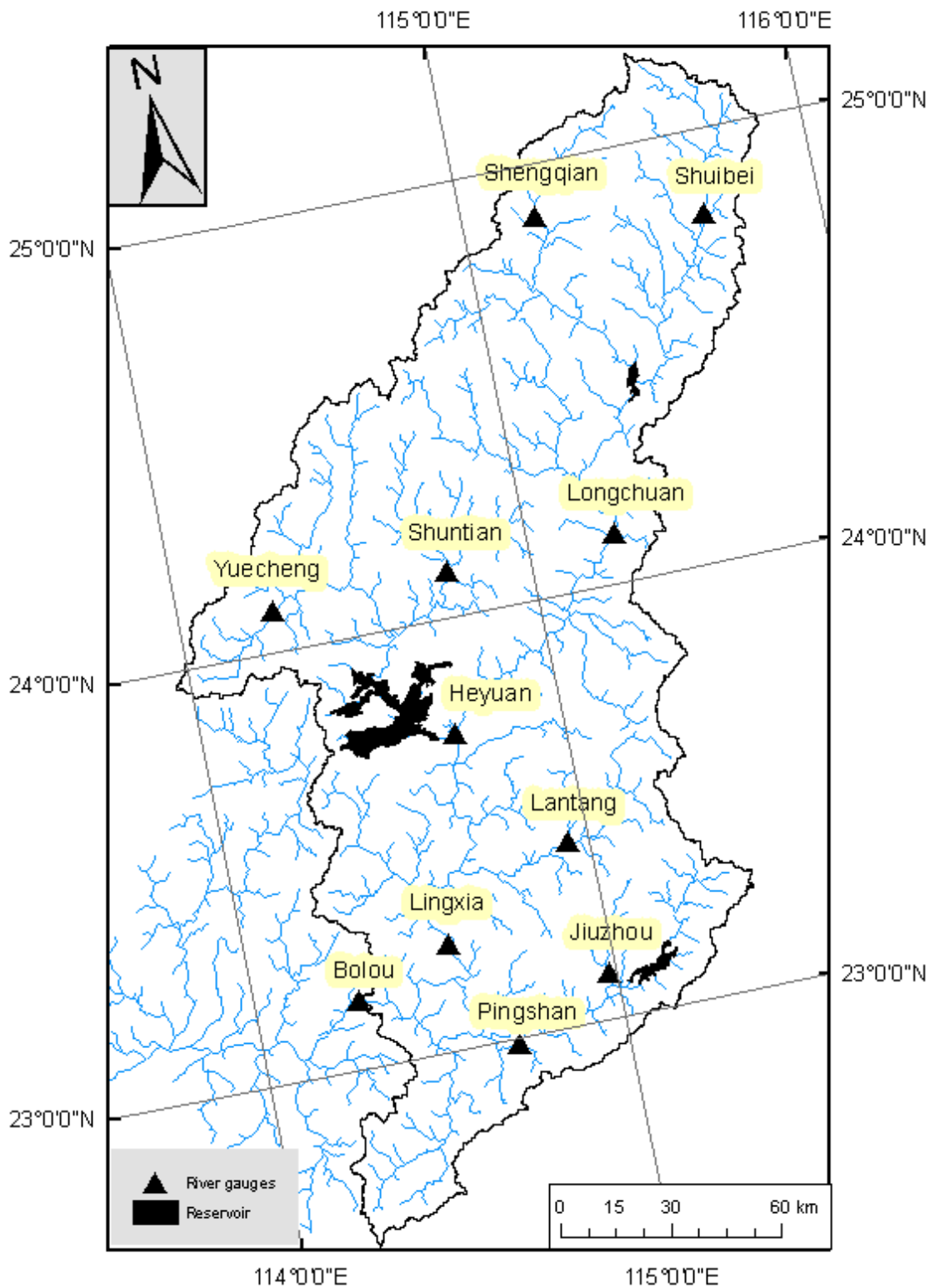


Figure 25 - Location of all river gauges within the East river catchment. Where, Jiuzhou, Lantang, Shuntian, Yuecheng, Shuibe and Shengqian are upstream of the three major reservoirs and are not affected by significant artificial influences.

Name	Catchment area (km <sup>2</sup> )	Flow data period	January flow (m <sup>3</sup> /s)		December flow (m <sup>3</sup> /s)		Upstream of reservoirs?	Longitude	Latitude
			Mean flow	Q95	Mean flow	Q95			
Longchuan	7699	2006-2013	125.4	82.2	114.4	55.6	No	115° 15'	24° 07'
Jiuzhou	385	2006-2013	3.1	1.8	4.9	1.9	Yes	114° 59'	23° 07'
Heyuan	15750	2007-2013	321.7	249	306	214	No	114° 42'	23° 44'
Lingxia	20557	2007-2013	364	296	362	261	No	114° 34'	23° 15'
Boluo	25325	2006-2013	377	287	437	290	No	114° 18'	23° 10'
Shengqian	751	2006-2013	6.9	3.2	8.2	2.7	Yes	115° 12'	24° 52'
Yuecheng	531	2006-2013	8.1	4.3	8.9	5.2	Yes	114° 16'	24° 06'
Shuntian	1357	2006-2013	12	3.2	15.8	5	Yes	114° 46'	24° 07'
Lantang	1080	2006-2013	7.8	4.9	10.5	4.9	Yes	114° 56'	23° 26'
Pingshan	2091	2006-2013	32.7	15.8	37	23	No	114° 43'	22° 59'
Shuibe	987	2009-2013	12	7.1	14.5	7.87	Yes	115° 41'	24° 48'

Table 9- River gauges, used within the East River catchment.

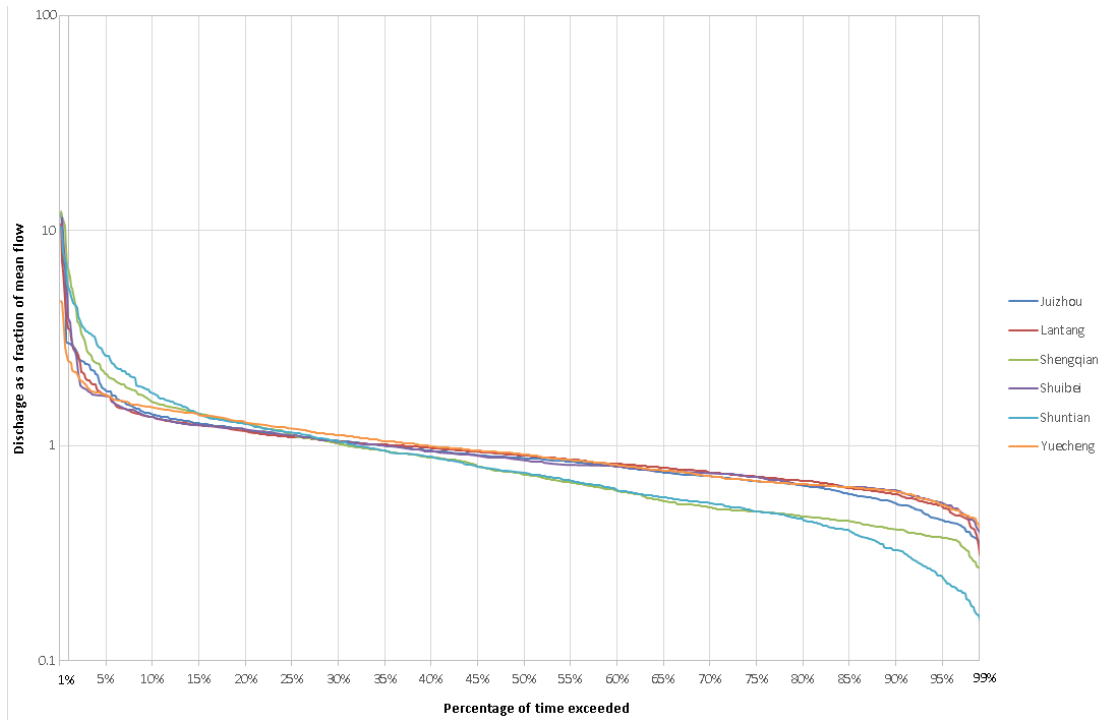


Figure 26 – Dry season (December – February) flow duration curves for the East river, where flow is normalised by mean flow ( $\text{m}^3/\text{s}$ ) - for gauges with little or no artificial influences.

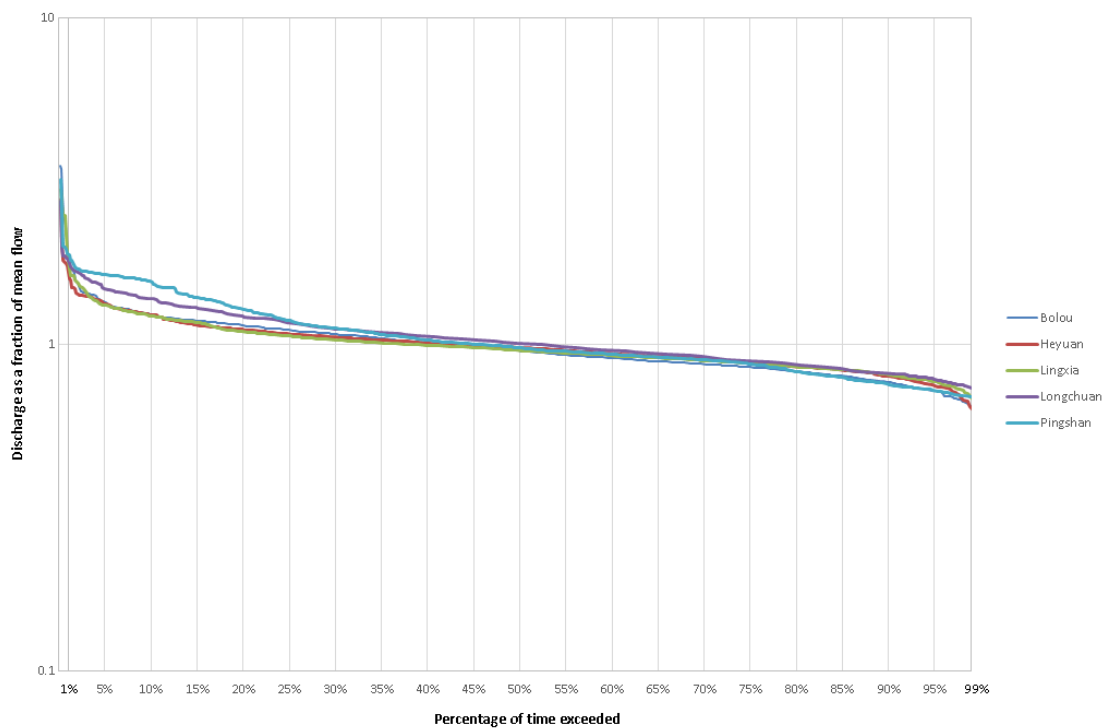


Figure 27 - Dry season (December – February) flow duration curves, where flow is normalised by mean flow ( $\text{m}^3/\text{s}$ )- for gauges with artificial influences. The curve is relatively shallow, as a result of reservoir containing flood waters and enhancing the flow in low-flow conditions (Su et al., 2011).

This was a shorter period than desired for the estimation of low-flow (Rees, 2009) and therefore the natural variability of natural flow may not be contained within the dataset. In addition, the inflow-outflow data for the major reservoirs in the catchment was from a slightly different period; the reservoir inflow-outflow data was for 2011-2016, whereas the river gauge data covered the period 2006-2013. This limitation relates to the difficulty of obtaining hydrological data in China; initial attempts to obtain flow data were met with some resistance. The data was located by a 3<sup>rd</sup> party in print format at a university library in Beijing, which had to be digitised manually. As a result, there was an implied limit to the amount of data that could be obtained.

### 3.3.1. Estimation of catchment descriptors

To estimate the mean value for each descriptor, the descriptor was used as a weight for the flow accumulation algorithm in a GIS. As shown in Figure 10, a flow accumulation algorithm involves calculating the number of cells that are upslope of each cell. The algorithm identifies all cells upslope to have a value of "1". However when applying this algorithm, a weight may be applied (e.g. slope), which changes the value of every cell from 1 to a parameter of interest (e.g. slope). Therefore, rather than estimating the number of cells that drain to a given cell, the sum of a given attribute can be generated, which may be divided by the number of accumulated cells to provide the mean.

The initial selection of catchment descriptors was determined based upon data availability and the nature of the catchment.

Low-flow is often driven by catchment storage which is characterised by the release of water stored in lakes, soil, groundwater and other catchment stores. The size of catchment stores

is likely to be important for the East river during the dry season. Therefore, catchment characteristics were chosen that may characterise the storage of water.

Spatial variation of precipitation may also be important. During the monsoonal period, precipitation is higher in the coastal Southern region and decreases to the North-West (Chen et al., 2007). However, other mechanisms are likely to be significant in the dry season.

Precipitation data and various other characteristics that may further describe precipitation in the area were also explored.

Prior to analysis, flow was normalised by catchment area, which minimises the effect of scale. Low flow indices were calculated from gauged data for the respective month only. Catchment characteristics were estimated as the mean for the catchment area for each gauge. Relationships between flow indices and catchment characteristics were examined using correlation matrices and scatterplots



### 3.3.2. Catchment descriptors

#### 1) Geology

Geology is an important descriptor of catchment storage, which is relatively complex within the East river catchment. However, the availability of geology data was limited. Data was available from Onegeology ([www.onegeology.org](http://www.onegeology.org)) at a scale of 1:2 million, with data on rock type and age. The percentage rock type was explored as a candidate descriptor.

#### 2) Soil

The harmonised water soil database (HWSD) (FAO et al., 2009) was used, which is a global dataset at the 30 arc-second resolution (~1km at the equator). The HWSD provides standardised parameters for soil data based upon multiple datasets across the globe. Various parameters are provided, some of which are estimated based upon other measured parameters. Bulk density, soil texture and soil drainage class were explored. Bulk density was estimated from soil texture using equations developed by Saxton et al. (1986) and soil drainage class represents drainage conditions based upon soil type, soil texture and soil phase.

#### 3) Land cover

Land cover data was obtained at a resolution of 0.5km, based upon moderate resolution spectroradiometer imagery (MODIS) (Broxton et al., 2014). The dataset was used to examine the effect of different land use types upon flow.

#### 4) Topography

The unmodified SRTM 1 arc-second DEM was used to generate various topographic characteristics for the catchment. Catchment area, mean elevation, slope, stream order and the mean distance to stream were generated.

#### 5) Precipitation data

A gridded global long-term mean monthly precipitation dataset, created by Hijmans et al. (2005), was obtained. This consists of a set of 12 grids each representing the mean monthly precipitation depth between 1950-2000. This was calculated using measured precipitation point data, interpolated using a spline algorithm based upon latitude, longitude, and elevation data.

#### 6) Direction and distance from an arbitrary datum.

A datum was arbitrarily placed in the North-East region of the catchment to explore the possible use of direction and distance from this datum to represent the effect of decreasing precipitation to the North-East. This was similar to the approach taken by Rees et al. (2004).

### 3.3.3. Candidate catchment characteristics

Conceptually, geology has a strong influence upon low-flows. Rock type is a potential descriptor of water storage within aquifers, which is released in times of low-flow. A strong, positive relationship between low-flow and plutonic rock (% of catchment area) was found (Table 10), which was unexpected. Plutonic rock is formed when molten rock cools and hardens beneath the surface, forming large crystals. Plutonic rock is neither permeable nor porous, with a lower water storage capacity than sedimentary and volcanic rock.

Sedimentary rock is associated with greater water storage capacities, lower runoff, but greater low-flows (Jowett and Duncan, 1990; Holmes et al., 2002a). However in contrast, in the United States, a low-flow study noted that much of the variation in low-flows may relate to overlaying regolith, which may have been of greater importance than the underlying bedrock (Smith, 1981). It is possible that this may be of relevance to the East river catchment. Less porous, crystalline bedrock in many areas may be overlain by significant, thick regolith which provides significant storage potential (Price, 2011).

Mean elevation displayed a relatively strong relationship with normalised mean flow (Table 10). Elevation is likely to be an indicator of precipitation, which tends to be high in upland regions.

Topsoil bulk density is a parameter provided by the HWSD, and represents dry bulk density (measured bulk density following being dried in an oven). The parameter may reflect the permeability of the soil and potential for soil water storage, porosity and hydraulic conductivity.

	January Q95	January Mean	December Q95	December Mean	Plutonic rock (% area)	Top soil bulk density (kg/dm <sup>3</sup> )	Mean elevation (m)
Plutonic rock (% area)	0.83	0.743	0.89	0.74	1.00		
Top soil bulk density (kg/dm <sup>3</sup> )	-0.88	-0.80	-0.87	-0.87	0.57	1.00	
Mean elevation (m)	0.60	0.84	0.54	0.71	0.33	-0.64	1.00

Table 10 - Correlation coefficients of significant characteristics and normalised low-flow indices.

As shown by scatter graphs in Figure 28 and correlation coefficients in Table 10, top soil bulk density appears to be the strongest predictor for both Q95 and mean flow. Only one

parameter was used for regression due to strong inter-correlation and a small sample set (Babyak, 2004). With additional gauges, it would perhaps be possible to improve the model whilst avoiding overfitting.

Bulk density was selected to describe normalised flow for December. This was also the case for January normalised Q95; however, January normalised mean flow was more strongly related to mean elevation than bulk density. However, to model two low flow indices with different spatial parameters is likely to result in, for some subcatchments, mean flow < Q95, which would not be a good prediction. Therefore, Q95/mean flow was calculated, which is described as the low-flow index. However, no relationship of sufficient strength was found for the low-flow index. To simplify, only bulk density was used for all low-flow indices. The disadvantage of this approach is that Q95/mean flow is relatively similar for all gauges, which does not reflect measured ratios. This approach is similar to a previous GREAT-ER study by Schulze and Matthies (2001), who estimated mean flow and Q95 flow using a separate regression model for each, using accumulated river length as the predictor; although the approach here is more complex.

The form of the regression model was explored. Other than performance, the form of regression must not produce a regression line which may result in negative flow.

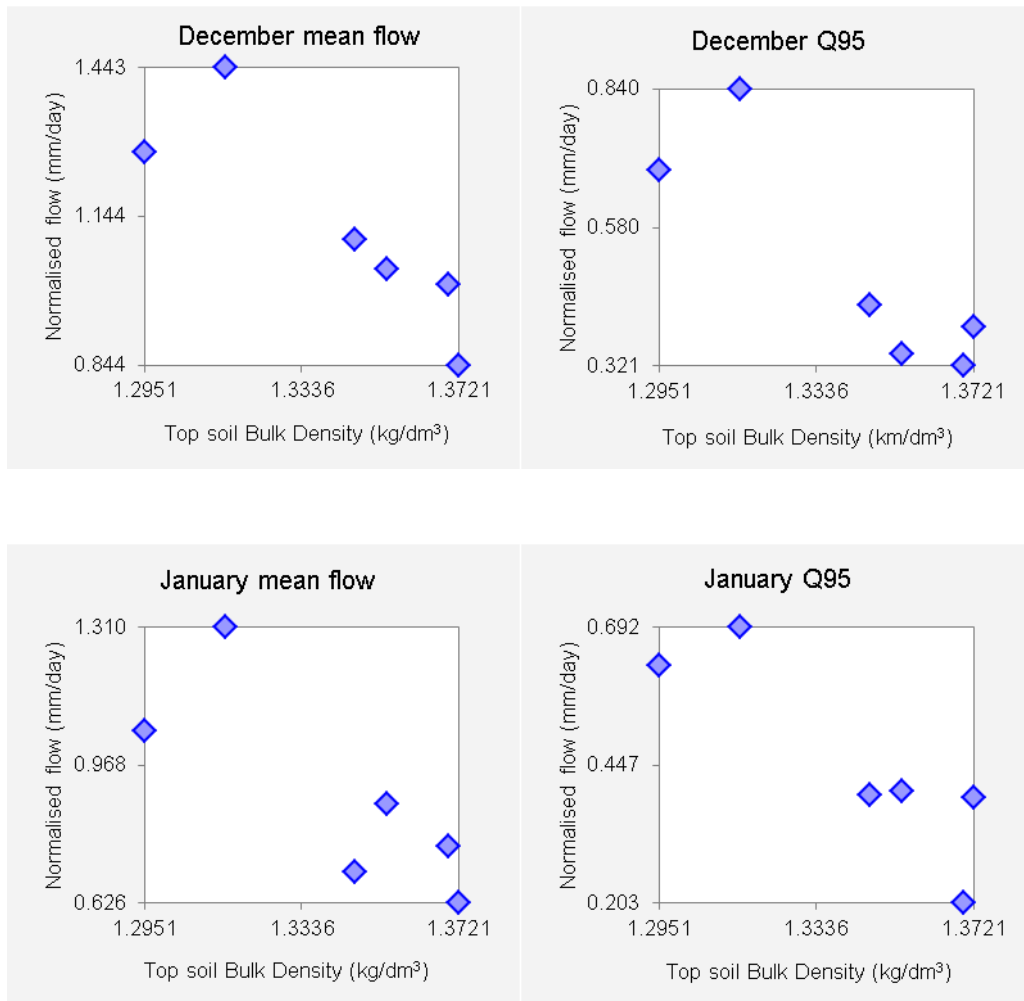


Figure 28 - Scatterplots displaying the relationship between flow indices and bulk density

The curve estimation function within the statistical software, IBM SPSS v22 was used to generate fitted regression lines and associated coefficient of determination for 11 different curve estimation models (Table 11). The exponential form was chosen, based upon performance for both Q95 and mean flow. The coefficients of performance are shown by Table 11. Equations generated (Equations 39-42) are shown below:

$$\text{Mean}_{\text{Dec}} = (2 \times 10^{-5} e^{-5.306 \times \text{BulkDensity}}) \quad (39)$$

$$\text{Mean}_{\text{Jan}} = (2 \times 10^{-4} e^{-7.201 \times \text{BulkDensity}}) \quad (40)$$

$$\text{Q95}_{\text{Dec}} = (0.0194 e^{-11.24 \times \text{BulkDensity}}) \quad (41)$$

$$\text{Q95}_{\text{Jan}} = (0.0262 e^{-11.55 \times \text{BulkDensity}}) \quad (42)$$

January Mean flow vs Bulk density		January Q95 flow vs Bulk density	
Equation	R <sup>2</sup>	Equation	R <sup>2</sup>
Compound	0.66	Compound	0.68
Power	0.66	Power	0.67
S	0.66	S	0.67
Growth	0.66	Growth	0.68
<b>Exponential</b>	0.66	<b>Exponential</b>	0.68
December Mean flow vs Bulk density		December Q95 flow vs Bulk density	
Equation	R <sup>2</sup>	Equation	R <sup>2</sup>
Compound	0.76	Compound	0.79
Power	0.76	Power	0.79
S	0.75	S	0.79
Growth	0.76	Growth	0.79
<b>Exponential</b>	<b>0.76</b>	<b>Exponential</b>	<b>0.79</b>

Table 11 - Coefficients of performance for different regression model types, generated using IBM SPSS v22. Bold indicates the selected regression form. Some regression types were not included here as they were deemed unsuitable.

### 3.3.4. Artificial influences to flow

Artificial influences to flow are significant within the East river catchment. Reservoirs may augment flow during low-flow periods and reduce flow during high-flow. Water abstractions

reduce flow, but vary significantly between seasons. Unfortunately insufficient data are available to account for abstractions. STWs discharge water from their outlets, which will augment flow. It is possible to obtain the average and maximum discharge rate for STWs that have been identified, which may be used to estimate the individual influence of a STW to flow.

### *Reservoir influence*

Three large reservoirs are located in the upper reaches of the catchment, all of which have a considerable influence upon flow, particularly low flows. The Xinfengjiang (XFJ) reservoir is the largest reservoir with a capacity of 13.98 billion m<sup>3</sup> (Zhou et al., 2012b). Therefore their influence must be accounted for within the model.

Flow was calculated for the outlets of all three reservoirs. The difference between reservoir outflows for January and December and the calculated mean and Q95 flow was observed (Table 12).

	Mean flow (m <sup>3</sup> /s)		Q95 (m <sup>3</sup> /s)	
	January	December	January	December
Baipenzhu reservoir	18.6	16.0	14.0	9.0
Fengshuba reservoir	45.3	-2.5	13.7	-12.6
Xinfengjiang reservoir	115.7	107.0	21.1	93.1

Table 12 - Difference between estimated and observed flow at the outlets of the three major reservoirs within the East river catchment.

### *STW influence*

In addition the influence of STW discharge was taken into account (Equation 43). The mean annual discharge (outflow) was available for STWs that were identified, which included all

STWs in the Huizhou/Shenzhen area and Heyuan city. Other STWs were not identified and therefore not accounted for.

*Artificial influence application*

The difference was applied to all stretches downstream:

$$\text{Adjusted}_{\text{stretch}(s)} = \sum_{i=1}^n (\text{Res}_{\text{diff}(i)}) + \sum_{j=1}^m (\text{STW}_{\text{disch}(j)}) + \text{Calc}_{\text{stretch}(s)} \quad (43)$$

where:

$\text{Adjusted}_{\text{stretch}(s)}$  - flow index for stretch(s), adjusted for artificial influences (m3/s)

$\text{Calc}_{\text{stretch}(s)}$  – natural flow index calculated for stretch(s) (m3/s)

$\text{Res}_{\text{diff}(i)}$  - arithmetic difference between the measured and calculated flow for the outlet of reservoir(i) upstream of stretch(s) (m3/s)

$\text{STW}_{\text{disch}(j)}$  - discharge from STW(j) (m3/s).

This is illustrated by Figure 29.



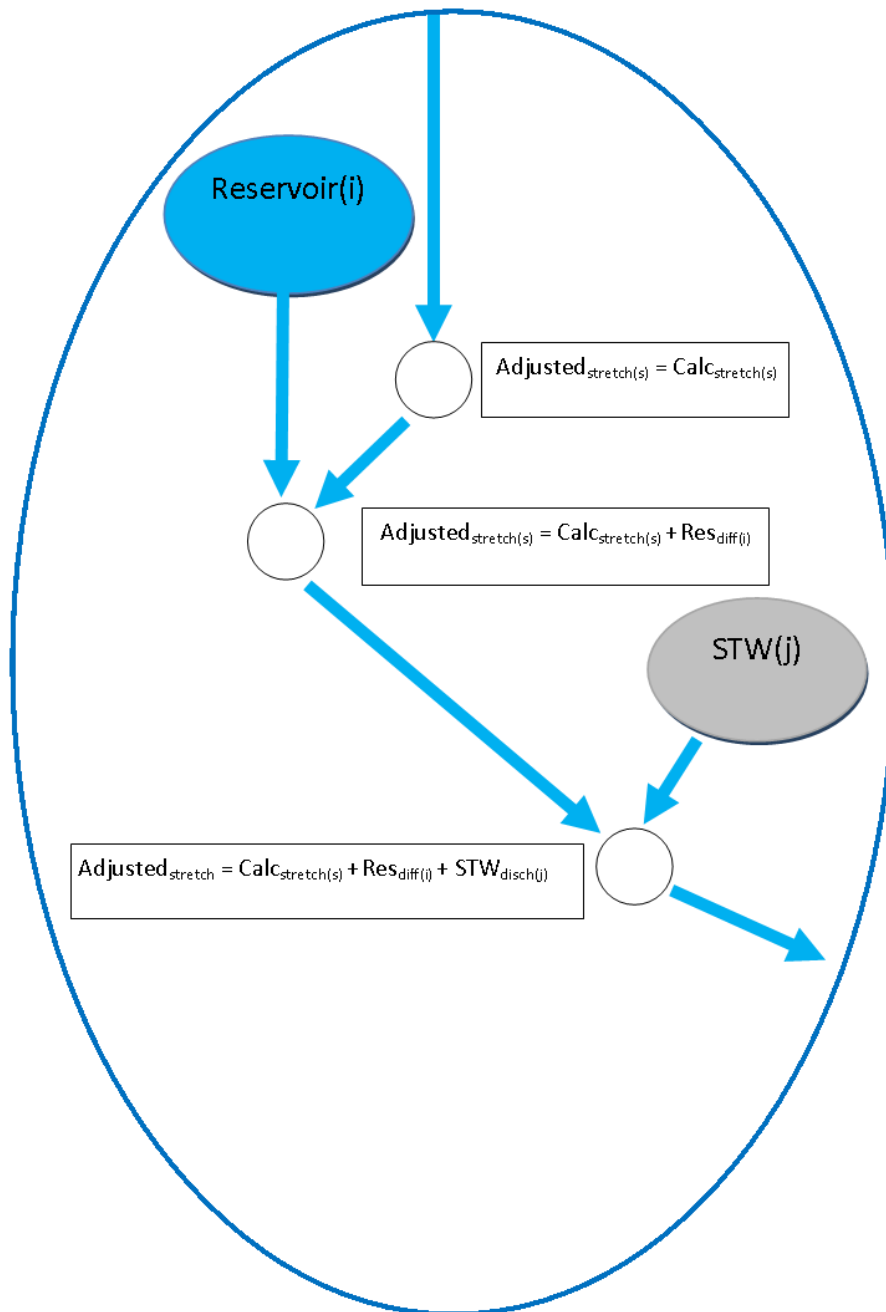


Figure 29 – The calculation of artificial influences to flow in a river network. Circles indicate nodes in the network.

Where:  $Adjusted_{stretch(s)}$  – estimated flow, taking into account influence from STW and reservoir outflows ( $m^3/s$ );

$Calc_{stretch(s)}$  - flow calculated for stretch(s) ( $m^3/s$ );  $Res_{diff(i)}$  - arithmetic difference between the measured and

calculated flow for the outlet of reservoir(i) upstream of stretch(s) ( $m^3/s$ );  $STW_{disch(j)}$  - discharge from STW(j)

( $m^3/s$ ).

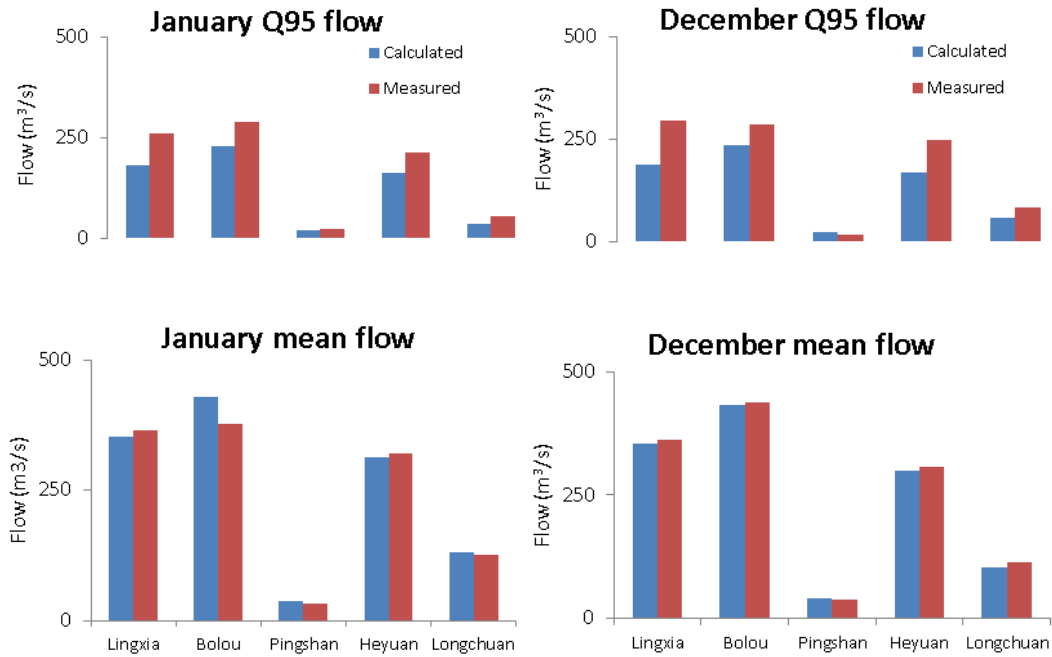


Figure 30 - Measured and calculated flow at river gauges; flow is calculated using Equations 39-42 and is subsequently adjusted for the influence of reservoir and STW outflow.

#### *Application of adjustment factors*

The flow estimated at the five gauges downstream of the three reservoirs, against measured flow, is displayed by Figure 30. The difference between estimated and actual mean flow is low, however this is not the case for the Q95 flow. Gauges downstream of XFI reservoir displayed the greatest deviation, especially at Heyuan and Lingxia gauges. This is likely to be largely the result of artificial influences that are not accounted for. During low flow, the proportion of flow from artificial sources is much greater (Young et al., 2000a) and the magnitude of these influences is likely to be quite high for these gauges. Characterising these artificial influences is unrealistic, and therefore a more pragmatic approach is to adjust the estimated flow by these downstream gauges.

This approach has been utilised in previous GREAT-ER studies (e.g. Young et al., 2000a; Schulze and Matthies, 2001; Schowanek and Webb, 2002). The approach here was modified

from Young et al. (2000a). The basis is that flow is adjusted by the proportion of measured and estimated flow at a gauged reach. It is assumed that estimated flow already accounts for the influence of the reservoirs. Each stretch is adjusted by up to two gauges upstream and the next downstream gauge. To determine the influence at each gauge (j), an adjustment factor (AF) is estimated as shown below:

$$AF(j) = \frac{Gauge_{meas}(j)}{Gauge_{est}(j)} - 1 \quad (44)$$

where:

$Gauge_{meas}(j)$  - measured low-flow index at gauge j ( $m^3/s$ )

$Gauge_{est}(j)$  - estimated low-flow index at gauge j ( $m^3/s$ ).

The reservoirs were also utilised as gauges, however the AF will always be 0 as the estimated flow was already adjusted to meet the low flow indices calculated at the reservoir outlet.

Flow is adjusted by at least one upstream gauge, and one downstream gauge. The flow is adjusted by taking into account of the relative (estimated) flow of the stretch and each gauge. Gauges with an estimated flow similar to the stretch have a greater influence.

Stretches that are closer to a gauge will generally have a similar estimate for flow and therefore the AF for this gauge is more influential than other gauges. However, using distance to determine similarity would not be appropriate as this does not account for other important factors such as catchment area and artificial influences. Therefore, for each stretch, weight factors (WF) were applied to each gauge (j) upstream or downstream of the stretch. WF defines the similarity of estimated flow at the stretch and the gauge (Equation 45 and Equation 46). This is calculated differently for gauges upstream and gauges downstream of the stretch. This is explained below:

$$WF(j) = \frac{Gauge_{est(j)}}{Reach_{est(i)}} \quad \text{- Gauge upstream of stretch} \quad (45)$$

$$WF(j) = \frac{Reach_{est(i)}}{Gauge_{est(j)}} \quad \text{- Gauge downstream of stretch} \quad (46)$$

where:

$Reach_{est(i)}$  - estimated low-flow index at reach (i).

The adjusted flow,  $Reach_{adjust}$  ( $m^3/s$ ), at each reach (i), is calculated differently for reaches with two upstream gauges and reaches with only one upstream gauge. The equations to calculate both are:

*Two gauges upstream:*

$$Reach_{adjust(i)} = Reach_{est(i)} \times \left[ 1 + \left( \frac{\sum_{j=1}^n WF(j) \times AF(j)}{\sum_{j=1}^n WF(j)} \right) \right] \quad (47)$$

*One gauge upstream:*

$Gauge_{est(up)}$  - estimated low-flow index at upstream gauge ( $m^3/s$ )

$$Reach_{adjust(i)} = Reach_{est(i)} \times \left[ 1 + \left( \frac{\sum_{j=1}^n \left( \left( WF(j) - \frac{Gauge_{est(up)}}{Gauge_{est(down)}} \right) \times AF(j) \right)}{\sum_{j=1}^n \left( WF(j) - \frac{Gauge_{est(up)}}{Gauge_{est(down)}} \right)} \right) \right] \quad (48)$$

$Gauge_{est(down)}$  - estimated low-flow index at downstream gauge ( $m^3/s$ ).

This is described using a hypothetical example as shown in Figure 31.

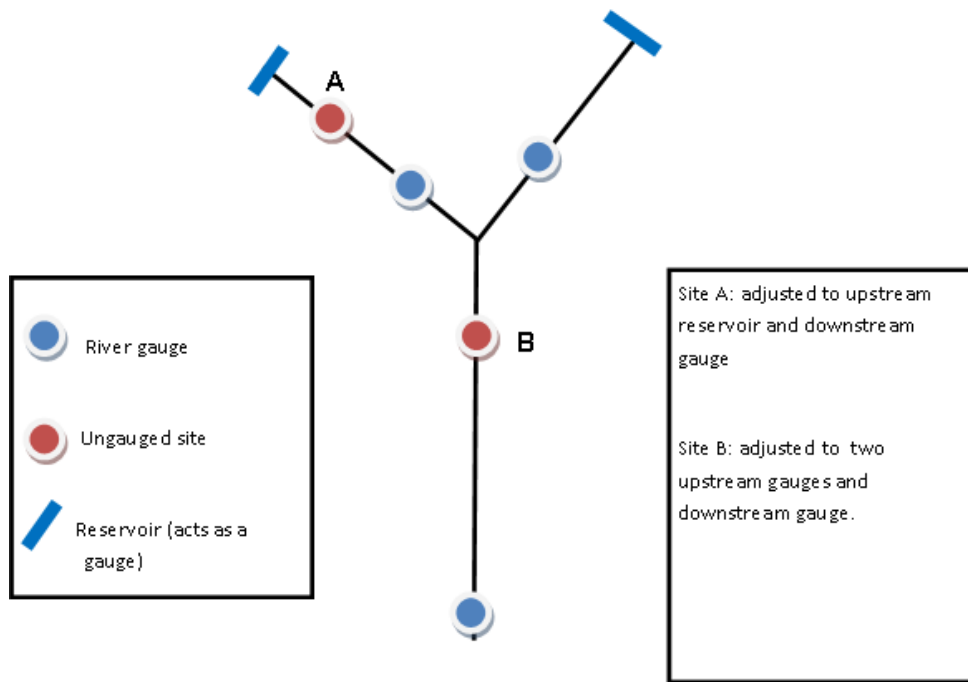


Figure 31 - Example of final adjustments to flow based upon flow gauges and reservoirs for ungauged sites in a hypothetical river network.

### *Evaluation*

The Shenzhen catchment, within the Huizhou sampling zone (Figure 38), is subject to numerous artificial influences. The outflow from STWs is accounted for by cumulatively applying the mean flow from STWs downstream. With many large STWs within a relatively small catchment, the flow increasingly becomes dominated by wastewater as the river passes through the main urban area. However, many of the artificial influences remain unaccounted for. Table 13 suggests that a large number of abstraction points could be located within the Huizhou zone. In addition, other than the three large reservoirs, a large number of smaller reservoirs are unaccounted for, including four small reservoirs in the Shenzhen subcatchment. As this catchment is ungauged, it is uncertain as to how accurate our estimate of flow was for this subcatchment.

The main stream within the Heyuan area required a relatively large correction to flow at Heyuan and Lingxia gauges. This suggests that a substantial number of artificial influences are unaccounted for, which may affect the accuracy of estimated flow in tributaries in areas that are downstream of urban area and are not corrected by a river gauge.

The rural area of Longchuan is mostly free of artificial influences to flow, other than the Fengshuba reservoir upon the main stream. Therefore, this region is primarily reliant upon the natural flow estimation.

	Guangzhou	Dongguan	Shenzhen	Huizhou	Heyuan	Shaoguan	Total
Class 1 tributaries	1	1	0	10	14	0	26
Large reservoirs	0	0	0	3	2	1	5
Medium reservoirs	6	8	4	19	12	0	49
Small reservoirs	0	4	0	1	0	0	5
Dykes protecting over 10,000 mu (1mu = 0.0667 ha)	4	2	0	17	0	0	23
Water extraction points	11	369	20	235	622	0	1257
Wastewater discharge outlets	0	6	0	13	0	0	19
Stairstep hydropower plants	0	1	0	2	11	0	14
Extractable river sediment (10,000 m <sup>3</sup> )	0	0	0	230.7	0	0	230.7

Table 13 - Table detailing the different artificial influences within the catchment in 2008, from Su et al. (2011).

### 3.4 E2 to E1 conversion

E2 biodegrades to E1 in the environment, and so this process was represented in the model. The assumption that one mole of E2 degrades to one mole of E1 was adapted from the approach by Williams et al. (2009). The model was first used to estimate E2 using a

combined first-order removal rate. Following this, E2 was simulated again, but with only biodegradation as a degradation mechanism. E2 losses via biodegradation were calculated for each stretch, noting the mean and standard deviation. This was then used as a diffuse input when modelling E1. The GREAT-ER sediment module provides a diffuse function, which allows the user to release the chosen chemical steadily along the stretch, using the mean and standard deviation as a distributed input from the Monte Carlo simulation.

### **3.5 Parameterisation**

Parameterisation of the model is described here with full details of the parameters used described in Table 14.

The initial parametrisation of chemical removal required the best available data from literature and models. A range of different values were obtained whenever possible. Distributions are not supported for in-stream removal rates, and therefore single values were used.

It was important to acquire reliable information regarding the removal of each respective chemical in-stream. This includes several tracer studies, process-focused laboratory experiments and a microcosm experiment. A tracer study involves the injection of a substance into the stream that may be used to track a single parcel of water downstream, in doing so water samples may be collected when the parcel passes set positions (Sabaliunas et al., 2003; Writer et al., 2012). A comparison of the concentration between set points may be used to determine the rate of removal in-stream, but is also important to take into account any additional dilution and other hydrological influences between sampling points (Writer et al., 2012). Process focused removal experiments tended to focus upon the rate of removal for single processes such as biodegradation or photolysis. This is the least preferable form of

analysis as removal under natural conditions tends to vary significantly in comparison to laboratory experiments (Robinson et al., 2007).

In the case of TCC and E1, data were available from only a single study each. For E1, it was noted that it is difficult to measure the removal under natural conditions due to the conversion of E2 to E1, as noted by Writer et al. (2012). Therefore a laboratory based experiment was used (Jürgens et al., 2002), which also provided degradation data for E2. For this study, water samples were collected from various rivers in the UK; these water samples were then spiked with a stock solution of E2. The samples were then regularly sampled to observe the biodegradation of E2, and subsequently, the by-product, E1 (Jürgens et al., 2002). In addition, the study also noted the effects of photolysis on a stock solution of E2, using a filtered Xenon lamp, configured to radiate at a spectrum similar to natural sunlight. Samples were taken daily to note the change in concentration of E2 as a result of photodegradation (Jürgens et al., 2002).

A single plume study was also available for E2 (Writer et al., 2012), in which the conservative tracer bromide was released into a stream in the US, and samples were collected at two sites downstream of a STW. In-stream removal was calculated based upon the change in mass, relative to bromide. This study produced similar results to the laboratory study mentioned above (Jürgens et al., 2002). As such the results from the study by Jürgens et al. (2002) were utilised in order to estimate the effects of biodegradation alone, which is used to determine the conversion of E2 to E1.

As GREAT-ER v3 does not allow for in-stream removal distributions, it was deemed necessary to run the model for several in-stream removal scenarios for TCS. For E1 and E2, the biodegradation rate used was the median of a large number of samples taken for a single study within a river in the UK (Jürgens et al., 2002). It would have been valuable to be able



to define a distribution for in-stream removal, or to be able to assign in-stream removal to vary in space, and/or time.

When parameterising STW removal rates, data was obtained for activated sludge (AS), trickling filter (TF) and other treatment types. All identified STWs were determined to be AS and those not identified were assumed to be AS. This was reflected by the STW list for the area, which suggested the majority of STWs were AS. Unfortunately, data for sub-types of STWs were limited and therefore disregarded.

From published literature, 43, 15, 54 and 41 estimates of STW removal were obtained for TCS, TCC, E1 and E2 respectively. Literature which focused upon studies of STW removal of the target chemicals was used, with no restriction to geographic area. Ideally, it would have been best to focus upon Chinese STW literature. However, it was deemed more important to acquire a larger sample size. Although a significant amount of data was collected, there is still a need for more data on STW removal. It is particularly important for data to be made available for different sub-types of STW, which may vary significantly in performance.

However, it was not always possible to identify the treatment sub-type of the STW within the study catchment.

Usage data for TCS and TCC was estimated and described by Zhu et al. (2016). In summary, personal and home care products that are both sold to the Chinese market and include TCS and TCC were identified. The tonnage of these products sold to the market and the inclusion levels of chemicals within each product were then identified, providing an estimation of chemical usage across China. Then, as described by Hodges et al. (2014), the usage was distributed across China by linking product affordability to GDP. In China, wealth is not distributed evenly and therefore higher value products may not be affordable to all. This is especially the case in rural regions, where usage of personal care products is likely to be

significantly lower. GDP data was available at the county administrative level and therefore usage for each county was estimated.

An estimate for usage (excretion rate) for E1 and E2 was generated from data acquired by back calculation based upon the concentration of Chinese STW influent concentration, flow and known STW served data. This is based upon the approach of Liu et al. (2015). This was calculated by acquiring data about STW population served, STW discharge rate and measured estrogen concentrations within influent. Usage was then calculated using:-

$$E = \frac{D}{P} * C \quad (49)$$

where:

E - estimated estrogen usage rate per capita per day (kg/cap/year)

D - STW average discharge rate per year (m<sup>3</sup>/year)

P - STW population served estimate

C - measured estrogen concentration in effluent (kg/L).

Chinese data was used exclusively as it has been suggested that the excretion of estrogen varies significantly between western and Chinese populations (Xu et al., 2012; Adlercreutz et al., 1994; Trichopoulos et al., 1984). This is partially related to the proportion of females and the proportion of post-menopausal women (Johnson et al., 2000); menstruating women excrete significantly more than post-menopausal women, whilst post-menopausal women excrete significantly more than men. Within the Chinese population, the proportion of females is relatively low (48.5% of population was female in 2016) in comparison with the EU and North America (51% and 50.5% respectively) (World Bank, 2017).

Outliers were identified and removed by means of box-plot analysis. A standard Tukey methodology (Tukey, 1977) was used to identify outliers, where suspected outliers were

identified as 1.5 - 3 \* interquartile range, and outliers are identified as those values >3 \* interquartile range. Boxplots were examined (Figure 32) and it was determined that potential outliers were likely to be true outliers as a result of a visual check and, therefore, all outliers and potential outliers were removed. These outliers are likely to be a result of errors in chemical analysis, a lower than normal STW discharge (dilution) or errors with population served estimates. As a result, 5 and 1 estimates were removed for E1 and E2 respectively. STW data was not found to be normally or log-normally distributed (established via a Shapiro-Wilk test (Shapiro and Wilk, 1965), performed in IBM SPSS v22). However, usage data for E1 and E2 were determined to be log-normal, with a significance value on 0.264 and 0.362 for E1 and E2 respectively. For E1 and E2, 32 estimates of usage were calculated for each chemical.

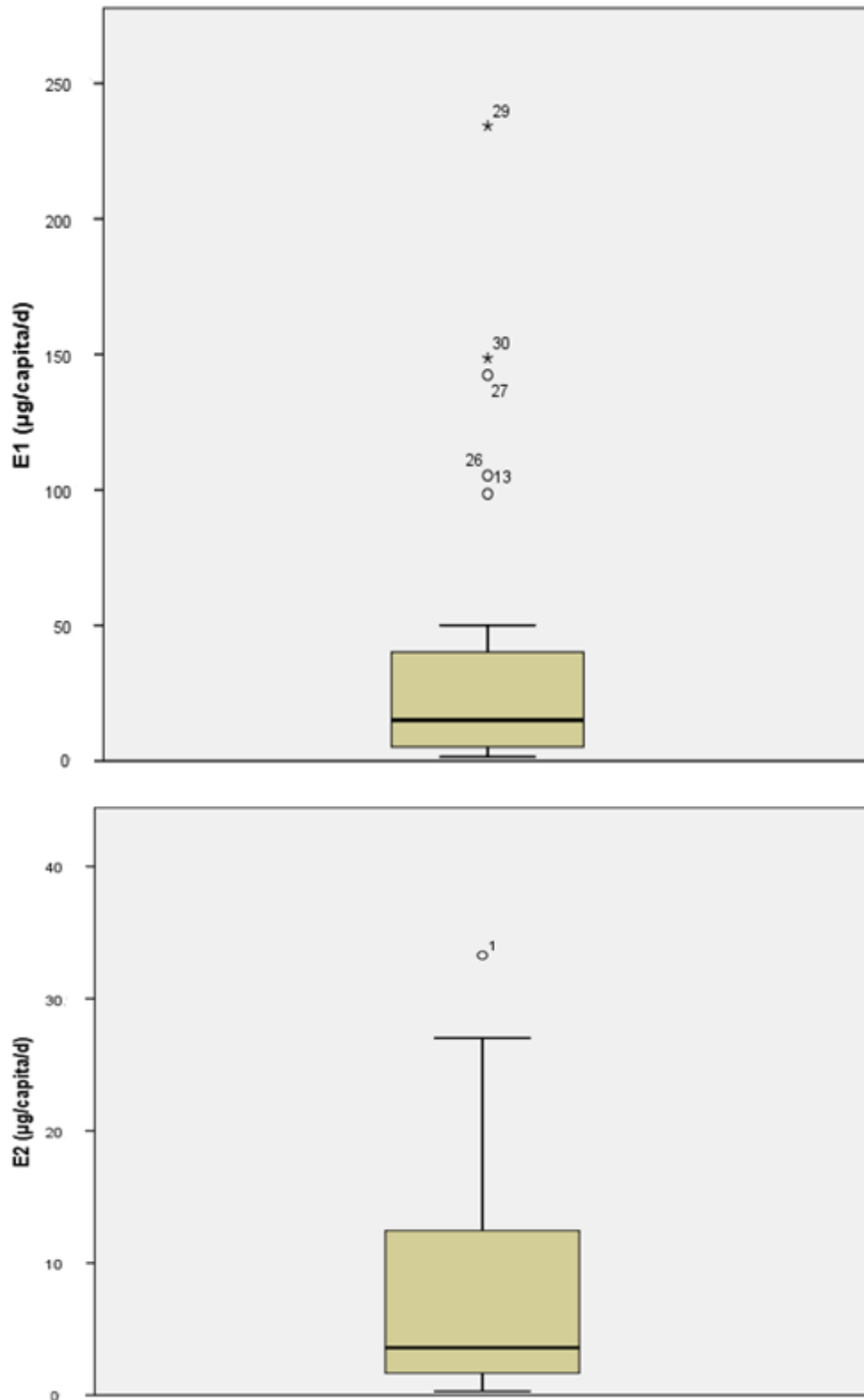


Figure 32 - Boxplots for calculated usage of E1 and E2. Open circle represent possible outliers (1.5-3 \* interquartile range) and asterisks represent extreme outliers (>3 \* interquartile range).

	<b>STW removal (%)</b>			
TCS <sup>1</sup>	45 - 99			
TCC <sup>2</sup>	51 – 97.5			
E1 <sup>3</sup>	<b>47.3 – 99.9</b>			
E2 <sup>3</sup>	39.4 – 99.4			
<b>Usage</b>	<i>Spatially distributed (by county)</i>			
<b>kg/capita/year</b>	<b>Mean</b>	<b>Standard deviation</b>	<b>Min</b>	<b>Max</b>
<b>TCS</b>	1.67E-4	5.9E-5	1.02E-4	3.12E-4
<b>TCC</b>	7.4E-5	2.5E-5	4.7E-5	1.3E-4
<i>Lognormal distribution</i>	<i>Spatially uniform</i>			
<b>kg/capita/year</b>	<b>Mean</b>	<b>Standard deviation</b>		
<b>E1 <sup>3</sup></b>	6.18E-6	7.80E-6		
<b>E2 <sup>3</sup></b>	3.21E-6	5.80E-6		
<b>In-stream removal k (h<sup>-1</sup>)</b>				
	TCS	E1	E2	E2 biodegradation only
<b>TCC</b>	<b>0.0138 <sup>4,a</sup></b>	<b>0.00983 <sup>5,b</sup></b>	<b>0.0132 <sup>5,b,c</sup></b>	<b>0.0103 <sup>5,b</sup></b>
	0.0610 <sup>6</sup>			
	0.210 <sup>7</sup>			
<b>Sorption</b>	TCS	TCC	E1	E2
<b>KOC <sup>e</sup> (L kg<sup>-1</sup>)</b>	15892 <sup>8, d</sup>	48865 <sup>8, d</sup>	3709 <sup>9</sup>	2378.3 <sup>10, e</sup>
<b>Fraction organic carbon</b>	0.1	0.1	0.1	0.1
<b>Mean suspended solids concentration (mg/l)</b>	18	18	18	18
<p>Table 14 - Parameters used for input into the GREAT-ER model.</p> <p><sup>1</sup> - Bendz et al. (2005); Bester (2005); Dotan et al. (2016); Gómez et al. (2007); Guerra et al. (2014); Heidler and Halden (2007); Kanda et al. (2003); Kasprzyk-Hordern et al. (2009); Lishman et al. (2006); McAvoy et al. (2002); Nakada et al. (2006); Sabaliunas et al. (2003); Schatowitz (1999); Singer et al. (2002); Thompson et al. (2005); Waltman et al. (2006); Winkler et al. (2007); Ying and Kookana (2007); Yu et al. (2006)</p> <p><sup>2</sup> - Yu et al. (2011); TCC Consortium (2002); Ryu et al. (2014); Lozano et al. (2013); Heidler et al. (2006); Guerra et al. (2014)</p> <p><sup>3</sup> - Liu et al. (2015); Dotan et al. (2016); Lishman et al. (2006)</p> <p><sup>4</sup> - Lv et al. (2014)</p> <p><sup>5</sup> - Jürgens et al. (2002)</p> <p><sup>6</sup> - Reiss et al. (2002)</p> <p><sup>7</sup> - Sabaliunas et al. (2003)</p> <p><sup>8</sup> - Wu et al. (2009)</p> <p><sup>9</sup> - Yu et al. (2004)</p> <p><sup>10</sup> - Holthaus et al. (2002); Yu et al. (2004)</p> <p><sup>a</sup> - Based upon mean value of an experiment by Lv et al. (2014), whom exposed water samples collected from the Jiulong river (South China) to a number of different conditions. For this study, the mean value of removal rates for "Light surface" samples was used for Triclosan and Triclocarban, which represents a condition where river water is exposed to natural sunlight. This provided a combined estimate for biodegradation and photodegradation under climatic conditions similar to that of the East river.</p> <p><sup>b</sup> - Based upon the median value of biodegradation experiments by Jürgens et al. (2002). The value estimated by Jürgens et al. (2002) was determined for 20°C. Furthermore an estimate for the mean temperature observed during sample collection in January 2016, 16degrees C. This was calculated using the modified Arrhenius equation: <math>KT=K20 \times \theta^{(T-20)}</math>. For which KT: K at temperature T; K20: K at temperature 20 degrees C; <math>\theta</math>: Arrhenius temperature coefficient. For E2, <math>\theta = 1.075</math> (Liu et al., 2015). To estimate the conversion of E2 to E1, the estimation for biodegradation was used alone.</p> <p><sup>c</sup> - Also based upon photodegradation experiments by Jürgens et al. (2002).</p> <p><sup>d</sup> - Estimated KOC values were selected for two soil types: sandy loam and silty clay. The catchment is predominately formed of the fine grained red soil, and therefore the KOC value for the silty clay was used.</p> <p><sup>e</sup> - The mean KOC value was used out of the values estimated by two studies.</p>				

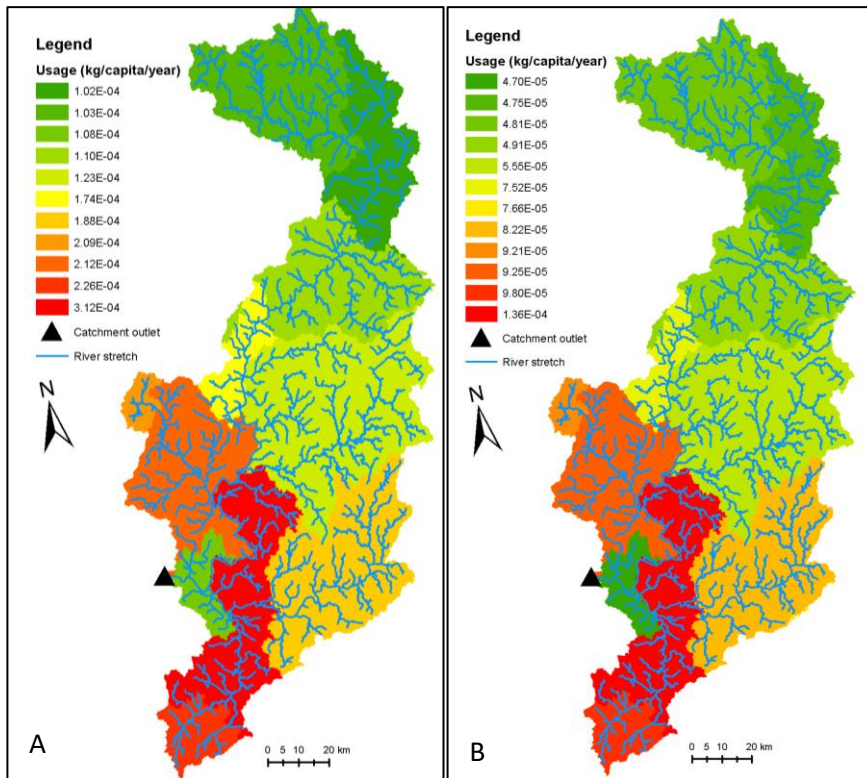


Figure 33 - Estimated spatial distribution of (A) TCS and (B) TCC usage.

### 3.4.1 Sensitivity analysis

In order to determine the relative importance of model parameters, a sensitivity analysis was performed. Understanding the relative importance of parameters may be useful to determine, for example, which parameter would be most useful to collect further data for, in order to better define the parameter.

The model parameters were adjusted by +/- 20%, one-at-a-time, and the relative change in modelled concentration was observed.

### **3.5 Wastewatershed delineation**

Wastewatershed delineation was performed as discussed in Chapter 2. Delineation within Huizhou and Shenzhen city (Figure 38) required additional information regarding population served by STWs, which was obtained from internet sources and communicating with STW plant operators. However, for many of the STW plants this information was not available and therefore it was estimated as described in Chapter 2.

The accuracy of the STW population served estimates, and the area served by each STW is uncertain. Actual population served data was available only for STWs in city areas, and without this data it would have been very difficult to estimate the population served, as there was no way to determine the extent of the wastewatersheds in a continuous urban area (e.g. Figure 17). A similar approach to estimate population served was described by Keller et al. (2006) for use in the UK; they found that their methodology produced reliable results in comparison to actual data.

The delineation methodology is subject to arbitrary decisions, although an attempt had been made to mitigate this. This is more significant in large urban areas where boundaries are difficult to identify. This was acknowledged by Keller et al. (2006). Outside of large cities, the effects of the variance caused by arbitrary decisions are likely to be minimal outside of high risk areas as the decisions are more constrained. In these areas further investigation should be considered.

### **3.6 Population**

A gridded population dataset is essential to predict spatially explicit emissions across the catchment. A population dataset is used to determine the population served and/or the area served by each sewage treatment plant. The population served by a STW can be used to

determine a site specific chemical emission and to calculate the spatial distribution of diffuse emissions.

There are a limited number of gridded population datasets available at the appropriate resolution. Most notable are Landscan (Bright et al., 2011), Worldpop (Gaughan et al., 2013) and the Gridded Population of the World version 4 (GPWv4) (CIESIN, 2016a). GPWv4 utilises raw census data and applies that to the respective vector based census boundary. This is converted to raster, assuming a uniform distribution throughout the census area. Landscan and Worldpop utilise census data similarly, however they also utilise additional datasets such as road networks and nightlights to predict the spatial distribution of population within the census boundaries.

GPWv4 lacks spatial variability within census boundaries (e.g. Figure 35) and therefore is unsuitable for the working scale. This is particularly problematic in rural areas, within which boundaries are large. The Landscan dataset, whilst allowing for spatial variation within census boundaries, utilises data from the previous census in 2000. GPWv4 and Worldpop utilise the latest census in 2010.

Worldpop distributes population count at a relatively high resolution of approximately 100m at the equator. However, the population is distributed in such a way that overestimates the population in rural areas and green spaces at the cost of urban areas. As shown by Figure 34, the green fields in the North-West of the mapped area have been identified as containing little or no population by Landscan, whilst Worldpop identifies the area to contain a low, but still significant population; this is clearly incorrect, and will lead to overestimated population outside of urban areas, and underestimated population in urban areas. The population distribution should be highest in the areas containing housing, as shown by the satellite imagery in Figure 34C. Landscan appears to represent the population distribution more accurately, but does not utilise the most recent census data. Therefore, a new dataset was



required. GPWv4 can be used to adjust Landscan to better reflect recent high resolution census data. This results in a dataset that is far more reliable and trustworthy on the back of high quality census data. It was assumed that the census data used by GPWv4 was reliable and reflected the true population in 2010. It is also assumed that population had not significantly changed between December 2008 and 2010.

The boundaries used by GPWv4 were not freely available. However, it was possible to backwards calculate in order to recreate them. The slice tool within the ArcGIS spatial analysis toolbox was used using the "natural breaks" setting. This reclassifies the data into its natural groupings (groups similar values) whilst maximising the differences between the classes (<http://desktop.arcgis.com/en/arcmap/10.3/tools/spatial-analyst-toolbox/slice.htm>). Cell values within a boundary are identical as they are grouped together by the tool and reclassified as such. This allows the resulting raster to be converted to polygons. The flaw in this method is that the developers of GPWv4, CIESIN (2016a) assigned cells that lay on the boundary to share the value of all intersecting boundaries. And therefore these cells are unique and when backcalculating census boundaries, these cells were grouped only with themselves. This effect is shown by Figure 36. Furthermore, the eliminate tool in ArcGIS spatial analysis toolbox was used to assign the majority of these unique cells to surrounding polygons. The eliminate tool merges selected polygons with neighbouring polygons that have the largest shared border.

The polygons are used to determine the sum of population within each boundary for GPWv4 and Landscan. Furthermore the total population in each boundary area is adjusted to that registered by GPWv4 whilst retaining the population within each cell relative to the original total population in its census boundary. This was achieved using the ArcGIS toolbox raster calculator, using the following equation:

$$\text{AdjustedPop} = \text{Census polygon sum} * \left( \frac{\text{RasterPopValue}}{\text{RasterPopPolygon}} \right) \quad (50)$$

where:

AdjustedPop - adjusted population value of a cell within the raster being modified

Census polygon sum - total census population within a given census boundary

RasterPopValue- value of a cell within the raster being modified

RasterPopPolygon - within a given census boundary, the population sum calculated from the population raster being modified.

A final adjustment was made to correct against population data for each city region within the catchment. Population data for the city regions within the catchment was obtained from the 2010 census for Guangdong and Jiangxi provinces. This was achieved using Equation 50 above. This adjustment was made to solve modest differences between the adjusted dataset and the census data, but also to ensure consistency when upgrading the population.

To create the population dataset for the 2016 model, data were obtained from the 1% population survey in 2015. This survey is a stratified sample designed to provide an estimate for population within a full census. It is assumed that it is accurate. This upgrade was performed using Equation 50. Again, it was assumed that population had not changed significantly between 2015 and 2016.

This approach results in all data cells within a city boundary increasing in proportion to the change in population for the containing city region as a whole. As a result, greenfield construction sites that were developed between this period are still considered to be undeveloped by the 2015 population dataset. As a result, emissions are underestimated for subcatchments that contain significant new developments.

However overall, this adjustment enabled greater confidence in our predictions of point and diffuse emissions.

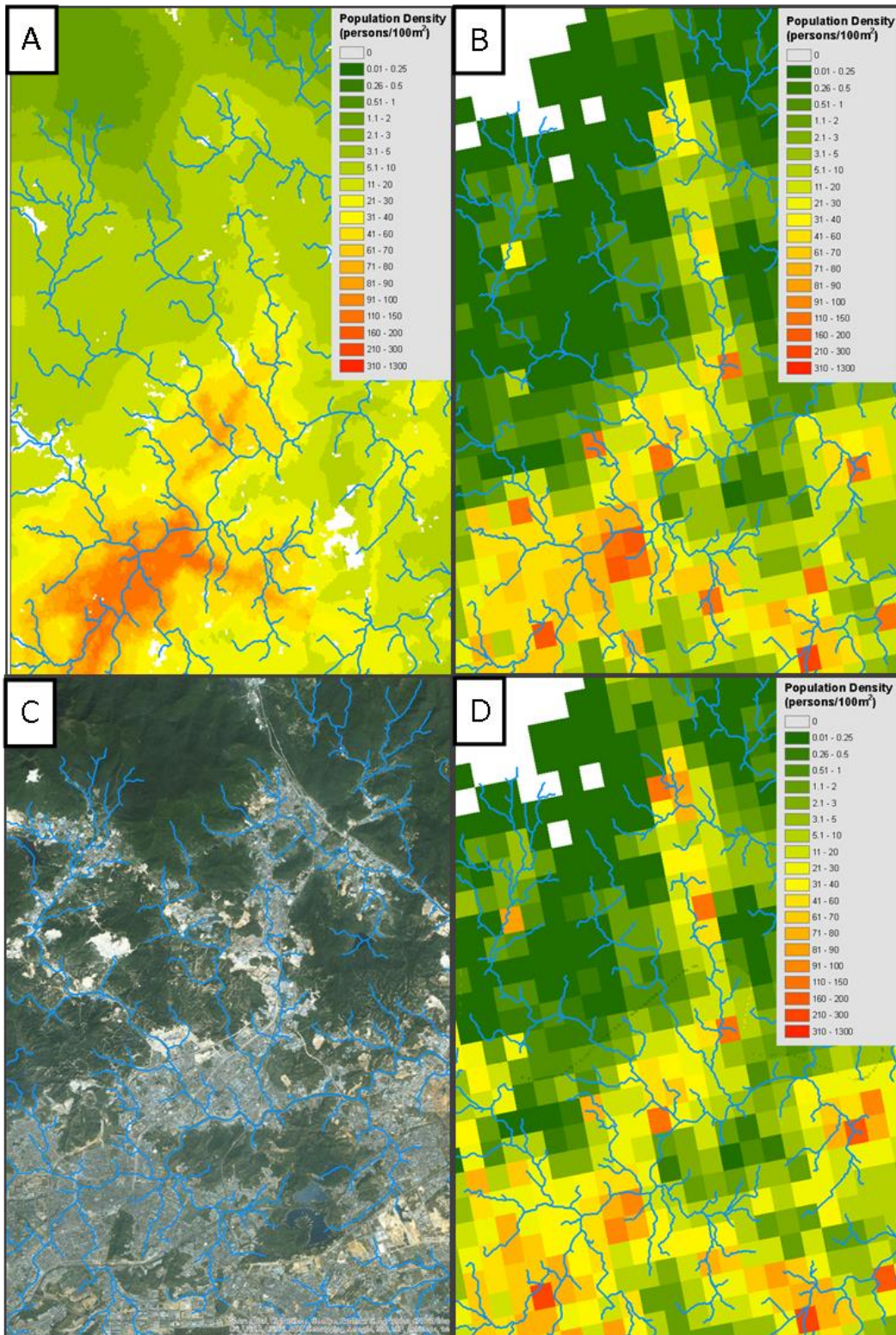


Figure 34 - Comparison of population datasets. The Worldpop dataset (A) boasts a higher resolution in comparison to Landscan (B). However when compared to satellite imagery (C), it is likely that Landscan is a more realistic representation of the underlying population. Sparsely populated areas such as the region to the North-West are poorly represented by Worldpop. The census data used by Landscan is older than the data used by Worldpop, however utilising the GPWv4 dataset, Landscan was adjusted to 2010 population levels (D).

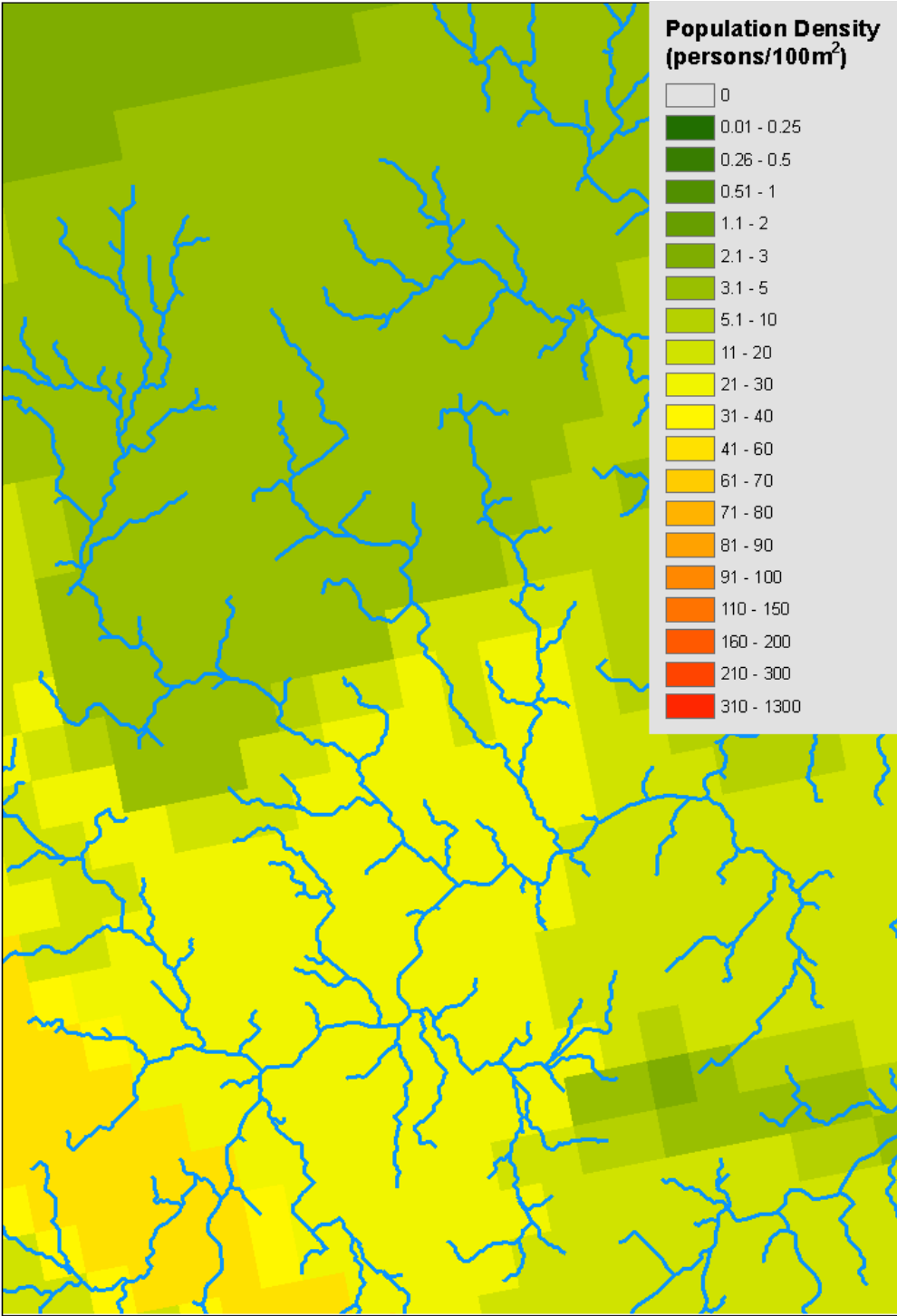


Figure 35 – Population density surface generated from the GPWv4 dataset.



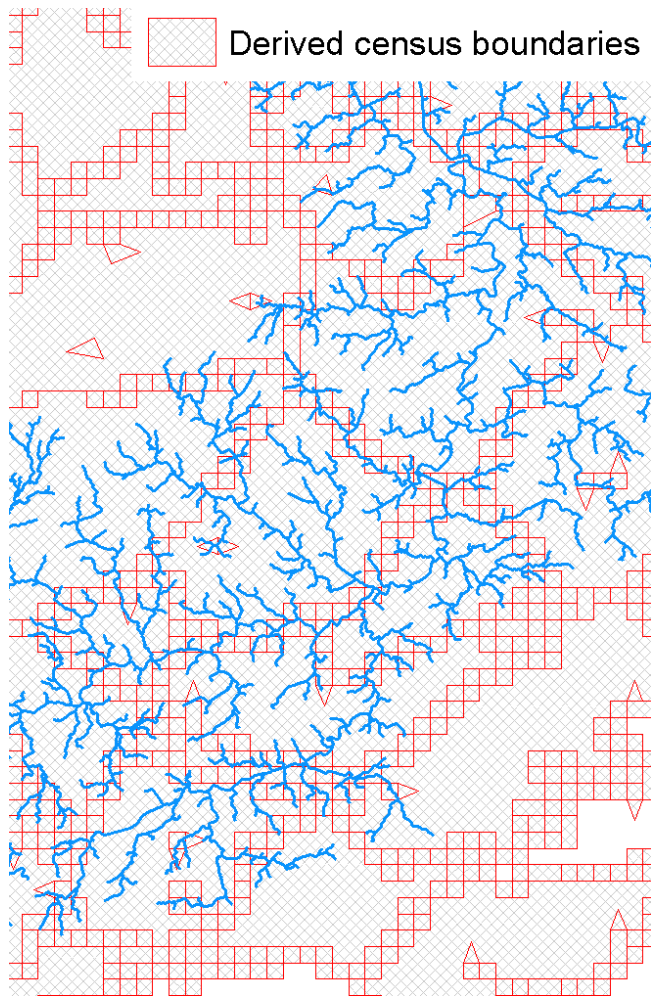


Figure 36 - Census boundaries derived from GPWv4. As part of the development of GPWv4, the developers assigned cells that lay on the boundary to share the value of all intersecting boundaries. And therefore these cells are unique and when backcalculating census boundaries, these cells grouped only with themselves. These are shown here as boundaries that include only a single cell each.

### 3.7 Delineating upgraded STWs

Delineating wastewatersheds for the 2016 model was completed prior to the 2008 model. For the 2008 model, wastewatersheds for STWs that were constructed after 2008 were removed and STWs that had been upgraded since 2008 were downgraded. In order to achieve this, data were obtained for population and service areas of STWs for 2008 if available, which was used to assist the process.

The methodology used here assumes that areas within an upgraded STW's wastewatershed (in 2016) that had been developed between 2008-2016 were served by the upgraded STW in 2016, and not by the pre-upgraded 2008 STW.

It was also assumed that sewer pipes connecting to the STW did not exist within these new development sites in 2008. Using Google Earth's historic imagery, new developments within the upgraded STW's wastewatershed were digitised. Subcatchments within these new developments were removed from 2008 wastewatersheds. New developments were treated like barriers and therefore subcatchments beyond these new developments were also removed in order to maintain a semi-continuous wastewatershed with no significant gaps.

Figure 37 shows an example of this process.

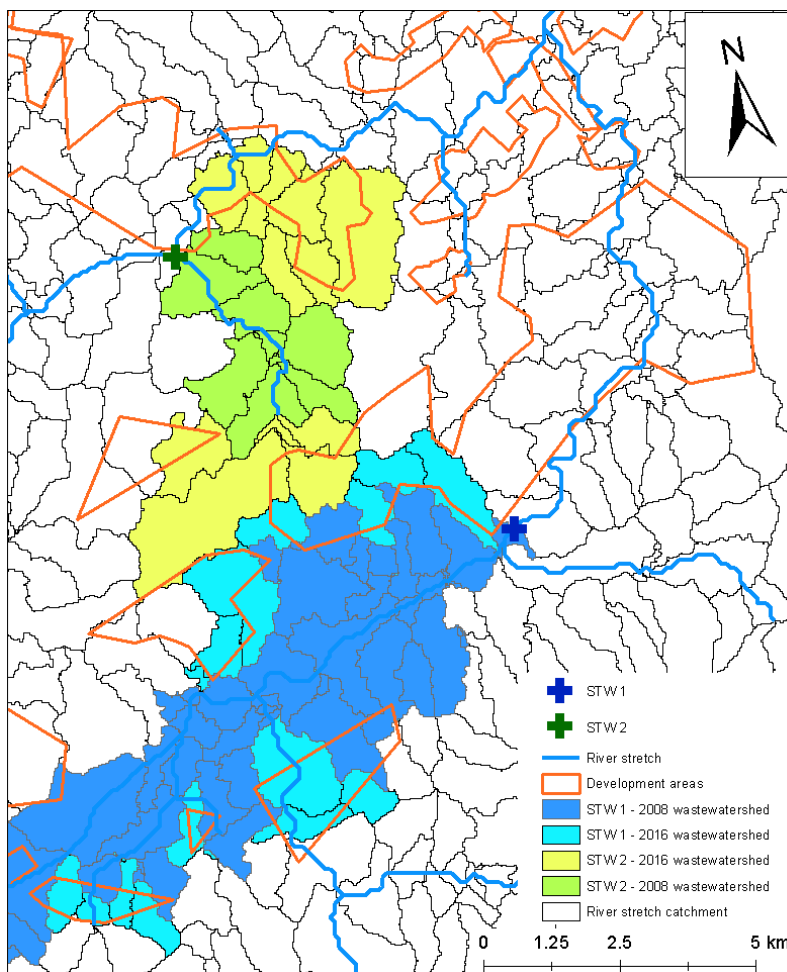


Figure 37 - Use of digitised development areas to aid the delineation of downgraded STWs. Developed areas, those plots of land that were developed between 2008 and 2016 were not included in the 2008 wastewatershed.

The assumption behind this strategy was based upon the likelihood that following STW upgrade, new developments are more likely to connect to the STW as opposed to retrofitting the required infrastructure for existing properties. Sewer pipes and other related infrastructure for new builds can be completed prior to construction and are therefore relatively cost-efficient. This is as opposed to the costs of laying pipes below existing properties (unsewered properties), which would involve considerable work and disruption removing the surface to place the new pipes. However, it is possible retrofitting could be implicitly accounted for to some extent. The new developments were identified by indications of significant construction from the imagery, which could include infrastructure retrofit.

This procedure was only required for two STWs (Figure 37), one of which was well confined by a relatively small catchment and the other with information about the size of the service area before and after upgrade.

Population data was available for a single STW prior to and following upgrade which was used for evaluation purposes. Using the methodology described, the population served prior to upgrade was estimated. The relative difference between predicted and actual 2008 population deviated by 24%. This is reasonable considering the uncertainties around the method and the data.

### **3.8 Sampling**

In January 2016, water samples were collected throughout the catchment (by the author) with the intention of quantifying the concentration of the four target chemicals. Samples were required for the purpose of validating the model. The objective of the campaign was to:-

- Sample all major subcatchments
- To sample upstream and downstream of a selection of representative STWs
- Sample subcatchments with no known STWs present

This was designed to evaluate the model's capability to simulate emissions from both treated and untreated sources. It was also important to test how representative the model was for different areas of the catchment.

With a relatively large catchment to sample, subcatchments with high population were preferentially selected for sampling. The transformed population data described in the STW identification section was used to highlight populated areas of the catchment. All subcatchments containing a STW were sampled and 4 sampling points were placed in subcatchments without a STW.

Sampling sites were divided into three zones as shown by Figure 38. The first zone (A), within the city regions of Huizhou and Shenzhen, was the most densely populated, and therefore contained the largest number of sampling sites. The second zone (B) was within the Heyuan city region, representing the middle section of the East river. Samples were collected from around Heyuan city and from the rural surroundings. The final zone (C) represented the upper reaches, which contained Longchuan and a number of small towns and villages in the largely rural region.

Samples were collected from bridges where possible to allow for access to the centre of the channel, otherwise samples were taken from the river bank or in singular case, a boat was hired to collect a sample from the centre of the channel.

Sampling area A was sampled between the 12<sup>th</sup>-13<sup>th</sup> of January, area C was sampled between 14<sup>th</sup>-15<sup>th</sup> of January and area B was sampled on the 15<sup>th</sup> and 18<sup>th</sup> of January. Weather



conditions for the sampling period are shown by Table 15. Conditions for the first sampling campaign, in 2008, were not available.

<b>Site</b>	<b>Date</b>	<b>Weather conditions</b>
A	12 <sup>th</sup> -13 <sup>th</sup> January 2016	Cool and dry.
B	14 <sup>th</sup> January 2016	Dry during sampling, but 9.8mm recorded in nearby rain gauge.
B	15 <sup>th</sup> January 2016	Light rain during sampling, 7.3mm recorded in nearby rain gauge.
C	15 <sup>th</sup> January 2016	Intermittent rainfall during sampling, 19.6mm recorded in nearby rain gauge.
C	18 <sup>th</sup> January 2016	Warm and dry.

Table 15 - Weather conditions during sampling in 2016.

The samples were collected using a bucket and stored in duplicate 1L amber glass bottles. The bucket and bottles were first rinsed with river water from the sampling site and 50ml MeOH. Then, 0.4ml 4M H<sub>2</sub>SO<sub>4</sub> was added to the samples to reduce the pH and stabilise the water samples. Water pH and temperature were also measured at each sampling site. The campaign involved a total of 36 sampling sites, with duplicate samples taken at each site.

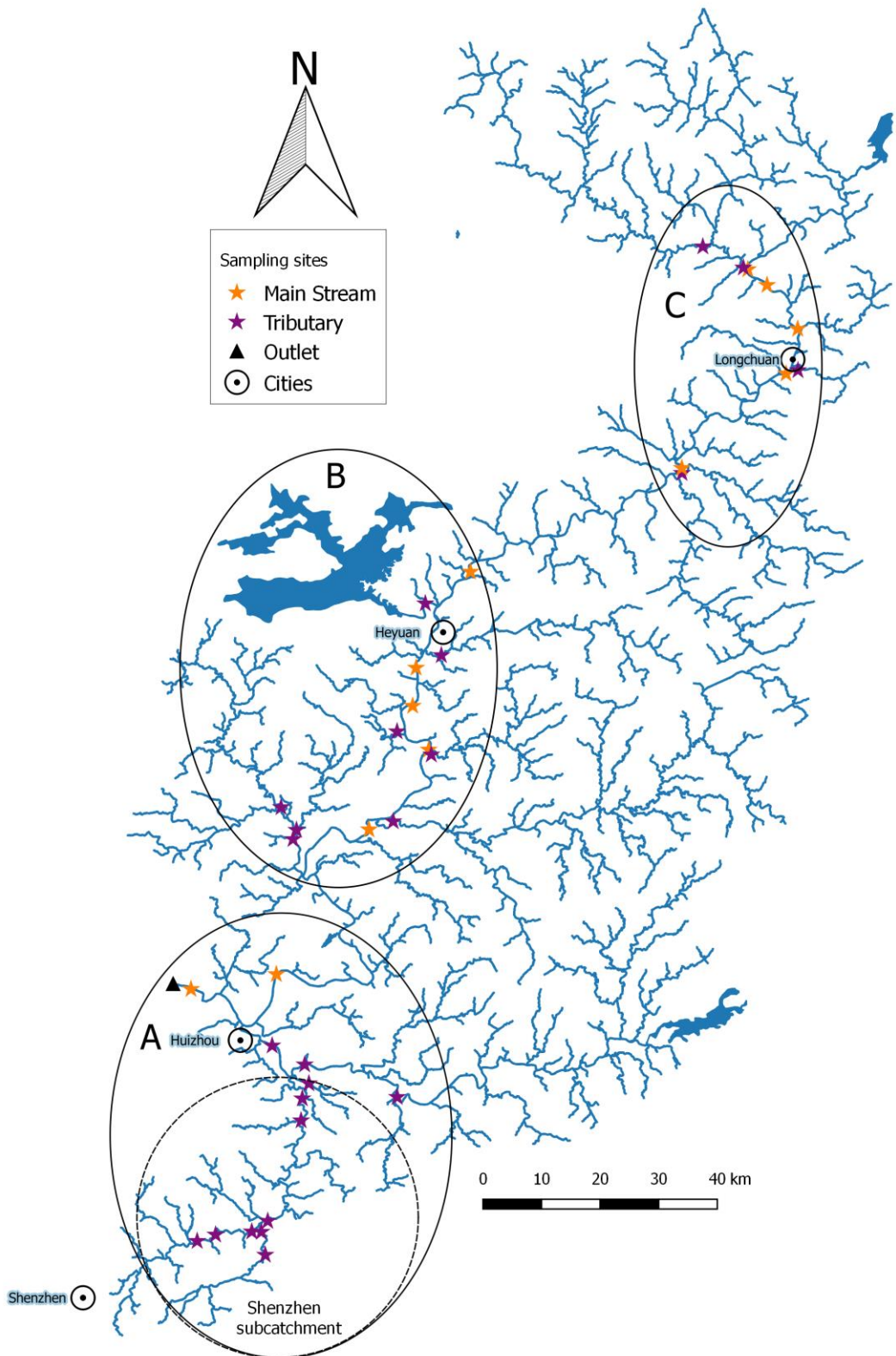


Figure 38 - Sampling sites, divided into three zones. Zone A represents Huizhou and Shenzhen, Zone B represents Heyuan City region and Zone C represents Longchuan area.

### 3.9 Analytical method

#### 3.9.1 Extraction

Bottles were immediately placed in a cooler and then extracted within 60 hours. Samples were filtered using 0.7µm G/F filter. At this point two laboratory blanks were prepared by mixing 1L MQ water with 50ml MeOH and 0.4 H<sub>2</sub>SO<sub>4</sub>. The samples were then spiked with 100ng internal standard (Table 17), and then shaken. Finally, the samples were then extracted using solid phase extraction (SPE). SPE cartridges (Sigma HLB 200mg, 6mL) were conditioned using 10ml MeOH and 10ml Mili-Q water. Samples were extracted at approximately 10ml/minute, and then dried using a vacuum pump. After extraction SPE cartridges were wrapped in aluminium foil and stored in a freezer. Following the conclusion of the sampling campaign, the SPE cartridges were returned to the UK and placed in a freezer within 24 hours.

#### 3.9.2 Elution and reconstitution

SPE cartridges were dried again using an extraction pump to remove any water that may have accumulated during freezing. The samples were eluted with a solvent mixture of 50/50 Acetonitrile and Ethyl Acetate at a rate of about 1ml/minute. The extracts then were placed in 15 mL amber vials for reduction to 0.1 mL under a stream of high purity nitrogen. The samples were then filtered using 0.2 µm PTFE syringe filters before storage in 2 mL vials.

An extract aliquot of 0.2 mL was reduced to just dryness, and reconstituted by a 0.1 mL mixture of MQ water and methanol mixture with 5mM NH<sub>4</sub>OH (50% : 50%, v/v) in micro vials just before instrument analysis.

### 3.9.3 Analysis

#### *Instrument*

The instrument consisted of an Agilent 1100 series high performance liquid chromatography (HPLC) system and a Quattro Micro triple-quadrupole mass spectrometer (Waters, Micromass, Manchester, UK). The HPLC system comprised of a binary pump, a vacuum micro-degasser, auto-sampler and a thermostatic column compartment. The Quattro Micro triple-quadrupole mass spectrometer was equipped with an electrospray ionisation (ESI) source. High-purity nitrogen was used as a nebulising and desolvation gas supplied by a generator (Peak Scientific, UK), bottled argon (99.999%) was used as the collision gas. The instrument control and data acquisition were controlled by Masslynx 4.1 software. The sample injection volume was 5  $\mu\text{L}$ . The instrument was optimised and operated in negative ion mode with a capillary voltage of 3 kV, a source temperature of 120  $^{\circ}\text{C}$  and a desolvation temperature of 300  $^{\circ}\text{C}$ , no cone gas flow and a desolvation gas flow of 600  $\text{L h}^{-1}$ .

#### *Mobile phase composition*

Two mobile phases were prepared:- A: 95% MQ water + 5% ACN with 5mM  $\text{NH}_4\text{OH}$ ; B: 95% ACN + 5% MQ water with 5mM  $\text{NH}_4\text{OH}$ .

#### *Column and column temperature*

A Waters Xbridge BEH C18 column was employed with a pre-column: 100 mm  $\times$  21. mm, 2.5  $\mu\text{m}$ . The column compartment temperature was kept at 25  $^{\circ}\text{C}$ .

Time (minutes)	Mobile phase A (%)	Mobile phase B (%)	Flow (ml min <sup>-1</sup> )
0	85	15	0.2
1	85	15	0.2
10	20	80	0.2
15	0	100	0.2
23	0	100	0.2
24	85	15	0.2
37	85	15	0.2

Table 16 – Gradient program used by the HPLC for analysis.

### *Quantification*

Quantification of the target PCP ingredients and estrogens were based on the precursor ion/product ion transitions or target ions using the MRM scan of the negative ion mode. The details of the MS transitions and parameters for the target chemicals are listed in Table 17.

Chemical	RT (minutes)	Parent ion	Daughter ions	CV	CE	Internal standard
TCS	11.22	287/ 289	35	15	5	TCS-d <sub>3</sub>
TCC	15.47	313/315	160/162	20	15/15	TCS-d <sub>3</sub>
E1	12.33	269	145/143	50	35/55	E1-d <sub>4</sub>
E2	11.53	271	183/145	55	40/40	E2-d <sub>5</sub>

Table 17 - MS transitions and parameters for the target chemicals, including retention time (RT), collision energy (CE), cone voltage (CV), parent ion, daughter ions and internal standard used for each target chemical.

Concentrations of analytes were corrected for losses by normalising by the recovery of internal standards. The Instrument detection limit (IDL) and method detection limit (MDL) for each chemical are contained in Table 18, along with an estimate of each method quantification limit (MQL). The IDL were calculated using low concentration standards, whilst MDLs were determined based upon the IDL, SPE recovery (%) and the concentration factor (1500), this is described by Equation 51:

$$MDL = \frac{IDL}{RE_{SPE} * CF} * 100 \quad (51)$$

where:

MDL - method detection limit (ng/L)

IDL - instrument detection limit (ng/ml)

RE<sub>SPE</sub> - SPE absolute recoveries (%)

CF - concentration factor.

This produced a set of chromatograms, examples of which are presented in Appendix A.

Analysis of the chromatograms provided an estimate for the concentration of each target compound within each sample.

Chemical	IDL (ng/ml)	MDL (ng/L)	MLQ (ng/L)
E1	0.40	0.14	0.48
E2	0.96	0.34	1.12
TCS	0.40	0.14	0.46
TCC	0.83	0.30	1.00

Table 18 –Detection limits for the target chemicals.

The quality of the data measured from samples taken in 2016 is assessed here. For both campaigns, duplicates were taken at each site. For the majority of the samples taken, the concentration of each chemical was similar for both duplicate samples. However in some cases, particularly in samples taken at Heyuan, significant variation was observed. It is also important to note that all four chemicals were detected within the blank control samples (Table 19). This may suggest that errors during analysis, contamination during extraction, storage or transportation may have occurred. As the number of samples taken is relatively low, none of the sampling data has been discarded. As such, the variation of each duplicate pair is presented and referred to when the data is referenced, especially when in comparison to modelling results.

E1	E2	TCC	TCS
0.3	0	0.3	3.6
0.4	0.8	0.2	3.7

Table 19 - Concentration of target chemicals within blank control samples (ng/l)

### **3.10 Scenario based assessment**

The use of scenarios may be used for the purpose of risk assessment and catchment management. Firstly, a simple risk assessment was completed based upon the PEC/PNEC ratio for each chemical, based upon the 50<sup>th</sup> and 90<sup>th</sup> percentile data.

Secondly, future scenarios were examined. The first examined the potential effect of increased population, mitigated by improved sewage treatment. The near future scenario for the year 2020 was selected as a suitable timepoint, with the assumption that all planned STWs would be completed. Projected population data for Huizhou and Shenzhen was acquired from the two city authorities and used to upgrade the gridded population. For Heyuan, no such data was available and therefore it was assumed that the same population growth rate for 2010-2015 continued for the period of 2015-2020.

As discussed in Chapter 2, when attempting to locate STWs for settlements currently without a STW, information was sought from internet sources which might suggest plans for construction of a STW in the future. Plans for two new STWs were located and a number of upgrade plans using this method. A dummy STW was placed just downstream of the planned Shiba and Mabei STWs (Figure 39), and the population served was estimated using the methodology presented in Chapter 2. It was estimated that Shiba and Mabei STWs will serve a population of 36,000 and 19,000 respectively. It was assumed that all existing STWs served any additional population within their respective service area. Plans from Shenzhen city authority reflected this, with upgrades for the majority of STWs to account for this change in population.

Following this, an updated risk assessment was performed, noting any changes in risk between the two models. Finally, solutions for high risk areas were devised, focusing upon construction and upgrade of STWs in the area.



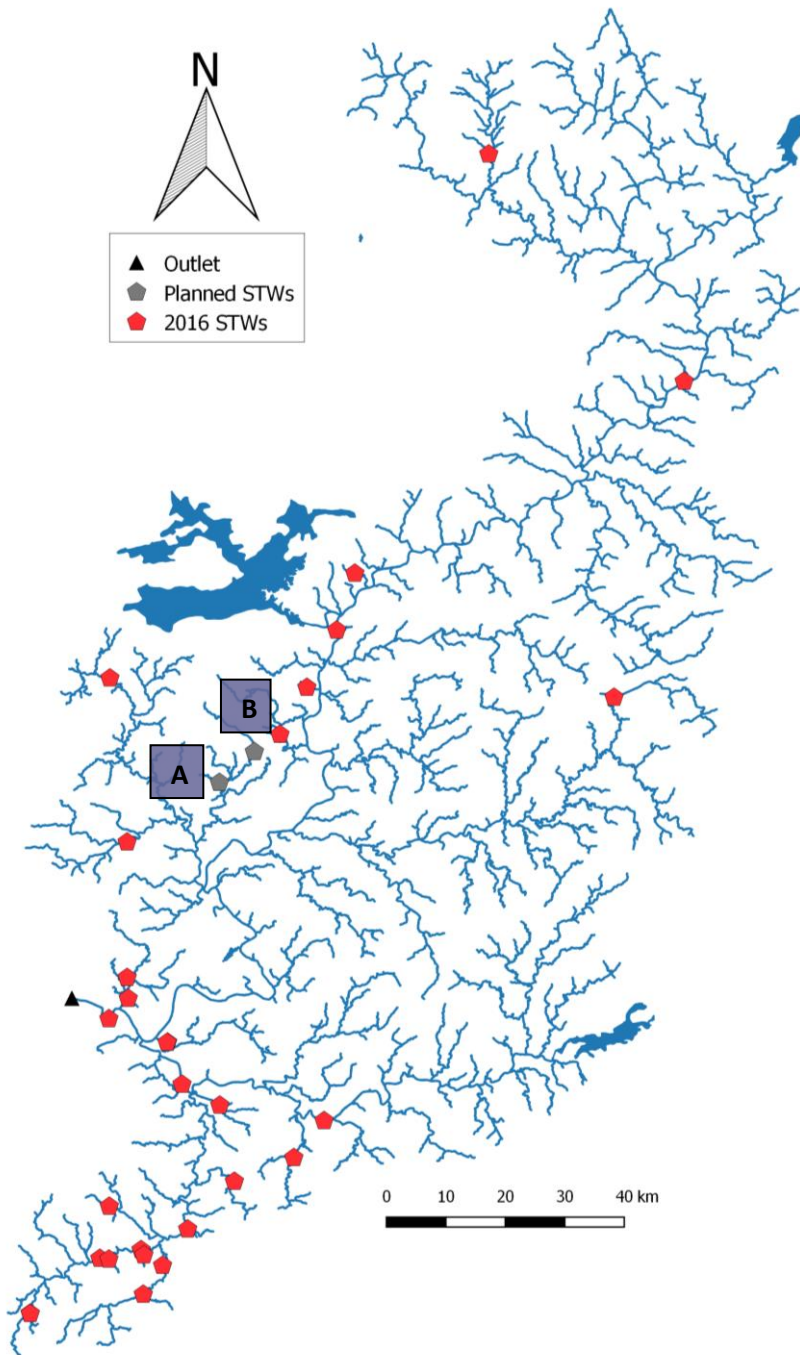


Figure 39 - Planned STWs within the East River catchment - the Shiba (A) and Mabei (B) STWs.

## Chapter 4 – East river modelling results and discussion

### 4.1. Introduction

The objective of this section is to assess whether the thesis aim: “To be able to reliably predict the in-stream concentration of down-the-drain chemicals TCS, TCC, E1 and E2” has been achieved.

To assess this, the simulation results for 2008 and 2016 were compared to measured concentrations. Attempts have been made to critique the different elements of the methodology, assessing the uncertainty around each element and the suitability of the approach taken.

Finally, the model was also parameterised for two future scenarios, which predict the effects of increasing population, usage and wastewater treatment capabilities upon chemical exposure. An assessment of the appropriateness of these scenarios was made, and the potential implications of these scenarios. This was used to assess whether thesis aim 3: “To demonstrate the potential of GREAT-ER for both risk assessment and catchment management purposes, based upon the present and year 2020 scenario” has been achieved.

### 4.2. Comparison of measured and modelled concentrations

The results of the model are presented here in comparison to measurements taken from water sampling campaigns in 2008 and 2016. Separate model results are presented for different in-stream removal constants, for TCS. These models are described as TCS A (removal constant =  $0.0138\text{h}^{-1}$ ), TCS B (removal constant =  $0.061\text{h}^{-1}$ ) and TCS C (removal constant =  $0.21\text{h}^{-1}$ ).

The root mean square error (RMSE) between the median estimated concentration and the mean measured concentration was calculated for samples collected at sampling sites within specified spatial units (e.g. all tributary sampling sites, or sites within the Heyuan sampling zone). Box plots have been used to illustrate the distribution of the estimated concentrations at each sampling site; the legend that applies to all box plots is shown in Figure 40. Maps are also provided showing the location of sampling sites and the mean population for each subcatchment. Subcatchment population was provided rather than raw data in order to provide an indication of the actual input to the model. Finally, scatterplots are presented, plotting the mean measured concentration against the median estimated concentration.

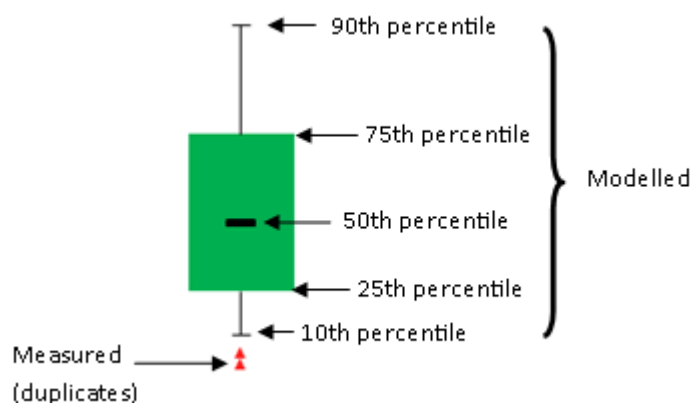


Figure 40 - Legend for measured vs modelled concentration box plots (ng/l).

#### 4.2.1. The 2008 model

2008 modelled and measured chemical concentrations are displayed graphically in boxplots (Figure 41 and Figure 42), and scatterplots (Figure 43). The majority of sampling sites are in the highly populated lower catchment; a map of the catchment with locations of sample sites is shown in Figure 44. Calculated RMSE values are presented in Table 20.

On the main stream, the RMSE for E1 and E2 is low, and the modelled 10<sup>th</sup> percentile concentration is close to 0 at all sampling sites where E1/E2 was not detected. The RMSE is

higher for TCC, but still relatively low, however the model underestimates the concentration of TCC at M2, M3, and M4. For TCS, the main stream RMSE varies according to the in-stream removal rate constant used. TCS B resulted in the smallest main stream RMSE, although the estimated concentrations for M1-M3 are underestimated; whereas the measured concentration for M1-M3 is within the 10<sup>th</sup>-90<sup>th</sup> percentile concentration range for TCS A. TCS C performs relatively poorly, with the model underestimating the measured concentration at all main stream sampling sites.

	E1	E2	TCC	TCS A	TCS B	TCS C
Catchment	12.56	2.0	43.84	124.21	108.77	63.58
Main stream	0.7	0.09	3.47	4.63	3.41	5.1
Tributaries	17.75	2.82	61.9	175.59	153.79	89.77

Table 20- RMSE (ng/l) between the median estimated concentration and the mean measured concentration for samples collected at sampling sites within specified spatial units - for the 2008 model. Triclosan is parameterised with different in-stream removal constants, where: (TCS A) – 0.0138h<sup>-1</sup>, (TCS B) – 0.061h<sup>-1</sup>, (TCS C) – 0.21h<sup>-1</sup>.

All tributaries are located within the city regions of Huizhou and Shenzhen. The RMSE for E1 is significantly higher than E2. The model underestimates the concentration of E1 at T1-T3; whilst for E2, the measured concentrations for T1,T2,T4 and T5 are within the estimated 10<sup>th</sup>-90<sup>th</sup> range and the 10<sup>th</sup> percentile estimated concentration is relatively close to 0 (0.32ng/l) for the sampling site T3, which was not detected within the samples collected.

For TCC, the tributary RMSE is much higher than the RMSE for E1/E2, and for the sampling sites T1-T3, the model overestimates the concentration of TCC. Finally, for TCS, the tributary RMSE varies considerably depending on the in-stream removal scenario. TCS A performs worst, with the greatest RMSE, underestimating the concentration of TCS at T1-T5. For TCS B, the measured value is within the estimated 10<sup>th</sup>-90<sup>th</sup> range, but underestimates the

concentration of samples taken at T3 and T5. The RMSE for TCS C is the lowest of the three scenarios and the measured value for samples taken at T1 and T3 is within the 10<sup>th</sup>-90<sup>th</sup> percentile, but underestimates T2, T4 and T5.

The scatterplots suggest that overall, the model's estimates for the concentration of E1 at most sampling sites is similar to that measured, although three sampling sites were underestimated by the 50<sup>th</sup> percentile. For E2, the model's estimated concentration at the majority of sampling sites is close to the measured concentration, with the exception of a single site, which the model overestimates. For TCC, the model's estimate for approximately half of the sites appear to be relatively close to the concentration measured, however the remaining sites are overestimated by the 50<sup>th</sup> percentile. Finally, scatter graphs for different in-stream removal constants for TCS suggest that the TCS B simulation ( $0.061\text{h}^{-1}$ ) produces estimates that are the closest to measured concentrations overall, although a few sampling sites are still overestimated by the 50<sup>th</sup> percentile.

Many of the estimates for chemical concentration deviate, sometimes significantly, from the measured concentrations. However overall, the model seems to be able to represent many of the elements that are important for chemical emission, dilution and removal. The results for 2008 are significant because of the complexity of the catchment and the uncertainty regarding the estimation of many of the emission elements. For the majority of STWs, the population served was unknown, and for many of these STWs, the population served was available only after upgrade. Therefore this may suggest that the estimation methodology used may have some merit.

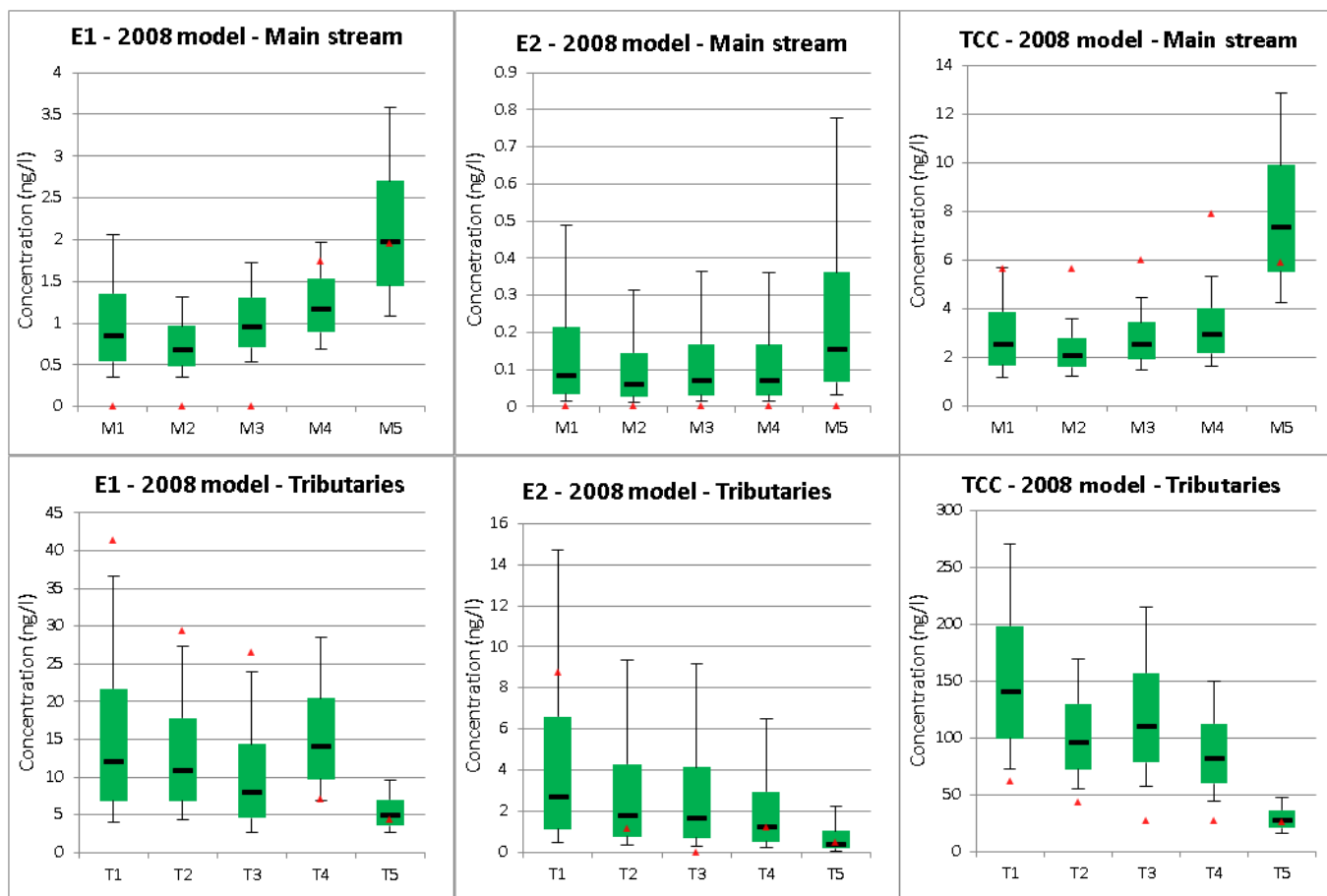


Figure 41 – A comparison between the measured and modelled concentrations for Estrone, 17β-estradiol and Triclocarban, for the December 2008 scenario.

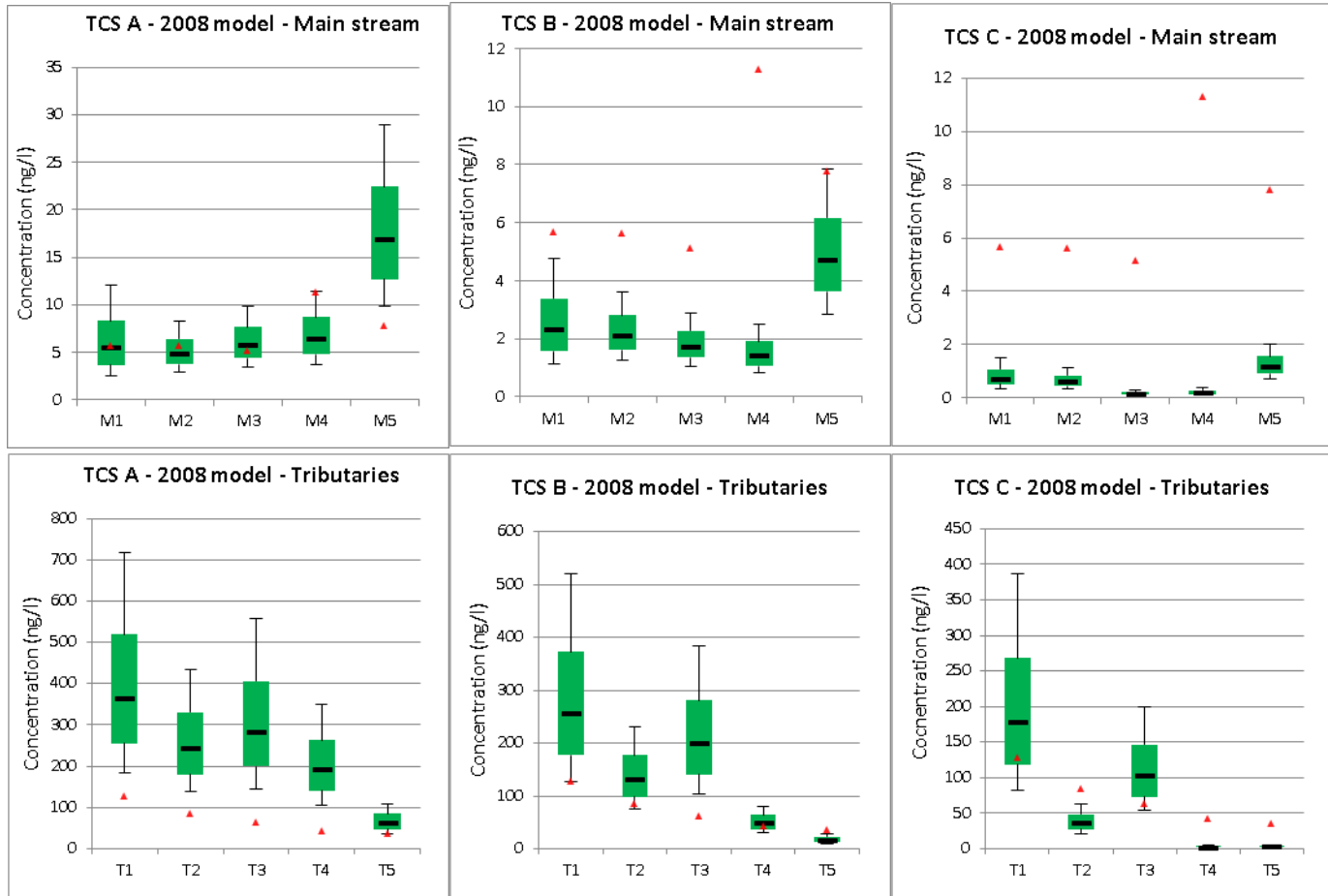


Figure 42 – A comparison between the measured and modelled concentrations for Triclosan, parameterised with different in-stream removal constants, for the December 2008 scenario. Where: (A) – 0.0138h<sup>-1</sup>, (B) – 0.061h<sup>-1</sup>, (C) – 0.21h<sup>-1</sup>.

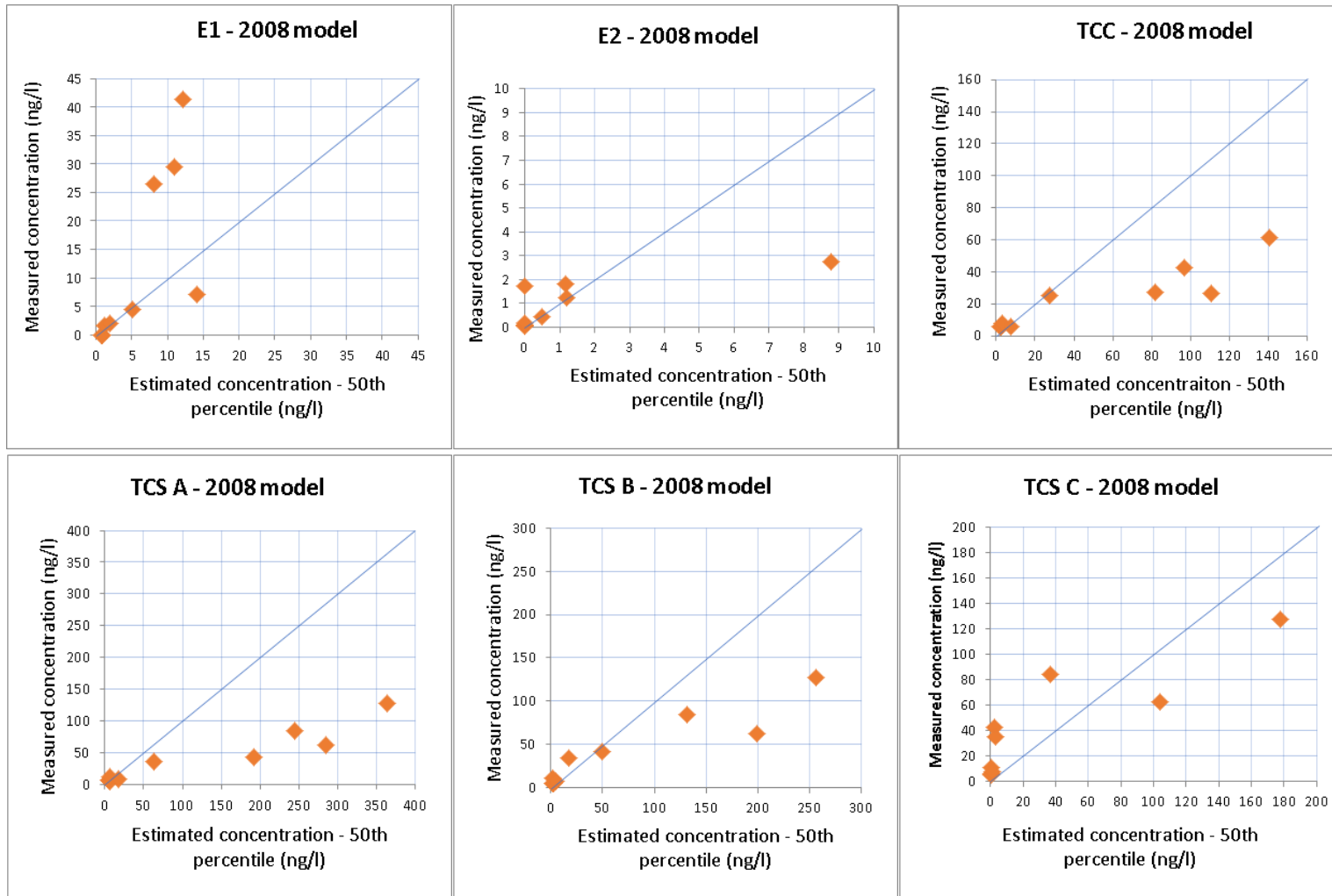




Figure 43 – Scatterplots displaying measured concentration against estimated concentration of Estrone, 17 $\beta$ -estradiol, Triclocarban and Triclosan for the 2008 model. Triclosan is parameterised with different in-stream removal constants, where: TCS A – removal constant =  $0.0138\text{h}^{-1}$ , TCS B – removal constant =  $0.061\text{h}^{-1}$ , TCS C – removal constant =  $0.21\text{h}^{-1}$ . A line is drawn on all graphs, where: measured = modelled.

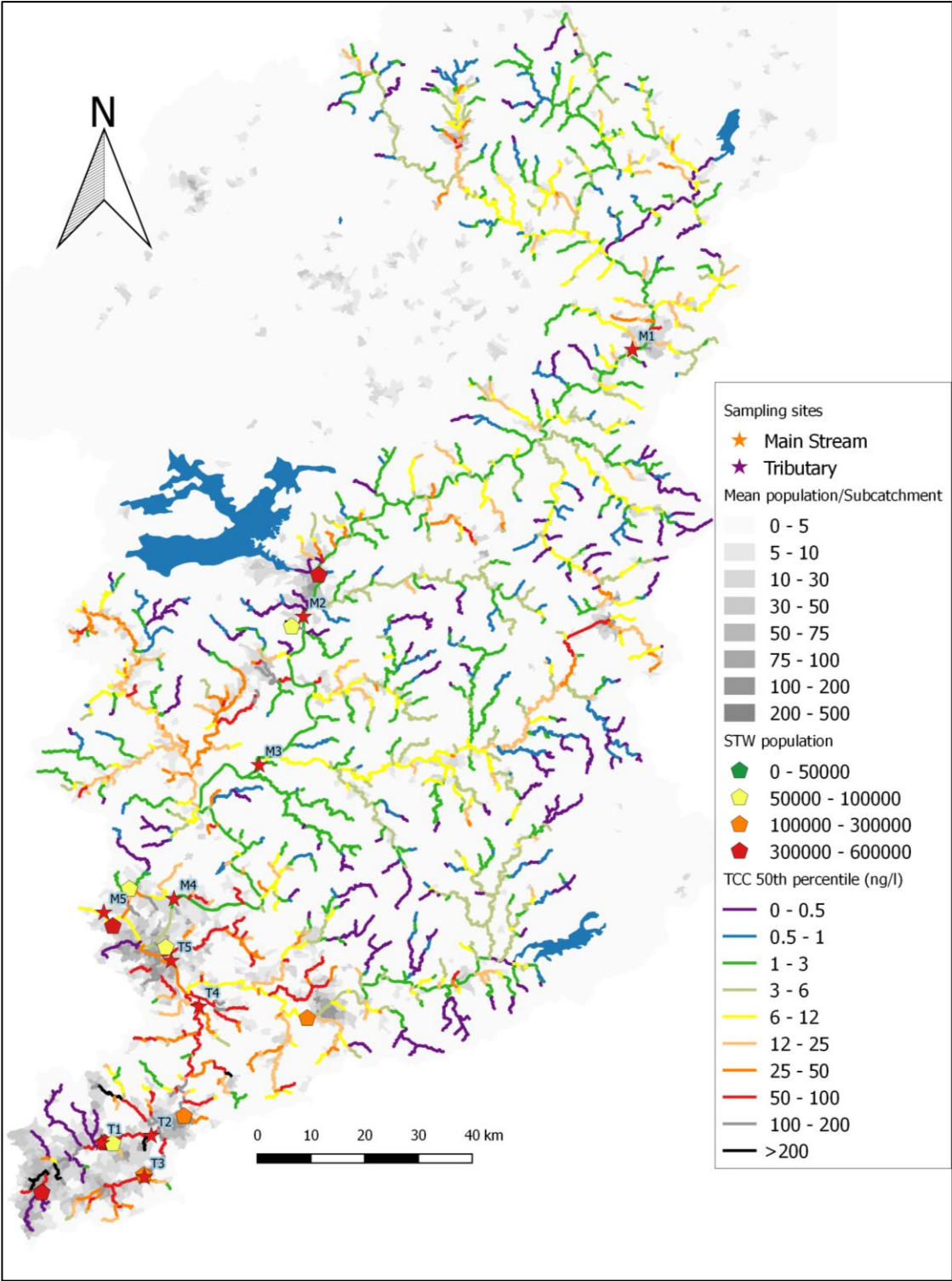


Figure 44 – Median simulated concentration of Triclocarban in 2008.

#### 4.2.1.1. The 2016 model

The 2016 modelling results for the three sampling zones are presented in this section.

Comparisons to measurements at sampling sites in the Longchuan and Heyuan sampling zones are displayed within boxplots (Figure 45, Figure 46, Figure 54 and Figure 55), whereas the spatial distribution of TCC is presented in each sampling area as an example (Figure 47, and Figure 56). TCS, E1 and E2 are also presented in maps of the Huizhou zone (Figure 57 - Figure 62). Maps for TCS, E1 and E2 for the other two zones are shown in Appendix B. The calculated RMSE values are presented in Table 21, Table 22, Table 24 and Table 25.

##### *Longchuan*

The Longchuan sampling zone is the most upstream subcatchment and represents a largely rural area, with the only major settlement being the town of Longchuan.

For E1, the measured concentration is within the estimated 10<sup>th</sup> - 90<sup>th</sup> percentile range for all main stream sites apart from LM1, which is underestimated. For E2, the modelled 10<sup>th</sup> percentile concentration is close to 0 at all sampling sites where E2 is not detected, and the measured concentration for LM2 is within the estimated 10<sup>th</sup> - 90<sup>th</sup> percentile range. The Longchuan tributary RMSE for E1 is much higher than E2, but neither chemical appears to be modelled inadequately.

For TCC, the measured concentration for samples collected at sites LM2-LM4 are within the estimated 10<sup>th</sup>-90<sup>th</sup> percentile range, however, the model underestimates the concentration for LM1 and overestimates the concentration for LM5. As shown by Table 21, the RMSE is relatively low for E1, E2 and TCC at main stream sampling sites in Longchuan. For TCS, the RMSE is significantly higher than the other three chemicals, but is still low in absolute terms. The measured concentrations at LM1, LM3, and LM4, are underestimated by the TCS A model, but LM2 is inside the estimated 10<sup>th</sup>-90<sup>th</sup> percentile range, and the measured

concentration for LM5 is within the estimated 25<sup>th</sup>-75<sup>th</sup> percentile range. For TCS B and TCS C, the concentration at all main stream sites are underestimated, more so by TCS C than TCS B.

	E1	E2	TCC	TCS A	TCS B	TCS C
All sites	4.07	0.61	3.7	4.89	7.58	11.27
Main stream	0.211	0.13	0.69	3.16	4.73	5.45
Tributaries	6.11	0.90	5.49	6.43	10.06	15.78

Table 21- RMSE (ng/l) between the median estimated concentration and the mean measured concentration for samples collected at sampling sites within specified spatial units - for the Longchuan sampling zone, 2016 model. Triclosan is parameterised with different in-stream removal constants, where: (A) – 0.0138h<sup>-1</sup>, (B) – 0.061h<sup>-1</sup>, (C) – 0.21h<sup>-1</sup>.

The boxplots in Figure 46 and the calculations of RMSE shown in Table 21 suggest that TCS A provides the closest estimate in comparison to the concentrations measured.

For the Longchuan tributary sites, the RMSE is much higher for E1 than E2, and this is largely a result of a significant deviation (7.33ng/l deviation) between the estimated and measured concentration at the LT3 sample site. LT3 is in Longchuan town and is therefore the most urbanised sampling point within the zone. It is assumed that the majority of the town is served by the STW on the main stream; however it is likely that significant untreated discharges remain. Measured concentrations of E1 at other tributary sampling sites in Longchuan are within the estimated 10<sup>th</sup>-90<sup>th</sup> percentile range, as are all measured concentrations for E2. The RMSE for TCC is similar to that of E1, but measured concentrations for sites LT1-LT3 are underestimated by the model.

The RMSE for TCS varies considerably for Longchuan tributary sites. As with main stream sites, estimates for TCS A are more comparable with measured concentrations, in

comparison to the other in-stream scenarios; measured concentrations are within the 10<sup>th</sup>-90<sup>th</sup> range at sampling sites LT2-LT4, although LT1 is underestimated. For TCS B, the measured concentration for LT1 is within the 10<sup>th</sup>-90<sup>th</sup> percentile range, however the concentrations at LT2-LT4 are significantly underestimated. The worst performing scenario is TCS C, which underestimates concentrations at all sampling sites.

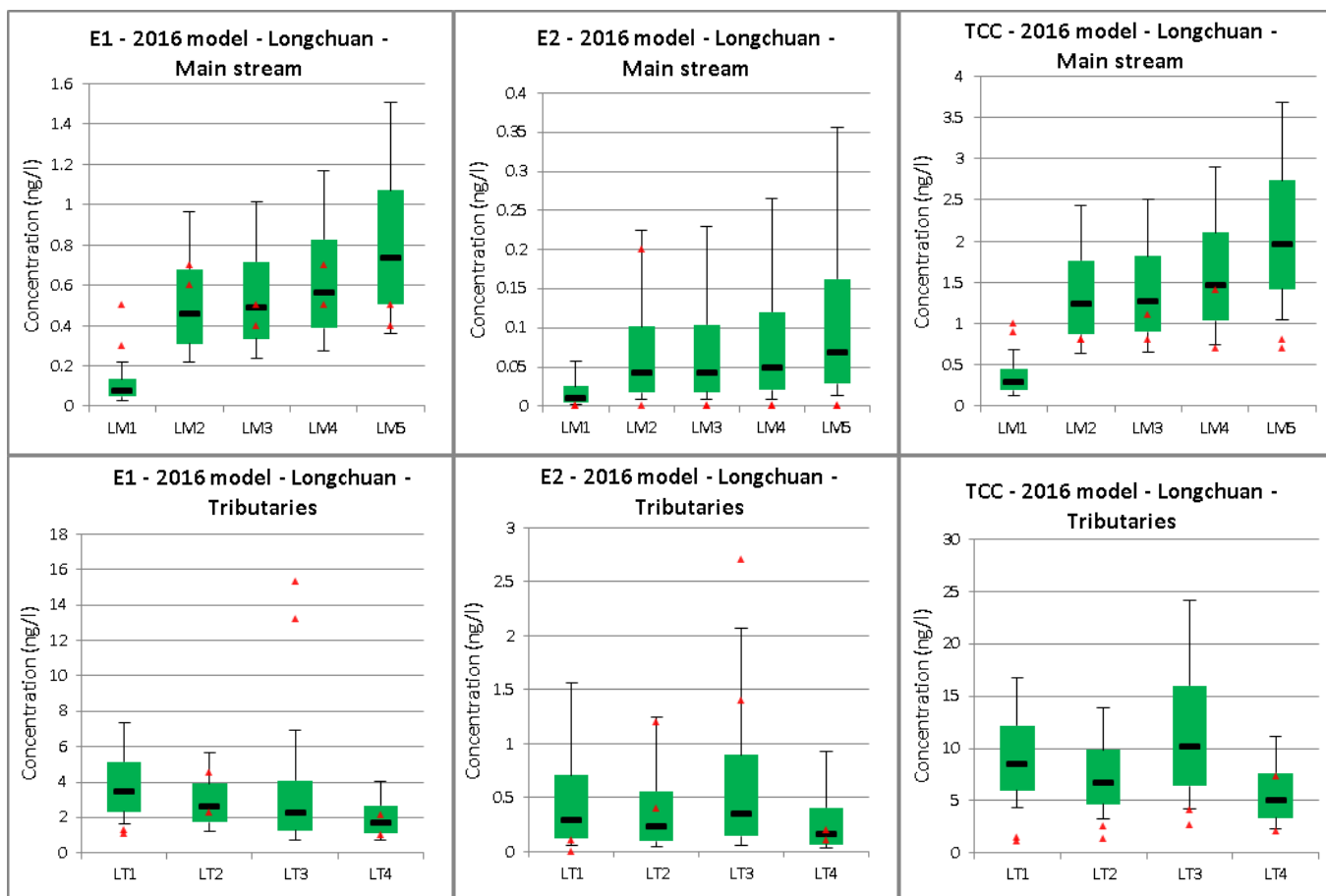


Figure 45 – Simulated and measured results for the 9 sampling sites within the Longchuan sampling zone in 2016 – for Estrone, 17β-estradiol and Triclocarban.

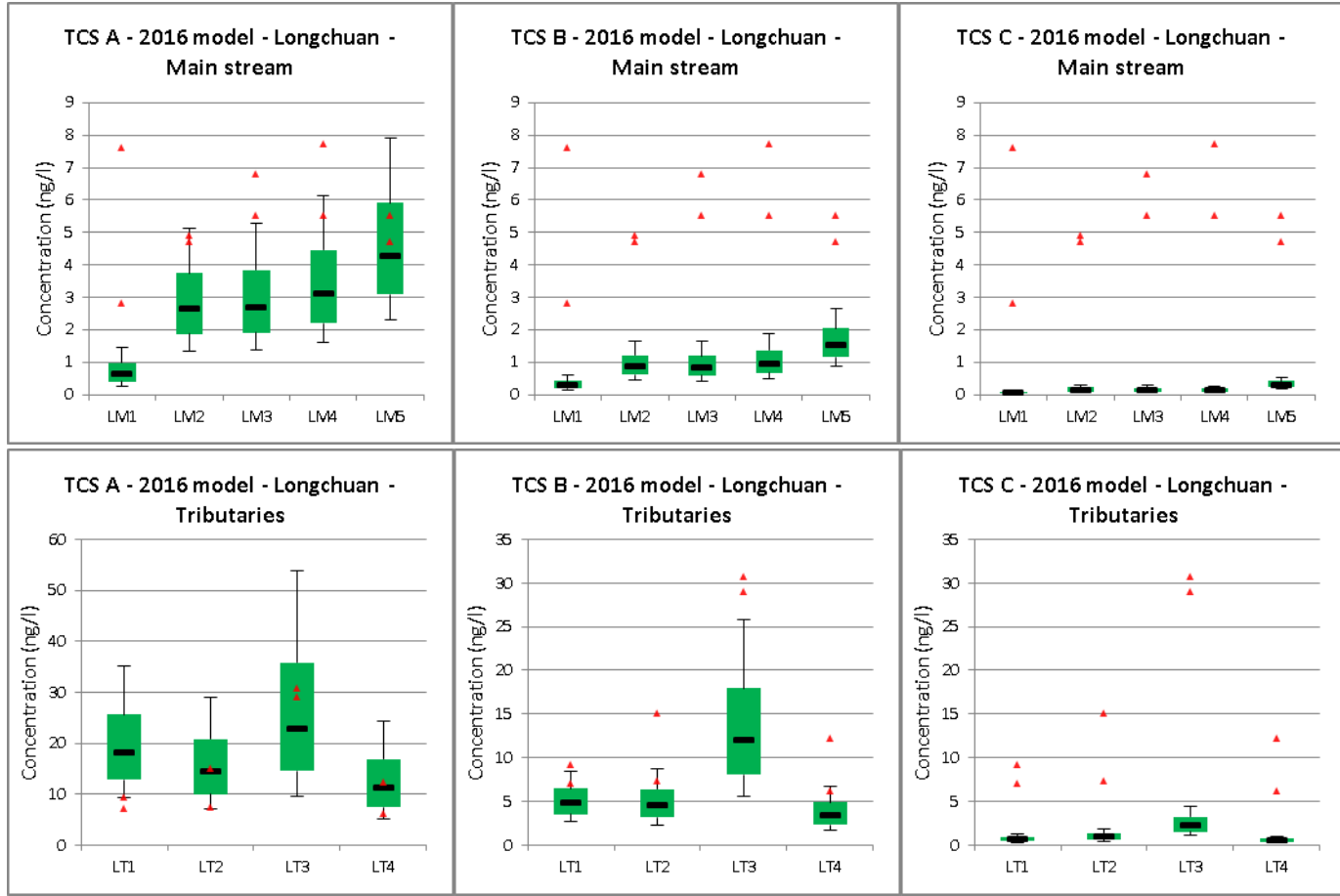


Figure 46 – Simulated and measured results for the 9 sampling sites within the Longchuan sampling zone in 2016 – For Triclosan. Triclosan is parameterised with different in-stream removal constants, where: (TCS A) – removal constant =  $0.0138\text{h}^{-1}$ , (TCS B) – removal constant =  $0.061\text{h}^{-1}$ , (TCS C) – removal constant =  $0.21\text{h}^{-1}$ .

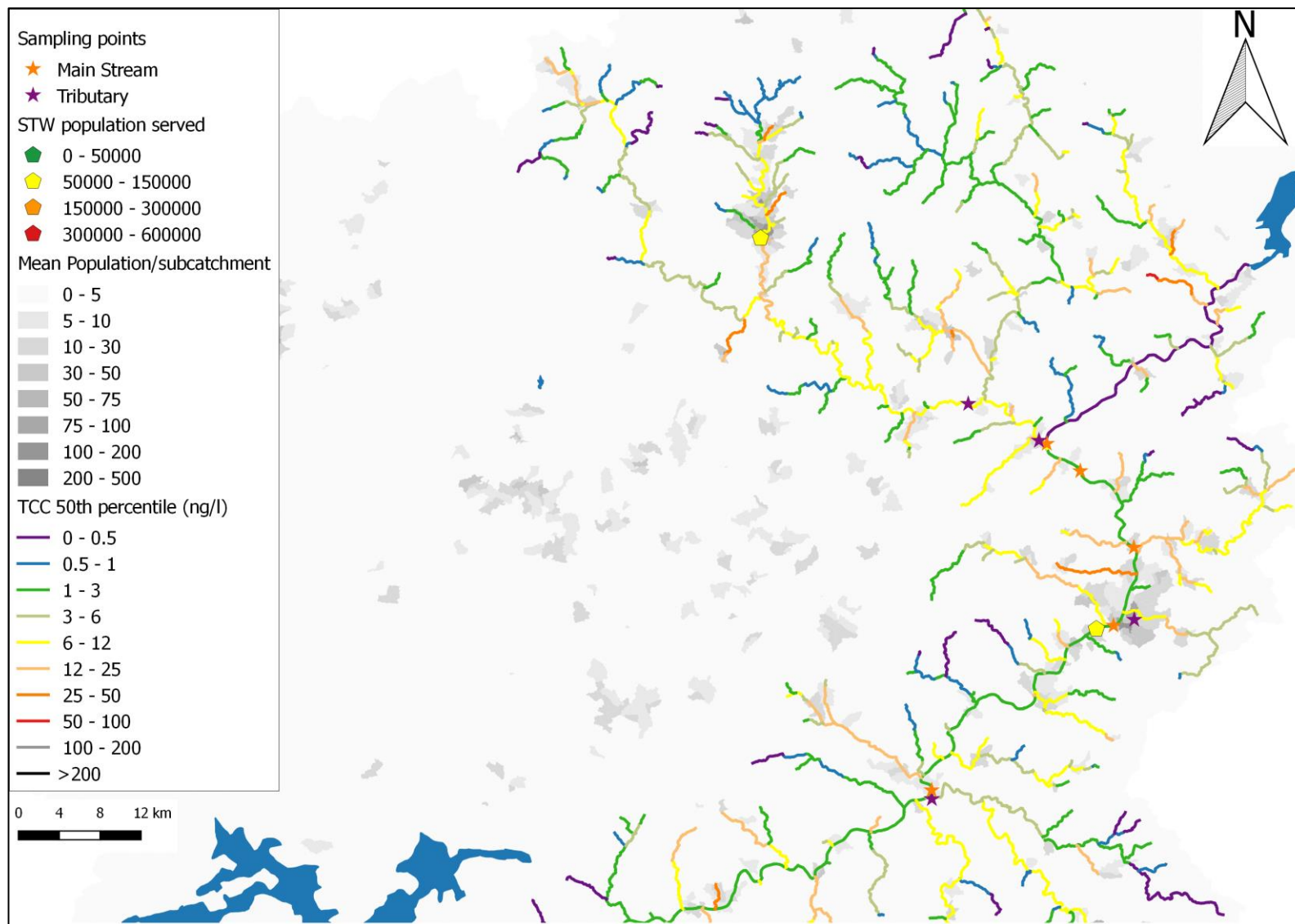


Figure 47 – Median simulated concentration of TCC in 2016 in the Longchuan sampling zone (ng/l).



## *Heyuan*

The Heyuan zone represents the mid-catchment. The zone is predominantly rural, however it also contains Heyuan city, which the main stream passes through. HT1 is located in Heyuan city (Figure 56), and the majority of the upstream catchment is assumed to be treated by the largest Heyuan STW. HT5 is on the outlet to a semi-rural catchment, containing a small number of towns. HT2-HT4, and HT6-HT8, are located in a relatively remote rural area as illustrated by Figures 48-53. In the case of HT6, this is directly downstream of a rural discharge pipe, as shown by Figure 48.

The calculated RMSE for E1 and E2 is relatively low. For E1, the concentration at HM1 is overestimated, and is underestimated at HM2 and HM4. For all other sites, measurements are within the estimated 10<sup>th</sup>-90<sup>th</sup> percentile range. For E2, HM2 and HM4 were underestimated by the model, but for all other sites, the measured concentrations were within the estimated 10<sup>th</sup>-90<sup>th</sup> percentile range.

For TCC, the concentration at HM1 and HM5 is overestimated, whilst the concentration at HM2, HM3 and HM4 are underestimated. The RMSE for TCC is greater than E1 and E2, but lower than that of all TCS simulations.

In the case of TCS, the best performing in-stream removal scenario is TCS A, for which the measured concentrations at HM1, HM3 and HM5 are within the estimated 10<sup>th</sup>-90<sup>th</sup> percentile range. HM2 and HM4 are underestimated by the model. For the other two scenarios, the measured concentration is underestimated at all sites, particularly under TCS C.

The deviations between the duplicates of some of the samples on the main stream are relatively large, and therefore it is difficult to assess how well the model performs. However, the calculated RMSE for E1, E2, TCC and the best estimate for TCS, TCS A, is less than 5ng/l.

	E1	E2	TCC	TCS A	TCS B	TCS C
All sites	3.65	1.06	21.3	46.55	17.89	8.51
Main stream	0.99	1.57	3.84	4.16	6.13	7.34
Tributaries	4.59	0.54	26.98	59.25	22.29	9.17

Table 22- RMSE (ng/l) between the median estimated concentration and the mean measured concentration for samples collected at sampling sites within specified spatial units - for the Heyuan sampling zone, 2016 model.

Triclosan is parameterised with different in-stream removal constants, where: (A) –  $0.0138\text{h}^{-1}$ , (B) –  $0.061\text{h}^{-1}$ , (C) –  $0.21\text{h}^{-1}$ .

The RMSE for E1 is ~8.5 times higher than E2 at tributary sites, however, the concentration at HT2, HT3 and HT5-HT8 are within the estimated 10<sup>th</sup>-90<sup>th</sup> percentile range. There is much uncertainty in these catchments, as the majority of the catchment is not served by a STW.

The concentration of E1 is underestimated at HT1 and HT5, although, HT1 is also underestimated for all other chemicals. The STW upstream of HT1 is stated to serve 1 million people, which according to the gridded population dataset used in this study (see section 3.6), is estimated to be well in excess of the number of people in the nearby area and, therefore, was defined to serve all of the area near the STW, including almost all of the catchment area upstream of the sample site. Therefore, the model is defined to release only a very small volume of wastewater upstream of the sampling site. This suggests that the area may be subject to illegal wastewater discharge or possibly some inefficiency in the sewage system. Precipitation records during the sampled month suggest that no sewer overflows are likely, although blocked pipes may still lead to overflows of untreated wastewater due to backed up flow. Alternatively this area may not be served, although considering the vicinity to the STW this would be unlikely.



Figure 48 - Rural wastewater discharge at site HT6.

The RMSE for E2 is low, and the measured concentrations at HT2-HT8 are within the estimated 10<sup>th</sup>-90<sup>th</sup> percentile range. Therefore the model seems to represent E2 well here.

The model performs quite poorly for TCC, as it overestimates the concentration at every tributary site in the Heyuan sampling zone. It is possible that the usage for sampling sites located in more remote rural areas may be overestimated. Rural life in these areas appears

to be relatively simple (as noted during the field sampling campaign), with more emphasis on low-technology (e.g. using animals for transportation), and as such it is plausible that the local population may not be able to afford personal care products.

For TCS, the in-stream removal scenario with the lowest RMSE is TCS C. However, as shown by Figure 54, the performance of each in-stream removal scenario varies considerably depending upon the sampling site. For HT2, HT3, HT6 and HT7, scenario TCS C has the lowest RMSE. For HT4 and HT5, TCS A has the lowest RMSE and for HT8, TCS B provides the closest estimate with a deviation of 0.05ng/l. Therefore, it is difficult to determine which scenario best represents the area, if any. It is possible that there is a relationship between river discharge and removal rates. The mean flow at each tributary site in the Heyuan sampling region is shown by Table 24. At HT6 and HT3, the flow is estimated to be very low, and as shown by Figure 48, a photo taken at HT6, the cross-sectional area of the stream is small, and therefore the estimation of flow is plausible. The concentration of TCS at sites HT3 and HT6 is best estimated when using a higher in-stream removal scenario, and at site HT5, which is estimated to have a much greater discharge, is best estimated when using a low in-stream removal scenario.

Site	Flow (m <sup>3</sup> /s)
HT1	163.97
HT2	3.37
HT3	0.68
HT4	3.75
HT5	13.83
HT6	0.2
HT7	1.74
HT8	7.04

Table 23 - Mean flow estimated at tributary sites in the Heyuan sampling zone.

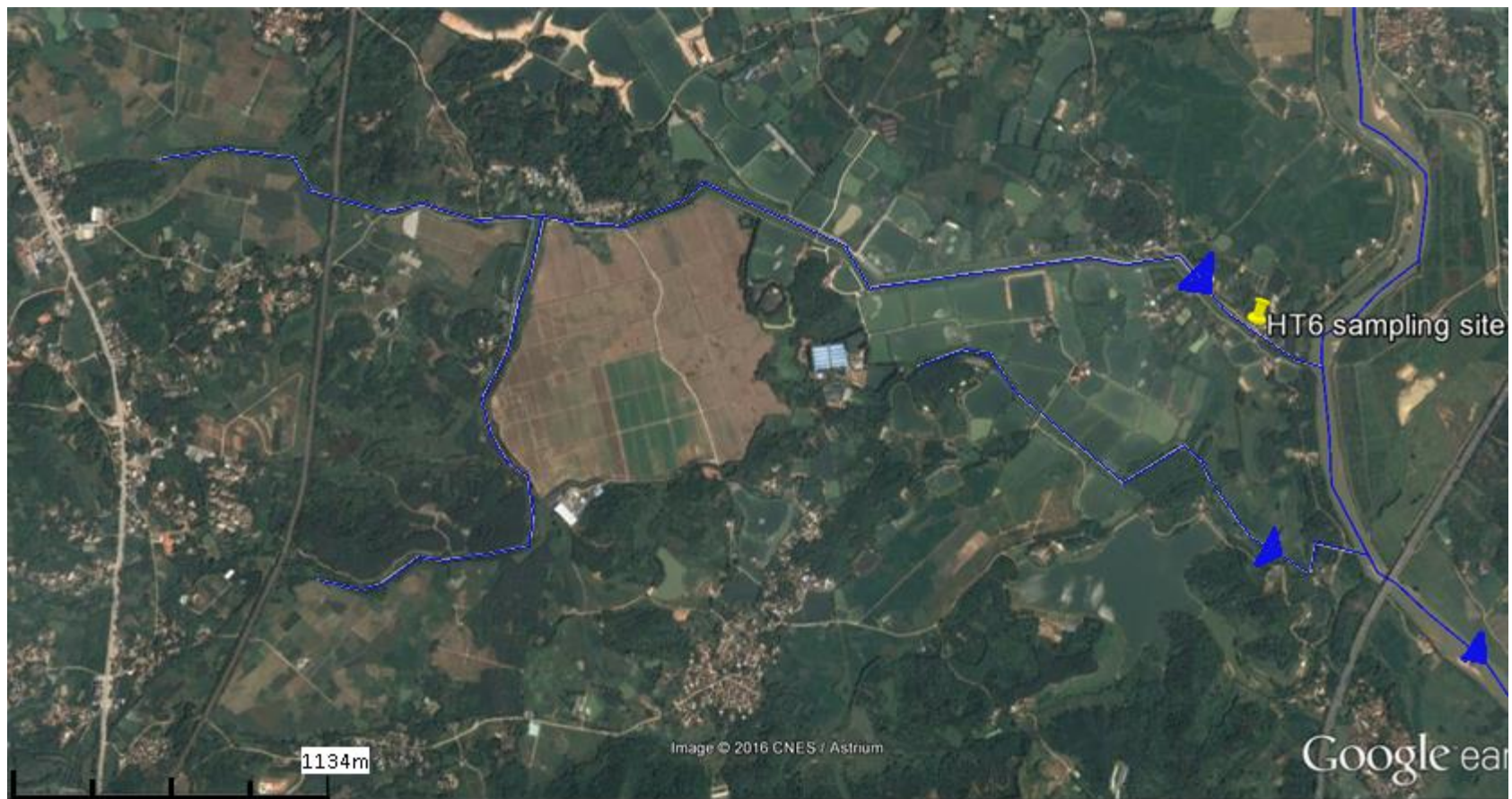


Figure 49 - Satellite imagery of sampling site HT6 in a rural catchment within the Heyuan zone. Arrows indicate direction of flow. Imagery from Google Earth





Figure 50 - Photo taken from the area near sample site HT6. This small, unstable bridge and a ferry is the only means for accessing the other side of the river. This photo provides an example the level of development in the area.



Figure 51 – Photo taken from the area near sampling site HT6. These residents appear to tend a small amount of crops, and chickens. This is an example of small-scale, subsistence farming observed in the area.

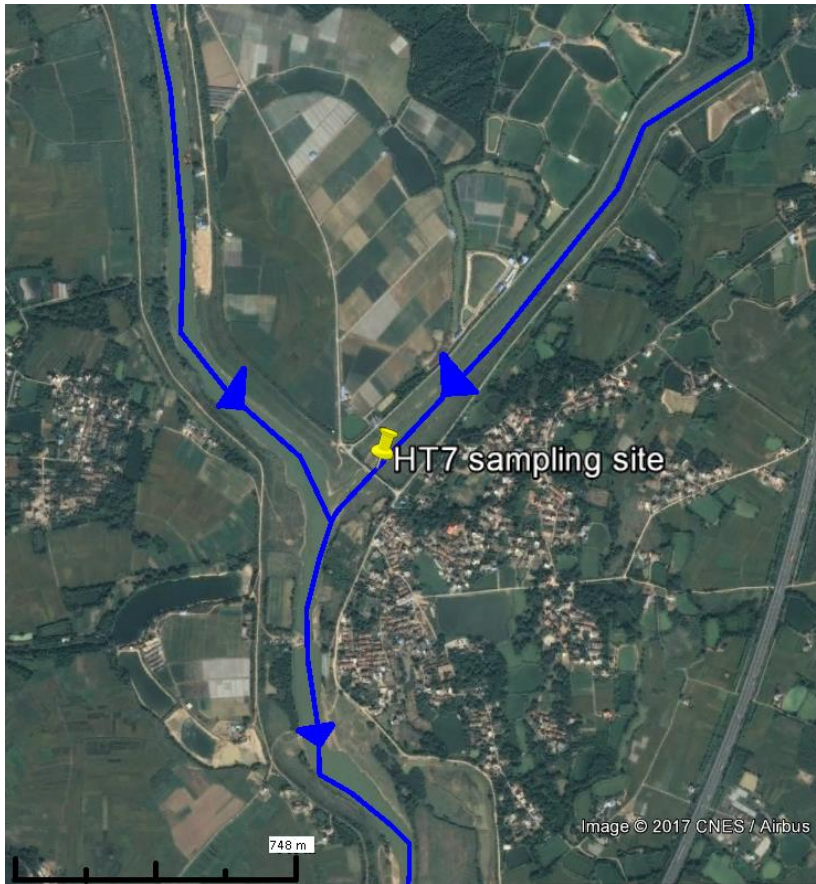


Figure 52 - Satellite imagery of the catchment of HT7 in a rural area within Heyuan zone. Arrows indicate direction of flow.

Imagery from Google Earth.



Figure 53 -Photo taken at sampling site HT7 - looking upstream. This area is rural with a sparse population, as illustrated here.



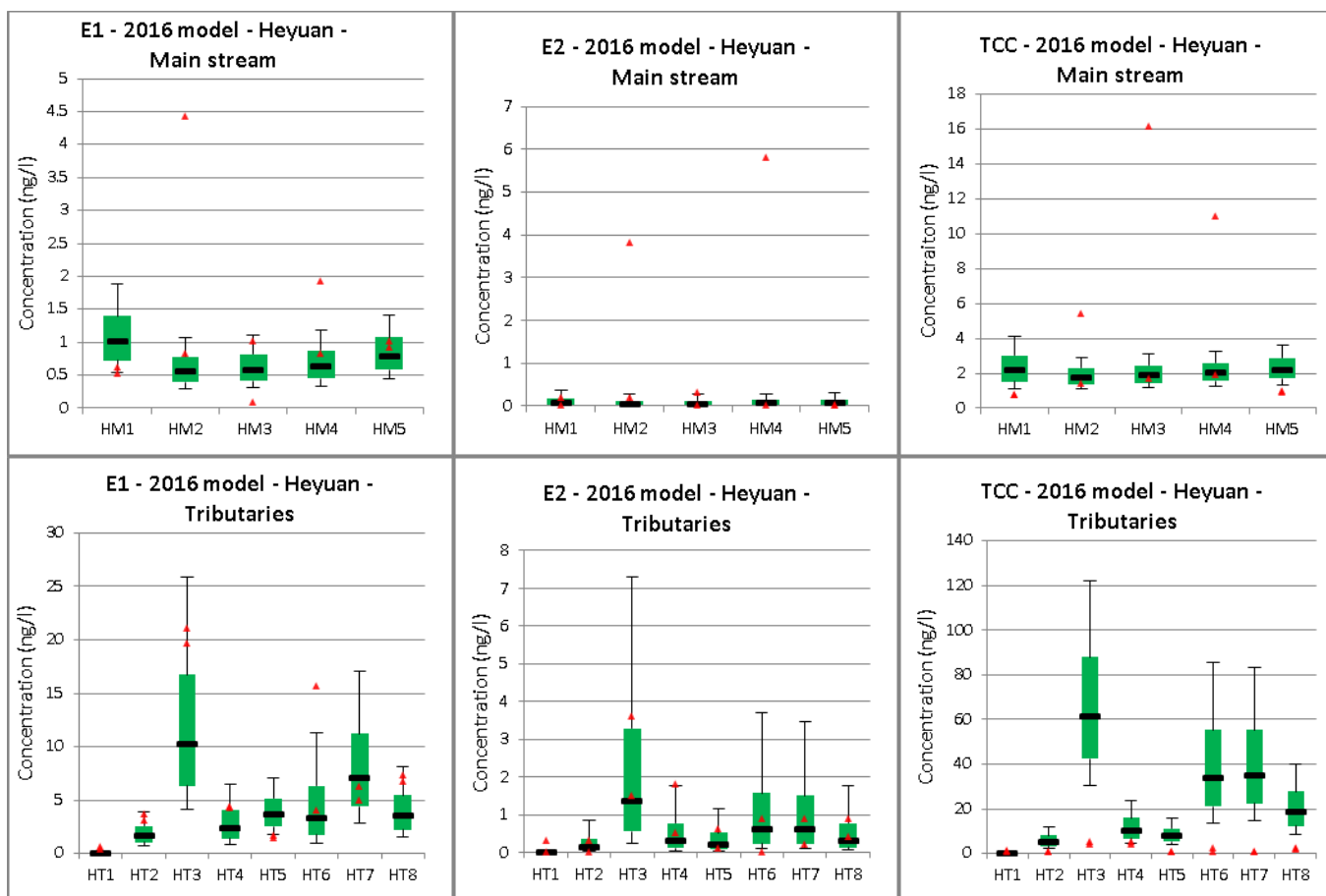


Figure 54 - Simulated and measured results for the 13 sampling sites within the Heyuan sampling zone in 2016 - for Estrone, 17β-estradiol and Triclocarban.

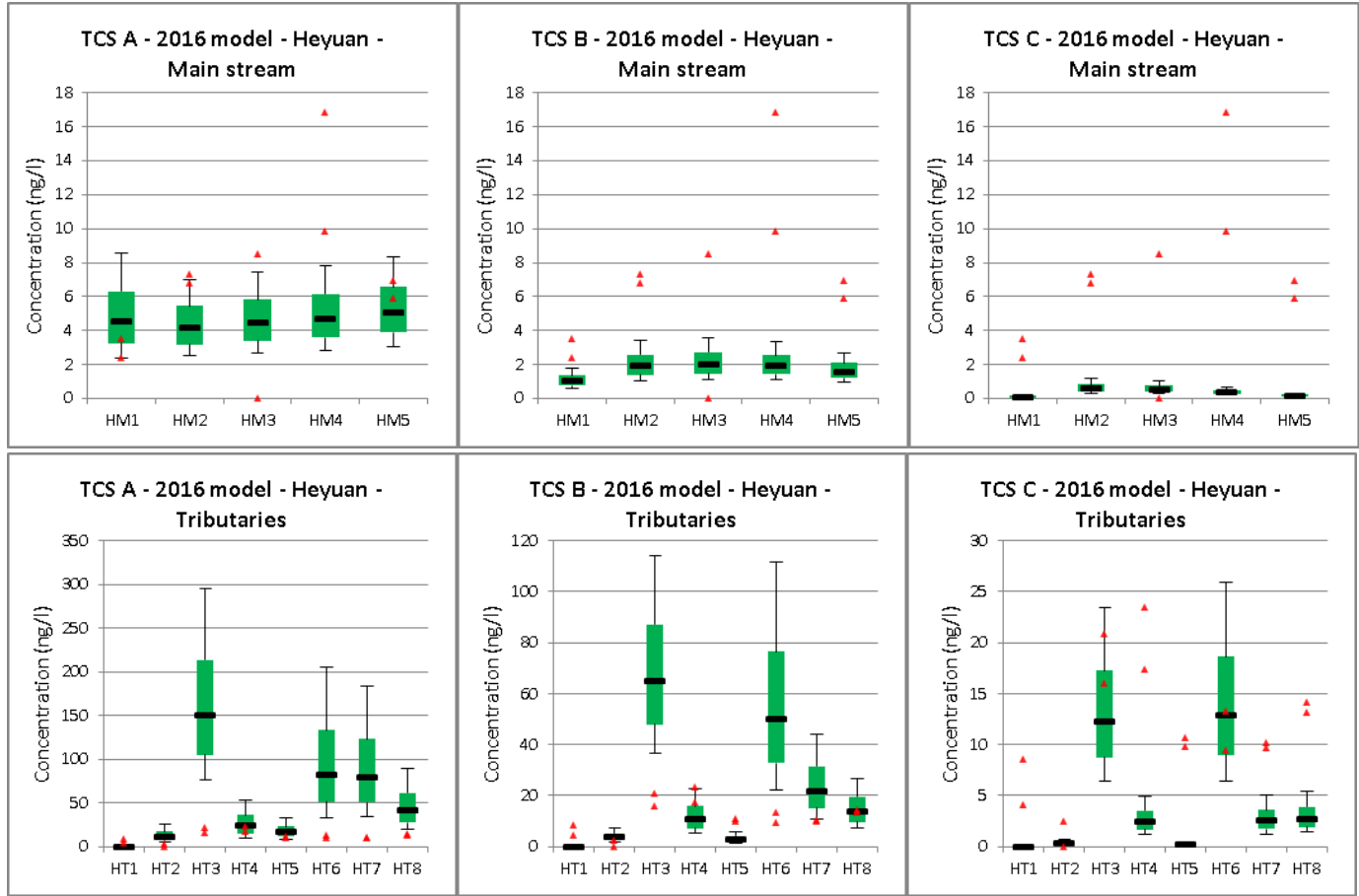


Figure 55 - Simulated and measured results for the 9 sampling sites within the Longchuan sampling zone in 2016 – For Triclosan. Triclosan is parameterised with different in-stream removal constants, where: (TCS A) – removal constant =  $0.0138h^{-1}$ , (TCS B) – removal constant =  $0.061h^{-1}$ , (TCS C) – removal constant =  $0.21h^{-1}$ .

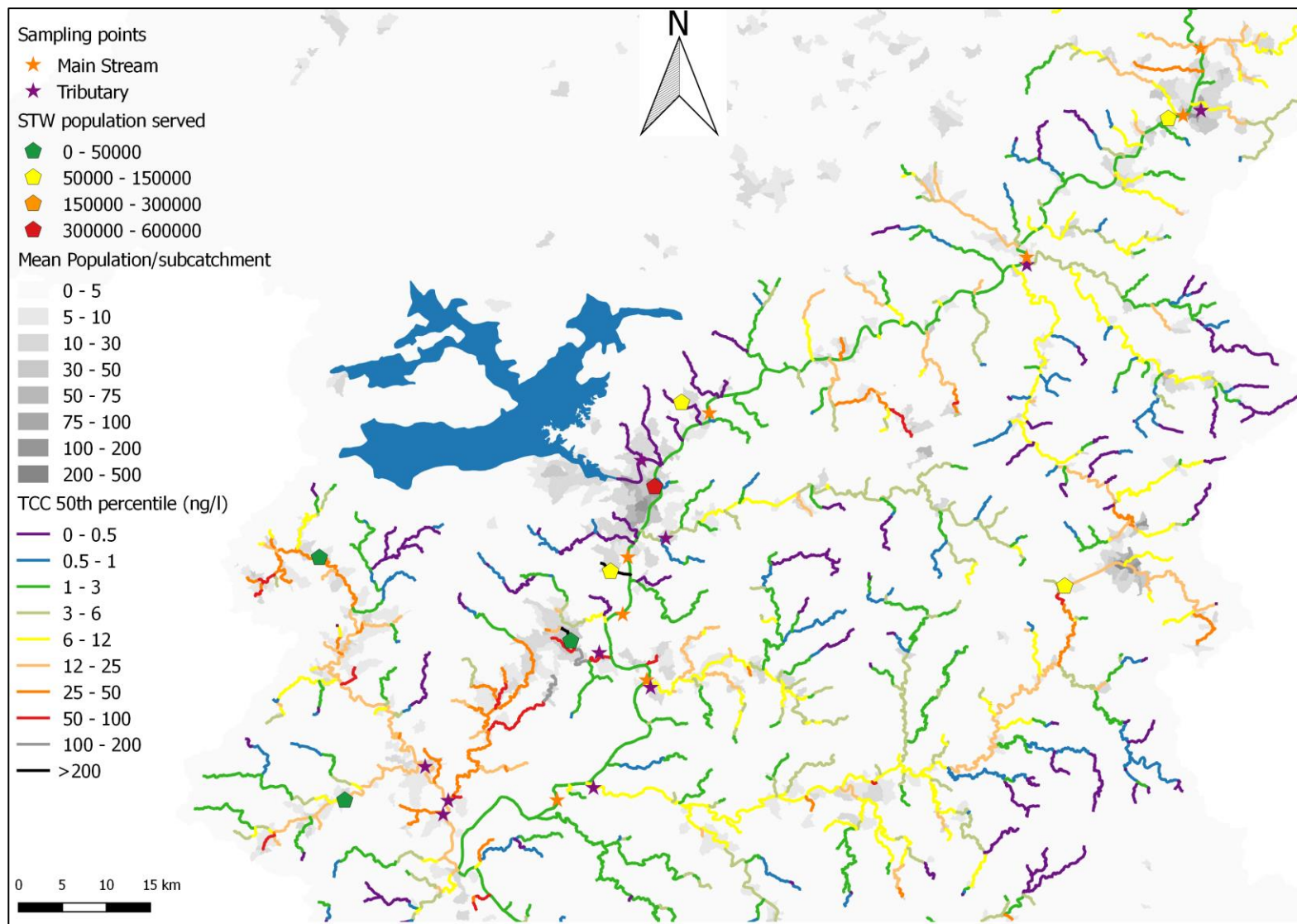


Figure 56 - Median simulated concentration of Triclocarban in 2016 in the Heyuan sampling zone (ng/l).

## Huizhou

The Huizhou zone represents a densely populated area that contains a portion of Huizhou and Shenzhen city (Figure 19). Chemical inputs are significantly higher than in the other two zones and therefore wastewater removal and dilution are important.

	E1	E2	TCC	TCS A	TCS B	TCS C
All sites	4.59	0.67	45.71	89.96	47.69	37.96
Main stream	0.93	0.22	2.87	5.26	9.11	11.23
Tributaries	5.20	0.71	49.35	97.15	51.37	40.74
H1-H4	6.14	0.49	33.73	54.21	17.27	55.70
HA1-HA3	4.86	0.79	67.86	130.03	74.24	35.53
HB1-HB2	7.08	1.27	44.80	79.92	28.58	33.51
T1-T3	0.91	0.06	47.78	112.55	64.05	22.15

Table 24- RMSE (ng/l) between the median estimated concentration and the mean measured concentration for samples collected at sampling sites within specified spatial units - for the Huizhou sampling zone, 2016 model.

Triclosan is parameterised with different in-stream removal constants, where: (A) – 0.0138 h<sup>-1</sup>, (B) – 0.061 h<sup>-1</sup>, (C) – 0.21 h<sup>-1</sup>.

The main stream in this section leads to the outlet to the study area and therefore the discharge is high. However, the chemical load is very high, accumulating from the wastewater from several million people living in this region; Huizhou and Shenzhen have a population of ~3 and 11 million respectively (Guangdong Provincial Bureau of Statistics, n.d.). The model underestimates the concentration of E1 at both sites, although the RMSE is <1 ng/l. For E2, the RMSE for the main stream is very low, and the measured concentrations are within the estimated 10<sup>th</sup>-90<sup>th</sup> percentile range. The measured concentration of TCC is within the estimated 10<sup>th</sup>-90<sup>th</sup> percentile range at HZM1, however, the concentration at HZM2 is

overestimated. Finally, for TCS, the RMSE is at its lowest for the TCS A in-stream removal scenario. HZM1 is underestimated by TCS A, but the measured concentration of TCS is within the estimated 10<sup>th</sup>-90<sup>th</sup> percentile range for HZM2. Both TCS B and TCS C underestimate the concentration at both sites.

The catchment area containing HA and HB sites is densely populated with some of the largest STWs in the catchment. As the majority of the HA sub catchments are served by a STW it is perhaps expected that the subcatchment is easier to characterise. However, the population served by the STWs in the HB sampling tributary is not known and a significant proportion of the catchment is not served. In addition, the accuracy of the flow estimation is uncertain for the Shenzhen subcatchment (Figure 38), as no gauging data is available, this area includes H, HA and HB sampling sites.

For all HA and HB tributary sampling sites, the measured concentration of E1 and E2 is within the estimated 10<sup>th</sup>-90<sup>th</sup> percentile range, with the exception of HB2, which is underestimated by the model for E1.

TCC is overestimated at every HA and HB sampling site, with a RMSE significantly higher than E1 and E2. The RMSE for TCS is lower for HA and HB for the TCS C or TCS B in-stream removal scenarios respectively. Measured concentrations for samples taken at HA and HB sites are within the estimated 10<sup>th</sup>-90<sup>th</sup> percentile range for TCS B, apart from HA1 which is overestimated. For the TCS C scenario, both HA3 and HB2 are underestimated by the model. Finally, the TCS A scenario overestimates every HA and HB sample site.

The H sample sites represent the longitudinal change from the outskirts of the city at H1 to the inlet of the East river main stem at H4 (Figure 57-62). Mid-profile, H2 and H3 are located near towns that surround the city. This sampling region is far more uncertain than the HA and HB subcatchments, as a high proportion of the catchment outside of HA/HB area is untreated. In addition, there are five STWs for which the population served is estimated.

HZT1, HZT2 and HZT3 are located downstream of 3 of these STWs. The measured concentration of E2 is within the estimated 10<sup>th</sup>-90<sup>th</sup> percentile concentration range for all H sites. For E1, H2 and H3 measured concentrations are within the estimated 10<sup>th</sup>-90<sup>th</sup> percentile range, whereas H1 is underestimated and H4 is overestimated. The in-stream removal scenario with the lowest RMSE for TCS is the B scenario, with all measured concentrations within the estimated 10<sup>th</sup>-90<sup>th</sup> percentile range. Regarding TCC, the model overestimates the concentration at all H sites.

T1 is located in a rural subcatchment, with a low population density (relative to the rest of the sampling area), as shown by Figure 63. T2 and T3 are both located upstream of the Shenzhen subcatchment confluence but are located downstream of two STWs and the Baipenzhu reservoir. The measured concentration of E1 is within the estimated 10<sup>th</sup>-90<sup>th</sup> percentile range for T1 and T2, but overestimates at T3. For E2, measured concentrations are either within the estimated 10<sup>th</sup>-90<sup>th</sup> percentile range, or the modelled 10<sup>th</sup> percentile concentrations are close to 0 at all sampling sites where E2 is not detected in the samples collected. TCC is again overestimated at all sample sites, suggesting that TCC is modelled poorly in Huizhou. For TCS, the RMSE is lowest for in-stream removal scenario C, although for the TCS B scenario, the measured concentration is within the 10<sup>th</sup>-90<sup>th</sup> percentile range for T2 and T3. TCS C underestimates T2 and T3, and all TCS scenarios overestimate T1.

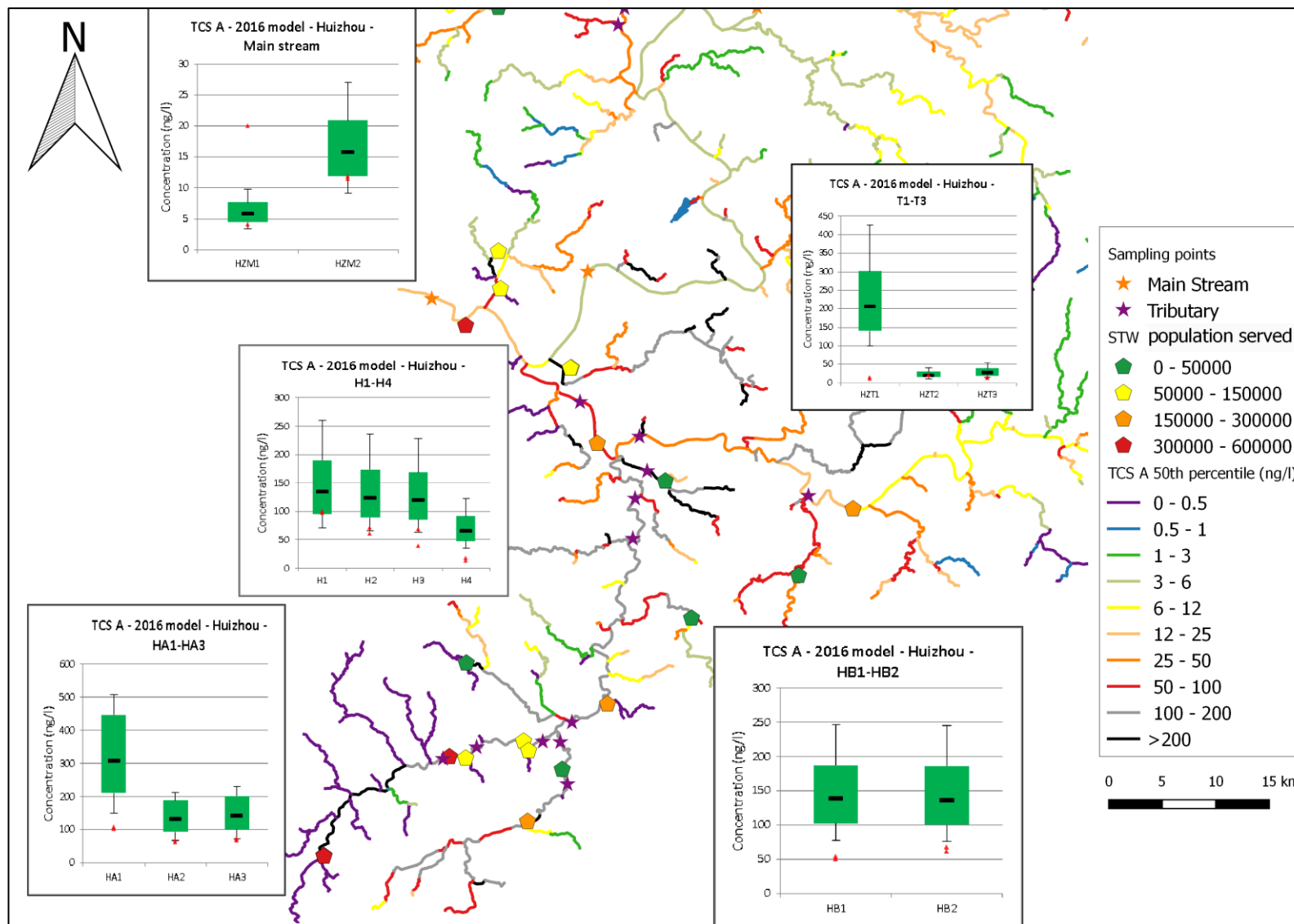


Figure 57 - Median simulated concentration of Triclosan A in 2016 in the 14 sites within Huizhou sampling zone (ng/l).

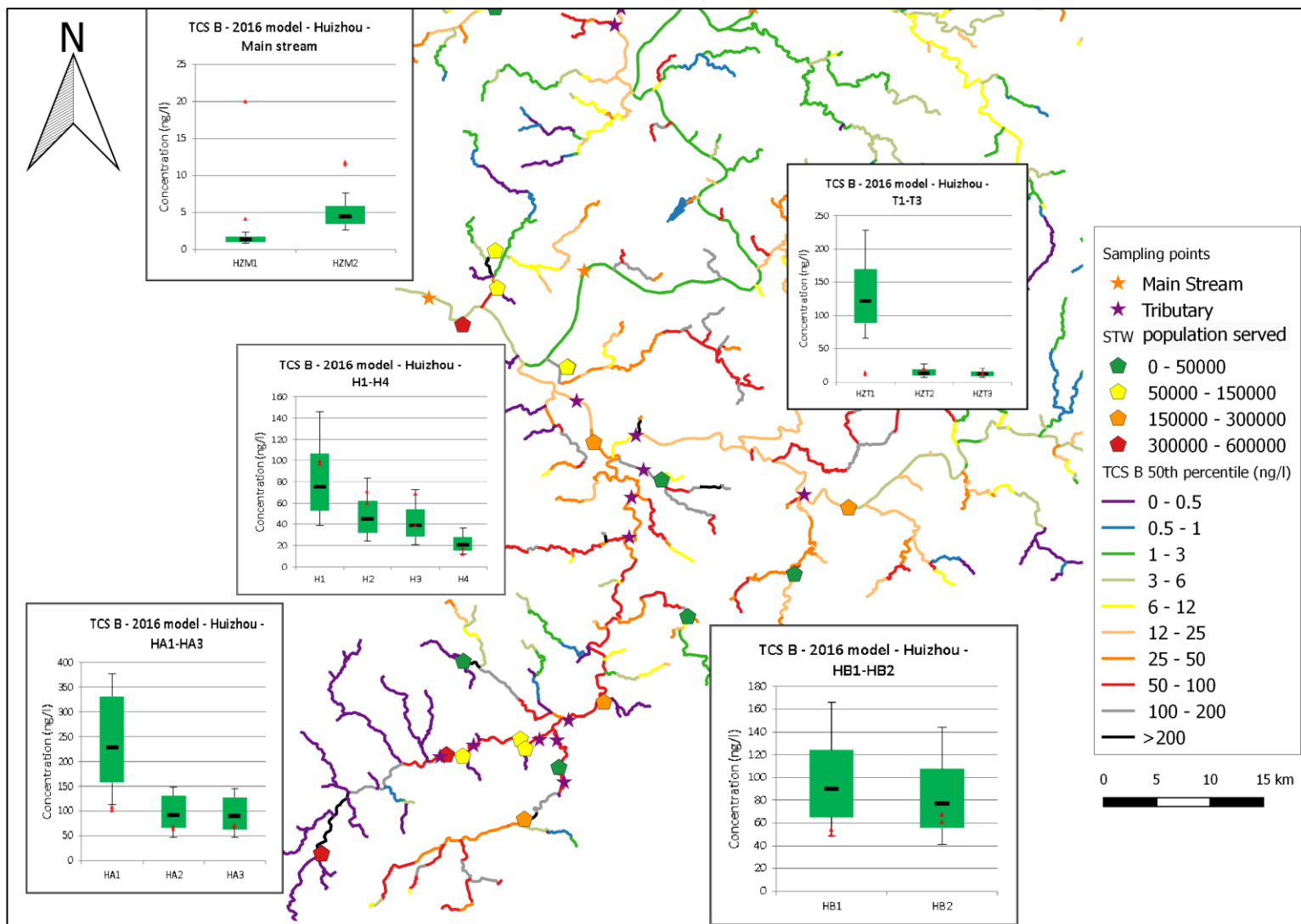


Figure 58 - Median simulated concentration of Triclosan B in 2016 for the 14 sites within the Huizhou sampling zone (ng/l).



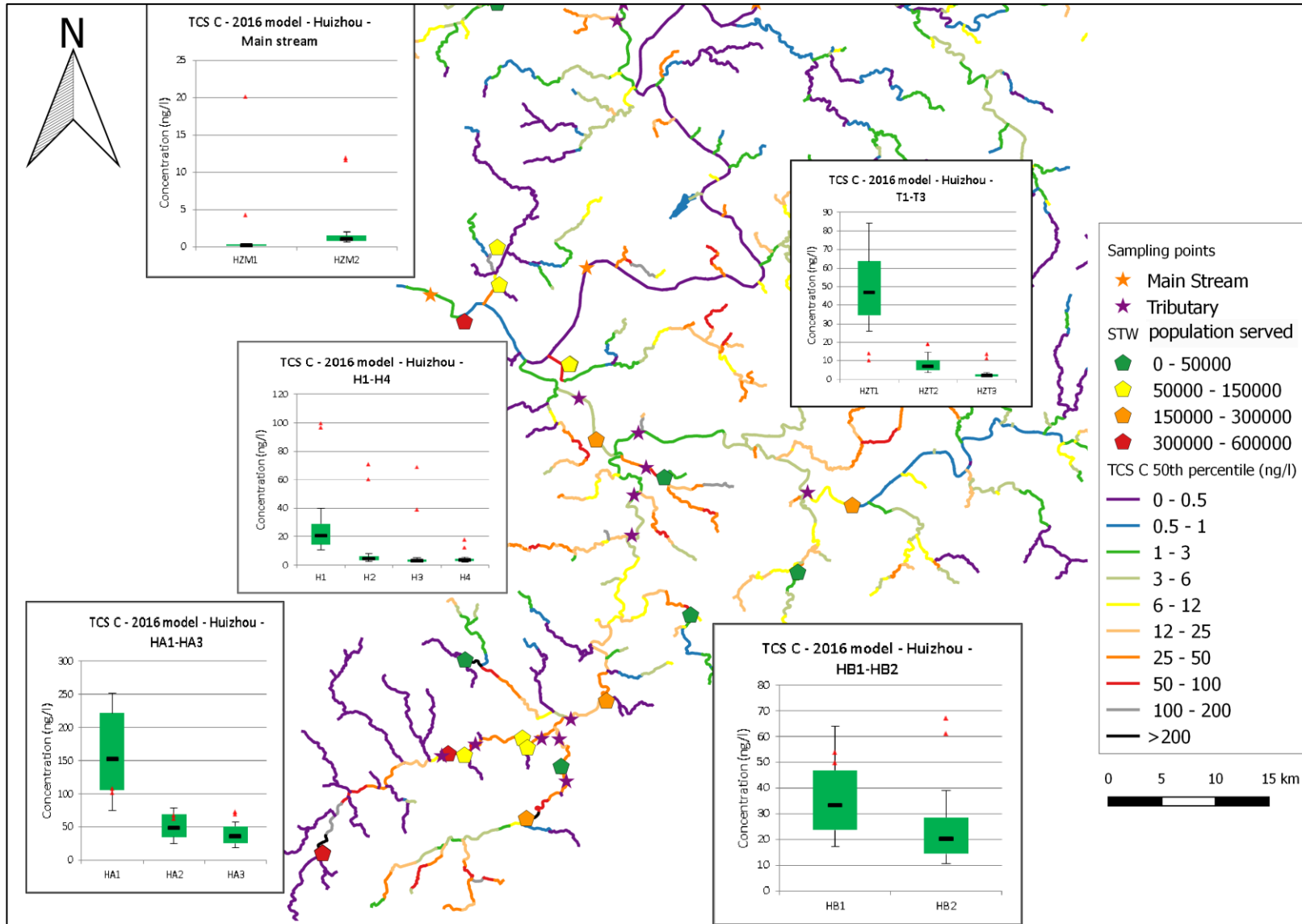


Figure 59- Median simulated concentration of Triclosan C in 2016 for the 14 sites within the 14 Huizhou sampling zone (ng/l).

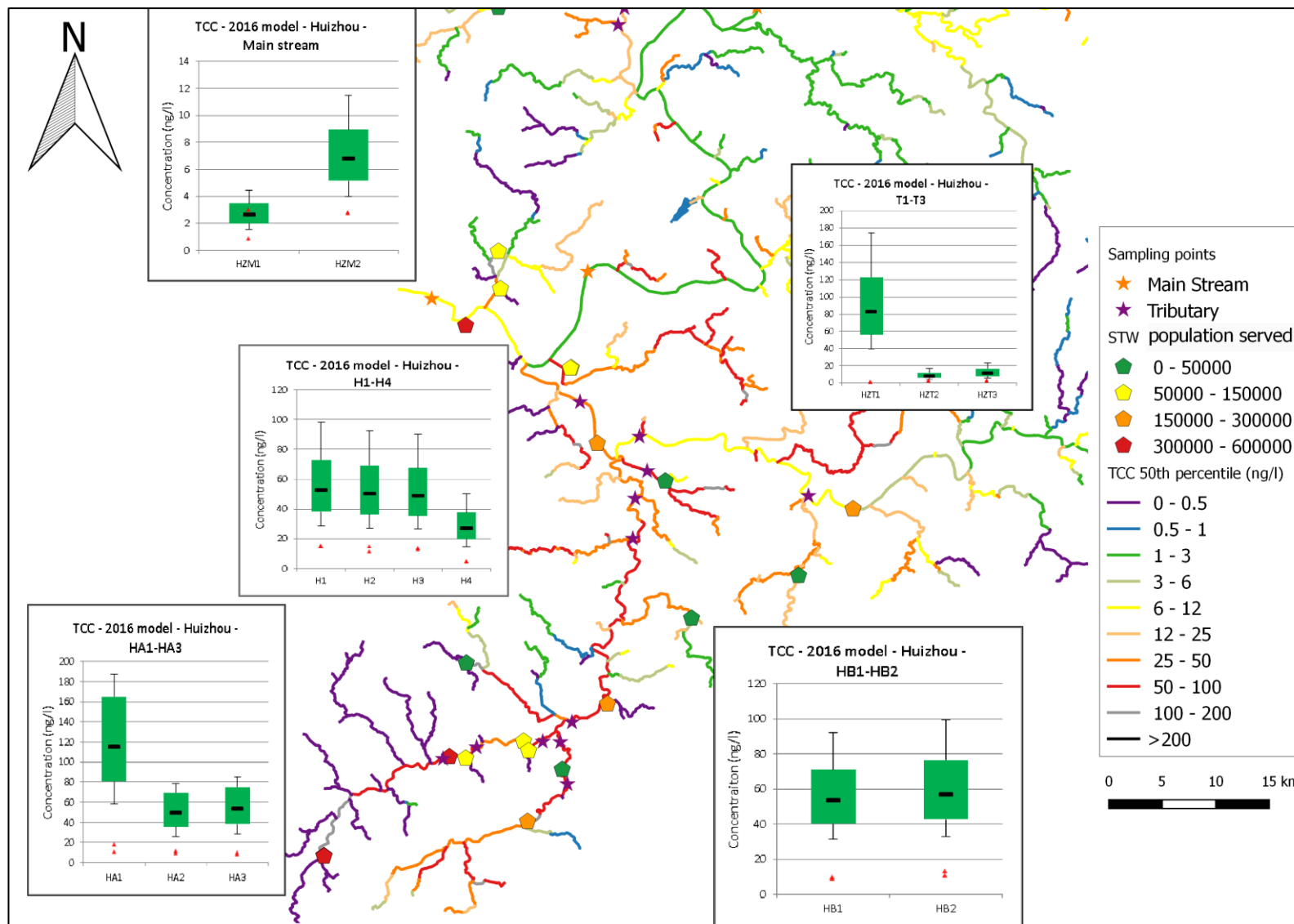


Figure 60 - Median simulated concentration of Triclocarban in 2016 for the 14 sites within the Huizhou sampling zone (ng/l).

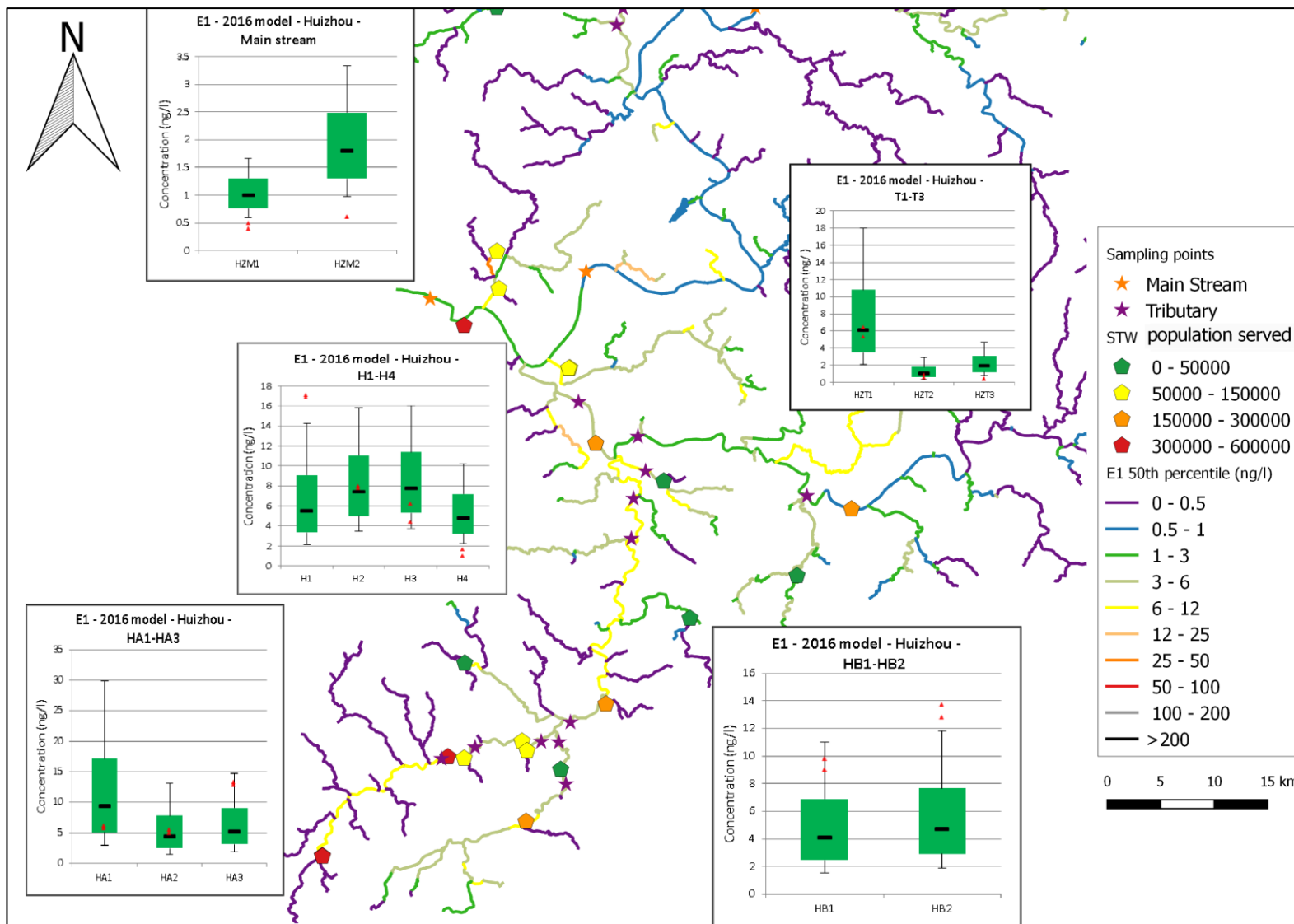


Figure 61 - Median simulated concentration of Estrone in 2016 for the 14 sites within the Huizhou sampling zone (ng/l).

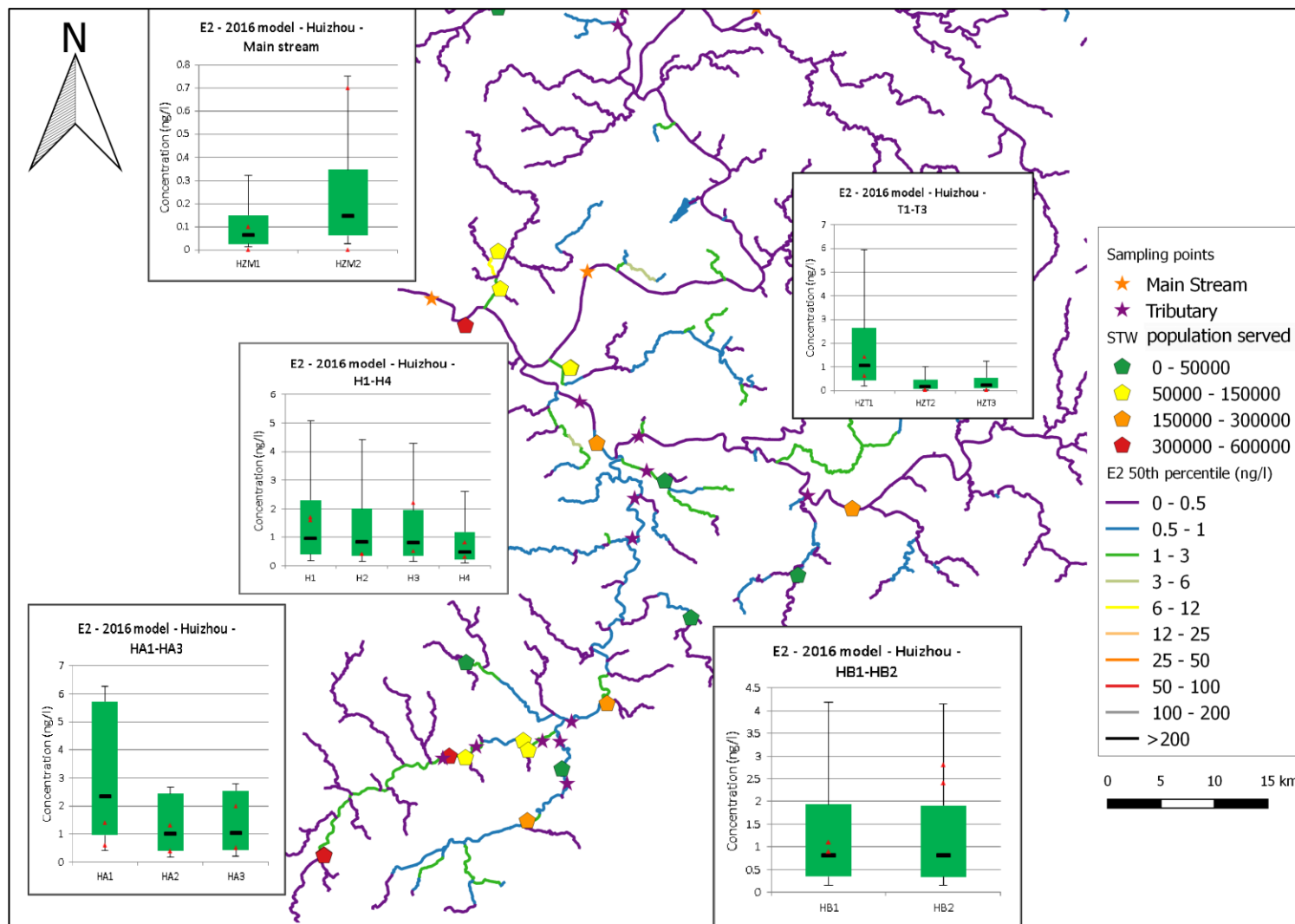


Figure 62 - Median simulated concentration of 17β-estradiol in 2016 for the 14 sites within the Huizhou sampling zone (ng/l).

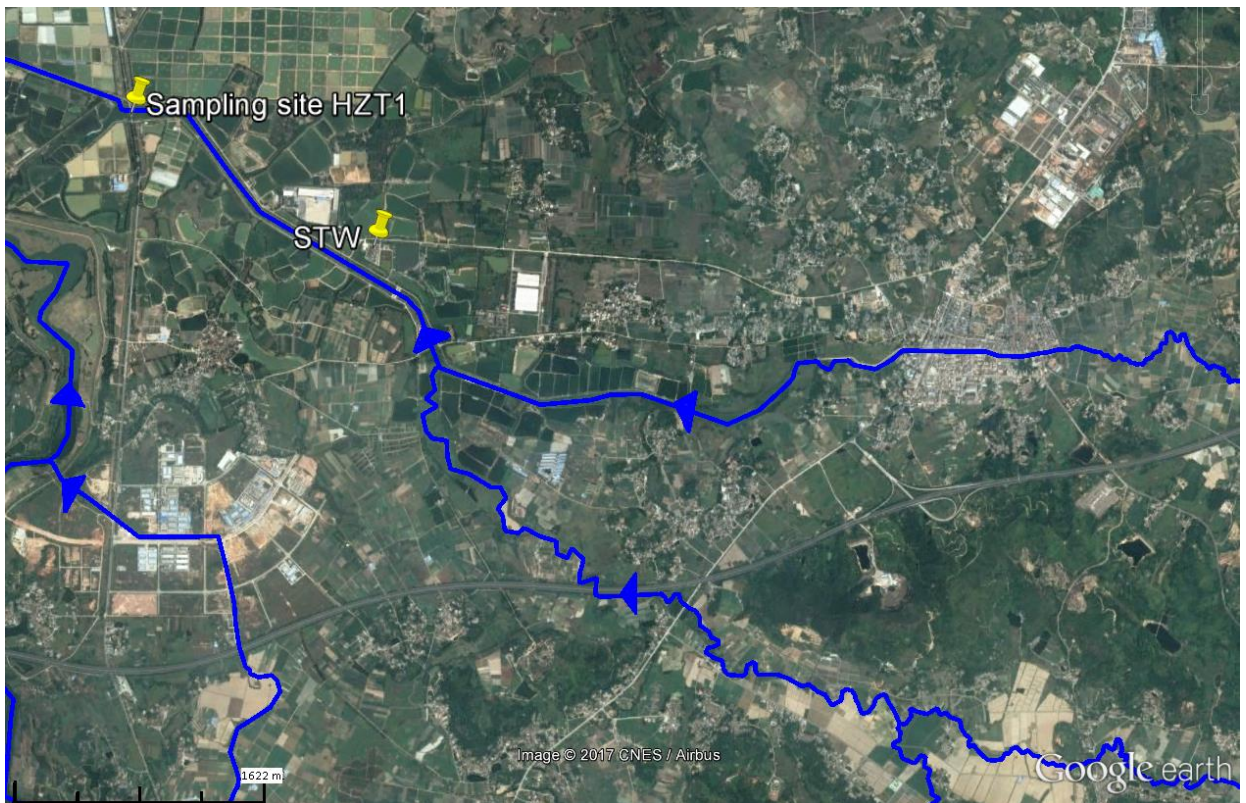


Figure 63 - Satellite imagery of sampling site HZT1, in a rural area of Huizhou zone. Arrows indicate direction of flow. Imagery from Google Earth.

## Summary

The ability of the model to simulate the catchment as a whole is assessed for each chemical here. Table 25 displays the RMSE for each chemical, as a whole, for the main stream and for tributary sampling sites. Figure 64 displays scatter graphs for each chemical, plotting the measured concentration against the estimated 50<sup>th</sup> percentile concentration.

E1 and E2 both have a relatively low RMSE overall, and scatter graphs suggest that the 50<sup>th</sup> percentile is relatively similar to the measured concentration in most cases, although when this is not the case, the estimated 50<sup>th</sup> percentile concentration is less than the measured concentration. The model appears to estimate the concentration of TCC on the main stream

with reasonable accuracy, as suggested by the RMSE value of 2.77ng/l. However, the performance in the tributary sites is relatively poor as described previously. Finally, for TCS, it appears that the lowest and highest in-stream removal constant is most appropriate for the main stream and the tributaries respectively. However, as discussed earlier, the most appropriate in-stream removal scenario varies between individual sampling sites. Examining the scatter graphs, TCS A tends to overestimate, TCS C tends to underestimate and for TCS B, modelled results are relatively similar to measured concentrations.

	E1	E2	TCC	TCS A	TCS B	TCS C
All sites	4.25	0.82	31.30	62.74	31.85	24.86
Main stream	0.76	1.02	2.77	4	6.23	7.47
Tributaries	5.17	0.68	38.28	76.79	38.76	29.99

Table 25- RMSE (ng/l) between the median estimated concentration and the mean measured concentration for samples collected at sampling sites within the East river catchment as a whole, for the 2016 model. Triclosan is parameterised with different in-stream removal constants, where: (A) –  $0.0138h^{-1}$ , (B) –  $0.061h^{-1}$ , (C) –  $0.21h^{-1}$ .



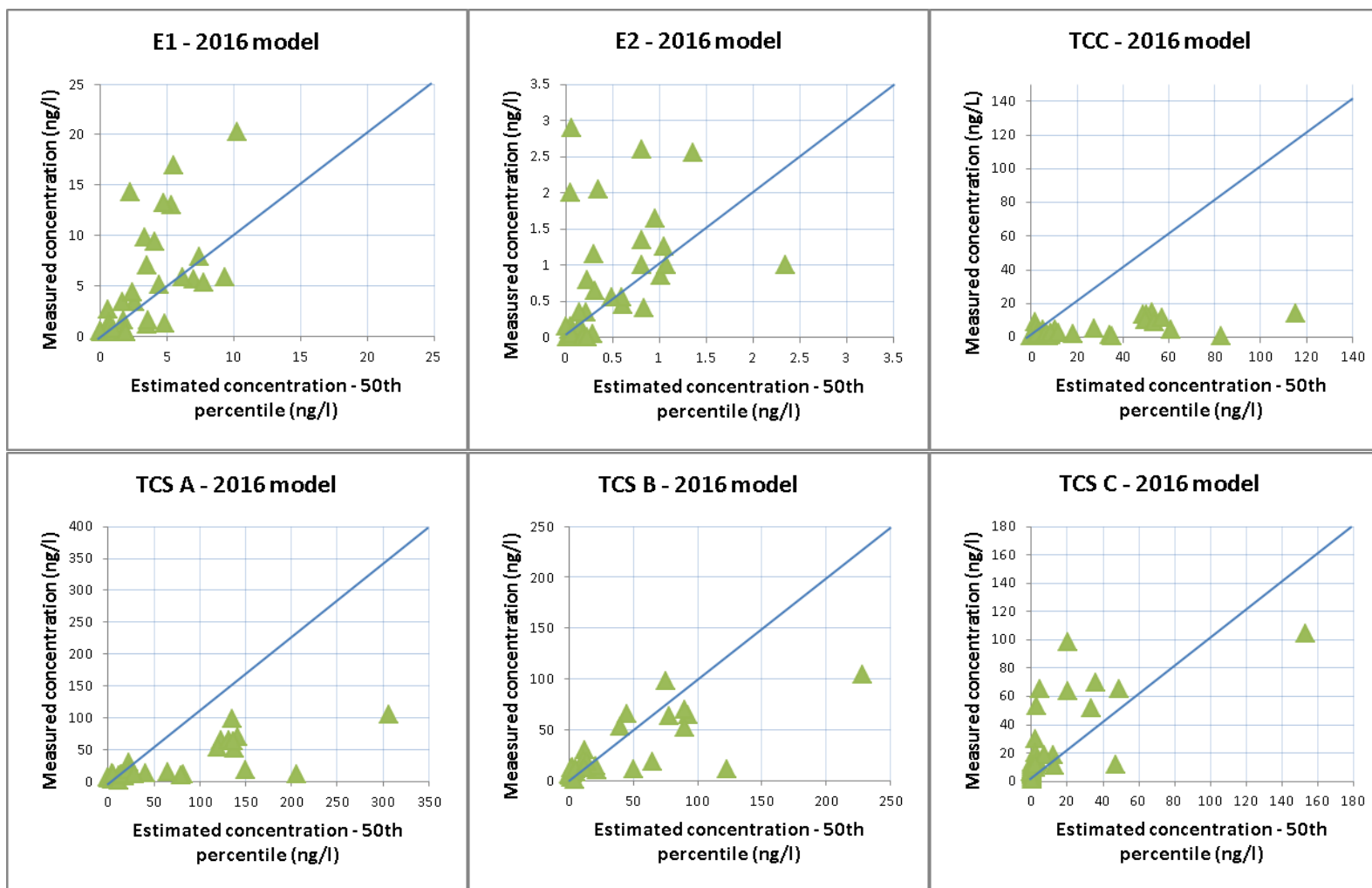


Figure 64 – Scatter graphs displaying measured concentration against estimated concentration of Estrone, 17 $\beta$ -estradiol, Triclocarban and Triclosan for the 2016 model. Triclosan is parameterised with different in-stream removal constants, where: (TCS A) – removal constant = 0.0138h<sup>-1</sup>, (TCS B) – removal constant = 0.061h<sup>-1</sup>, (TCS C) – removal constant = 0.21h<sup>-1</sup>. A line is drawn on all graphs, where: measured = modelled.



### 4.3. Model analysis

It is important to be able to explain the distribution of modelled results in space and time, in order to be able to make a sound assessment of its capabilities. A comparison of modelled results between the 2008 and 2016 models at 2016 sampling sites is provided here. The initial purpose of selecting these locations was for sampling only. The ratio of modelled concentrations in 2008 and 2016 (Table 26), and scatter graphs with 2008 concentration (C2008) plotted against 2016 concentration (C2008) (Figure 65A and Figure 66A) are included for the purpose of this analysis.

Concentration is lower in the 2016 model overall, but although the concentration at the majority of sampled sites is relatively similar, there are a small number of sites where the concentration in the 2016 model is much lower than the 2008 model. These sites are the HA and HB Huizhou tributary sites, and within the catchment areas of these sampling sites, large improvements to the wastewater infrastructure occurred between 2008 and 2016. However, for the majority of sites, the most significant change is flow, which is illustrated by Figure 65B and Figure 66B. Discharge was generally greater in the 2016 model, for which the primary effect was to increase dilution, which is reflected by the strong relationship between the ratios:  $Q_{2016}/Q_{2008}$  and  $C_{2016}/C_{2008}$ . However, this relationship is weaker for TCS C. This appears to relate to in-stream removal, which has a positive relationship with the ratio of  $C_{2016}/C_{2008}$  for TCS, as shown by Figure 67. Increasing river discharge also increases velocity which reduces the removal of a chemical between one stretch and the next, which is more significant for higher in-stream removal constants (e.g. TCS C); this therefore counteracts the effects of increased dilution, and weakens the relationship between discharge and  $C_{2016}/C_{2008}$ .

Overall the model appears to be a reasonable representation of the catchment for E1 and E2. However there are notable errors for TCC and for TCS under specific conditions and areas

of the catchment. Results from different in-stream removal scenarios for TCS seem to suggest that in-stream removal may be lower than estimated in larger catchments with higher discharge. In previous GREAT-ER (or models of similar design) studies, it became apparent that with larger catchments the errors in simulating in-stream removal processes increase with increasing residence time (Johnson et al., 2008b; Anderson et al., 2003; Alder et al., 2010). It was noted by Price et al. (2009) that applying different in-stream removal rates for different areas of the catchment may significantly improve the GREAT-ER model's predictions. They suggested that higher removal rates are likely to dominate in the shallow water of tributaries whereas in the main stream, lower removal rates may be more appropriate due to lower contact between fixed-film microbial biomass and the water column, which relates to a lower biodegradation rate. In addition, photolysis will be reduced due to increased light-extinction. This contrasts with the conclusion made by Grill et al. (2016) who suggested that differences in in-stream removal was not significant.

Correctly defining chemical removal for in-stream processes is important. There is significant spatial and temporal variation for all removal processes, which leads to difficulties when attempting to characterise these processes.

Site	Concentration ratio (2016/2008)
E1	0.82
E2	0.86
TCC	0.84
TCS A	0.85
TCS B	0.88
TCS C	0.93

Table 26 - Ratio of modelled concentration between the 2008 and 2016 models.

The methodologies used to generate the in-stream removal rates examined in this study do not estimate removal in deep water. Therefore, in-stream removal may be overestimated in

deep water. However, this is likely to be not the only factor influencing the accuracy of the model. There may be other factors that are not represented by the model that become significant for catchments with greater contributing areas. It has also been suggested that sediment may be a significant sink and potential source for TCC and TCS (Zhao et al., 2010). This may be released following resuspension, which is more likely outside of low-flow conditions.

Tributaries to the East river are clearly of greater concern, because they are less diluted than the main stream. This has been noted in previous studies, which has led to modelling approaches that focus heavily upon dilution and population (e.g. Keller et al., 2014). In the case of the Shenzhen catchment, the proportion of population that is treated is relatively high, although as the population is very high and dilution is relatively low, concentrations can still be high after treatment.

Rural catchments tend to have lower dilution and are treated to a lesser extent; this is the case for both developed and developing countries. This is reflected in a study by Johnson et al. (2007a), who noted that the contribution of a small STW in a small rural stream was much more significant than large STWs on the main stream. Often the largest populations are located in the lower catchment, which then discharge into rivers with greater dilution than found upstream. In the case of the East river, treatment of sparse populations is likely to be limited and crude. The model assumes that populations that are not treated by a STW are not treated at all, which may not be the case for all regions within the catchment, although it is conservative. These regions may be of concern as these areas may be of greater ecological significance. Zhang et al. (2010) noted that macroinvertebrate diversity was significantly higher in upper reaches in comparison to lower reaches. They suggested this related to stream disturbance from anthropogenic activity, particularly urban activity and water

quality. Therefore, protection of the upper reaches is important in order to preserve the resident ecological communities.

For remote rural sampling sites in Heyuan, it was suggested that usage for TCC and TCS may possibly be overestimated. In contrast, the model is able to simulate natural estrogens in the area relatively well. It is also important to reiterate that natural estrogens are released from all humans, but product use will vary quite significantly. It is likely that the usage of personal care products in the local area is relatively low; the area is much less developed in comparison to the cities in the region. Observations during the sampling campaign revealed buildings and transport links that are much more basic, and the use of technology in the region appears to be much lower, with many residents observed to be reliant upon animals to transport goods and machinery. It is likely that income in the region is much lower in comparison to urban areas in the country, and therefore many products would be unaffordable for the population. This might be confirmed by conducting a product use survey, and interviewing residents in the region.

The approach used to determine usage for TCC and TCS assumed usage was dependent on GDP. The major limitation is that GDP is determined at the county level. In rural areas, counties may be very large and therefore the spatial resolution is low. Furthermore, a more refined approach may be required to improve the estimation of product usage spatially. However, TCC was overestimated in sites across the catchment, not just in rural tributary sites, which suggests that usage may be overestimated for the entire catchment. Back-calculation of usage for E1 and E2 had significant advantages. There are many studies regarding the concentration of E1 and E2 in influent and effluent for STWs in China and therefore it was possible to describe the usage of E1 and E2 as a log-normal distribution. This is a significant reason as to why E1 and E2 often outperformed TCS and TCC. In addition, a fraction of a given chemical may be removed during transportation in sewers. This is often

an unknown proportion but has been shown to be significant for surfactants (Matthijs et al., 1995). These results suggest that back-calculating usage may be more appropriate at the catchment scale. This will provide a range of values that may be input as a distribution to represent the uncertainty of the parameter. However, high resolution GDP datasets are emerging, which may potentially be utilised to refine the usage estimate.

Estimates in some of the smallest rivers were deemed to be unrealistically high. For example for TCS, there are a small number (<0.3%) of stretches that were estimated to have a concentration >500ng/l, for stretches immediately downstream of major STWs, which rapidly become diluted downstream of the point. Flow is likely to be significantly underestimated at these points, which is a particular problem within the heavily urbanised areas. However, as these are of a minority they are considered to be insignificant. This effect has been observed in previous GREAT-ER studies, with concentrations noted above that of untreated STW effluent in some stretches (Hannah et al., 2009). No explanation was provided by the author of this work, however it is plausible that the discharge of the receiving stream may have been defined to be less than that of the untreated wastewater discharge. This may occur if the flow estimate was calculated before a STW was constructed or simply if the modeller did not account for the effects of the STW discharge upon flow.

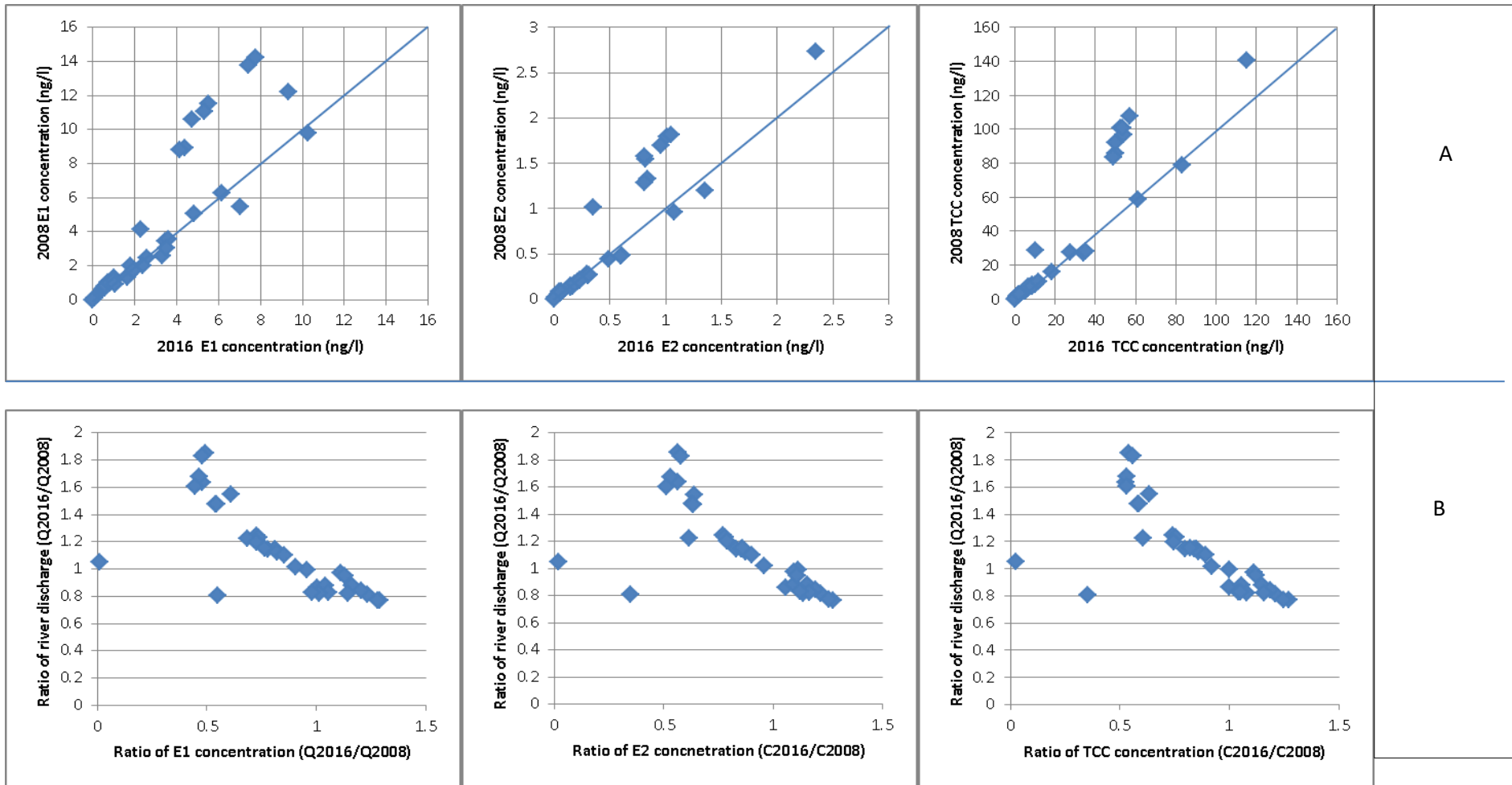


Figure 65 - Scatter graphs for the analysis of Estrone, 17β-estradiol and Triclocarban between the 2008 and 2016 models, where: (A) concentration in 2016 (C2016) against concentration in 2008 (C2008); and (B) ratio of C2016/C2008 against ratio of Q2016/Q2008. Line drawn on graphs is where: C2008 = C2016.

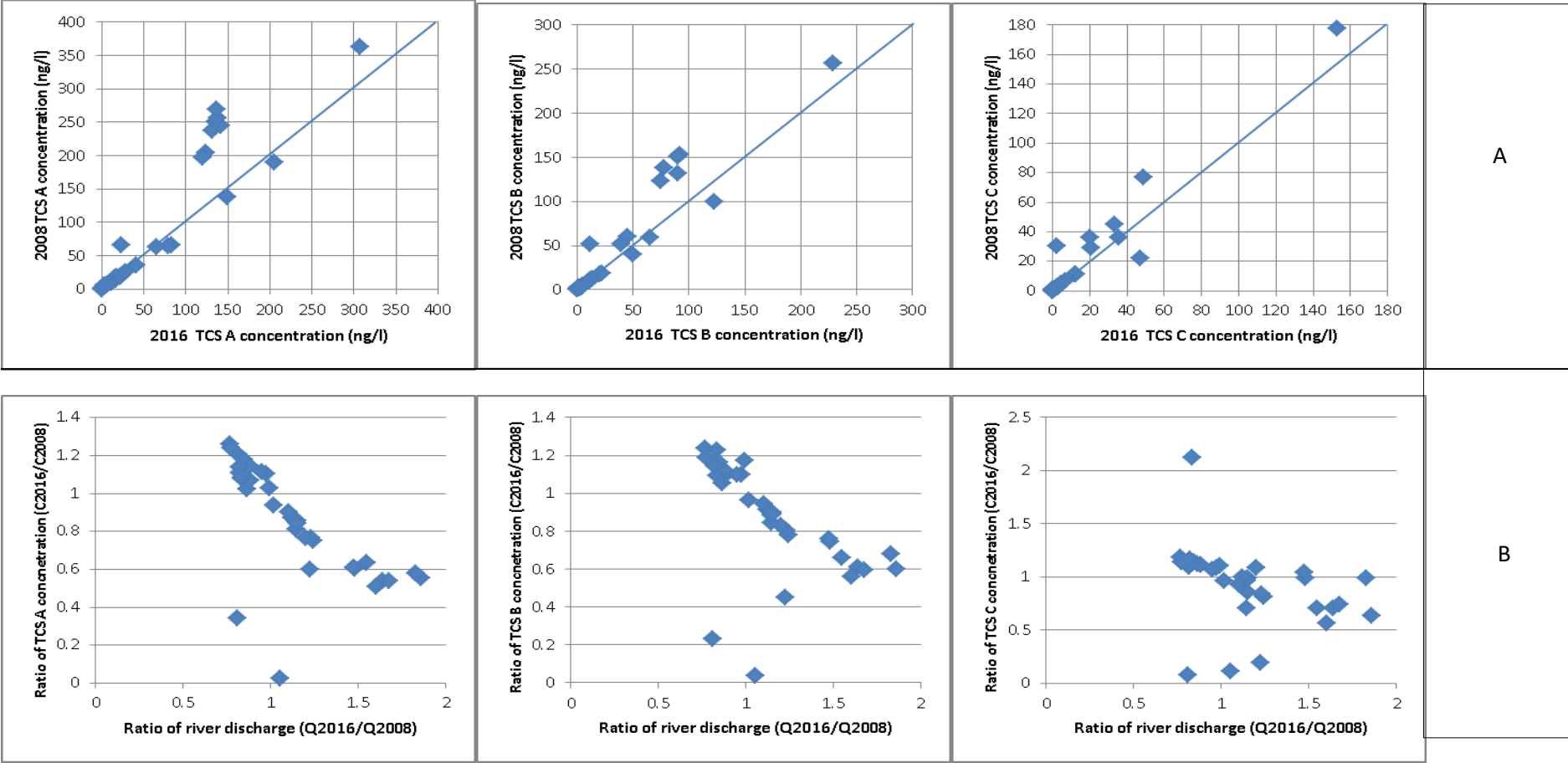


Figure 66 - Scatter graphs for the analysis of Triclosan between the 2008 and 2016 models, where: (A) concentration in 2016 (C2016) against concentration in 2008 (C2008), and (B) ratio of C2016/C2008 against ratio of Q2016/Q2008. Triclosan is parameterised with different in-stream removal constants, where: (TCS A) – removal constant =  $0.0138\text{h}^{-1}$ , (TCS B) – removal constant =  $0.061\text{h}^{-1}$ , (TCS C) – removal constant =  $0.21\text{h}^{-1}$ . Line drawn on graphs is where:  $C2008 = C2016$ .



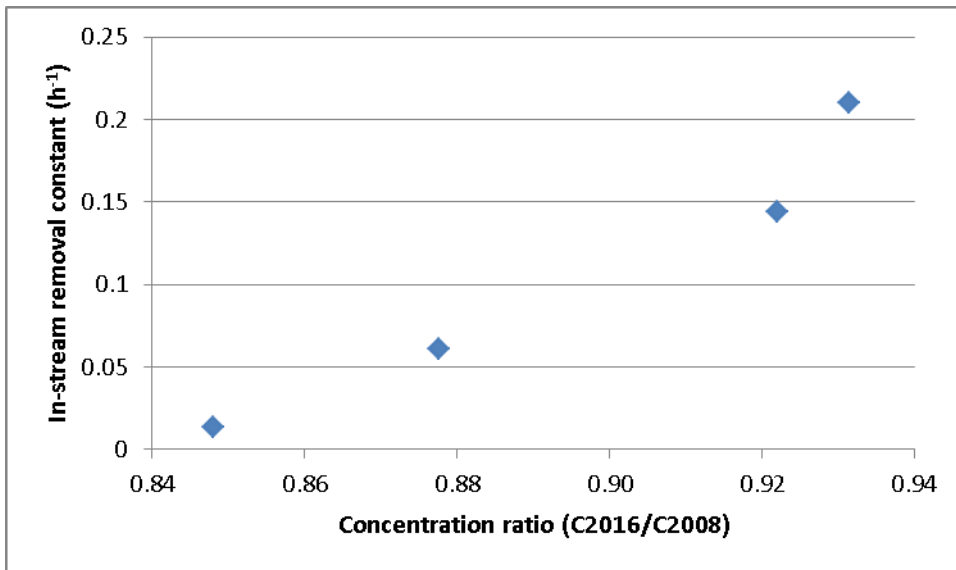


Figure 67 - Scatter graph illustrating the relationship between in-stream removal and the ratio between the concentration in 2016 (C2016) and 2008 (C2008).

#### 4.3.1. Sensitivity analysis

The sensitivity of the model to physio-chemical and environmental parameters was investigated through the means of a one-at-a-time sensitivity analysis. The change in predicted concentrations at 2016 sample sites was observed, following the change of a single parameter from its original value (base state) to a different value (sensitivity state). For results from this analysis to be comparable, this analysis aimed to determine the percentage change of chemical concentration as a result of a 20% change in a model input.

For this analysis, the stochastic nature of the model was removed; all parameters were defined as single values, including flow, which was defined by the mean flow only. The base and sensitivity states of each parameter are tabulated in Table 27. This analysis focuses on TCC, using the 2016 model.

Parameter	Base case	Sensitivity case +20%	Sensitivity case -20%
STW removal	0.5	0.6	0.4
DER	0.5	0.6	0.4
Usage (kg/capita/year)	7.4e-05	8.88E-05	5.92E-05
In-stream removal (h <sup>-1</sup> )	0.0102	0.01224	0.00816
Koc (L kg <sup>-1</sup> )	71687.0	86024.4	57349.6
Suspended solids concentration (mg/l)	18	21.6	14.4
Flow (m <sup>3</sup> /s)	-	+20%	-20%
Velocity (m/s)	-	+20%	-20%

Table 27 – Parameter set for TCC used for the purpose of sensitivity analysis of the 2016 East river model. The base state is the default state and the sensitivity state is the value 20% above/below the base state, used to test the sensitivity of the model to changes in this parameter.

Parameter	+20%	-20%
Koc	-2.23%	2.34%
Suspended solids concentration	-2.23%	2.34%
Velocity	3.9%	-5.8%
In-stream removal constant	-4.7%	5.0%
STW removal	-9.3%	9.3%
DER	12.3%	-12.3%
Flow	-20.0%	20.0%
Usage	20.0%	-20.0%

Table 28 - Sensitivity of the model to changes of each parameter by +/- 20%. Sensitivity is the percentage change in concentration normalised by the percentage change in the parameter (20%).

The most significant observation from this analysis is the ranking of parameter sensitivity; this information is illustrated by results tabulated in Table 28. Firstly, there is little or no difference between the response from positive and negative changes to each parameter. As for the relative importance of each parameter, results suggest that parameters that describe chemical input (usage) and chemical dilution (flow) are of most importance. DER is of greater importance than STW removal; STW removal relates to the chemical emission from areas of the catchment with the highest population, however, the majority of the catchment is untreated, and therefore the effect of DER is more important overall. In-stream removal constant and velocity are of equal importance as they both relate to the degradation of the chemical, as described by Equation 11. Previous analysis has suggested that in-stream removal may be of importance, however the sensitivity analysis suggests that its relative importance is less than parameters that describe emission and dilution. The parameters that relate to sorption, Koc and suspended solids concentration, are of the least importance. A value for suspended solids was obtained based on the mean suspended solids concentration at the catchment outlet (Bolou flow gauge), however the spatial and temporal variability of suspended solids is likely to vary significantly, but, the results of the sensitivity analysis suggest that this would likely have little impact upon the model result.

#### 4.4. Scenario based assessment

##### 4.4.1 Risk assessment

A full risk assessment was not a specific aim for this thesis. However, to present the viability of the model for risk assessment purposes PNECs for the four chemicals were used as thresholds to estimate risk for the catchment in 2016. As a conservative measure, the lowest in-stream removal scenario for TCS, TCS A, was used.

Firstly, it was important to assess whether the model was suitable as a predictive tool for risk assessment. At the majority of sample sites for the 2016 model, the 90<sup>th</sup> percentile exceeds the measured concentration, as illustrated by Figure 69. This suggests that the model may be acceptable as a preventative tool in the majority of cases, although there is clearly room for improvement, with a need to refine the model in order to reduce the number of cases where the estimated 90<sup>th</sup> percentile is exceeded by the measured concentration.

As shown by Figure 70, modelled results at the 50<sup>th</sup> percentile suggest that much of the catchment is at risk from TCS exposure, with much of the catchment estimated to be exposed to a factor of over 5 times the PNEC. The estimated concentration of TCS at the 90<sup>th</sup> percentile (Figure 71) exceeds its PNEC value for a slightly larger area than the 50<sup>th</sup> percentile estimate but also generally exceeds the PNEC by a greater margin.

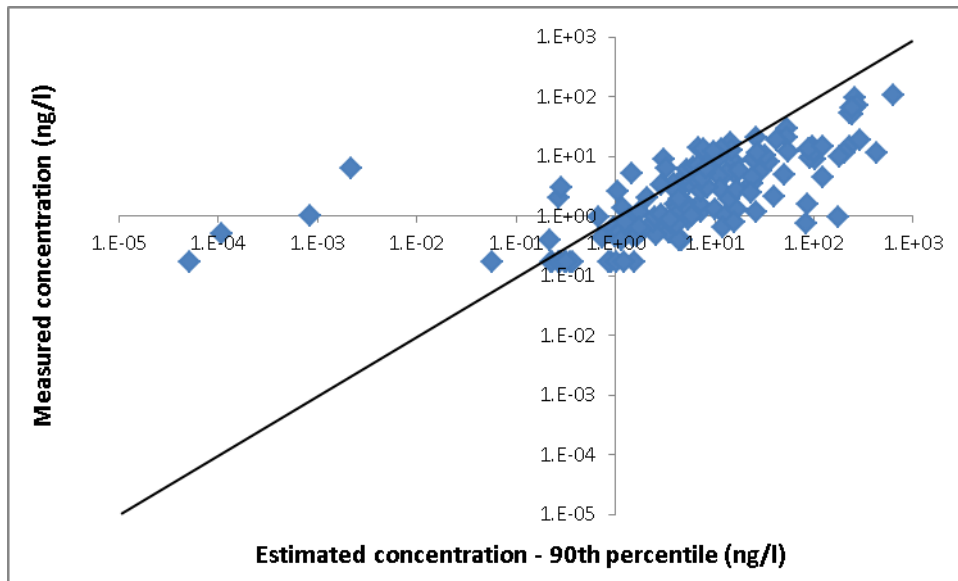


Figure 69 – Scatter graph displaying measured concentration against estimated concentration for all chemicals, using the 2016 model. A line is drawn on the graph, where: measured = modelled.

In contrast to TCS, at the 50<sup>th</sup> percentile, the model predicts that no region of the catchment is exposed to a concentration that exceeds the PNEC (Figure 70). However, concentration of TCC at the 90<sup>th</sup> percentile (Figure 71) exceeds the PNEC threshold for stretches mostly within the Huizhou and Shenzhen area, but also a few short stretches in small streams throughout the catchment.

Risk from E1 and E2 is largely acceptable for the catchment. However, there are notable hotspots within the catchment as shown by Figure 72. For E1, areas with unacceptable risk appear to be largely confined to the Shenzhen subcatchment (Figure 38), and a few small tributaries throughout the catchment. For E2, the area at risk is significantly smaller, which includes the upper Shenzhen catchment and minor stretches located just downstream of population centres with insufficient dilution relative to the population size. At the 90<sup>th</sup> percentile (Figure 73), the area that the model estimates to exceed the PNEC for E1 and E2 extends to relatively small tributaries within the Longchuan sampling zone to the North, and to tributaries in the West and East in the Heyuan sampling zone.

#### 4.4.2 Catchment management scenarios

In Chapter 1 it was suggested that the GREAT-ER model could have the potential to be used for catchment management. To test this potential, scenarios are used here to determine the effect of different management decisions on chemical risk; specifically focused on wastewater infrastructure. Firstly, population was upgraded to estimate 2020 levels and all existing STWs were assumed to be upgraded to incorporate additional population within their service areas. Secondly, two planned STWs (Figure 39) were identified through various reports (in Chinese), which were acknowledged when locating STWs as discussed in Chapter 2. These were incorporated into the catchment model. In addition, plans were identified for an upgrade of the service area for a STW upstream of sampling site HB1, the entire subcatchment was assumed to be served by this STW. An additional risk assessment was then completed for each chemical, at the 50<sup>th</sup> percentile.

As shown by Figure 74, the number of stretches that exceed the PNEC for TCS does not change significantly in comparison to 2016; however, the concentration of TCS is predicted to be higher overall, apart from stretches in catchments with enhanced wastewater infrastructure. As a result of increased population, the number of stretches that exceed the PNEC for TCC increases from 0 to 3, all of which are located downstream of STWs in the Heyuan and Huizhou sampling zones. For estimates of E1 and E2 at the 50<sup>th</sup> percentile, the number of stretches that exceed the PNEC values within subcatchments with improvements to wastewater infrastructure decreased; however the area estimated to exceed the PNEC value extended (Figure 75), this is due to the increase in population.

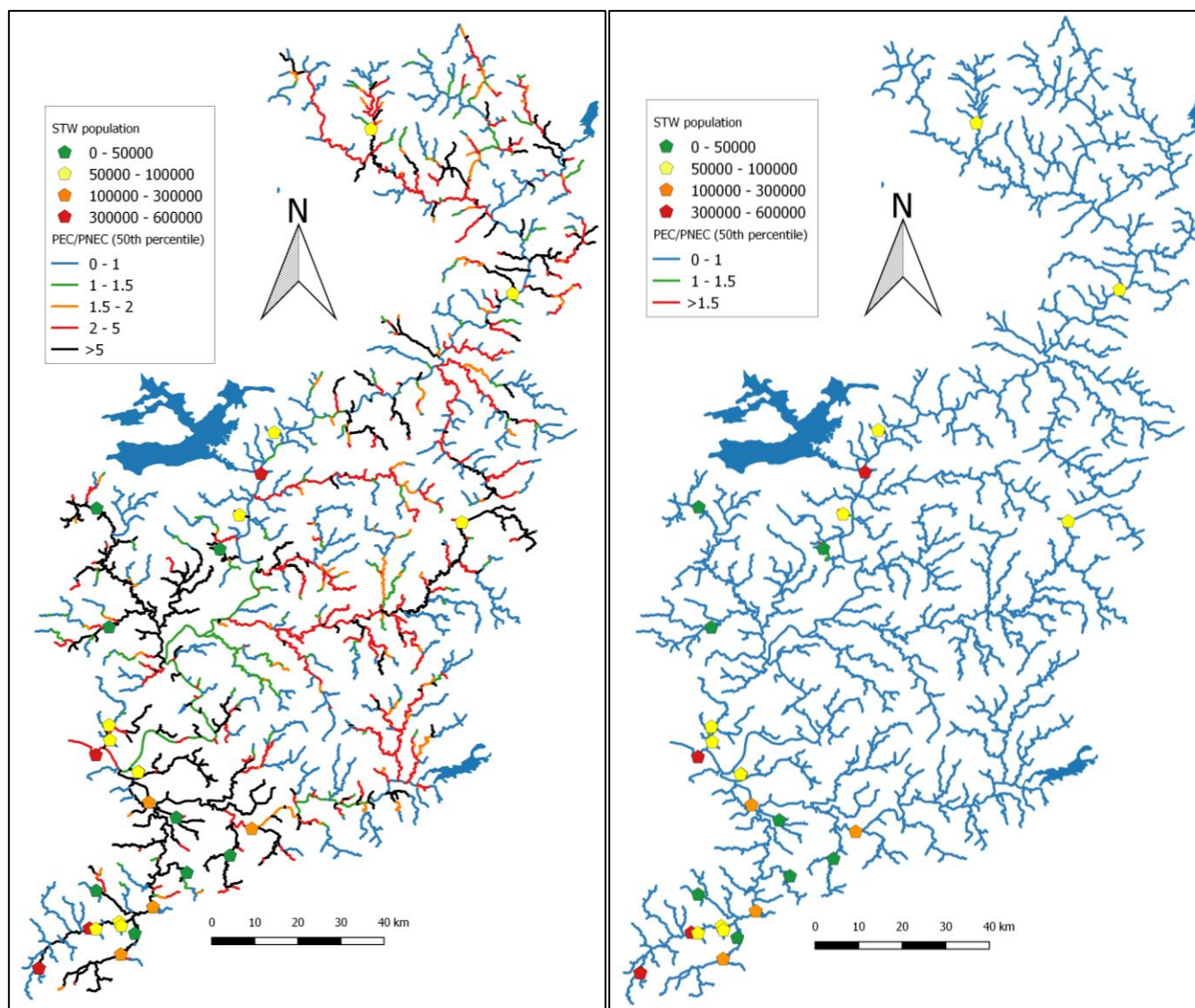


Figure 70 - Assessment of risk, at the 50<sup>th</sup> percentile concentration, from TCS (left) and TCC (right) for the 2016 model, assuming a PNEC of 4.7 and 146ng/l respectively.

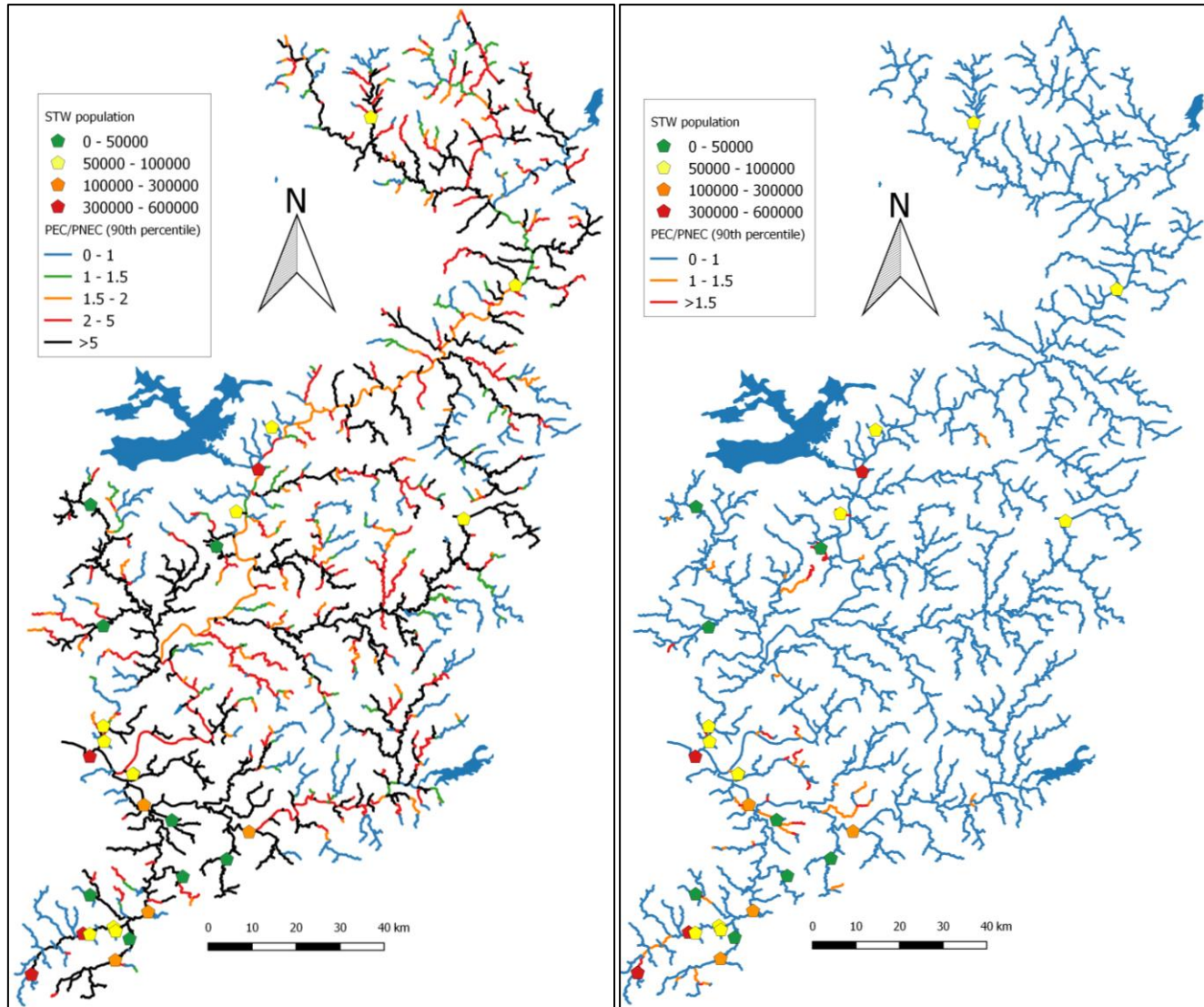


Figure 71 - Assessment of risk at the 90<sup>th</sup> percentile concentration from TCS (left) and TCC (right) for the 2016 model, assuming a PNEC of 4.7 and 146ng/l respectively.



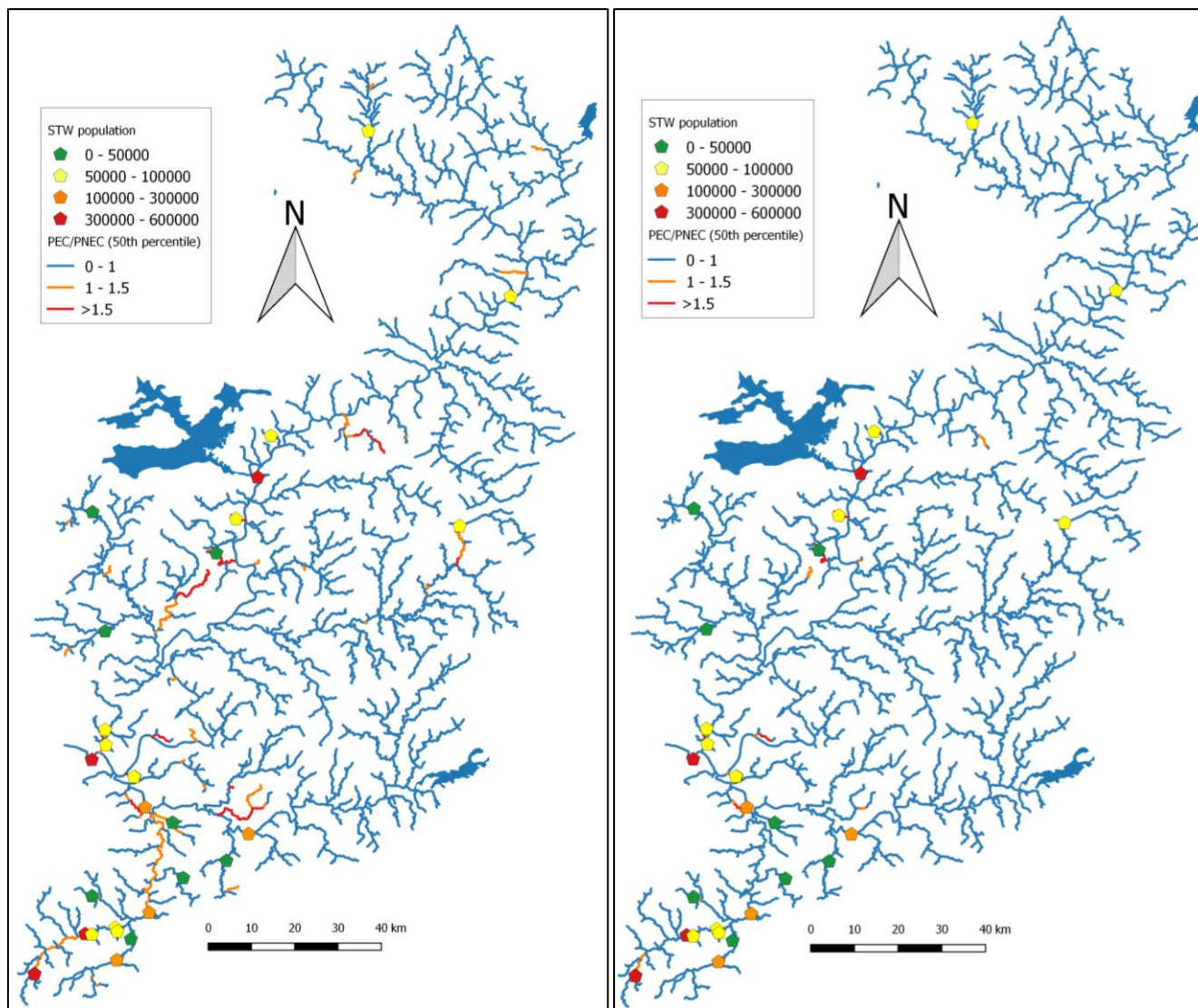


Figure 72 - Assessment of risk, at the 50<sup>th</sup> percentile concentration, from E1 (left) and E2 (right) for the 2016 model, assuming a PNEC of 6 and 2ng/l respectively.

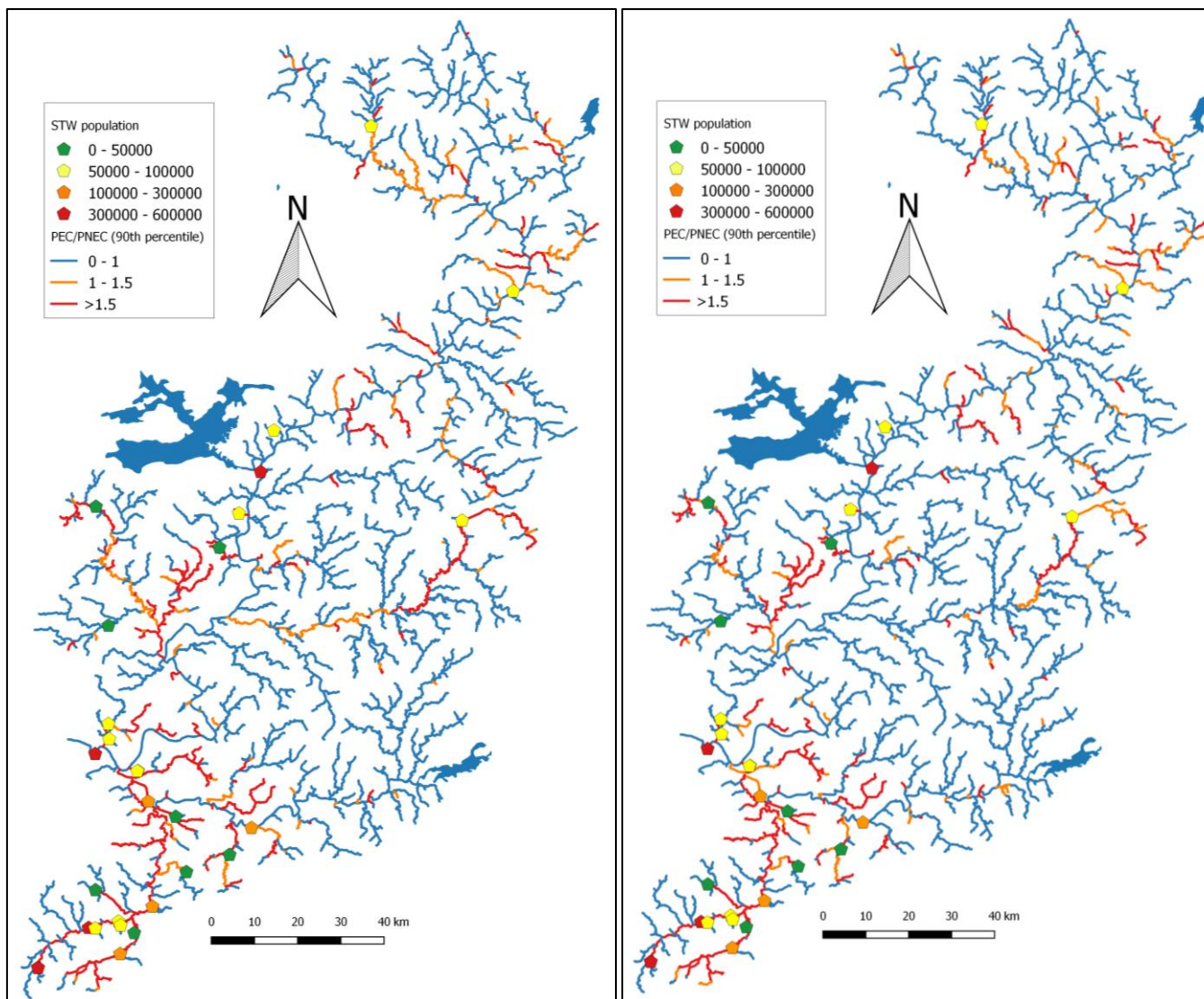


Figure 73 - Assessment of risk at the 90<sup>th</sup> modelling percentile concentration from E1 (left) and E2 (right) for the 2016 model, assuming a PNEC of 6 and 2ng/l respectively.

A further scenario was performed which predicted the effect of improved STW removal efficiency. From data pooled from literature sources regarding the fraction removed in STWs (described in section 3.5), STW removal was redefined as a uniform distribution with a minimum and maximum value defined by the 75<sup>th</sup> percentile and the maximum removal fraction (from these pooled data) respectively (Table 29).

<b>Chemical</b>	<b>STW removal (%)</b>
Triclosan	95.1-99
Triclocarban	90.5-97.5
Estrone	93.6-99.9
17 $\beta$ -Estradiol	93.9-99.4

Table 29 - The fraction removed by STWs defined for use within a management scenario assuming increased STW efficiency.

Applying increased STW removal for TCS appears to make little difference in the risk as shown by Figure 76. In terms of wastewater treatment, as a result, there is little else that can be done to significantly reduce the area that is at risk within the catchment. However, increasing STW removal reduces the number of stretches in the catchment exceeding the PNEC value for TCC to 0. As for E1 and E2, the area that is estimated to exceed the PNEC values is reduced considerably, as shown by Figure 77. Unacceptable risk still remains for a small number of stretches without treatment; however this may be mitigated by expanding the service area of existing STWs and constructing new STWs in areas where this is not possible. These regions are highlighted in Figure 77.

This second part of the assessment focuses upon E1 and E2. For areas at risk, STW service areas were expanded to serve subcatchments containing a relatively high population upstream of stretches highlighted to be at risk, or if there was no nearby STW, a new STW

was implemented for areas with a total population exceeding 2000. These measures, as shown by Figure 78, result in risk being reduced to an acceptable level for all areas targeted, albeit with 0.4% and 0.1% of stretches with unacceptable risk remaining for E1 and E2 respectively. Of course it is important to note that this scenario does not account for the monetary expense for this solution which is likely to be considerable. It must also be noted that the proposal to increase STW efficiency has no actual real meaning, as there is no mention of specific technology to apply and where. Unfortunately, there is not enough data available within the literature that describes the removal of any of the target chemicals by treatment sub-type (e.g. oxidation ditch or membrane bioreactor treatment technology), which would be required in order to determine an appropriate treatment technology that would meet the performance specified by this scenario.

However, this exercise demonstrates the possible solutions available to a catchment manager, who may be able to update the model to represent the true state of wastewater treatment within the catchment, for example treatment efficiencies for STWs and service area.



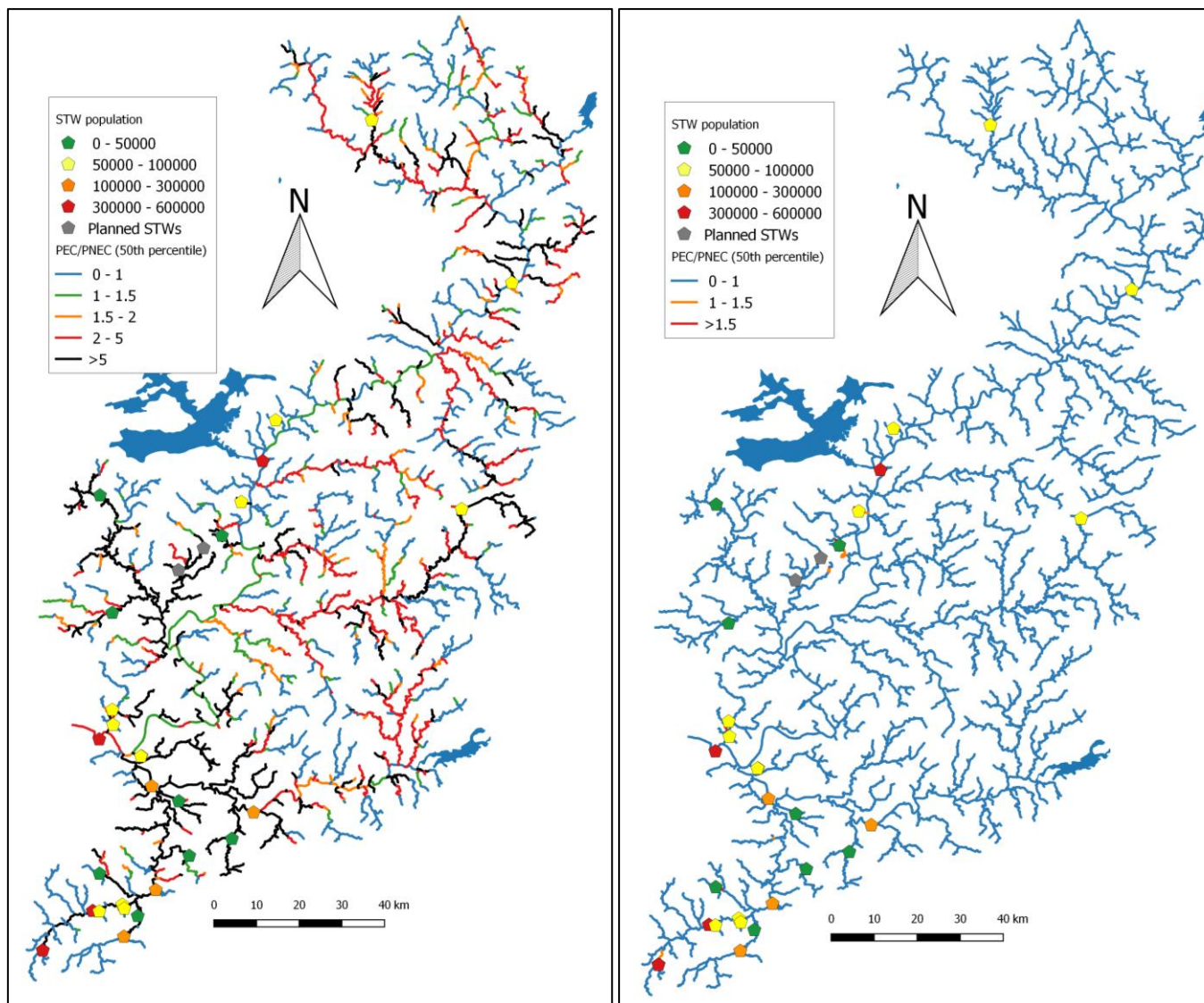


Figure 74 - Assessment of risk, at the 50<sup>th</sup> percentile concentration, from TCS (left) and TCC (right) in the year 2020 base scenario, assuming a PNEC of 4.7 and 146ng/l respectively.

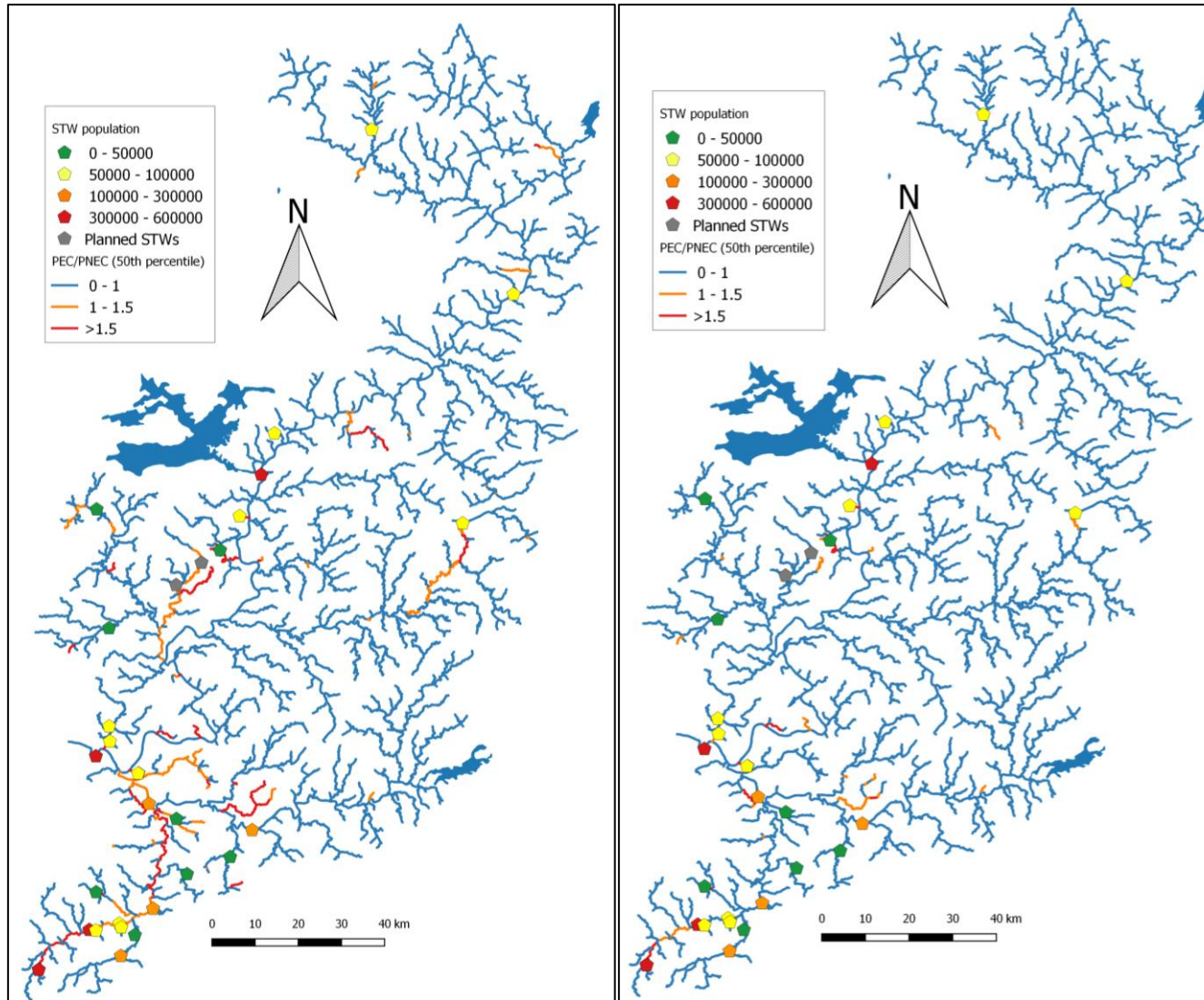


Figure 75 - Assessment of risk, at the 50<sup>th</sup> percentile concentration, from E1 (left) and E2 (right) in the year 2020 base scenario, assuming a PNEC of 6 and 2ng/l respectively.

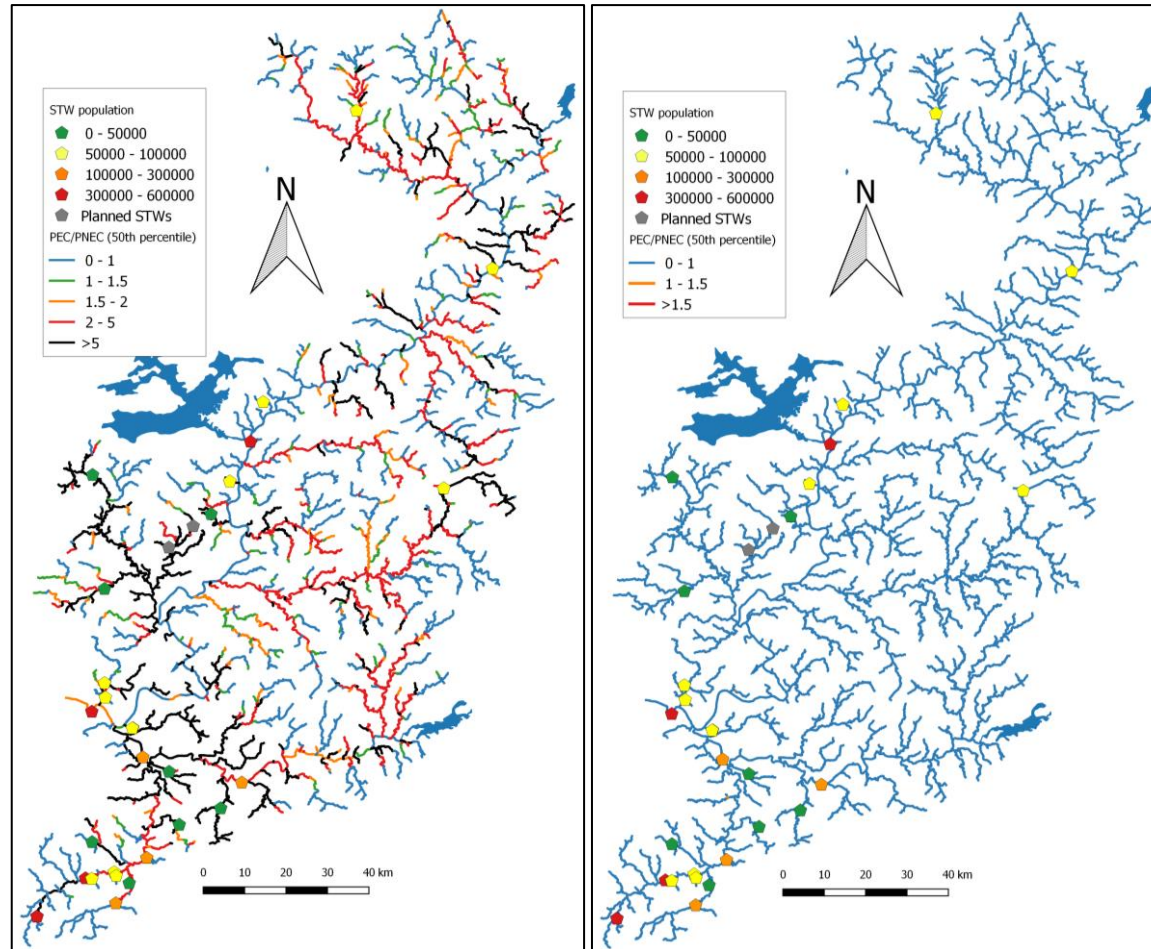


Figure 76 - Assessment of risk, at the 50<sup>th</sup> percentile concentration, from TCS (left) and TCC (right) in the year 2020 with high STW removal (95.1-99% and 90.5-97.5% respectively); assuming a PNEC of 4.7 and 146ng/l respectively.



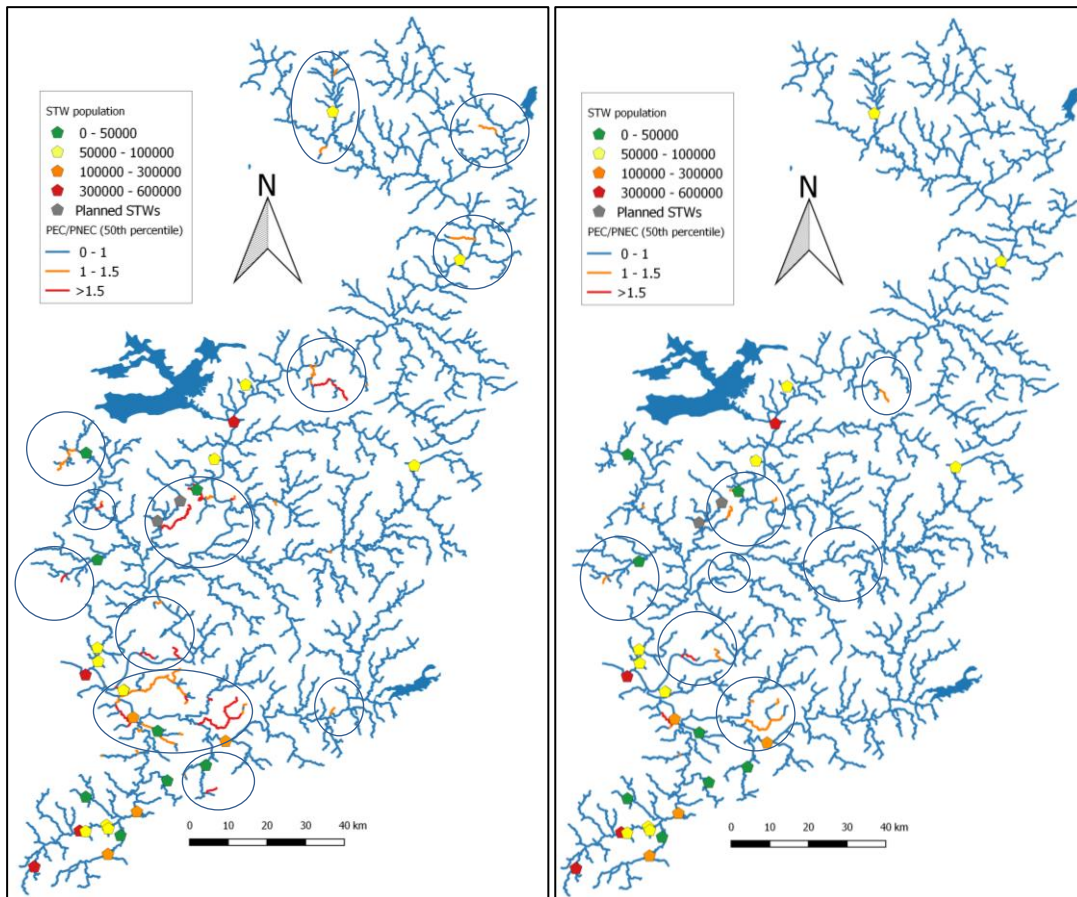


Figure 77 - Assessment of risk, at the 50<sup>th</sup> percentile concentration from E1 (left) and E2 (right) in the year 2020 with high STW removal (93.6-99.9% and 93.9-99.4% respectively); assuming a PNEC of 6 and 2ng/l respectively. Circles indicate areas in need of improvement.

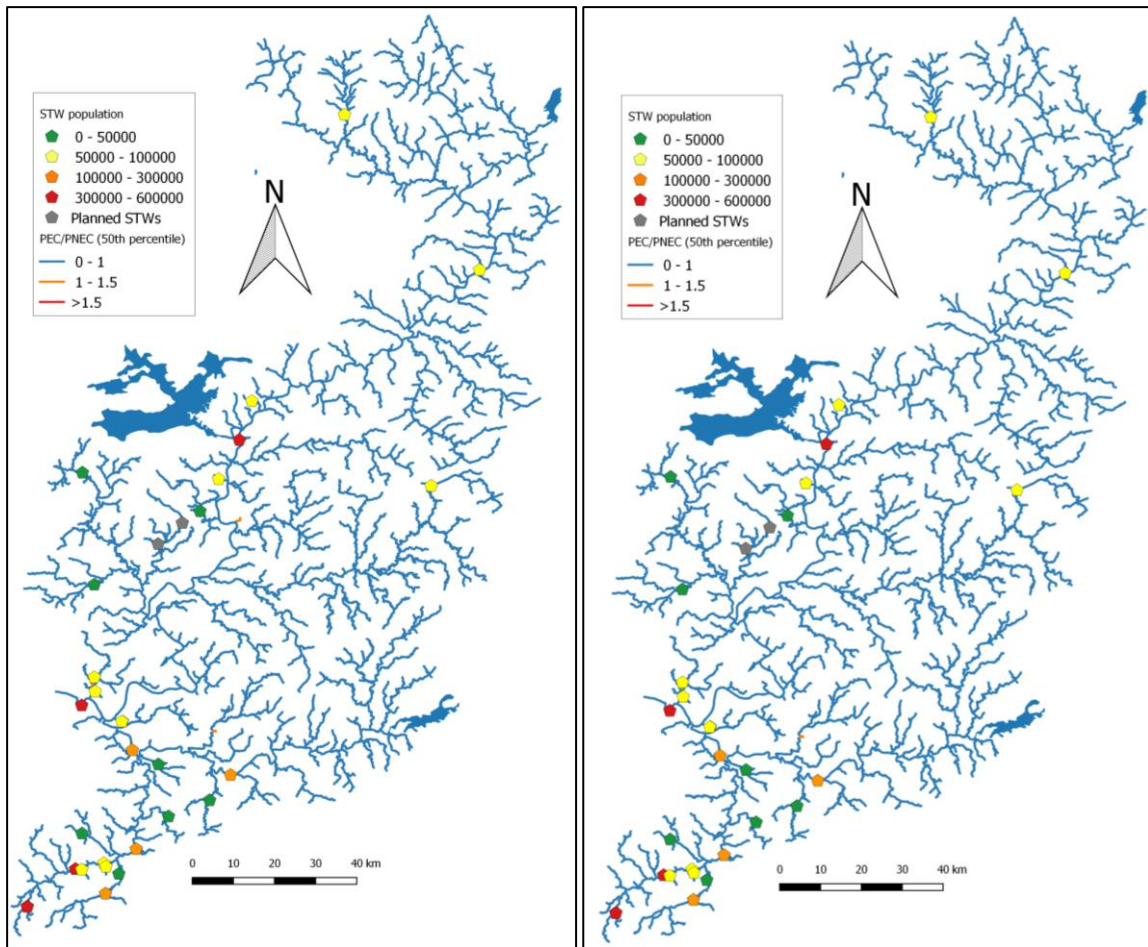


Figure 78 - Risk from E1 (left) and E2 (right), at the 50<sup>th</sup> percentile concentration, in 2020 following proposed STW management scenario; assuming a PNEC of 6 and 2ng/l respectively.

#### 4.5. Conclusions

This study suggests that the GREAT-ER model may be used with some success in both a rural and urban Chinese environments. However, significant deviations have been observed between estimated and measured concentrations at some of the sample sites. The model's estimate of the 90<sup>th</sup> percentile concentration exceeds the measured concentration in the majority of cases. However, improvements are still required in order for the GREAT-ER model to be used as a reliable risk assessment tool for the East river.

The most significant improvements include an improved estimate of usage for TCC and TCS, and implementing variable in-stream removal rates for all chemicals. In addition, greater detail about the wastewater infrastructure in the catchment should help to improve the accuracy of the model, although this would be quite difficult to obtain.

Using management scenarios, it was demonstrated that the GREAT-ER model is capable of assisting catchment management, with the aim of minimising chemical risk within the catchment. The model would likely be most useful for scoping purposes, to define areas of concern, and derive possible solutions.

Addressing the thesis aim: "To be able to predict reliably the in-stream concentration of down-the-drain chemicals TCS, TCC, E1 and E2"; this has been achieved to some extent. There are significant errors between some of the model's predictions and measured concentrations, but overall there is some agreement between modelled and measured concentrations.

The final thesis aim has been achieved: "To demonstrate the potential of GREAT-ER for both risk assessment and catchment management purposes, based upon the present and year 2020 scenario". The GREAT-ER model may be used within China successfully, albeit with some

difficulty, and it has been demonstrated that there is potential for its use in catchment management and chemical risk assessment.

## Chapter 5 – Evaluation

### 5.1. Overview

The first aim of this thesis was to be able to develop a complete methodology that allows one to reasonably setup a catchment model in China using the GREAT-ER model. This required a number of modelling challenges to be overcome. The modelling challenges primarily derived from data availability. The availability of high quality data provides the potential for higher quality models. Therefore, a methodology was developed to estimate the data required using reliable global datasets such as DEMs, satellite imagery and population datasets. There is now the potential to model other data poor regions.

A general methodology to apply the GREAT-ER model to China is described in Chapter 2; whilst in Chapter 3 a specific methodology for application of the GREAT-ER model in the East river catchment was described. As described by Chapter 4, the application of the GREAT-ER model in the East river catchment was, to some extent, successful. The GREAT-ER model was used to simulate the possible exposure of triclosan, triclocarban, estrone and 17 $\beta$ -estradiol. In comparison with measurements from two sampling campaigns, the modelled results largely agreed with the concentrations measured. However, there were a few significant limitations and barriers noted. These elements will be discussed in more detail, with suggestions for their resolution. Finally, a discussion on the future of GREAT-ER and future research directions is presented.

## 5.2. Suggested methodological improvements

### 5.2.1. Validation of flow and untreated discharge

Other than flow data availability, the primary identified concern was that of the estimation of artificial influences upon flow, which was considerable within the East river catchment. An approach that could identify and/or estimate the location and magnitude of artificial influences would be useful, as would the ability to determine the relative accuracy of flow within artificially influenced, ungauged catchments.

In previous GREAT-ER studies, conservative wastewater constituents (e.g. Boron), were initially selected for simulation. As removal by STW and in-stream processes is deemed to be insignificant for these conservative substances, the outputs of the model are entirely dependent on the estimates for dilution and chemical emission, and therefore the accuracy of these elements can be assessed by comparison of modelled to measured concentrations (Johnson et al., 2008b; Schulze et al., 1999; Fox et al., 2000; Wind et al., 2004). Boron was particularly favoured due to its conservative nature (Matthijs et al., 1997), the ease of analysis and the strong relationship with wastewater sources; boron is commonly used within detergents, although some natural sources may exist (Wind et al., 2004; Johnson et al., 2008b). In an environment with few untreated sources and a conservative nature, the accuracy of the model can be assumed to be entirely related to emission estimation and flow estimation. However, Boron is no longer widely used (Personal communication, Unilever) and therefore it is no longer appropriate for use for this purpose.

It is possible to estimate the relative flow between multiple sample sites along a stream by releasing a fluorescent dye, for example, Rhodamine WT, which can be measured on-site (e.g. using a fluorometer) (Kunkel and Radke, 2011; Fox et al., 2000; Hubbard et al., 1982). The area

under a plotted curve for measured Rhodamine WT fluorescence intensity against time may be used to estimate the relative dilution between sampling sites; the area under the curve is used to account for dispersion of the dye. The area under the curve is expected to decrease at downstream sampling sites, which may provide an indication of the change in dilution; this information may be useful when interpreting the relative change in concentration for target chemicals. Rhodamine WT is resistant to degradation processes (Turner et al., 1991), however it does adsorb to sediment (Fox et al., 2000; Kunkel and Radke, 2011), and therefore shouldn't be considered to be a conservative tracer. Runkel (2015) suggested that it is reasonable to use Rhodamine WT in large river systems, as the volume of water is much larger than the surface area of the streambed and therefore there is less interaction with solids in the bank and bed. However, use of Rhodamine WT in smaller systems was not recommended by Runkel, as sorption may be more significant. Another disadvantage is that it may not be feasible to perform a dye study for every sampled reach as it is more resource intensive. Finally, there may be political obstacles to the use of a dye. Prior to the East river sampling campaign, it was suggested to collaborators that we should complete our own dye study in order to estimate in-stream removal; however the response from our collaborators was that the local authorities would not agree to a campaign of this nature, as the locals might mistake the dye for a pollutant spill, which would have political ramifications.

Sucralose and other artificial sweeteners have been previously identified as suitable wastewater tracers as they are conservative and are primarily sourced from domestic wastewater (Tran et al., 2014). The production of Sucralose increased significantly after the expiry of its patents in 2009. However, it has been suggested that the majority of sucralose produced is exported (Research and Markets, 2013). It is uncertain as to how widespread the use of sucralose in China is, although it has been detected within urban environments (Gan et al., 2013; Heeb et al., 2012)

and seawater (Sang et al., 2014). Caffeine has also been suggested for use as a tracer for untreated effluent (Buerge et al., 2003) as it undergoes near-complete removal in biological sewage treatment (Sui et al., 2010; Qi et al., 2015) and is used frequently and widely within China.

Van Stempvoort et al. (2013) proposed that the use of multiple co-tracers is the most appropriate approach, given that many tracers have multiple sources, may be subject to varied in-stream removal, or their use may not be regular or widespread. Further research may be necessary to determine which tracers may be effective for use in China.

Scholefield et al. (2008) described a novel approach to sampling which involved the deployment of a GPS-enabled drogoue which may be released to traverse downstream, measuring velocity, conductivity, dissolved oxygen, pH and temperature, which it then maps as a function of time and space. They also attached a diffusive gradients in thin films (DGT) (Davison and Zhang, 1994; Zhang and Davison, 1995; Chen et al., 2012) sampler in an attempt to determine the average concentration for the stretch. These DGT devices consist of a membrane filter, a diffusive gel and a binding gel. Chemical substances diffuse through the membrane filter and the diffusive gel, and are then assimilated by the binding gel. However, the practical application of a DGT sampler is likely to be limited, as the time exposed to the water is not likely to be sufficient to reach a mass above detection limits.

The drogoue based technology has the potential to map the location and magnitude of untreated discharges and to validate estimates of surface water velocity. However, due to obstacles such as weirs, reservoirs and vegetation, it is challenging to sample significant distances downstream.



### 5.2.2. Refining estimates of in-stream removal

It is clear that in-stream removal can vary significantly in time and space. A removal rate for a given chemical determined within one catchment may not be appropriate for use within another catchment (Sabaliunas et al., 2003; Morrall et al., 2004), and therefore it is most appropriate to measure in-stream removal within the catchment of interest. Removal rates may vary significantly within the catchment itself, (Jürgens et al., 2002) depending upon water depth, suspended solid concentration, light penetration, weather, biological activity and various other factors (Ciffroy et al., 2017). It was suggested that the in-stream removal rate within the main channel of the East river catchment was likely to be less than that of its tributaries, which was a conclusion shared with other GREAT-ER studies (Price et al., 2009; Fox et al., 2000).

Laboratory derived removal rates may be available for the chemical of interest (Robinson et al., 2007). However, these do not necessarily reflect natural conditions; it may be difficult to apply these removal rates directly to models. Therefore it is important to estimate the factors within the natural environment that may enhance or reduce laboratory derived removal estimates. For example, Robinson et al. (2007) adjusted laboratory derived photodegradation rates to account for: season, latitude, water depth, light extinction from turbidity and river mixing. Alternatively, the software GCSOLAR (Zepp and Cline, 1977), may be used to adjust the photodegradation rate based upon season, latitude, time of day, water depth and ozone thickness. GCSOLAR was also utilised by Tixier et al. (2002) in order to adjust photodegradation rates of TCS and by Gerecke et al. (2001) to adjust the photodegradation rates for various phenylurea herbicides derived within the laboratory, with both studies adjusting photodegradation rates for the Lake Greifensee, Switzerland. In addition to adjustments made in GCSOLAR, both studies also adjusted to account for reduced sunlight intensity due to cloud cover, calculated using the hourly measured global

radiation at Dübendorf, the actual zenith angle and a correction factor for aerosol scattering (0.92) (Gerecke et al., 2001; Tixier et al., 2002). All environmental data required are relatively abundant and therefore the methodology is relatively simple to apply.

A more in depth approach may be used such as the use of the more recently developed “higher tier” chemical risk assessment models such as the hydro-biogeochemical model INCA-Contaminants (Nizzetto et al., 2016). This model is able to estimate the concentration within soil, water and sediment, but also focuses upon the biological and chemical processes within the whole catchment, not limited to in-stream processes. However, the use of models of this complexity may be hindered by data availability in China, although it may be plausible for research catchments and for regions where there is substantial support from authorities.

### 5.2.3. Wet season mechanics

The majority of China experiences a well-defined wet season. The South of China is by far the wettest, and experiences both monsoonal and frontal rainfall in the summer months. This includes the East river catchment. Modelling of the East river catchment was confined to the winter months due to the difficulties of representing the mechanics of the wet season. It was noted that a number of previous studies observed higher concentrations of TCS and TCC in the wet season, despite a significant increase in dilution. It was suggested that two different mechanisms may explain this phenomenon. The first involved the wash off of chemicals that are contained in wastewater storage ditches, the second is the resuspension of sediment and subsequent desorption. These wet season mechanics are challenging to model. The effects of sewer overflows have been taken into account in the past by previous GREAT-ER studies (Hüffmeyer et al., 2009) and similar models (Whelan et al., 1999). However, as many of more

significant overflow events occur from unlocated untreated sources this is difficult to characterise without additional data. As for resuspension, it is likely that the most appropriate option would be to utilise a “higher tier” chemical risk model that takes into account sediment resuspension in response to changes in flow, such as INCA-Contaminants (Nizzetto et al., 2016). However, this would require a significant amount of data. It may be possible to provide a more simplistic model to address this, although it is uncertain as to what and how successful this would be.

### **5.3. Addressing data limitations**

Data limitations were overcome for the East river study. However, two significant barriers were observed, which are likely to remain a problem for future studies.

#### **5.3.1. Hydrological data**

The acquisition of hydrological data is the greatest barrier in the modelling methodology. Several flow gauges, with relatively long records were located within the East river catchment. However, obtaining these data was a significant challenge. Hydrological data is often confidential in China, although policy varies between regions. Hydrological data may be politically sensitive in certain contexts, especially for high and low flows. Data is available in hard copy format which are often distributed to various governmental and academic institutions.

Hydrological data for the East river were made available from an academic institution in Beijing.

Data was stored as a hard copy and therefore data had to be copied manually into electronic

format. Copying data into electronic format had the potential for human error and limited the quantity of data that could be obtained. Data was also available in electronic format from the river authority's website. However, the data obtained was of poor quality with numerous errors and missing data. Data available in hard copy hydrological yearbooks was fully processed, and relatively free of errors. It is clearly essential for foreign nationals to find an appropriate 3<sup>rd</sup> party contact to obtain hydrological data, which may not always be possible.

### 5.3.2. Locating STWs

STWs of importance should be located and digitised, which is a time consuming process. The precise location must be obtained manually using satellite imagery. Satellite imagery is not always available for recent periods, and therefore it is possible that STWs may have been built after the most recent image was captured. Therefore, for populations without STWs, further investigation should be taken to determine whether a STW is present or if one will be constructed in the future. This is time consuming, which may be a problem for large catchments.

However, spatial and non-spatial data has been collected and published by multiple organisations and individuals. As mentioned in Chapter 2, a partial geodatabase of STW locations is provided by [www.ipe.org.cn](http://www.ipe.org.cn). This database has recently been expanded to include the locations of industrial/commercial discharges and monitoring data for many of the discharges. Non-spatial databases have also been developed, with over 3000 STWs documented by Li et al. (2017). Data availability is improving over time, which may improve the efficiency of model setup.

### 5.3.3. STW data

Estimating or acquiring STW data may be time consuming, particularly population served. It is therefore important to establish which STWs should be digitised and which should be ignored. Conclusions from the East river modelling exercise suggests that only large STWs will have any significant impact upon streams of high dilution such as the main stem of the East river. Small or medium STWs that discharge into large rivers are likely to be of little importance. However, small STWs that discharge to very small streams may have a significant impact. If information regarding the STW discharge is available, it may be useful to calculate the ratio of STW discharge and river discharge.

Population served may be estimated for towns and villages relatively quickly. A semi-automatic approach similar to that described by Keller et al. (2006) may be developed to increase the efficiency and repeatability of this process.

However, for large urban areas this data should ideally be from published sources or wastewater managers. Without this information it may be extremely challenging to estimate population served with a reasonable degree of accuracy. Population served is sometimes reported in news publications. However, the accuracy of these reports is uncertain. It may also be obtained directly from the plant operator. However, this is very time consuming and therefore it is not always possible for large catchments. In some cases, this information is confidential and, therefore, it may not be possible to obtain. It is perhaps inevitable that a significant amount of time is necessary to determine the population served. This is likely to prove to be the most inhibitive factor when attempting to model a large catchment.

For the East river catchment it was assumed that all STWs used activated sludge treatment technology. This was supported by the list of STWs within the area, although this may not be the case for other catchments. The difference in treatment efficiency between activated sludge and trickling filter is often significant. For example, trickling filters have been reported to remove E1 with an average efficiency of 30% (Johnson et al., 2007b), this contrasts with a mean efficiency of ~84% for activated sludge technology, determined from a literature review for the East river study. However, according to STW lists released by the China Ministry of Environmental Protection (<http://www.mep.gov.cn>), trickling filter technology does not appear to be prevalent in China.

It is particularly important to increase the availability of STW removal information for multiple treatment types in order to capture the variation in removal efficiency, which may be significant even for a single STW (Johnson et al., 2008b; Williams et al., 2003; Vieno et al., 2005). If a modeller is able to determine the particular type of treatment for a STW, then potentially the uncertainty of the model may be significantly reduced, as different treatment technologies may have significantly different efficiencies. However, this may only be achieved with sufficient data describing the removal efficiency for multiple treatment types and sub-treatment types.

#### 5.3.4. Chemical validation data

Measured sample data is required for validation purposes; however, measured data is often not available and may be difficult to acquire. It may be possible to use surrogate data for chemicals that are similar to the chemical of interest for validation (Grill et al., 2016; Chen et al., 2014). For the initial setup phase of a model, it may be plausible to utilise more readily available water

quality data such as BOD. However, water quality data in China is often released heavily aggregated in the form of water quality classes (Chen et al., 2015). These were utilised by Whelan et al. (2012) who compared the predicted concentration of LAS with water quality classes throughout China. Although water quality classes are not directly indicative of the presence of the chemical of interest, it does provide an indication of the level of human influence. Sampling campaigns are still necessary to confirm the presence and magnitude of the chemical of interest, although utilising alternative measurements such as water quality classes may either increase the confidence in the model or may allow the modeller to reassess areas for which water quality data conflicts with the model results.

#### 5.3.5. Open data

A major barrier to undertaking scientific activities within China relates to data policy and legislation of the Chinese government. Large datasets covering a wide range of subjects is stored by the Chinese government. Unfortunately, data sharing by the Chinese government has been very restricted historically, and data that is released is highly aggregated (Chen et al., 2015), especially for spatial data.

Collection of data is also a significant challenge, especially geographic data. The distribution and mapping of geographic data is restricted by Chinese law. Requirements of the 'Surveying and Mapping Law of the People's Republic of China' include approval before surveying activities, applying of a state approved co-ordinate system and approval before publication of mapping activities. The crowd source mapping project, OpenStreetMap (OSM) states that: "This seems to outlaw the entire OSM project and any participation or contribution" (Openstreetmap, n.d.).

This is particularly significant for foreign nationals, who have to form a Chinese-foreign

partnership. For those in breach of the law fines or imprisonment may follow (Hvistendahl, 2013).

However, in March 2015 the Chinese Premier announced that government data should be open to the public. This was followed by the announcement of the TPWP in April of the same year, insisting upon increased public participation in the process. If this is a serious deviation of policy then this may have a significant impact upon science in China. This depends upon whether the government now recognises the true value of open data to science, culture, the environment and the economy. China's TPWP recognises the need for an increased role from science, technology and the market. Scientists are restricted as to the extent they may contribute as a result of poor data availability. Increased data sharing from government sources to scientists, including foreign nationals, will lead to the development of tools, policy and data which may advance the goals of the TPWP. The primary purpose of this section is to illustrate how open data and collaboration from the Chinese government may be beneficial for the advancement of environmental policy, specifically in the context of water pollution from point sources.

The GREAT-ER model, and other similar chemical exposure models, may provide useful functionality for the purpose of risk assessment and catchment management. Both the MEP order 7 (Wang et al., 2012) and the TPWP would benefit from tools that provide an assessment of the exposure of contaminants within surface waters. Tools that provide an assessment of risk and to provide possible solutions to alleviate said risk would be valuable for governmental use. Therefore, it is important to communicate the value of these models and to describe the data barriers that are in place and where governmental support would help.

A new discharge permit system has been proposed as part of the TPWP. At present China already registers new and old STWs which are published in lists to the public. There is the



potential to expand this reporting system to also provide specific locations of STWs and to potentially provide population or population equivalents for each.

The Ministry of Water Resources manages a vast dataset of hydrological information for gauges across the country. The release of hydrological data has significant benefits to science, the environment and the economy (Hannah et al., 2011). The release of hydrological data may benefit the environmental protection service industry which TPWP aims to expand. More significantly, the release of hydrological data allows for risk to river catchments to be better assessed and managed. For high resolution chemical exposure models like GREAT-ER, hydrological data is essential. Flow may be estimated without hydrological data using mechanistic hydrological models, but most Chinese catchments are affected by complex artificial influences to flow and, therefore, this is likely to be inaccurate.

From a catchment management perspective, the GREAT-ER model may be used to provide solutions to complex catchment issues. The potential of the model may be reached if the model can be presented as an effective management tool to the appropriate authorities. With much greater data accessibility, a greater number of applications become available. For example, with detailed information about the different artificial influences within a catchment it may be possible to determine the effects of changing water use, different reservoir management strategies and other issues relating to water resources. In the context of the East river, it would be possible to create a scenario that provides a possible solution to chemical risk by increasing dilution in the Shenzhen catchment. However, this would require much more detailed information about the reservoir release profiles and the abstraction and discharge points.

#### 5.4. Potential for GREATER

Following the completion of the East river study, there are two examples of the application of GREAT-ER in China; this study and a heavily urbanised catchment in Beijing (Zhang et al., 2015a). The creation of the East river model was challenging but there are many areas of China where the challenge presented by the environment is significantly reduced. The first GREAT-ER study in China investigated the heavily urbanised Wenyu catchment, Beijing (Zhang et al., 2015a). The area was subject to little or no untreated discharges and the authors were able to obtain population served data from the plant managers. There was also a readily available, calibrated SWAT model parameterised for the catchment. It may be reasonable to initially focus upon relatively simple catchments, with readily accessible data. China is a large, diverse country with many complex river catchments that are difficult to represent other than at the catchment scale. It is, therefore, important to model a diverse range of river catchments within China. It is also important to model high risk areas of the country, which may have been previously identified to be at risk either by large scale risk assessment models, or monitoring studies.

##### 5.4.1. Modelling climate extremes

The climate of China varies significantly between regions (Figure 79). There are regions of severe cold to the North-East and Western China, a wet and hot South-East and an arid/semi-arid North-West China (Domrös and Peng, 2012; Qin et al., 2015). Each of these regions provides a unique modelling challenge.

*Severe cold climate*

Severe cold conditions are prevalent over much of China. However, from a risk assessment perspective, the most significant region is likely to be the North-East, which has a relatively high population density. The city of Harbin (Figure 80), with a population of 10.64 million, experiences a mean January temperature of  $-18^{\circ}\text{C}$ . The Songhua river flows through Harbin, which freezes over during the winter months with ice approximately 1 meter thick. During freeze-up, discharge and velocity decreases and flow depth increases (Ferrick and Calkins, 1996). Flow decreases further later in the year as groundwater sources deplete; in the case of North flowing rivers, precipitation and subsequent runoff also decrease. A critical problem when attempting to model cold climates such as this is that the measurement of flow is often difficult during freeze-over and is often interpolated between less frequent observations (Prowse, 2001). The formation of an ice-cover has implications for biochemical activity. In particular the exchange of gasses with the atmosphere is drastically reduced. This leads to a lowering of dissolved-oxygen within the river channel (Prowse, 2001), which has implications for biological activity. In addition, there is also significant attenuation of solar radiation by covering ice and snow (Prowse, 2001) and therefore a reduction in the photolysis rate. Sediment load is also significantly related to the formation and break up of ice. During the ice covered period, as a result of reduced flow velocity, transport capacity is reduced (Prowse, 2001). During ice breakup suspended sediment transport increases dramatically as a result of surge conditions (Prowse, 2001). This has significant implications for chemical risk assessment, with conditions likely favouring a significant reduction of in-stream removal and dilution. It is likely that a model such as GREAT-ER would be unsuitable for use within these complex conditions. There are also significant barriers to obtaining grab samples, especially when a thick ice-cover is present. Therefore calibration and validation of a model is difficult. In addition, in-stream removal would likely be difficult to derive by means of tracer based studies.

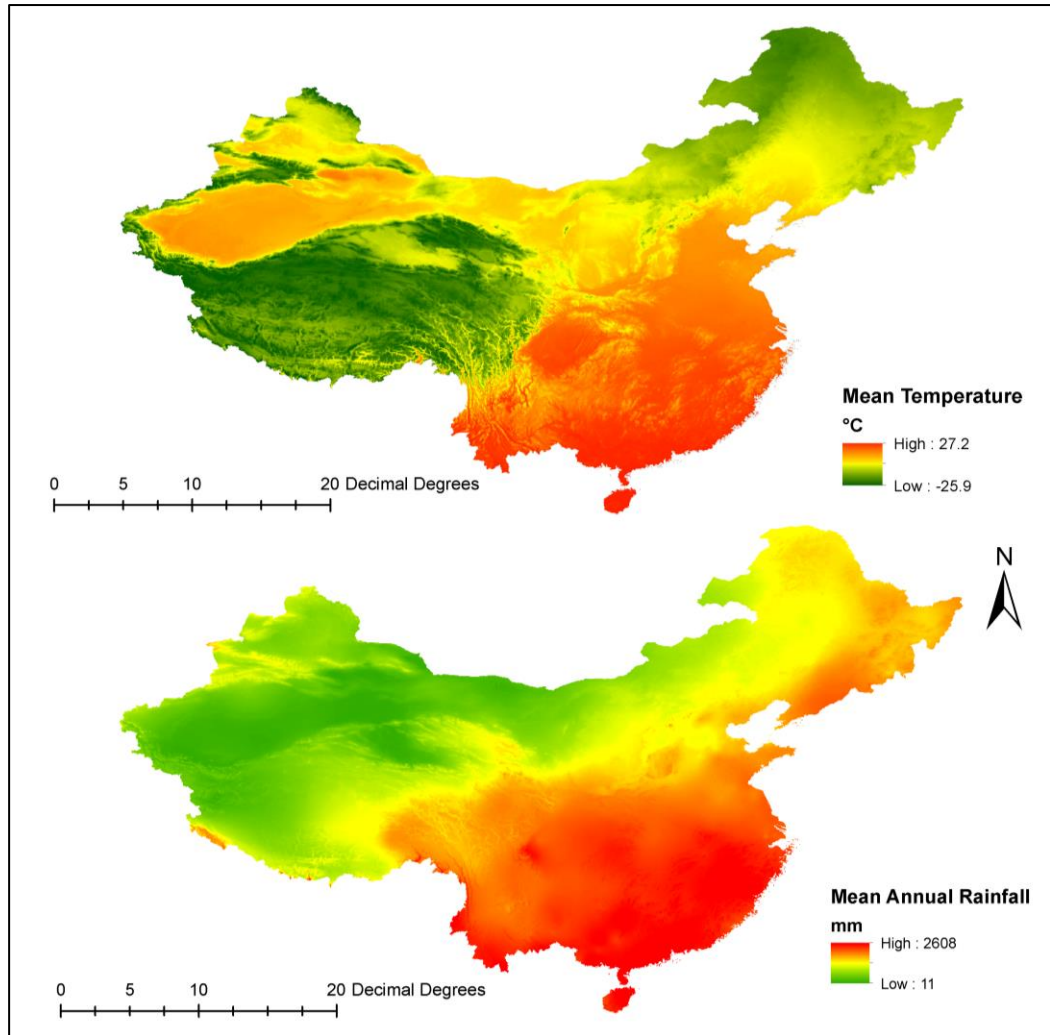


Figure 79 – Mean annual temperature and mean annual precipitation of China produced based upon data produced by Fick and Hijmans (2017).

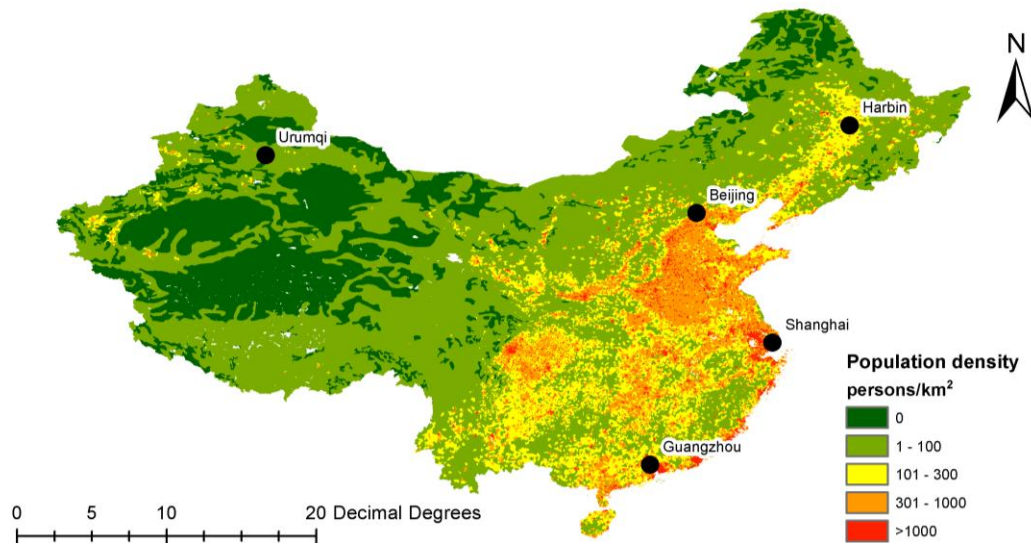


Figure 80 - Population in China, based upon GPWv4 dataset (CIESIN, 2016b). The majority of the population is within South-East China; whilst much of North-West China is uninhabited, or sparsely populated.

### *Arid conditions*

Flow in river catchments in arid climates may reach critically low levels during part of the year, in some cases drying out completely. In urban catchments, flow may become dominated by wastewater flow which results in the water quality of the river strongly depending upon the efficiency of wastewater treatment (Carey and Migliaccio, 2009).

The natural flow regime is likely to be affected by significant abstractions to flow, and in many arid catchments flow may become intermittent as a result of over abstraction (Smakhtin, 2001). Consequently, estimation of low-flows would be strongly dependent upon artificial influences to flow and therefore obtaining high quality data on the location and effects of artificial influences to flow would be essential.

The arid regions of China are of a relatively low population density and as such chemical emissions are likely to be much lower in comparison to other regions. However, the available flow to dilute wastewater discharges is much lower, with some streams ephemeral in nature. For example the North-Western city of Ürümqi (Figure 80) hosts a population of over 3 million (2010 figures). Water demand significantly exceeds the available water resources and as such the dilution of wastewater is critically low during the dry season (Yao, 2013). The city's population continues to grow and a need for alternative sources of water has led to suggestions to reuse wastewater for irrigation, industry and other urban uses but instead, much of the wastewater is discharged directly into a watercourse untreated (Yao, 2013).

From a modelling perspective, the element of complexity is flow estimation. In the case of Ürümqi, annual potential evaporation (2300 mm/year) is much greater than annual precipitation (304mm/year) (Yao, 2013), and therefore flow may potentially decrease downstream as result of losses from evaporation and abstraction. Therefore a methodology for flow estimation in this region must take into account complex natural drivers of low-flows and utilise high quality artificial influence data. This is a significant challenge and as such requires a much more sophisticated approach in comparison to the East river catchment.

It has been suggested that effluent-dominant streams may present the maximum hazard to in-stream biota (Brooks et al., 2003). However, the effects of wastewater discharges may potentially be of benefit to downstream biota if additional habitat is created or if elements within the effluent reduce the bioavailability of upstream pollutants (Brooks et al., 2006). It was even suggested by Luthy et al. (2015) that the release of treated effluent to intermittent streams may be an effective management solution in order to improve or restore a stream's physical habitat, leading to enhanced biodiversity. Ecological risk assessment in this environment is more

complex as, in some cases, without the release of wastewater, the ecosystem would not exist (Luthy et al., 2015). The impact zone concept, first introduced by Limlette III Workshop (1995), offers an alternative approach; this was originally conceived as an approach towards assessing the risk of consumer product ingredients in a river system that receives untreated wastewater. The 'impact zone' is the stretch of heavily polluted water downstream of an untreated discharge, primarily characterised as containing low levels of DO (McAvoy et al., 2003; Limlette III Workshop, 1995). It is argued that this zone is already impacted by pollutants and therefore the aims of a chemical risk assessment should include: 1) whether the chemical of interest affects the rate of self-purification and, 2) whether the concentration of the chemical of interest exceeds the PNEC beyond the impact zone. Self-purification occurs due to organisms within the stream acting to breakdown wastewater constituents (McAvoy et al., 2003). Arid, wastewater dominated streams, are likely to contain high concentrations of pollutants due to the low level of dilution; this impact zone approach could therefore be useful here, even for streams receiving treated wastewater. Regardless of whether the release of pollutants would create habitat or not, the two aims of the impact zone approach are important, as they would minimise the risk from the target chemical and from other contaminants to less polluted stretches downstream. To apply this approach, it is important to determine whether the degradation rate of the chemical in the impact zone is affected; as the level of DO may inhibit aerobic biodegradation (Whelan et al., 2007; Finnegan et al., 2009). This may be determined by means of plume studies at sites affected by untreated wastewater discharge (e.g. Whelan et al., 2007), or by means of laboratory simulation (e.g. Finnegan et al., 2009). To determine how the chemical of interest affects the self-purification process, tests may focus upon the concentration at which the chemical affects the rate of BOD decay (McAvoy et al., 2003).

## 5.5. Future modelling approaches

The TPWP provides ambitious goals to improve water quality in China's major river catchments. Management of water quality in a country of China's size and complexity is very challenging and requires management at many different scales. At the national scale, an assessment of risk posed to individual catchments is required, which assist in the prioritisation of resources and chemicals of concern. At the catchment scale, specific areas within a catchment that may be at risk can be identified and measures which may lead to improvements in these areas may be assessed in suitable scenarios.

### 5.5.1. Modelling at large scales

National and global scale chemical risk assessment models have been developed in recent years. Data availability for large scale models are generally greater than for small-scale; a large number of global datasets are available for use. The primary use for large-scale models is to provide estimates for exposure with a high spatial coverage and to represent the long-range transportation of persistent chemicals (e.g. Zhu et al., 2014).

### 5.5.2. Dilution based large-scale models

Dilution based models focus upon the water phase, with some consideration for hydrological realism (e.g. Whelan et al., 2012; Keller et al., 2014). Chemical emissions are distributed based upon population distribution and assumed rates for sewage treatment removal and usage. The concentration is then determined based upon calculated dilution for each element (grid cell or vector polyline). Dilution is often determined based upon a water balance approach which takes



into account spatially resolved evaporation rates and precipitation, or by using existing runoff calculations (e.g. Fekete et al., 2002). Gauged data may be used to calibrate such models, when available. The chemical is routed from cell to cell based upon estimates of flow direction, determined using a DEM (as described in Chapter 2). Removal is often calculated using a combined first-order removal rate and travel time. This model type may perhaps be analogous to a large-scale GREAT-ER model.

Hydrological data is available for many major rivers, made available through water authorities or from global datasets such as the global runoff database (GRDC) (<http://www.bafg.de/GRDC>), which includes many major river gauges in China. This approach has a number of disadvantages. Freely available hydrological data is often not available for the most recent decade and/or may be only available at a monthly resolution; in some cases this renders the data useless. Gauged data is more likely to be available for downstream sections of river that are more likely to be exposed to numerous artificial influences to flow (Rodda, 1998) and therefore may be inappropriate for use in regionalisation unless artificial influences are somehow taken into account .

Large reservoirs are likely to provide the largest influence and therefore their effects need to be quantified. This is taken into account to some extent by water use and availability models such as GWAVA (Meigh et al., 1999) and WaterGAP (Alcamo et al., 2003).

### 5.5.3. Multimedia modelling

Multimedia models are described in Chapter 1. At the large-scale, there are many advantages for their use. The data requirements can be larger than dilution models, however they have the

advantage of being able to estimate chemical exposure in different media. Therefore for chemicals which are primarily found in the water phase, dilution based models are clearly preferable.

#### 5.5.4.A cascading modelling system

Both the large and the small scale models have different applications. National and global models often focus upon major river systems, which provide an indication of catchments that may be at risk. This may be comparable to a scoping exercise. However, smaller tributaries may be subject to greater risk due to lower levels of dilution. Therefore, small-scale catchment models such as GREAT-ER are important to provide greater detail about of risk within river catchments.

Therefore, a cascading model system is proposed here. Global or national scale models may be used to highlight regions or catchments at risk. The catchment(s) with the greatest risk may then be investigated in greater detail using a small-scale model such as GREAT-ER. National scale chemical risk assessment models have already been developed for China (e.g. Zhu et al., 2016; Whelan et al., 2012). This could be investigated in even further detail for more critical catchment management applications by using emerging higher-tier chemical fate models. Examples include STREAM-EU (Lindim et al., 2016) which is a spatially and temporally explicit model with consideration of partitioning between groundwater, soil, water, sediment, snow/ice and air compartments. STREAM-EU is a dynamic model which requires modelled daily flow data, based upon an external hydrologic model. The model considers time variable temperatures, transport velocities and emissions.

## 5.6. More ecological relevance

One of the primary purposes for ecological risk assessment (ERA) is to be protective to the freshwater ecosystem. However, it has been argued that the ecological element in chemical risk assessments is far too limited (Bednarska et al., 2013). Toxicity tests are carried out under standard conditions which do not take into account the complexity of the environment and animal behavioural patterns. Protection goals generally focus upon the population level (or above), whilst standardised tests only provide data regarding the effects on individuals (Hommen et al., 2010; Martin et al., 2014). There is also little consideration for interactions between chemicals and other stressors in a mixture, and how this may enhance or reduce the biological response from aquatic organisms (Beyer et al., 2014; Heys et al., 2016). These issues will be discussed in more detail in this section, with reference to possible approaches to address these issues.

### 5.6.1. Ecological models

Population models enable effects to be predicted at the population-level and above, which is necessary in order to meet protection goals set at the population/community/ecosystem level (Forbes et al., 2011; Galic et al., 2010). It is plausible to utilise mesocosm/microcosm tests to determine effects at the population level; however, they often fail to take into account dispersal and recolonisation processes, usually do not include larger organisms (e.g. fish), and these tests are also often expensive to perform (Galic et al., 2010). Population models increase the realism of an ERA, and in doing so, may lead to estimated effects that are much higher or lower than expected, at the population level (Forbes et al., 2011). For example, Hayashi et al. (2009), by

using a population model, noted that population-level effects exceeded those at the individual level, as a result of the density-dependence of the population. The response of the population may differ significantly depending on the environmental conditions and habitat complexity, which may be accounted for in population models (Grimm and Railsback, 2013; Van den Brink et al., 2007). ERA currently does little to consider the life-history of organisms; however, population level effects may vary significantly between species with different life-history strategies (Calow et al., 1997; Stark et al., 2004). For example, a fish that reproduces multiple times a year may be more resilient as a population than a species that breeds once a year (Forbes et al., 2011). Finally, population models may take into account indirect effects, which are those that affect a species as a result of effects on another species, usually at another trophic level (Galic et al., 2010). This may include the suppression of a predator's prey as a result of toxic effects, which results in less food availability for the predator. These indirect effects may result in significant changes to the structure or functioning of the ecosystem (Galic et al., 2010). Indirect effects are best represented at the food-web level, however, it is also plausible to estimate indirect effects using models at the population level, for example, host-parasite interactions (Waage et al., 1985). Food-web models, which may also be described as ecosystem-level models, include the models: AQUATOX (Park et al., 2008), CASM (Naito et al., 2002) and CATS (Traas et al., 1998). Population-level models consider a single-species, which are used to estimate population change and abundance (Galic et al., 2010). These models may or may not be structured, which defines whether the model includes different characteristics for individuals at different stages of the life-cycle. Structure models include matrix population models (Billoir et al., 2007; An et al., 2006), which are able to calculate population growth for a set of life-cycle data (e.g. age dependent survival data) (Galic et al., 2010).

Another common type of population-level model is the individual based model (IBM) (e.g. Jaworska et al., 1997; Beaudouin et al., 2008; Madenjian et al., 1993), which regards all individuals as being unique (DeAngelis and Grimm, 2014). The behaviour of individuals includes interactions with the environment as well as interspecific and intraspecific interactions (Galic et al., 2010). IBMs represent the highest level of realism, but as a result, tend to have high data and computational requirements, although individual models are considered to be generally more viable for experimental testing, as experiments tend to focus on effects on individuals (Van den Brink, 2008). Toxicokinetic-Toxicodynamic effect models (TKTD models) are individual-level models that simulate how contaminants interact with the organism internally; toxicokinetics (TK) describe the uptake, transformation and elimination of the chemical and toxicodynamics (TD) describes damage, repair and mortality (Jager, 2016). These models attempt to relate exposure to effects, and to some extent, describe why this effect occurs. They may be coupled/incorporated into existing IBM models (Galic et al., 2010). For example, Gabsi et al. (2014) coupled the IBM, IDamP (Preuss et al., 2009), with the general unified threshold model of survival (GUTS) TKTD model (Jager et al., 2011). This enabled the effects of Dispersogen A on the survival of daphnid individuals to be extrapolated to the population level (Gabsi et al., 2014). GUTS is a unified framework of different existing TKTD models that determine the effect of a substance on survival (Ashauer et al., 2011). GUTS may operate on as few as 4 parameters, which may potentially be estimated based on standard toxicity data alone. For other quantal endpoints (endpoints that can only occur, or not occur, such as survival), the GUTS framework may be viable, if modified (Ashauer et al., 2011). Modifications include enabling the model to account for the reversibility of a response, which GUTS does not include (as death is not reversible). TKTD models may also be used to estimate the effects on life-history traits, such as maximum size and reproduction, but a more connected approach may be needed (Ashauer et

al., 2011). Life-history traits are linked, in that a limited pool of resources (e.g. energy) is allocated to each life-history trait, and therefore, if exposure to a contaminant inhibits a life-history trait, other life-history traits may be affected too (Ashauer et al., 2011). Species may be classified based upon the supply-demand continuum (Lika et al., 2014; Banavar et al., 2002). Demand systems relate to organisms that, for example, eat what is needed rather than what is available and reproduction is not typically restrained by the ability to acquire and use resources (energetics) (Ashauer et al., 2011). Demand systems include most birds and mammals, whereas the majority of species are closer to the supply end of the spectrum (Jager, 2016). For organisms on the supply end of the spectrum, responses such as growth and reproduction rate depend on environmental interactions, particularly food availability and temperature. Creating links between a contaminant and effects on life-history traits is generally more difficult as there may either be direct impacts upon traits or there may an effect that may limit the amount of food that is collected or assimilated, which subsequently has an impact upon life-history traits (Jager, 2016). Therefore, understanding which process is affected by a contaminant is important in order to predict effects upon relevant traits, and interactions with environmental conditions (Jager, 2016; Álvarez et al., 2006). It is particularly important to understand how individuals obtain and use food, and other resources (Martin et al., 2014). It is possible to represent this using an approach based upon the dynamic energy budget (Kooijman, 2001; Nisbet et al., 2000). The DEB is a representation of how individuals obtain and use resources, which accounts for feeding, assimilation, maintenance, growth, maturation and reproduction (Kooijman, 2001; Nisbet et al., 2000). Effects of pollutants are accounted for by adjusting the relevant parameters that relate to these processes in the model (Jager, 2016), this is determined by using partial life cycle tests, i.e. those focused upon observing the effects of individual physiological processes. These parameters are linearly (with threshold) related to the internal concentration (Jager,

2016). Therefore, the model parameters relate to the physiological functions and furthermore, it has been suggested that it is theoretically possible to extrapolate between chemicals, life stages and between species, although the methods of achieving these extrapolations is not fully developed (Jager, 2016). It is important to note that different species exposed by the same chemical may be affected in different ways, i.e. the chemical affects different physiological processes (Álvarez et al., 2006). To determine which processes are affected, short, molecular level tests may be used (Groh et al., 2015; Ankley et al., 2006).

A significant disadvantage of many TKTD models is that they often require additional experimental data in order to parameterise, and therefore wherever possible, estimating or extrapolating data is preferable (Jager and Kooijman, 2008; Jager, 2016; Ashauer et al., 2011). TK and TD parameters may be influenced by measurable chemical characteristics, for example, TK parameters may be influenced by physiochemical properties, and TD parameters may be influenced by the potency of the chemical (Ashauer and Escher, 2010). Therefore, if quantitative relationships are established between TK, TD and influential chemical characteristics, it may be possible to estimate the toxicity of previously untested chemicals (Hendriks et al., 2001; Gobas et al., 1999; Arnot and Gobas, 2004). Species traits may also relate to TK and TD, and if a quantitative relationship is determined, it might be possible to estimate the sensitivity of other, untested species (Rubach et al., 2011; Gergs et al., 2015). For example, it was noted by Gergs et al. (2015) that for the substance triphenyltin, toxicokinetics partially scaled with body size for the organisms: *Daphnia magna*, *Chaoborus crystallinus* and *Mesocyclops leuckarti*. Also, Rubach et al. (2012) noted that differences in the uptake rate of chlorpyrifos related to the traits: surface area, detritivore food preference, whether a species breathes atmospheric oxygen, and phylogeny, using multiple regression ( $R^2 = 0.87$ ). From this, TK parameters may potentially be extrapolated between species. There is the potential for the use of ecological traits to be used

without the need for additional effects testing on organisms, which is quite significant. However, based upon published literature, it is not currently possible to utilise this trait based approach to derive contaminant sensitivity. But with further development it is possible for traits to provide a more ecologically realistic assessment.

#### 5.2.1. Effects of multiple stressors

The combined effects of multiple stressors upon in-stream fauna and the possible interactions between them have been largely neglected in ecological risk assessments. The effects of naturally occurring stressing factors may directly or indirectly affect the toxicity of contaminants to aquatic organisms. For example, raising temperature has been observed to amplify the toxicity of acridine (a polycyclic aromatic compound) (Cooney et al., 1983), nickel (Bryant et al., 1985), and pesticides (Demon and Eijsackers, 1985). However, ERAs are almost entirely based upon bioassays under standard conditions (Bednarska et al., 2013). When these interacting effects are fully understood, they may be applied to the results from exposure assessments. For example, Orvos et al. (2002) demonstrated that the toxicity of Triclosan is significantly influenced by pH, as a result of ionisation. Zhu et al. (2016) estimated the spatial distribution of pH in freshwater and sediment based upon measured data across China. This was incorporated into the multimedia model, SESAMe. The PNEC for Triclosan in the neutral form was recalculated based upon carefully controlled conditions for multiple measures of pH (Roberts et al., 2014). Further, the neutral form PEC for Triclosan was estimated across China (Zhu et al., 2016). It was noted that only 0.03% of freshwater areas exceed the recalculated PNEC for neutral form TCS. In a higher-tier assessment, Price et al. (2010) utilised pH data from monitoring surveys in the UK to determine the predominant form of Triclosan, for which concentration was estimated using



the high resolution water quality model LF2000-WQX (Williams et al., 2009). The availability of water quality parameters (e.g. pH or DO) is limited in China (Chen et al., 2015), and therefore it may be difficult to estimate the combined effect of a chemical of interest and standard water quality parameters.

In the natural environment, a mixture of different chemicals will likely be present within the water, and it has been observed that exposure to a mixture of chemicals may result in toxic effects, even if the concentration of all individual chemicals are below their respective NOEC values (Brian et al., 2007; Kortenkamp, 2008; Silva et al., 2002). The effects of the combination of chemicals may be: additive, synergetic (total effect is more than sum of effects (Sabljic, 2009)) or antagonistic (blocks action of an agonist, a chemical that binds to a receptor (Matthews, 1993; Ashauer et al., 2007)). This needs to be considered in an ERA in order to assess the combined risk of these chemical mixtures, however, it is near-impossible to test every combination of chemicals, and therefore a different approach is required (Beyer et al., 2014). Two classical approaches to account for chemical mixtures are the concentration addition (CA) (Löewe and Muischnek, 1926) and the independent action (IA) (Bliss, 1939) approaches. The CA approach is applicable when multiple chemicals with a similar mechanism of action affect the same endpoint (Backhaus and Faust, 2012; Beyer et al., 2014). Whilst the IA approach assumes that each chemical affects the same endpoint, but through different mechanisms and acting on different subsystems of the organism. CA is an additive model and assumes all chemicals contribute to the total toxicity, even if some components are below the effect threshold (Heys et al., 2016). The mixture effect for CA is determined using Equation 52 below (Backhaus and Faust, 2012):

$$\sum_{i=1}^n \frac{c_i^*}{ECx_i} = 1 \quad (52)$$

where:

$c_i^*$  - concentration of the  $i$ th component in a  $n$ -component mixture, which contributes  $x\%$  of the total effect

$ECx_i$  - denotes the concentration of the  $i$ th component which would provoke an effect  $X$  if applied alone.

The fraction:  $c_i^*/ECx_i$  is described as a toxic unit, which is the concentration of a component normalised by the component's relative potency; if the summation of toxic units equals 1, then the mixture behaves according to CA (Backhaus and Faust, 2012).

The IA approach determines the mixture effect by calculating according to the joint probability of independent events, described by Equation 53 and 54. For when the value of a biological end point decreases with increasing concentration (e.g. survival), the mixture effect is determined using Equation 53 (Backhaus and Faust, 2012):

$$E(c_{\text{mix}}) = E(c_1 + \dots + c_n) = \prod_{i=1}^n E(c_i) \quad (53)$$

alternatively, for when the value of the biological end point increases with increasing concentration (e.g. immobility), Equation 54 is applied (Backhaus and Faust, 2012):

$$E(c_{\text{mix}}) = E(c_1 + \dots + c_n) = 1 - \prod_{i=1}^n [1 - E(c_i)] \quad (54)$$

where:

$E(C_{mix})$  - the overall effect predicted, normalised to a range of 0-1, for a mixture containing  $n$  components at a total concentration of  $C_{mix}$

$E(c_i)$  - the effect of component  $i$  if applied singly in a concentration  $c_i$ , which corresponds to the concentration of that component in the mixture.

If each component has a concentration below its respective effects threshold then no combination effects will apply (Heys et al., 2016; Kortenkamp et al., 2009). IA is frequently applied when evidence suggests that mixture toxicity is not additive (Kortenkamp et al., 2009). IA however, is not often applied, partially due to its assumptions (Backhaus and Faust, 2012). IA may only apply to quantal endpoints, and it has also been argued that chemicals may never truly act independently of each other (Cedergreen et al., 2008). CA is perhaps the most commonly used approach and although there is a danger of missing potential mixture interactions (particularly synergetic interactions), it is suggested that CA is appropriate in most cases (Backhaus and Faust, 2012; Belden et al., 2007; Heys et al., 2016).

Attempts have been made to try to account for chemical interactions. The first is the adjusted hazard index (HI) or weight of evidence (WOE) approach (Heys et al., 2016; Mumtaz et al., 1993). The HI approach summates hazard quotients which are calculated based on the exposure and the reference effect level for the chemical (e.g. NOEC), if this summated value is greater than one, it is assumed to exceed acceptable toxicity levels (Heys et al., 2016). The adjusted HI/WOE approach assesses the likelihood of the toxicity being over- or under-estimated based on factors such as data quality and pairwise assessment of potential interactions between all mixture chemicals; this is more often used when data used to calculate HI is based on different

endpoints (Heys et al., 2016; Mumtaz et al., 1993). This is quite an intensive process which become less feasible with increasing number of chemicals within the mixture (Heys et al., 2016).

## Chapter 6 – Conclusions

This thesis describes a methodology to facilitate the use of the GREAT-ER model in China. The two key barriers to its use were data requirements and the estimation of the distribution and magnitude of the discharge of untreated wastewater; the major data challenge was to obtain data regarding the location and population served by STWs. These were overcome with the development of a methodology to locate STWs, to estimate the catchment area (wastewatersheds) for each STW and thus estimate the population served. Further, wastewater generated by the population outside of these wastewatersheds was assumed to be untreated. For untreated wastewater, the fraction released to the river network was defined by the DER. The GREAT-ER model was successfully used to model the East river catchment, for the purpose of estimating the concentrations of Triclosan, Triclocarban, Estrone and 17 $\beta$ -estradiol.

Regional regression was used to estimate low-flow statistics, which were adjusted for the influence of upstream reservoirs and other artificial influences. There was uncertainty regarding the influence of artificial influences on low-flows, especially for ungauged catchments. There was also uncertainty as to the distribution and extent of untreated discharge, which is likely to vary significantly throughout the catchment. The use of wastewater tracers and drogue technology should be explored in order to better estimate flow and to detect wastewater discharge points; however, it was noted that it may be difficult to obtain permission from Chinese authorities to undertake these measures.

It was also highlighted that the estimation of population served for STWs within large urban areas was a significant barrier for the use of the model. It is essential to acquire either population served or service area data for the majority of STWs within these large areas.

Overall, E1 and E2 were modelled with reasonable accuracy; with an overall RMSE (between the median estimated concentration and the mean measured concentration) of 4.25 and 0.82 ng/l for E1 and E2 respectively. However, the model's estimate for the concentration of both TCC and TCS was subject to some significant errors. Overall, the RMSE of TCC was 31.3 ng/l, and the RMSE for TCS, which depended on the in-stream removal rate, ranged between 24.86-62.74 ng/l. TCC and TCS were significantly overestimated at some rural sampling sites, which was likely due to the underuse of products containing TCC and TCS as a result of a lack of affordability or tradition. Further research should be undertaken to better understand and represent the spatial distribution of chemical usage. It was also noted that in-stream removal was potentially quite important to describe the concentration of TCC and TCS, with a greater in-stream removal noted to be more effective to model rural tributary sites with a lower in-stream removal rate for the main stream. It was postulated that in-stream removal, particular biodegradation, may be related to river discharge, which is likely to be lower in rural areas and higher in the main stream. Representation of in-stream removal could be refined, with standard water quality parameters modelled in tandem with the target pollutants. In-stream removal rate constants are sometimes based upon laboratory tests, which do not necessarily represent realistic conditions. Water quality parameters, along with data such as water depth and climate, may be used to adjust the estimate to conditions present within the modelled catchment, or with enough data, to consider in-stream removal as a spatially explicit process. Estimates of water quality parameters could also be used to better estimate the effects upon stream biota. Water quality parameters such as temperature may regulate the effects of organic chemicals upon biota, and therefore including this element would improve the ecological relevance of the model. The challenge with this approach is to do so whilst minimising model complexity and data requirements. For ecological risk assessments, it is also important to determine the effects of mixtures of chemicals, to estimate effects at the population level or above, and to take into account

indirect effects on the ecosystem. This may be improved further by involvement of ecological models, including TKTD, DEB and individual-based population models.

A risk assessment was performed for the four chemicals for both 2016 and 2020 scenarios, with comparison to PNECs determined from literature. The assessment considered there to be little or no risk from TCC for the East river catchment in 2016 at the 50<sup>th</sup> percentile, whilst at the 90<sup>th</sup> percentile areas that exceed the PNEC threshold were largely confined to the Huizhou and Shenzhen area, but also a few short stretches in small streams throughout the catchment. Risk from E1 and E2 is largely acceptable for the catchment. However, there are notable hotspots within the catchment, largely confined to the city of Shenzhen. In contrast, large areas of the catchment were predicted to exceed the PNEC for TCS for both the 50<sup>th</sup> and the 90<sup>th</sup> percentile in 2016. E1 and E2 were estimated to exceed the 50<sup>th</sup> and the 90<sup>th</sup> percentile in stretches mostly confined to large urban areas with lower dilution in 2016.

In 2020, 3 stretches located downstream of major STWs were predicted to exceed the PNEC for TCC at the 50<sup>th</sup> percentile. As for E1 and E2, the area that exceeded the PNEC expanded in 2020, apart from in areas with improved infrastructure, where stretches downstream of new STWs dropped below the PNEC threshold. Finally, for TCS the area that exceeded the PNEC threshold did not change, however the threshold was exceeded by a greater extent.

Catchment management scenarios were implemented in order to determine possible mitigation strategies for the catchment. This reduced the number of stretches that exceeded the PNEC value for TCC, for the 50<sup>th</sup> percentile, to 0. For E1 and E2, the number of stretches that exceeded their PNEC threshold reduced significantly, however, there was no reduction of the number of stretches that exceeded the PNEC value for TCS at the 50<sup>th</sup> percentile. A second scenario was implemented for E1 and E2 alone, with a focus upon remaining stretches indicating high risk. STW service areas were expanded to serve subcatchments containing a relatively high population upstream of stretches highlighted to be at risk or if

there was no nearby STW, a new STW was implemented. For areas targeted, estimated concentrations were reduced to below the PNEC threshold, at the 50<sup>th</sup> percentile. This provided confidence in the model as a catchment management tool.

There is confidence that GREAT-ER may now be used in other catchments in China. Future implementations of GREAT-ER should focus upon areas which may prove a high risk, which may be determined using a large-scale risk assessment model (e.g. Zhu et al., 2014). The North-East of China is likely to experience the greatest risks from down-the-drain chemicals, due to the fact that population is very high, and river discharge is relatively low. Of particular interest are the cold regions; during the freeze-over period complex conditions are likely to result in low dilution and degradation, which may result in significant inputs to streams that flow through large population areas.

The arid North-West may also experience elevated risks, in particular, large urban areas such as the city of Ürümqi. Dilution is very low during the dry season and there may be examples of streams that are fed entirely by wastewater discharge, much of which may be untreated. However, this water is likely to be already affected by pollutants, and that the release of wastewater may create habitat, where there was none before. Therefore, for the purpose of risk assessment this scenario may be best approached using the impact zone concept (Limlette III Workshop, 1995); where the impact zone is a heavily polluted stretch of river downstream of a wastewater discharge outlet. The aim behind this concept is to ensure that the chemical of interest does not affect self-purification within the “impact zone”, and does not exceed the PNEC beyond the “impact zone”.



## Reference list

- ABBOTT, M. B., BATHURST, J. C., CUNGE, J. A., O'CONNELL, P. E. & RASMUSSEN, J. 1986. An introduction to the European Hydrological System — Systeme Hydrologique Europeen, "SHE", 1: History and philosophy of a physically-based, distributed modelling system. *Journal of Hydrology*, 87, 45-59.
- ADLERCREUTZ, H., GORBACH, S. L., GOLDIN, B. R., WOODS, M. N., DWYER, J. T. & HÄMÄLÄINEN, E. 1994. Estrogen Metabolism and Excretion in Oriental and Caucasian Women. *JNCI: Journal of the National Cancer Institute*, 86, 1076-1082.
- ALCAMO, J., DÖLL, P., HENRICH, T., KASPAR, F., LEHNER, B., RÖSCH, T. & SIEBERT, S. 2003. Development and testing of the WaterGAP 2 global model of water use and availability. *Hydrological Sciences Journal*, 48, 317-337.
- ALDEKOA, J., MEDICI, C., OSORIO, V., PÉREZ, S., MARCÉ, R., BARCELÓ, D. & FRANCÉS, F. 2013. Modelling the emerging pollutant diclofenac with the GREAT-ER model: Application to the Llobregat River Basin. *Journal of Hazardous Materials*, 263, Part 1, 207-213.
- ALDER, A. C., SCHAFFNER, C., MAJEWSKY, M., KLASMEIER, J. & FENNER, K. 2010. Fate of  $\beta$ -blocker human pharmaceuticals in surface water: Comparison of measured and simulated concentrations in the Glatt Valley Watershed, Switzerland. *Water research*, 44, 936-948.
- ALMEIDA, M. C., BUTLER, D. & FRIEDLER, E. 1999. At-source domestic wastewater quality. *Urban Water*, 1, 49-55.
- ALTMAN, D. G. & ANDERSEN, P. K. 1989. Bootstrap investigation of the stability of a cox regression model. *Statistics in Medicine*, 8, 771-783.
- ÁLVAREZ, O. A., JAGER, T., REDONDO, E. M. & KAMMENGA, J. E. 2006. Physiological modes of action of toxic chemicals in the nematode *Acrobeloides nanus*. *Environmental Toxicology and Chemistry*, 25, 3230-3237.
- AN, W., HU, J.-Y. & YAO, F. 2006. A method of assessing ecological risk to night heron, *Nycticorax nycticorax*, population persistence from dichlorodiphenyltrichloroethane exposure. *Environmental Toxicology and Chemistry*, 25, 281-286.
- ANDERSON, P. D., D'ACO, V. J., SHANAHAN, P., CHAPRA, S. C., BUZBY, M. E., CUNNINGHAM, V. L., DUPLESSIE, B. M., HAYES, E. P., MASTROCCO, F. J., PARKE, N. J., RADER, J. C., SAMUELIAN, J. H. & SCHWAB, B. W. 2003. Screening Analysis of Human Pharmaceutical Compounds in U.S. Surface Waters. *Environmental Science & Technology*, 38, 838-849.
- ANGLE, G., GOWDA, S., JENNINGS, P., PETRIE, R., CHEN, R., DELLARCO, V., LEIGHTON, T., MCMAHON, T., SHAMIM, A. N., GARVIE, H., ISBELL, D. & ROSS, P. 2008. Reregistration Eligibility Decision for Triclosan. United States Environmental Protection Agency.
- ANKLEY, G. T., DASTON, G. P., DEGITZ, S. J., DENSLOW, N. D., HOKE, R. A., KENNEDY, S. W., MIRACLE, A. L., PERKINS, E. J., SNAPE, J., TILLITT, D. E., TYLER, C. R. & VERSTEEG, D. 2006. TOXICOGENOMICS in Regulatory Ecotoxicology. *Environmental science & technology*, 40, 4055-4065.
- ARNOLD, J. G., ALLEN, P. M. & BERNHARDT, G. 1993. A comprehensive surface-groundwater flow model. *Journal of Hydrology*, 142, 47-69.
- ARNOLD, J. G., KINIRY, J. R., SRINIVASAN, R., WILLIAMS, J. R. & HANEY, E. B. 2012. *Soil and Water Assessment Tool: Input/Output Documentation - Version 2012*.
- ARNOT, J. A. & GOBAS, F. A. P. C. 2004. A food web bioaccumulation model for organic chemicals in aquatic ecosystems. *Environmental Toxicology and Chemistry*, 23, 2343-2355.

- ASHAUER, R., AGATZ, A., ALBERT, C., DUCROT, V., GALIC, N., HENDRIKS, J., JAGER, T., KRETSCHMANN, A., O'CONNOR, I., RUBACH, M. N., NYMAN, A.-M., SCHMITT, W., STADNICKA, J., VAN DEN BRINK, P. J. & PREUSS, T. G. 2011. Toxicokinetic-toxicodynamic modeling of quantal and graded sublethal endpoints: A brief discussion of concepts. *Environmental Toxicology and Chemistry*, 30, 2519-2524.
- ASHAUER, R., BOXALL, A. B. A. & BROWN, C. D. 2007. Simulating Toxicity of Carbaryl to *Gammarus pulex* after Sequential Pulsed Exposure. *Environmental Science & Technology*, 41, 5528-5534.
- ASHAUER, R. & ESCHER, B. I. 2010. Advantages of toxicokinetic and toxicodynamic modelling in aquatic ecotoxicology and risk assessment. *J Environ Monit*, 12, 2056-61.
- BABYAK, M. A. 2004. What You See May Not Be What You Get: A Brief, Nontechnical Introduction to Overfitting in Regression-Type Models. *Psychosomatic Medicine*, 66, 411-421.
- BACKHAUS, T. & FAUST, M. 2012. Predictive Environmental Risk Assessment of Chemical Mixtures: A Conceptual Framework. *Environmental Science & Technology*, 46, 2564-2573.
- BAKER, M. E., WELLER, D. E. & JORDAN, T. E. 2006. Comparison of Automated Watershed Delineations. *Photogrammetric Engineering & Remote Sensing*, 72, 159-168.
- BANAVAR, J. R., DAMUTH, J., MARITAN, A. & RINALDO, A. 2002. Supply–demand balance and metabolic scaling. *Proceedings of the National Academy of Sciences*, 99, 10506-10509.
- BARRON, L., HAVEL, J., PURCELL, M., SZPAK, M., KELLEHER, B. & PAULL, B. 2009. Predicting sorption of pharmaceuticals and personal care products onto soil and digested sludge using artificial neural networks. *Analyst*, 134, 663-670.
- BEAUDOUIN, R., MONOD, G. & GINOT, V. 2008. Selecting parameters for calibration via sensitivity analysis: An individual-based model of mosquitofish population dynamics. *Ecological Modelling*, 218, 29-48.
- BEDNARSKA, A. J., JEVTIĆ, D. M. & LASKOWSKI, R. 2013. More ecological ERA: Incorporating natural environmental factors and animal behavior. *Integrated Environmental Assessment and Management*, 9, e39-e46.
- BEI, Z. G., HU, T. S., LIU, J. J., YU, W. W., PAERL, H. W. & CARMICHAEL, W. M. 2009. Study of water environmental pollution model and control strategy. *China Rural Water Hydropower*, 326, 15-23.
- BELDEN, J. B., GILLIOM, R. J. & LYDY, M. J. 2007. How well can we predict the toxicity of pesticide mixtures to aquatic life? *Integrated Environmental Assessment and Management*, 3, 364-372.
- BENDZ, D., PAXÉUS, N. A., GINN, T. R. & LOGE, F. J. 2005. Occurrence and fate of pharmaceutically active compounds in the environment, a case study: Höje River in Sweden. *Journal of Hazardous Materials*, 122, 195-204.
- BESTER, K. 2005. Fate of Triclosan and Triclosan-Methyl in Sewage Treatment Plants and Surface Waters. *Archives of Environmental Contamination and Toxicology*, 49, 9-17.
- BEVEN, K. 2006. A manifesto for the equifinality thesis. *Journal of Hydrology*, 320, 18-36.
- BEVEN, K. 2012a. Down to Basics: Runoff Processes and the Modelling Process. *Rainfall-Runoff Modelling*. John Wiley & Sons, Ltd.
- BEVEN, K. 2012b. Hydrological Similarity, Distribution Functions and Semi-Distributed Rainfall–Runoff Models. *Rainfall-Runoff Modelling*. John Wiley & Sons, Ltd.
- BEVEN, K. 2012c. Predicting Hydrographs Using Distributed Models Based on Process Descriptions. *Rainfall-Runoff Modelling*. John Wiley & Sons, Ltd.
- BEVEN, K. 2012d. Predicting Hydrographs Using Models Based on Data. *Rainfall-Runoff Modelling*. John Wiley & Sons, Ltd.

- BEYER, J., PETERSEN, K., SONG, Y., RUUS, A., GRUNG, M., BAKKE, T. & TOLLEFSEN, K. E. 2014. Environmental risk assessment of combined effects in aquatic ecotoxicology: A discussion paper. *Marine Environmental Research*, 96, 81-91.
- BHARGAVA, H. N. & LEONARD, P. A. 1996. Triclosan: Applications and safety. *American Journal of Infection Control*, 24, 209-218.
- BILLOIR, E., PÉRY, A. R. R. & CHARLES, S. 2007. Integrating the lethal and sublethal effects of toxic compounds into the population dynamics of *Daphnia magna*: A combination of the DEBtox and matrix population models. *Ecological Modelling*, 203, 204-214.
- BLISS, C. I. 1939. The Toxicity of Poisons Applied Jointly. *Annals of Applied Biology*, 26, 585-615.
- BOEIJE, G. 1999. GREAT-ER - Technical Documentation - Chemical Fate Models. Gent, Belgium: Ghent University.
- BOWDEN, K. & BROWN, S. R. 1984. Relating Effluent Control Parameters to River Quality Objectives Using a Generalised Catchment Simulation Model. *Water Science and Technology*, 16, 197-206.
- BRADY, N. C. 1999. *The nature and properties of soils*, Upper Saddle River, N.J. : Prentice Hall.
- BRIAN, J. V., HARRIS, C. A., SCHOLZE, M., KORTENKAMP, A., BOOY, P., LAMOREE, M., POJANA, G., JONKERS, N., MARCOMINI, A. & SUMPTER, J. P. 2007. Evidence of Estrogenic Mixture Effects on the Reproductive Performance of Fish. *Environmental Science & Technology*, 41, 337-344.
- BRIÈRE, F. G. 2007. *Drinking-Water Distribution, Sewage, and Rainfall Collection*, Polytechnic International Press.
- BRIGHT, E. A., COLEMAN, P. R. & KING, A. L. 2006. LandScan 2005. 2005 ed. Oak Ridge, TN: Oak Ridge National Laboratory.
- BRIGHT, E. A., COLEMAN, P. R., ROSE, A. N. & URBAN, M. L. 2011. LandScan 2010. 2010 ed. Oak Ridge, TN: Oak Ridge National Laboratory.
- BROOKS, B. W., FORAN, C. M., RICHARDS, S. M., WESTON, J., TURNER, P. K., STANLEY, J. K., SOLOMON, K. R., SLATTERY, M. & LA POINT, T. W. 2003. Aquatic ecotoxicology of fluoxetine. *Toxicology Letters*, 142, 169-183.
- BROOKS, B. W., RILEY, T. M. & TAYLOR, R. D. 2006. Water Quality of Effluent-dominated Ecosystems: Ecotoxicological, Hydrological, and Management Considerations. *Hydrobiologia*, 556, 365-379.
- BROXTON, P. D., ZENG, X., SULLA-MENASHE, D. & TROCH, P. A. 2014. A Global Land Cover Climatology Using MODIS Data. *Journal of Applied Meteorology and Climatology*, 53, 1593-1605.
- BRYANT, V., NEWBERY, D. M., MCLUSKY, D. S. & CAMPBELL, R. 1985. Effect of temperature and salinity on the toxicity of nickel and zinc to two estuarine invertebrates (*Corophium volutator*, *Macoma balthica*). *Marine Ecology Progress Series*, 24, 139-153.
- BUERGE, I. J., POIGER, T., MÜLLER, M. D. & BUSER, H.-R. 2003. Caffeine, an Anthropogenic Marker for Wastewater Contamination of Surface Waters. *Environmental Science & Technology*, 37, 691-700.
- BUIS, A. & COLE, S. 2014. *U.S. Releases Enhanced Shuttle Land Elevation Data* [Online]. Available: <https://www.jpl.nasa.gov/news/news.php?release=2014-321> [Accessed 26/09/2017].
- CALDWELL, D. J., MASTROCCO, F., ANDERSON, P. D., LÄNGE, R. & SUMPTER, J. P. 2012. Predicted-no-effect concentrations for the steroid estrogens estrone, 17 $\beta$ -estradiol, estriol, and 17 $\alpha$ -ethinylestradiol. *Environmental Toxicology and Chemistry*, 31, 1396-1406.
- CALOW, P., SIBLY, R. M. & FORBES, V. 1997. Risk assessment on the basis of simplified life-history scenarios. *Environmental Toxicology and Chemistry*, 16, 1983-1989.

- CALVER, A. & WOOD, W. L. 1995. The Institute of Hydrology Distributed Model. *In*: SINGH, V. P. (ed.) *Computer models of watershed hydrology*. Highlands Ranch, Colorado, US: Water resource publications
- CAPDEVIELLE, M., VAN EGMOND, R., WHELAN, M., VERSTEEG, D., HOFMANN-KAMENSKY, M., INAUEN, J., CUNNINGHAM, V. & WOLTERING, D. 2008. Consideration of exposure and species sensitivity of triclosan in the freshwater environment. *Integrated Environmental Assessment and Management*, 4, 15-23.
- CAREY, R. O. & MIGLIACCIO, K. W. 2009. Contribution of Wastewater Treatment Plant Effluents to Nutrient Dynamics in Aquatic Systems: A Review. *Environmental Management*, 44, 205-217.
- CASSIE, D. & EL-JABI, N. 1995. Hydrology of the Miramichi River Drainage Basin. *In*: CHADWICK, E. M. P. (ed.) *Water, science and the public: the Miramichi ecosystem*. Canadian Special Publication of Fisheries and Aquatic Sciences No. 123.
- CASTELLARIN, A. 2014. Regional prediction of flow-duration curves using a three-dimensional kriging. *Journal of Hydrology*, 513, 179-191.
- CASTIGLIONI, S., CASTELLARIN, A. & MONTANARI, A. 2009. Prediction of low-flow indices in ungauged basins through physiographical space-based interpolation. *Journal of Hydrology*, 378, 272-280.
- CASTIGLIONI, S., CASTELLARIN, A., MONTANARI, A., SKØIEN, J. O., LAAHA, G. & BLÖSCHL, G. 2011. Smooth regional estimation of low-flow indices: physiographical space based interpolation and top-kriging. *Hydrology and Earth System Sciences*, 15, 715-727.
- CAUPOS, E., MAZELLIER, P. & CROUE, J.-P. 2011. Photodegradation of estrone enhanced by dissolved organic matter under simulated sunlight. *Water Research*, 45, 3341-3350.
- CEDERGREEN, N., CHRISTENSEN, A. M., KAMPER, A., KUDSK, P., MATHIASSEN, S. K., STREIBIG, J. C. & SØRENSEN, H. 2008. A review of independent action compared to concentration addition as reference models for mixtures of compounds with different molecular target sites. *Environmental Toxicology and Chemistry*, 27, 1621-1632.
- CEFIC 2016. The European Chemical Industry Facts and Figures 2016.
- CERVIONE, M. A., RICHARDSON, A. R. & WEISS, L. A. 1993. Low-flow characteristics of selected streams in Rhode Island. USGS Water-Resources Investigations Report 93-4046.
- CHANG, C. P. 2004. *East Asian Monsoon*, World Scientific.
- CHEN, C.-E., ZHANG, H. & JONES, K. C. 2012. A novel passive water sampler for in situ sampling of antibiotics. *Journal of Environmental Monitoring*, 14, 1523-1530.
- CHEN, J., AHN, K. C., GEE, N. A., AHMED, M. I., DULEBA, A. J., ZHAO, L., GEE, S. J., HAMMOCK, B. D. & LASLEY, B. L. 2008. Triclocarban Enhances Testosterone Action: A New Type of Endocrine Disruptor? *Endocrinology*, 149, 1173-1179.
- CHEN, R., SHERBININ, A. D. & YE, C. 2015. Time for a data revolution in China. *Science*, 348, 981-981.
- CHEN, X., CHEN, Y. D. & XU, C.-Y. 2007. A distributed monthly hydrological model for integrating spatial variations of basin topography and rainfall. *Hydrological Processes*, 21, 242-252.
- CHEN, Z.-F., YING, G.-G., LIU, Y.-S., ZHANG, Q.-Q., ZHAO, J.-L., LIU, S.-S., CHEN, J., PENG, F.-J., LAI, H.-J. & PAN, C.-G. 2014. Triclosan as a surrogate for household biocides: An investigation into biocides in aquatic environments of a highly urbanized region. *Water Research*, 58, 269-279.
- CHOKMANI, K. & OUARDA, T. B. M. J. 2004. Physiographical space-based kriging for regional flood frequency estimation at ungauged sites. *Water Resources Research*, 40, n/a-n/a.

- CHOWDHURY, R. R., CHARPENTIER, P. & RAY, M. B. 2010. Photodegradation of Estrone in Solar Irradiation. *Industrial & Engineering Chemistry Research*, 49, 6923-6930.
- CIAT 2004. Void-filled seamless SRTM data V2. International Centre for Tropical Agriculture.
- CIESIN 2016a. Gridded Population of the World, Version 4 (GPWv4): Population Count. Palisades, NY: NASA Socioeconomic Data and Applications Center (SEDAC).
- CIESIN 2016b. Gridded Population of the World, Version 4 (GPWv4): Population Density. Palisades, NY: NASA Socioeconomic Data and Applications Center (SEDAC).
- CIFFROY, P., TEDIOSI, A. & CAPRI, E. 2017. *Modelling the Fate of Chemicals in the Environment and the Human Body*, Springer International Publishing.
- COONEY, J. D., BEAUCHAMP, J. & GEHRS, C. W. 1983. Effects of temperature and nutritional state on the acute toxicity of acridine to the calanoid copepod, *Diaptomus clavipes schacht*. *Environmental Toxicology and Chemistry*, 2, 431-439.
- COWAN, C. E., CAPRARA, R. J., WHITE, C. E., MERVES, M. L. & GULLOTTI, M. K. A model for predicting the fate of 'down-the-drain' consumer product ingredients in United States rivers. Water Environment Federation - 66th annual conference and exposition, October 3-7 1993, Anaheim, United States. 351-358.
- COX, B. 2003. A review of currently available in-stream water-quality models and their applicability for simulating dissolved oxygen in lowland rivers. *The Science of The Total Environment*, 314-316, 335-377.
- CRABTREE, B., KELLY, S., GREEN, H., SQUIBBS, G. & MITCHELL, G. 2009. Water Framework Directive catchment planning: a case study apportioning loads and assessing environmental benefits of programme of measures. *Water Science and Technology*, 59, 407-416.
- CROFTON, K. M., PAUL, K. B., DEVITO, M. J. & HEDGE, J. M. 2007. Short-term in vivo exposure to the water contaminant triclosan: Evidence for disruption of thyroxine. *Environmental Toxicology and Pharmacology*, 24, 194-197.
- DAVLSON, W. & ZHANG, H. 1994. In situ speciation measurements of trace components in natural waters using thin-film gels. *Nature*, 367, 546.
- DEANGELIS, D. L. & GRIMM, V. 2014. Individual-based models in ecology after four decades. *F1000Prime Reports*, 6, 39.
- DEMON, A. & EIJSACKERS, H. 1985. The effects of lindane and azinphosmethyl on survival time of soil animals, under extreme or fluctuating temperature and moisture conditions. *Zeitschrift für Angewandte Entomologie*, 100, 504-510.
- DERKSEN, S. & KESELMAN, H. J. 1992. Backward, forward and stepwise automated subset selection algorithms: Frequency of obtaining authentic and noise variables. *British Journal of Mathematical and Statistical Psychology*, 45, 265-282.
- DESBROW, C., ROUTLEDGE, E. J., BRIGHTY, G. C., SUMPTER, J. P. & WALDOCK, M. 1998. Identification of Estrogenic Chemicals in STW Effluent. 1. Chemical Fractionation and in Vitro Biological Screening. *Environmental Science & Technology*, 32, 1549-1558.
- DING, S.-L., WANG, X.-K., JIANG, W.-Q., MENG, X., ZHAO, R.-S., WANG, C. & WANG, X. 2013. Photodegradation of the antimicrobial triclocarban in aqueous systems under ultraviolet radiation. *Environmental Science and Pollution Research*, 20, 3195-3201.
- DING, Y. 2013. *Monsoons over China*, Springer Netherlands.
- DOMRÖS, M. & PENG, G. 2012. *The Climate of China*, Springer Berlin Heidelberg.
- DONGJIANG RIVER BASIN AUTHORITY. 2010. *Dongjiang River in Guangdong Province 2009-2010 annual dry season water regulation work summary meeting held in Huizhou [In Chinese]* [Online]. Available: [http://www.djriver.cn/News\\_View.asp?NewsID=1182](http://www.djriver.cn/News_View.asp?NewsID=1182) [Accessed 05/01/2017].
- DONGJIANG RIVER BASIN AUTHORITY. 2014. *I organized the organization to organize the winter and spring dry season water scheduling work forum [In Chinese]* [Online]. Available: [http://www.djriver.cn/News\\_View.asp?NewsID=2358](http://www.djriver.cn/News_View.asp?NewsID=2358) [Accessed 05/01/2017].

- DOTAN, P., GODINGER, T., ODEH, W., GROISMAN, L., AL-KHATEEB, N., RABBO, A. A., TAL, A. & ARNON, S. 2016. Occurrence and fate of endocrine disrupting compounds in wastewater treatment plants in Israel and the Palestinian West Bank. *Chemosphere*, 155, 86-93.
- DRIESCH, H. 1908. *The science and philosophy of the organism*, London, UK, Adam and Charles Black.
- DUMONT, E., WILLIAMS, R., KELLER, V., VOß, A. & TATTARI, S. 2012. Modelling indicators of water security, water pollution and aquatic biodiversity in Europe. *Hydrological Sciences Journal*, 57, 1378-1403.
- EUROPEAN CHEMICAL AGENCY 2011. Guidance on information requirements and chemical safety assessment. Part B: Hazard assessment.
- EUROPEAN COMMISSION 91/676/EEC of 12 December 1991 concerning the protection of waters against pollution caused by nitrates from agricultural sources.
- EUROPEAN COMMISSION 91/271/EEC of 21 May 1991 concerning urban waste-water treatment.
- EUROPEAN COMMISSION 98/83/EC of 3 November 1998 on the quality of water intended for human consumption.
- EUROPEAN COMMISSION 1999. Revised proposal for a list of priority substances in the context of the water framework directive (COMMPS procedure). Schmollenberg: Fraunhofer Institute.
- EUROPEAN COMMISSION 2000/60/EC of 23 October 2000 establishing a framework for Community action in the field of water policy.
- EUROPEAN COMMISSION 2003. Technical guidance document on risk assessment in support of commission directive 93/67/EEC on risk assessment for new notified substances, commission regulation (EC) No 1488/94 on risk assessment for existing substances, and Directive 98/8/EC of the European parliament and of the council concerning the placing of biocidal products on the market: Part II.: Office for Official Publications of the European Communities.
- EUROPEAN COMMISSION 2006/7/EC of 15 February 2006 concerning the management of bathing water quality and repealing Directive 76/160/EEC.
- EUROPEAN COMMISSION 2006b. Reach in brief.
- FAO, IIASA, ISRIC, ISSCAS & JRC 2009. Harmonized World Soil Database (version 1.1). Rome, Italy and IIASA, Laxenburg, Austria.: FAO.
- FARR, T. G., ROSEN, P. A., CARO, E., CRIPPEN, R., DUREN, R., HENSLEY, S., KOBRICK, M., PALLER, M., RODRIGUEZ, E., ROTH, L., SEAL, D., SHAFFER, S., SHIMADA, J., UMLAND, J., WERNER, M., OSKIN, M., BURBANK, D. & ALSDORF, D. 2007. The Shuttle Radar Topography Mission. *Reviews of Geophysics*, 45, n/a-n/a.
- FEDERATION, W. E. 2009. *Wastewater Collection Systems Management MOP 7, Sixth Edition*, McGraw-Hill Education.
- FEDRA, K. & JAMIESON, D. G. 1996. The 'WaterWare' decision-support system for river-basin planning. 2. Planning capability. *Journal of Hydrology*, 177, 177-198.
- FEIJTEL, T., BOEIJE, G., MATTHIES, M., YOUNG, A., MORRIS, G., GANDOLFI, C., HANSEN, B., FOX, K., HOLT, M., KOCH, V., SCHRODER, R., CASSANI, G., SCHOWANEK, D., ROSENBLUM, J. & NIESSEN, H. 1997. Development of a geography-referenced regional exposure assessment tool for European rivers - great-er contribution to great-er #1. *Chemosphere*, 34, 2351-2373.
- FEKETE, B. M., VÖRÖSMARTY, C. J. & GRABS, W. 2002. High-resolution fields of global runoff combining observed river discharge and simulated water balances. *Global Biogeochemical Cycles*, 16, 15-1-15-10.

- FERRICK, M. G. & CALKINS, D. J. 1996. Discussion: Risk-Equivalent Seasonal Discharge Programs for Ice-Covered Rivers. *Journal of Water Resources Planning and Management*, 122, 442-444.
- FEWTRELL, L. & BARTRAM, J. (eds.) 2001. *Water Quality: Guidelines, Standards, and Health : Assessment of Risk and Risk Management for Water-related Infectious Disease*: World Health Organization.
- FICK, S. E. & HIJMANS, R. J. 2017. WorldClim 2: new 1-km spatial resolution climate surfaces for global land areas. *International Journal of Climatology*, 37, 4302-4315.
- FIELD, R., SULLIVAN, D. & TAFURI, A. N. 2003. *Management of Combined Sewer Overflows*, CRC Press.
- FINNEGAN, C. J., VAN EGMOND, R. A., PRICE, O. R. & WHELAN, M. J. 2009. Continuous-flow laboratory simulation of stream water quality changes downstream of an untreated wastewater discharge. *Water Res*, 43, 1993-2001.
- FORBES, V. E., CALOW, P., GRIMM, V., HAYASHI, T. I., JAGER, T., KATHOLM, A., PALMQVIST, A., PASTOROK, R., SALVITO, D., SIBLY, R., SPROMBERG, J., STARK, J. & STILLMAN, R. A. 2011. Adding Value to Ecological Risk Assessment with Population Modeling. *Human and Ecological Risk Assessment: An International Journal*, 17, 287-299.
- FOX, K., HOLT, M., DANIEL, M., BUCKLAND, H. & GUYMER, I. 2000. Removal of linear alkylbenzene sulfonate from a small Yorkshire stream: contribution to GREAT-ER project #7. *Science of The Total Environment*, 251–252, 265-275.
- GABSI, F., HAMMERS-WIRTZ, M., GRIMM, V., SCHÄFFER, A. & PREUSS, T. G. 2014. Coupling different mechanistic effect models for capturing individual- and population-level effects of chemicals: Lessons from a case where standard risk assessment failed. *Ecological Modelling*, 280, 18-29.
- GALIC, N., HOMMEN, U., BAVECO, J. M. & VAN DEN BRINK, P. J. 2010. Potential application of population models in the European ecological risk assessment of chemicals II: Review of models and their potential to address environmental protection aims. *Integrated Environmental Assessment and Management*, 6, 338-360.
- GAN, Z., SUN, H., FENG, B., WANG, R. & ZHANG, Y. 2013. Occurrence of seven artificial sweeteners in the aquatic environment and precipitation of Tianjin, China. *Water Research*, 47, 4928-4937.
- GARBRECHT, J. & MARTZ, L. W. 1997. The assignment of drainage direction over flat surfaces in raster digital elevation models. *Journal of Hydrology*, 193, 204-213.
- GAUGHAN, A. E., STEVENS, F. R., LINARD, C., JIA, P. & TATEM, A. J. 2013. High Resolution Population Distribution Maps for Southeast Asia in 2010 and 2015. *PLOS ONE*, 8, e55882.
- GE, F., SIELMANN, F., ZHU, X., FRAEDRICH, K., ZHI, X., PENG, T. & WANG, L. 2017. The link between Tibetan Plateau monsoon and Indian summer precipitation: a linear diagnostic perspective. *Climate Dynamics*.
- GERECKE, A. C., CANONICA, S., MÜLLER, S. R., SCHÄRER, M. & SCHWARZENBACH, R. P. 2001. Quantification of Dissolved Natural Organic Matter (DOM) Mediated Phototransformation of Phenylurea Herbicides in Lakes. *Environmental Science & Technology*, 35, 3915-3923.
- GERGS, A., KULKARNI, D. & PREUSS, T. G. 2015. Body size-dependent toxicokinetics and toxicodynamics could explain intra- and interspecies variability in sensitivity. *Environmental Pollution*, 206, 449-455.
- GESCH, D. B., VERDIN, K. L. & GREENLEE, S. K. 1999. New land surface digital elevation model covers the Earth. *Eos, Transactions American Geophysical Union*, 80, 69-70.
- GIGER, W., SCHAFFNER, C. & KOHLER, H.-P. E. 2006. Benzotriazole and Tolytriazole as Aquatic Contaminants. 1. Input and Occurrence in Rivers and Lakes. *Environmental Science & Technology*, 40, 7186-7192.

- GOBAS, F. A. P. C., WILCOCKSON, J. B., RUSSELL, R. W. & HAFFNER, G. D. 1999. Mechanism of Biomagnification in Fish under Laboratory and Field Conditions. *Environmental Science & Technology*, 33, 133-141.
- GÓMEZ, M. J., MARTÍNEZ BUENO, M. J., LACORTE, S., FERNÁNDEZ-ALBA, A. R. & AGÜERA, A. 2007. Pilot survey monitoring pharmaceuticals and related compounds in a sewage treatment plant located on the Mediterranean coast. *Chemosphere*, 66, 993-1002.
- GREEN, C., WILLIAMS, R., KANDA, R., CHURCHLEY, J., HE, Y., THOMAS, S., GOONAN, P., KUMAR, A. & JOBLING, S. 2013. Modeling of steroid estrogen contamination in UK and South Australian rivers predicts modest increases in concentrations in the future. *Environ Sci Technol*, 47, 7224-32.
- GRILL, G., KHAN, U., LEHNER, B., NICELL, J. & ARIWI, J. 2016. Risk assessment of down-the-drain chemicals at large spatial scales: Model development and application to contaminants originating from urban areas in the Saint Lawrence River Basin. *Science of The Total Environment*, 541, 825-838.
- GRIMM, V. & RAILSBACK, S. 2013. *Individual-based Modeling and Ecology*.
- GROH, K. J., CARVALHO, R. N., CHIPMAN, J. K., DENSLOW, N. D., HALDER, M., MURPHY, C. A., ROELOFS, D., ROLAKI, A., SCHIRMER, K. & WATANABE, K. H. 2015. Development and application of the adverse outcome pathway framework for understanding and predicting chronic toxicity: I. Challenges and research needs in ecotoxicology. *Chemosphere*, 120, 764-777.
- GUANGDONG PROVINCIAL BUREAU OF STATISTICS. n.d. *Guangdong statistics network* [Online]. Available: <http://www.gdstats.gov.cn/> [Accessed 19/12/2017].
- GUERARD, J. J., MILLER, P. L., TROUTS, T. D. & CHIN, Y.-P. 2009. The role of fulvic acid composition in the photosensitized degradation of aquatic contaminants. *Aquatic Sciences*, 71, 160-169.
- GUERRA, P., KIM, M., SHAH, A., ALAEE, M. & SMYTH, S. A. 2014. Occurrence and fate of antibiotic, analgesic/anti-inflammatory, and antifungal compounds in five wastewater treatment processes. *Science of The Total Environment*, 473-474, 235-243.
- GUSTARD, A. & YOUNG, A. 2009. Estimating low flows in artificially influenced rivers. *Manual on Low-flow estimation and prediction*. Geneva: World meteorological organization.
- HALDEN, R. U. 2014. On the Need and Speed of Regulating Triclosan and Triclocarban in the United States. *Environmental Science & Technology*, 48, 3603-3611.
- HALDEN, R. U. & PAULL, D. H. 2005. Co-Occurrence of Triclocarban and Triclosan in U.S. Water Resources. *Environmental Science & Technology*, 39, 1420-1426.
- HAN, D., CURRELL, M. J. & CAO, G. 2016. Deep challenges for China's war on water pollution. *Environmental Pollution*, 218, 1222-1233.
- HANKIN, B., BIELBY, S., POPE, L. & DOUGLASS, J. 2016. Catchment-scale sensitivity and uncertainty in water quality modelling. *Hydrological Processes*, 30, 4004-4018.
- HANNAH, D. M., DEMUTH, S., VAN LANEN, H. A. J., LOOSER, U., PRUDHOMME, C., REES, G., STAHL, K. & TALLAKSEN, L. M. 2011. Large-scale river flow archives: importance, current status and future needs. *Hydrological Processes*, 25, 1191-1200.
- HANNAH, R., D'ACO, V. J., ANDERSON, P. D., BUZBY, M. E., CALDWELL, D. J., CUNNINGHAM, V. L., ERICSON, J. F., JOHNSON, A. C., PARKE, N. J., SAMUELIAN, J. H. & SUMPTER, J. P. 2009. Exposure assessment of 17 $\alpha$ -ethinylestradiol in surface waters of the United States and Europe. *Environmental Toxicology and Chemistry*, 28, 2725-2732.
- HAWKINS, D. M. 2004. The Problem of Overfitting. *Journal of Chemical Information and Computer Sciences*, 44, 1-12.
- HAYASHI, T. I., KAMO, M. & TANAKA, Y. 2009. Population-level ecological effect assessment: estimating the effect of toxic chemicals on density-dependent populations. *Ecological Research*, 24, 945-954.



- HEEB, F., SINGER, H., PERNET-COUDRIER, B., QI, W., LIU, H., LONGRÉE, P., MÜLLER, B. & BERG, M. 2012. Organic Micropollutants in Rivers Downstream of the Megacity Beijing: Sources and Mass Fluxes in a Large-Scale Wastewater Irrigation System. *Environmental Science & Technology*, 46, 8680-8688.
- HEIDLER, J. & HALDEN, R. U. 2007. Mass balance assessment of triclosan removal during conventional sewage treatment. *Chemosphere*, 66, 362-369.
- HEIDLER, J., SAPKOTA, A. & HALDEN, R. U. 2006. Partitioning, Persistence, and Accumulation in Digested Sludge of the Topical Antiseptic Triclocarban during Wastewater Treatment. *Environmental Science & Technology*, 40, 3634-3639.
- HELLWEGER, F. L. 1997. *AGREE - DEM Surface Reconditioning System* [Online]. Available: <http://www.ce.utexas.edu/prof/maidment/gishydro/ferdi/research/agree/agree.html> [Accessed 09/11/2015] 2015]].
- HENDRIKS, A. J., VAN DER LINDE, A., CORNELISSEN, G. & SIJM, D. T. H. M. 2001. The power of size. 1. Rate constants and equilibrium ratios for accumulation of organic substances related to octanol-water partition ratio and species weight. *Environmental Toxicology and Chemistry*, 20, 1399-1420.
- HEYS, K. A., SHORE, R. F., PEREIRA, M. G., JONES, K. C. & MARTIN, F. L. 2016. Risk assessment of environmental mixture effects. *RSC Advances*, 6, 47844-47857.
- HIJMANS, R. J., CAMERON, S. E., PARRA, J. L., JONES, P. G. & JARVIS, A. 2005. Very high resolution interpolated climate surfaces for global land areas. *International Journal of Climatology*, 25, 1965-1978.
- HODGES, J., HOLMES, C., VAMSHI, R., MAO, D. & PRICE, O. 2012. Estimating chemical emissions from home and personal care products in China. *Environmental Pollution*, 165, 199-207.
- HODGES, J. E. N., VAMSHI, R., HOLMES, C., ROWSON, M., MIAH, T. & PRICE, O. R. 2014. Combining high-resolution gross domestic product data with home and personal care product market research data to generate a subnational emission inventory for Asia. *Integrated Environmental Assessment and Management*, 10, 237-246.
- HOLDEN, J. 2012. *Introduction to Physical Geography and the Environment*, Pearson.
- HOLMES, M. G. R., YOUNG, A. R., GUSTARD, A. & GREW, R. 2002a. A region of influence approach to predicting flow duration curves within ungauged catchments. *Hydrology and Earth System Sciences*, 6, 721-731.
- HOLMES, M. G. R., YOUNG, A. R., GUSTARD, A. & GREW, R. 2002b. A region of influence approach to predicting flow duration curves within ungauged catchments. *Hydrology and Earth System Sciences Discussions*, 6, 721-731.
- HOLTHAUS, K. I. E., JOHNSON, A. C., JÜRGENS, M. D., WILLIAMS, R. J., SMITH, J. J. L. & CARTER, J. E. 2002. The potential for estradiol and ethinylestradiol to sorb to suspended and bed sediments in some English rivers. *Environmental Toxicology and Chemistry*, 21, 2526-2535.
- HOMMEN, U., BAVECO, J. M., GALIC, N. & VAN DEN BRINK, P. J. 2010. Potential application of ecological models in the European environmental risk assessment of chemicals I: Review of protection goals in EU directives and regulations. *Integrated Environmental Assessment and Management*, 6, 325-337.
- HONG KONG INFORMATION SERVICES DEPARTMENT. 2013. *Dongjiang water quality improving* [Online]. Available: [http://www.news.gov.hk/en/categories/infrastructure/html/2013/11/20131107\\_141139.shtml](http://www.news.gov.hk/en/categories/infrastructure/html/2013/11/20131107_141139.shtml) [Accessed 17/09/2014] 2014]].
- HONG KONG LEGISLATIVE COUNCIL RESEARCH OFFICE 2015. Water resources in Hong Kong - Research brief Issue No. 5. Hong Kong Legislative council research office.
- HONG KONG WATER SUPPLIES DEPARTMENT. 2009. *Water From Dongjiang at Guangdong* [Online]. Available: [http://www.wsd.gov.hk/en/water\\_resources/raw\\_water\\_sources/water\\_sources\\_in](http://www.wsd.gov.hk/en/water_resources/raw_water_sources/water_sources_in)

- [http://www.wsd.gov.hk/en/water\\_resources/raw\\_water\\_sources/dongjiang\\_raw\\_water/index.html](http://www.wsd.gov.hk/en/water_resources/raw_water_sources/dongjiang_raw_water/index.html) [Accessed 05/01/2017] 2017]].
- HONG KONG WATER SUPPLIES DEPARTMENT. 2015. *Dongjiang Raw Water* [Online]. Available: [http://www.wsd.gov.hk/en/water\\_resources/raw\\_water\\_sources/dongjiang\\_raw\\_water/index.html](http://www.wsd.gov.hk/en/water_resources/raw_water_sources/dongjiang_raw_water/index.html) [Accessed 05/01/2017] 2017]].
- HSU, A., DE SHERBININ, A. & SHI, H. 2012. Seeking truth from facts: The challenge of environmental indicator development in China. *Environmental Development*, 3, 39-51.
- HUBBARD, E. F., KILPATRICK, F. A., MARTENS, L. A. & WILSON JR, J. F. 1982. Measurement of time of travel and dispersion in streams by dye tracing. *Techniques of Water-Resources Investigations*. 1982 ed.
- HÜFFMEYER, N., KLASMEIER, J. & MATTHIES, M. 2009. Geo-referenced modeling of zinc concentrations in the Ruhr river basin (Germany) using the model GREAT-ER. *Science of The Total Environment*, 407, 2296-2305.
- HUTCHINSON, M. F. 1988. Calculation of hydrologically sound digital elevation model. *Third International Symposium on Spatial Data Handling*. Columbus, Ohio: International Geographical Union.
- HUTCHINSON, M. F. 1989. A new procedure for gridding elevation and stream line data with automatic removal of spurious pits. *Journal of Hydrology*, 106, 211-232.
- HVISTENDAHL, M. 2013. Foreigners Run Afoul of China's Tightening Secrecy Rules. *Science*, 339, 384-385.
- JAGER, T. 2016. Predicting environmental risk: A road map for the future. *Journal of Toxicology and Environmental Health, Part A*, 79, 572-584.
- JAGER, T., ALBERT, C., PREUSS, T. G. & ASHAUER, R. 2011. General Unified Threshold Model of Survival - a Toxicokinetic-Toxicodynamic Framework for Ecotoxicology. *Environmental Science & Technology*, 45, 2529-2540.
- JAGER, T. & KOUIJMAN, S. A. L. M. 2008. A biology-based approach for quantitative structure-activity relationships (QSARs) in ecotoxicity. *Ecotoxicology*, 18, 187.
- JAKEMAN, A. J. & HORNBERGER, G. M. 1993. How much complexity is warranted in a rainfall-runoff model? *Water Resources Research*, 29, 2637-2649.
- JAMIESON, D. G. & FEDRA, K. 1996a. The 'WaterWare' decision-support system for river-basin planning. 1. Conceptual design. *Journal of Hydrology*, 177, 163-175.
- JAMIESON, D. G. & FEDRA, K. 1996b. The 'WaterWare' decision-support system for river-basin planning. 3. Example applications. *Journal of Hydrology*, 177, 199-211.
- JARVIS, A., RUBIANO, A., NELSON, A. & FARROW, M. 2004. Practical use of SRTM data in the tropics: comparisons with digital elevation models generated from cartographic data. Working Document no. 198. Cali, Colombia: International Centre for Tropical Agriculture (CIAT).
- JAWORSKA, J. S., ROSE, K. A. & BRENKERT, A. L. 1997. Individual-based modeling of PCBs effects on young-of-the-year largemouth bass in southeastern USA reservoirs. *Ecological Modelling*, 99, 113-135.
- JENSON, S. K. & DOMINGUE, J. O. 1988. Extracting topographic structure from digital elevation data for geographic information-system analysis. *Photogrammetric Engineering and Remote Sensing*, 54, 1593-1600.
- JOHNSON, A. C., BELFROID, A. & DI CORCIA, A. 2000. Estimating steroid oestrogen inputs into activated sludge treatment works and observations on their removal from the effluent. *Science of The Total Environment*, 256, 163-173.
- JOHNSON, A. C., JÜRGENS, M. D., WILLIAMS, R. J., KÜMMERER, K., KORTENKAMP, A. & SUMPTER, J. P. 2008a. Do cytotoxic chemotherapy drugs discharged into rivers pose

- a risk to the environment and human health? An overview and UK case study. *Journal of Hydrology*, 348, 167-175.
- JOHNSON, A. C., KELLER, V., WILLIAMS, R. J. & YOUNG, A. 2007a. A practical demonstration in modelling diclofenac and propranolol river water concentrations using a GIS hydrology model in a rural UK catchment. *Environmental Pollution*, 146, 155-165.
- JOHNSON, A. C., TERNES, T., WILLIAMS, R. J. & SUMPTER, J. P. 2008b. Assessing the Concentrations of Polar Organic Microcontaminants from Point Sources in the Aquatic Environment: Measure or Model? *Environmental Science & Technology*, 42, 5390-5399.
- JOHNSON, A. C., WILLIAMS, R. J., SIMPSON, P. & KANDA, R. 2007b. What difference might sewage treatment performance make to endocrine disruption in rivers? *Environ Pollut*, 147, 194-202.
- JONES, R. D., JAMPANI, H. B., NEWMAN, J. L. & LEE, A. S. 2000. Triclosan: A review of effectiveness and safety in health care settings. *American Journal of Infection Control*, 28, 184-196.
- JOWETT, I. G. & DUNCAN, M. J. 1990. Flow variability in New Zealand rivers and its relationship to in - stream habitat and biota. *New Zealand Journal of Marine and Freshwater Research*, 24, 305-317.
- JÜRGENS, M. D., HOLTHAUS, K. I. E., JOHNSON, A. C., SMITH, J. J. L., HETHERIDGE, M. & WILLIAMS, R. J. 2002. The potential for estradiol and ethinylestradiol degradation in english rivers. *Environmental Toxicology and Chemistry*, 21, 480-488.
- KANDA, R., GRIFFIN, P., JAMES, H. A. & FOTHERGILL, J. 2003. Pharmaceutical and personal care products in sewage treatment works. *Journal of environmental monitoring : JEM*, 5, 823-830.
- KANNEL, P., KANEL, S., LEE, S., LEE, Y.-S. & GAN, T. 2011. A Review of Public Domain Water Quality Models for Simulating Dissolved Oxygen in Rivers and Streams. *Environmental Modeling & Assessment*, 16, 183-204.
- KAO, E. 2013. *Project succeeds in lifting Dongjiang water quality* [Online]. Available: <http://www.scmp.com/news/hong-kong/article/1350220/project-succeeds-lifting-dongjiang-water-quality> [Accessed 17/09/2014].
- KASPRZYK-HORDERN, B., DINSDALE, R. M. & GUWY, A. J. 2009. The removal of pharmaceuticals, personal care products, endocrine disruptors and illicit drugs during wastewater treatment and its impact on the quality of receiving waters. *Water Research*, 43, 363-380.
- KELLER, V. 2006. Risk assessment of “down-the-drain” chemicals: Search for a suitable model. *Science of The Total Environment*, 360, 305-318.
- KELLER, V., FOX, K., REES, H. G. & YOUNG, A. R. 2006. Estimating population served by sewage treatment works from readily available GIS data. *Science of The Total Environment*, 360, 319-327.
- KELLER, V. D. J., WILLIAMS, R. J., LOFTHOUSE, C. & JOHNSON, A. C. 2014. Worldwide estimation of river concentrations of any chemical originating from sewage-treatment plants using dilution factors. *Environmental Toxicology and Chemistry*, 33, 447-452.
- KESHAVAMURTHY, R. N. & RAO, M. S. 1992. *The Physics of Monsoons*, Allied Publishers Limited.
- KHANAL, S. K., XIE, B., THOMPSON, M. L., SUNG, S., ONG, S.-K. & VAN LEEUWEN, J. 2006. Fate, Transport, and Biodegradation of Natural Estrogens in the Environment and Engineered Systems. *Environmental Science & Technology*, 40, 6537-6546.
- KOLPIN, D. W., FURLONG, E. T., MEYER, M. T., THURMAN, E. M., ZAUGG, S. D., BARBER, L. B. & BUXTON, H. T. 2002. Pharmaceuticals, Hormones, and Other Organic Wastewater Contaminants in U.S. Streams, 1999–2000: A National Reconnaissance. *Environmental Science & Technology*, 36, 1202-1211.

- KOMORI, K., TANAKA, H., OKAYASU, Y., YASOJIMA, M. & SATO, C. 2004. Analysis and occurrence of estrogen in wastewater in Japan. *Water Sci Technol*, 50, 93-100.
- KOOIJMAN, S. A. 2001. Quantitative aspects of metabolic organization: a discussion of concepts. *Philosophical Transactions of the Royal Society of London. Series B*, 356, 331-349.
- KOOIJMAN, S. A. L. M. 1987. A safety factor for LC50 values allowing for differences in sensitivity among species. *Water Research*, 21, 269-276.
- KÖRNER, W., BOLZ, U., SÜßMUTH, W., HILLER, G., SCHULLER, W., HANF, V. & HAGENMAIER, H. 2000. Input/output balance of estrogenic active compounds in a major municipal sewage plant in Germany. *Chemosphere*, 40, 1131-1142.
- KORTENKAMP, A. 2008. Low dose mixture effects of endocrine disrupters: Implications for risk assessment and epidemiology. *International Journal of Andrology*, 31, 233-237.
- KORTENKAMP, A., BACKHAUS, T. & FAUST, M. 2009. State of the Art Report on Mixture Toxicity. In: COMMISSION, E. (ed.).
- KROLL, C. N. & STEDINGER, J. R. 1998. Regional hydrologic analysis: Ordinary and generalized least squares revisited. *Water Resources Research*, 34, 121-128.
- KUNKEL, U. & RADKE, M. 2011. Reactive Tracer Test To Evaluate the Fate of Pharmaceuticals in Rivers. *Environmental Science & Technology*, 45, 6296-6302.
- LAMB, R., CREWITT, J. & CALVER, A. Relating hydrological model parameters and catchment properties to estimate flood frequencies from simulated river flows. Proceedings of the British Hydrological Society Seventh National Hydrology Symposium, September, Newcastle. 3.57-3.64.
- LATCH, D. E., PACKER, J. L., STENDER, B. L., VANOVERBEKE, J., ARNOLD, W. A. & MCNEILL, K. 2005. Aqueous photochemistry of triclosan: Formation of 2,4-dichlorophenol, 2,8-dichlorodibenzo-p-dioxin, and oligomerization products. *Environmental Toxicology and Chemistry*, 24, 517-525.
- LEE, H. B. & PEART, T. E. 1998. Determination of 17 beta-estradiol and its metabolites in sewage effluent by solid-phase extraction and gas chromatography/mass spectrometry. *J AOAC Int*, 81, 1209-16.
- LEHNER, B., KRIS, V. & JARVIS, A. 2006. *HydroSHEDS - Technical documentation* [Online]. Available: [https://hydrosheds.cr.usgs.gov/webappcontent/HydroSHEDS\\_TechDoc\\_v10.pdf](https://hydrosheds.cr.usgs.gov/webappcontent/HydroSHEDS_TechDoc_v10.pdf) [Accessed 04/10/2017].
- LEVY, S. B. 2001. Antibacterial household products: cause for concern. *Emerging Infectious Diseases*, 7, 512-515.
- LI, W. 2015. Progresses of China's Water Action Plan. *Putting China's Water Pollution Action Plan into Action*. Washington: The Wilson Center.
- LI, Y., SHI, L., QIAN, Y. & TANG, J. 2017. Diffusion of municipal wastewater treatment technologies in China: a collaboration network perspective. *Frontiers of Environmental Science & Engineering*, 11, 11.
- LIKA, K., AUGUSTINE, S., PECQUERIE, L. & KOOIJMAN, S. A. L. M. 2014. The bijection from data to parameter space with the standard DEB model quantifies the supply-demand spectrum. *Journal of Theoretical Biology*, 354, 35-47.
- LIMLETTE III WORKSHOP. Environmental risk assessment of detergent chemicals. Proceedings of the AISE/CESIO Limlette III Workshop 28-29 November 1995. 49-50.
- LIN, A. Y. C. & REINHARD, M. 2005. Photodegradation of common environmental pharmaceuticals and estrogens in river water. *Environmental Toxicology and Chemistry*, 24, 1303-1309.
- LINDIM, C., VAN GILS, J. & COUSINS, I. T. 2016. A large-scale model for simulating the fate & transport of organic contaminants in river basins. *Chemosphere*, 144, 803-810.
- LIPNICK, R. 1995. Structure-activity relationships. *Fundamentals of Aquatic Toxicology*. Washington, DC: Taylor & Francis.

- LISHMAN, L., SMYTH, S. A., SARAFIN, K., KLEYWEGT, S., TOITO, J., PEART, T., LEE, B., SERVOS, M., BELAND, M. & SETO, P. 2006. Occurrence and reductions of pharmaceuticals and personal care products and estrogens by municipal wastewater treatment plants in Ontario, Canada. *Science of The Total Environment*, 367, 544-558.
- LIU, X., KELLER, V., DUMONT, E. L., SHI, J. & JOHNSON, A. C. 2015. Risk of endocrine disruption to fish in the Yellow River catchment in China assessed using a spatially explicit model. *Environmental Toxicology and Chemistry*, 34, 2870-2877.
- LIU, X., SHI, J., BO, T., MENG, Y., ZHAN, X., ZHANG, M. & ZHANG, Y. 2017. Distributions and ecological risk assessment of estrogens and bisphenol A in an arid and semiarid area in northwest China. *Environmental Science and Pollution Research*, 1-10.
- LÖEWE, S. & MUISCHNEK, H. 1926. Über Kombinationswirkungen Mitteilung: Hilfsmittel der Fragestellung. *Naunyn Schmiedeberg's Archives of Pharmacology*, 114, 313-326.
- LOZANO, N., RICE, C. P., RAMIREZ, M. & TORRENTS, A. 2013. Fate of Triclocarban, Triclosan and Methyltriclosan during wastewater and biosolids treatment processes. *Water Research*, 47, 4519-4527.
- LU, G. H., SONG, W. T., WANG, C. & YAN, Z. H. 2010. Assessment of in vivo estrogenic response and the identification of environmental estrogens in the Yangtze River (Nanjing section). *Chemosphere*, 80, 982-990.
- LUTHY, R. G., SEDLAK, D. L., PLUMLEE, M. H., AUSTIN, D. & RESH, V. H. 2015. Wastewater-effluent-dominated streams as ecosystem-management tools in a drier climate. *Frontiers in Ecology and the Environment*, 13, 477-485.
- LV, M., SUN, Q., XU, H., LIN, L., CHEN, M. & YU, C.-P. 2014. Occurrence and fate of triclosan and triclocarban in a subtropical river and its estuary. *Marine Pollution Bulletin*, 88, 383-388.
- LYON, J. G. 2003. *GIS for Water Resource and Watershed Management*, CRC Press.
- MACKAY, D., GUARDO, A. D., PATERSON, S., KICSI, G. & COWAN, C. E. 1996. Assessing the fate of new and existing chemicals: A five - stage process. *Environmental Toxicology and Chemistry*, 15, 1618-1626.
- MACKAY, D., PATERSON, S. & SHIU, W. Y. 1992. Generic models for evaluating the regional fate of chemicals. *Chemosphere*, 24, 695-717.
- MACKAY, D. & YEUN, A. T. 1983. Mass transfer coefficient correlations for volatilization of organic solutes from water. *Environ Sci Technol*, 17, 211-7.
- MACLEOD, M., WOODFINE, D. G., MACKAY, D., MCKONE, T., BENNETT, D. & MADDALENA, R. 2008. BETR North America: A regionally segmented multimedia contaminant fate model for North America. *Environmental Science and Pollution Research*, 8, 156.
- MADENJIAN, C. P., CARPENTER, S. R., ECK, G. W. & MILLER, M. A. 1993. Accumulation of PCBs by Lake Trout (*Salvelinus namaycush*): An Individual-Based Model Approach. *Canadian Journal of Fisheries and Aquatic Sciences*, 50, 97-109.
- MAIDMENT, D. R. & DJOKIC, D. 2000. *Hydrologic and hydraulic modeling support: With geographic information systems*, ESRI, Inc.
- MANSELL, J. & DREWES, J. E. 2004. Fate of Steroidal Hormones During Soil - Aquifer Treatment. *Groundwater Monitoring & Remediation*, 24, 94-101.
- MARK, D. M. 1988. Network Models in Geomorphology. In: ANDERSON, M. G. (ed.) *Modelling Geomorphological Systems*. New York: John Wiley.
- MARTIN, B., JAGER, T., NISBET, R. M., PREUSS, T. G. & GRIMM, V. 2014. Limitations of extrapolating toxic effects on reproduction to the population level. *Ecological Applications*, 24, 1972-1983.
- MARTIN, J. L. & MCCUTCHEON, S. C. 1998. *Hydrodynamics and Transport for Water Quality Modeling*, Taylor & Francis.
- MATSUI, S., TAKIGAMI, H., MATSUDA, T., TANIGUCHI, N., ADACHI, J., KAWAMI, H. & SHIMIZU, Y. 2000. Estrogen and estrogen mimics contamination in water and the role of sewage treatment. *Water Science and Technology*, 42, 173-179.

- MATTHEWS, J. C. 1993. *Fundamentals of Receptor, Enzyme, and Transport Kinetics*, Taylor & Francis.
- MATTHIJS, E., DEBAERE, G., ITRICH, N., MASSCHELEYN, P., ROTTIERS, A., STALMANS, M. & FEDERLE, T. 1995. The fate of detergent surfactants in sewer systems. *Water Science and Technology*, 31, 321-328.
- MATTHIJS, E., HOLT, M. S., KIEWIET, A. & RIJS, G. B. J. 1997. Fate of surfactants in activated sludge waste water treatment plants: Outcome of field studies. *Tenside, Surfactants, Detergents*, 34, 238-241.
- MCAVOY, D. C., MASSCHELEYN, P., PENG, C., MORRALL, S. W., CASILLA, A. B., LIM, J. M. U. & GREGORIO, E. G. 2003. Risk assessment approach for untreated wastewater using the QUAL2E water quality model. *Chemosphere*, 52, 55-66.
- MCAVOY, D. C., SCHATOWITZ, B., JACOB, M., HAUK, A. & ECKHOFF, W. S. 2002. Measurement of triclosan in wastewater treatment systems. *Environmental Toxicology and Chemistry*, 21, 1323-1329.
- MEIGH, J. R., MCKENZIE, A. A. & SENE, K. J. 1999. A Grid-Based Approach to Water Scarcity Estimates for Eastern and Southern Africa. *Water Resources Management*, 13, 85-115.
- MEYLAN, W. M. & HOWARD, P. H. 1991. Bond contribution method for estimating henry's law constants. *Environmental Toxicology and Chemistry*, 10, 1283-1293.
- MIDGLEY, D. C., PITMAN, W. V., MIDDLETON, B. J., SOUTH, A. & WATER RESEARCH, C. 1995. *Surface water resources of South Africa, 1990*, [Pretoria], Water Research Commission.
- MOORE, R. J. 1985. The probability-distributed principle and runoff production at point and basin scales. *Hydrological Sciences Journal*, 30, 273-297.
- MORRALL, D., MCAVOY, D., SCHATOWITZ, B., INAUEN, J., JACOB, M., HAUK, A. & ECKHOFF, W. 2004. A field study of triclosan loss rates in river water (Cibolo Creek, TX). *Chemosphere*, 54, 653-660.
- MOSS, M. E. & TASKER, G. D. 1991. An intercomparison of hydrological network-design technologies. *Hydrological Sciences Journal*, 36, 209-221.
- MUMTAZ, M. M., SIPES, I. G., CLEWELL, H. J. & YANG, R. S. H. 1993. Risk Assessment of Chemical Mixtures: Biologic and Toxicologic Issues. *Fundamental and Applied Toxicology*, 21, 258-269.
- NAITO, W., MIYAMOTO, K.-I., NAKANISHI, J., MASUNAGA, S. & BARTELL, S. M. 2002. Application of an ecosystem model for aquatic ecological risk assessment of chemicals for a Japanese lake. *Water Research*, 36, 1-14.
- NAKADA, N., TANISHIMA, T., SHINOHARA, H., KIRI, K. & TAKADA, H. 2006. Pharmaceutical chemicals and endocrine disrupters in municipal wastewater in Tokyo and their removal during activated sludge treatment. *Water Research*, 40, 3297-3303.
- NASA. 2003. *SRTM Data Editing Rules* [Online]. Available: [https://dds.cr.usgs.gov/srtm/version2\\_1/Documentation/SRTM\\_edit\\_rules.pdf](https://dds.cr.usgs.gov/srtm/version2_1/Documentation/SRTM_edit_rules.pdf) [Accessed 03/10/2017].
- NATIONAL DEVELOPMENT AND REFORM COMMISSION 2016. "Thirteen five" national town Sewage Treatment and Recycling Facilities Construction Planning.
- NATIONAL DEVELOPMENT AND REFORM COMMISSION, MINISTRY OF ENVIRONMENTAL PROTECTION & MINISTRY OF HEALTH OF CHINA 2007. 11th Five-Year Plan on National Rural Drinking Water Safety Project (In Chinese). Beijing: National Development and Reform Commission.
- NEITSCH, J. G., ARNOLD, J. G., KINIRY, J. R. & WILLIAMS, J. R. 2011. *Soil and Water Assessment Tool Theoretical Documentation Version 2009*.
- NIELD, R. 2015. *China's Foreign Places: The Foreign Presence in China in the Treaty Port Era, 1840-1943*, Hong Kong University Press.

- NISBET, R. M., MULLER, E. B., LIKA, K. & KOUIJMAN, S. A. L. M. 2000. From molecules to ecosystems through dynamic energy budget models. *Journal of Animal Ecology*, 69, 913-926.
- NIZZETTO, L., BUTTERFIELD, D., FUTTER, M., LIN, Y., ALLAN, I. & LARSEN, T. 2016. Assessment of contaminant fate in catchments using a novel integrated hydrobiogeochemical-multimedia fate model. *Science of The Total Environment*, 544, 553-563.
- O'CALLAGHAN, J. F. & MARK, D. M. 1984. The extraction of drainage networks from digital elevation data. *Computer Vision, Graphics, and Image Processing*, 28, 323-344.
- OIZUMI, K. 2011. The Emergence of the Pearl River Delta Economic Zone—Challenges on the Path to Megaregion Status and Sustainable Growth—. *Pacific Business and Industries*, 11.
- OPENSTREETMAP. n.d. *WikiProject China* [Online]. OpenStreetMap Wiki. Available: [http://wiki.openstreetmap.org/w/index.php?title=WikiProject\\_China&oldid=1437000](http://wiki.openstreetmap.org/w/index.php?title=WikiProject_China&oldid=1437000) [Accessed 04/04/2017].
- ORESQUES, N., SHRADER-FRECHETTE, K. & BELITZ, K. 1994. Verification, Validation, and Confirmation of Numerical Models in the Earth Sciences. *Science*, 263, 641.
- ORVOS, D. R., VERSTEEG, D. J., INAUEN, J., CAPDEVIELLE, M., ROTHENSTEIN, A. & CUNNINGHAM, V. 2002. Aquatic toxicity of triclosan. *Environmental Toxicology and Chemistry*, 21, 1338-1349.
- PARK, R. A., CLOUGH, J. S. & WELLMAN, M. C. 2008. AQUATOX: Modeling environmental fate and ecological effects in aquatic ecosystems. *Ecological Modelling*, 213, 1-15.
- PENG, X., YU, Y., TANG, C., TAN, J., HUANG, Q. & WANG, Z. 2008. Occurrence of steroid estrogens, endocrine-disrupting phenols, and acid pharmaceutical residues in urban riverine water of the Pearl River Delta, South China. *Science of The Total Environment*, 397, 158-166.
- PING, Z. & LONGXUN, C. 2001. Interannual variability of atmospheric heat source/sink over the Qinghai—Xizang (Tibetan) Plateau and its relation to circulation. *Advances in Atmospheric Sciences*, 18, 106-116.
- POINTURIER, R. & VOLZ, E. 1990. Report on water solubility. Basel, Switzerland: Ciba Specialty Chemical.
- POSTHUMA, L., SUTER, G. W. & TRAAS, T. P. 2001. *Species Sensitivity Distributions in Ecotoxicology*, CRC Press.
- PREUSS, T. G., HAMMERS-WIRTZ, M., HOMMEN, U., RUBACH, M. N. & RATTE, H. T. 2009. Development and validation of an individual based *Daphnia magna* population model: The influence of crowding on population dynamics. *Ecological Modelling*, 220, 310-329.
- PRICE, K. 2011. Effects of watershed topography, soils, land use, and climate on baseflow hydrology in humid regions: A review. *Progress in Physical Geography*, 35, 465-492.
- PRICE, O. R., MUNDAY, D. K., WHELAN, M. J., HOLT, M. S., FOX, K. K., MORRIS, G. & YOUNG, A. R. 2009. Data requirements of GREAT-ER: Modelling and validation using LAS in four UK catchments. *Environmental Pollution*, 157, 2610-2616.
- PRICE, O. R., WILLIAMS, R. J., VAN EGMOND, R., WILKINSON, M. J. & WHELAN, M. J. 2010. Predicting accurate and ecologically relevant regional scale concentrations of triclosan in rivers for use in higher-tier aquatic risk assessments. *Environment international*, 36, 521-526.
- PROWSE, T. D. 2001. River-ice ecology. I: hydrologic, geomorphic, and water-quality aspects. *Journal of Cold Regions Engineering*, 15, 1.
- QI, W., SINGER, H., BERG, M., MÜLLER, B., PERNET-COUDRIER, B., LIU, H. & QU, J. 2015. Elimination of polar micropollutants and anthropogenic markers by wastewater treatment in Beijing, China. *Chemosphere*, 119, 1054-1061.



- QIN, D., DING, Y. & MU, M. 2015. *Climate and Environmental Change in China: 1951–2012*, Springer Berlin Heidelberg.
- QU, Y. & DUFFY, C. J. 2007. A semidiscrete finite volume formulation for multiprocess watershed simulation. *Water Resources Research*, 43, n/a-n/a.
- REES, G. 2009. Hydrological data. *Manual on Low-flow estimation and prediction*. Geneva: World meteorological organization.
- REES, H. G., HOLMES, M. G. R., YOUNG, A. R. & KANSAKAR, S. R. 2004. Recession-based hydrological models for estimating low flows in ungauged catchments in the Himalayas. *Hydrology and Earth System Sciences Discussions*, 8, 891-902.
- REISS, R., MACKAY, N., HABIG, C. & GRIFFIN, J. 2002. An ecological risk assessment for triclosan in lotic systems following discharge from wastewater treatment plants in the United States. *Environmental Toxicology and Chemistry*, 21, 2483-2492.
- RESEARCH AND MARKETS. 2013. *Production and Market of Sucralose in China*. [Online]. Available: [http://www.researchandmarkets.com/research/08250a/production\\_and\\_market\\_of\\_sucralose\\_in\\_china](http://www.researchandmarkets.com/research/08250a/production_and_market_of_sucralose_in_china) [Accessed 23/03/2017].
- ROBERTS, J., PRICE, O. R., BETTLES, N., RENDAL, C. & VAN EGMOND, R. 2014. Accounting for dissociation and photolysis: A review of the algal toxicity of triclosan. *Environmental Toxicology and Chemistry*, 33, 2551-2559.
- ROBINSON, P. F., LIU, Q.-T., RIDDLE, A. M. & MURRAY-SMITH, R. 2007. Modeling the impact of direct phototransformation on predicted environmental concentrations (PECs) of propranolol hydrochloride in UK and US rivers. *Chemosphere*, 66, 757-766.
- RODDA, J. C. 1998. Hydrological networks need improving! *International Conference on World Water Resources at the Beginning of the 21st Century --IHP-V Technical Documents in Hydrology 18*. Paris.
- ROHLI, R. & VEGA, A. J. 2011. *Climatology*, Jones & Bartlett Learning.
- ROUND, C. E., YOUNG, A. R. & FOX, K. 1998. A Regionally Applicable Model for Estimating Flow Velocity at Ungauged River Sites in the UK. *Water and Environment Journal*, 12, 402-405.
- RUBACH, M. N., ASHAUER, R., BUCHWALTER, D. B., DE LANGE, H. J., HAMER, M., PREUSS, T. G., TÖPKE, K. & MAUND, S. J. 2011. Framework for traits-based assessment in ecotoxicology. *Integrated Environmental Assessment and Management*, 7, 172-186.
- RUBACH, M. N., BAIRD, D. J., BOERWINKEL, M.-C., MAUND, S. J., ROESSINK, I. & VAN DEN BRINK, P. J. 2012. Species traits as predictors for intrinsic sensitivity of aquatic invertebrates to the insecticide chlorpyrifos. *Ecotoxicology*, 21, 2088-2101.
- RUHRVERBAND 2005. Annual report on Ruhr River Quality [In German]. Essen: Ruhrverband.
- RUNKEL, R. L. 2015. On the use of rhodamine WT for the characterization of stream hydrodynamics and transient storage. *Water Resources Research*, 51, 6125-6142.
- RYU, J., OH, J., SNYDER, S. A. & YOON, Y. 2014. Determination of micropollutants in combined sewer overflows and their removal in a wastewater treatment plant (Seoul, South Korea). *Environmental Monitoring and Assessment*, 186, 3239-3251.
- SABALIUNAS, D., WEBB, S. F., HAUKE, A., JACOB, M. & ECKHOFF, W. S. 2003. Environmental fate of Triclosan in the River Aire Basin, UK. *Water research*, 37, 3145-3154.
- SABLJIC, A. 2009. *ENVIRONMENTAL AND ECOLOGICAL CHEMISTRY - Volume III*, EOLSS Publishers Company Limited.
- SANG, Z., JIANG, Y., TSOI, Y.-K. & LEUNG, K. S.-Y. 2014. Evaluating the environmental impact of artificial sweeteners: A study of their distributions, photodegradation and toxicities. *Water Research*, 52, 260-274.
- SAUVÉ, S. & DESROSIERS, M. 2014. A review of what is an emerging contaminant. *Chemistry Central Journal*, 8, 15.



- SAXTON, K. E., RAWLS, W. J., ROMBERGER, J. S. & PAPENDICK, R. I. 1986. Estimating Generalized Soil-water Characteristics from Texture. *Soil Science Society of America Journal*, 50, 1031-1036.
- SCHATOWITZ, B. 1999. Triclosan in WWTP samples of Slough and Chertsey, UK. Basel, Switzerland: Ciba Specialty Chemicals.
- SCHOLEFIELD, P., NEAL, C., KELLY, J., NUTTER, S., TAKEUCHI, Y., MABERLY, S., ZHANG, H., HAMILTON TAYLOR, J. & FOLKARD, A. An instrumented river buoy for measuring temporospatial water quality data on whole river reaches. European Geophysical Union General Assembly, 01/2008, Vienna.
- SCHOWANEK, D. & WEBB, S. 2002. Exposure simulation for pharmaceuticals in European surface waters with GREAT-ER. *Toxicology Letters*, 131, 39-50.
- SCHREIBER, P. & DEMUTH, S. 1997. Regionalization of low flows in southwest Germany. *Hydrological Sciences Journal*, 42, 845-858.
- SCHRÖDER, F., SCHULZE, C. & MATTHIES, M. 2002. Concentration of LAS and boron in the Itter. *Environmental Science and Pollution Research*, 9, 130-135.
- SCHULZE, C. & MATTHIES, M. 2001. Georeferenced aquatic fate simulation of cleaning agent and detergent ingredients in the river Rur catchment (Germany). *Science of The Total Environment*, 280, 55-77.
- SCHULZE, C., MATTHIES, M., TRAPP, S. & SCHRÖDER, F. R. 1999. Georeferenced fate modelling of las in the Itter stream. *Chemosphere*, 39, 1833-1852.
- SHAPIRO, S. S. & WILK, M. B. 1965. An analysis of variance test for normality (complete samples). *Biometrika*, 52, 591-611.
- SHAREEF, A., ANGOVE, M. J., WELLS, J. D. & JOHNSON, B. B. 2006. Aqueous Solubilities of Estrone, 17 $\beta$ -Estradiol, 17 $\alpha$ -Ethinylestradiol, and Bisphenol A. *Journal of Chemical & Engineering Data*, 51, 879-881.
- SHEN, C., RIAZ, Z., PALLE, M. S., JIN, Q. & PEÑA-MORA, F. 2015. Open Data Landscape: A Global Perspective and a Focus on China. In: JANSSEN, M., MÄNTYMÄKI, M., HIDDERS, J., KLIEVINK, B., LAMERSDORF, W., VAN LOENEN, B. & ZUIDERWIJK, A. (eds.) *Open and Big Data Management and Innovation : 14th IFIP WG 6.11 Conference on e-Business, e-Services, and e-Society, I3E 2015, Delft, The Netherlands, October 13-15, 2015, Proceedings*. Cham: Springer International Publishing.
- SILVA, E., RAJAPAKSE, N. & KORTENKAMP, A. 2002. Something from "Nothing" – Eight Weak Estrogenic Chemicals Combined at Concentrations below NOECs Produce Significant Mixture Effects. *Environmental Science & Technology*, 36, 1751-1756.
- SINGER, H., MÜLLER, S., TIXIER, C. & PILLONEL, L. 2002. Triclosan: Occurrence and Fate of a Widely Used Biocide in the Aquatic Environment: Field Measurements in Wastewater Treatment Plants, Surface Waters, and Lake Sediments. *Environmental Science & Technology*, 36, 4998-5004.
- SMAKHTIN, V. U. 2001. Low flow hydrology: a review. *Journal of Hydrology*, 240, 147-186.
- SMAKHTIN, V. Y., SAMI, K. & HUGHES, D. A. 1998. Evaluating the performance of a deterministic daily rainfall – runoff model in a low - flow context. *Hydrological Processes*, 12, 797-812.
- SMITH, R. E., GOODRICH, D. C., WOOLHISER, D. A. & UNKRICH, C. L. 1995. KINEROS - a KINematic runoff and EROsion model. In: SINGH, V. P. (ed.) *Computer models of watershed hydrology*. Highlands Ranch, Colorado, US: Water resource publications.
- SMITH, R. W. 1981. *Rock type and minimum 7-day/10-year flow in Virginia streams*. Blacksburg, Virginia Water Resource Research Center, Virginia Polytechnic Institute and State University.
- SNYDER, S. A., KEITH, T. L., VERBRUGGE, D. A., SNYDER, E. M., GROSS, T. S., KANNAN, K. & GIESY, J. P. 1999. Analytical Methods for Detection of Selected Estrogenic Compounds in Aqueous Mixtures. *Environmental Science & Technology*, 33, 2814-2820.

- SOUTHWORTH, G. R. 1979. The role of volatilization in removing polycyclic aromatic hydrocarbons from aquatic environments. *Bulletin of Environmental Contamination and Toxicology*, 21, 507-514.
- STARK, J. D., BANKS, J. E. & VARGAS, R. 2004. How risky is risk assessment: The role that life history strategies play in susceptibility of species to stress. *Proceedings of the National Academy of Sciences of the United States of America*, 101, 732.
- STATE COUNCIL. 2015. *China announces action plan to tackle water pollution* [Online]. Available: [http://english.gov.cn/policies/latest\\_releases/2015/04/16/content\\_281475090170164.htm](http://english.gov.cn/policies/latest_releases/2015/04/16/content_281475090170164.htm) [Accessed 09/05/2017].
- STEDINGER, J. R. & TASKER, G. D. 1986. Regional Hydrologic Analysis, 2, Model-Error Estimators, Estimation of Sigma and Log-Pearson Type 3 Distributions. *Water Resources Research*, 22, 1487-1499.
- STUETZ, R. M. & STEPHENSON, T. 2009. *Principles of Water and Wastewater Treatment Processes*, IWA Publishing.
- SU, D. H., ZHENG, Z., WANG, Y., LUO, X. Z. & WU, W. X. 2005. Discussion on treatment technology of rural domestic wastewater. *Environmental Science and Technology*, 28, 79-81.
- SU, L. & DAO, B. 2012. Liquid Assets II - Industrial relocation in Guangdong province: avoid repeating mistakes. Civic Exchange.
- SU, L., YONG, Y., HONGYI, L. & TIANCHENG, D. 2011. Dongjiang Overloaded-2011 Dongjiang Expedition Report.
- SUI, Q., HUANG, J., DENG, S., YU, G. & FAN, Q. 2010. Occurrence and removal of pharmaceuticals, caffeine and DEET in wastewater treatment plants of Beijing, China. *Water Research*, 44, 417-426.
- SUI, Y., JIANG, D. & TIAN, Z. 2013. Latest update of the climatology and changes in the seasonal distribution of precipitation over China. *Theoretical and Applied Climatology*, 113, 599-610.
- SUMPTER, J. P. & JOBLING, S. 1995. Vitellogenesis as a biomarker for estrogenic contamination of the aquatic environment. *Environmental Health Perspectives*, 103, 173-178.
- SUMPTER, J. P., JOHNSON, A. C., WILLIAMS, R. J., KORTENKAMP, A. & SCHOLZE, M. 2006. Modeling Effects of Mixtures of Endocrine Disrupting Chemicals at the River Catchment Scale. *Environmental Science & Technology*, 40, 5478-5489.
- TALLAKSEN, L. M. & VAN LANEN, H. A. J. 2004. *Hydrological Drought: Processes and Estimation Methods for Streamflow and Groundwater*, Elsevier.
- TAMURA, I., KAGOTA, K.-I., YASUDA, Y., YONEDA, S., MORITA, J., NAKADA, N., KAMEDA, Y., KIMURA, K., TATARAZAKO, N. & YAMAMOTO, H. 2013. Ecotoxicity and screening level ecotoxicological risk assessment of five antimicrobial agents: triclosan, triclocarban, resorcinol, phenoxyethanol and p-thymol. *Journal of Applied Toxicology*, 33, 1222-1229.
- TCC CONSORTIUM 2002. High production volume (HPV) chemical challenge program - Data availability and screening level assessment for Triclocarban.
- TELIS, P. A. 1991. *Low-flow and flow-duration characteristics of Mississippi streams*, Mississippi, USGS.
- TERNES, T. A., STUMPF, M., MUELLER, J., HABERER, K., WILKEN, R. D. & SERVOS, M. 1999. Behavior and occurrence of estrogens in municipal sewage treatment plants — I. Investigations in Germany, Canada and Brazil. *Science of The Total Environment*, 225, 81-90.
- THE STATE COUNCIL. 2012. *Planning for wastewater treatment during 12th-five plan. (In Chinese)* [Online]. Available: [http://www.gov.cn/zwggk/2012-05/04/content\\_2129670.htm](http://www.gov.cn/zwggk/2012-05/04/content_2129670.htm) [Accessed 07/04/2017].

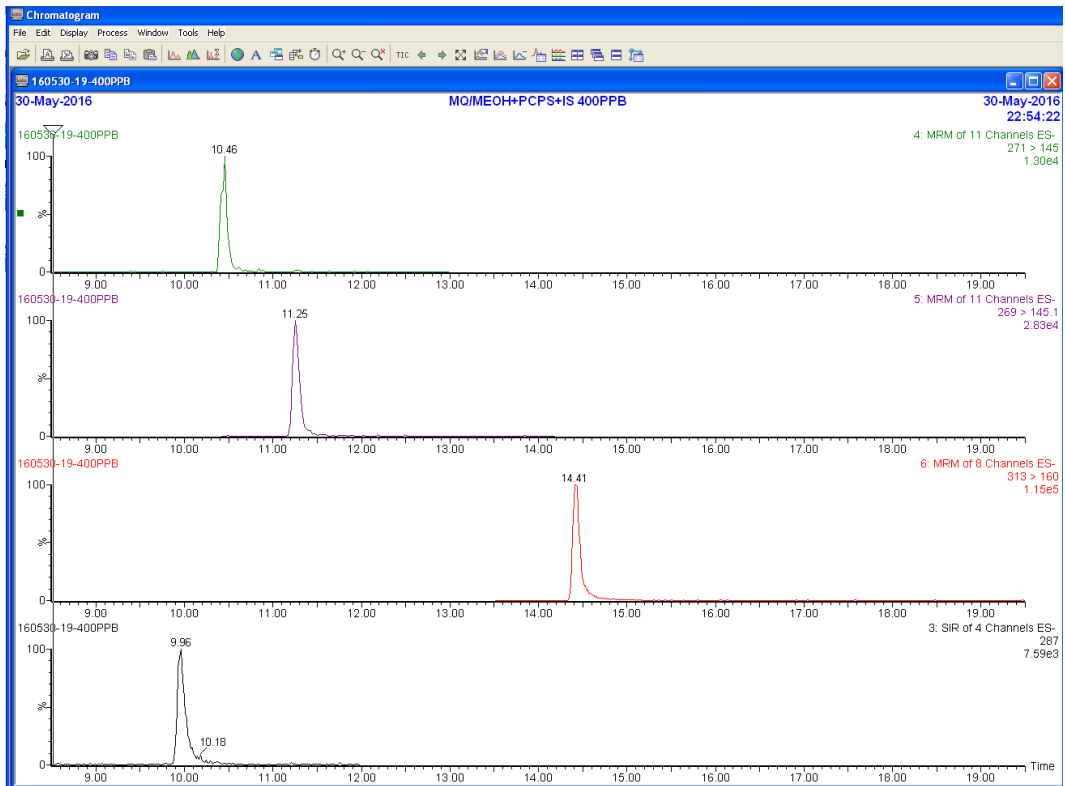
- THOMPSON, A., GRIFFIN, P., STUETZ, R. & CARTMELL, E. 2005. The Fate and Removal of Triclosan during Wastewater Treatment. *Water Environment Research*, 77, 63-67.
- TIXIER, C., SINGER, H. P., CANONICA, S. & MÜLLER, S. R. 2002. Phototransformation of Triclosan in Surface Waters: A Relevant Elimination Process for This Widely Used Biocide Laboratory Studies, Field Measurements, and Modeling. *Environmental Science & Technology*, 36, 3482-3489.
- TIXIER, C., SINGER, H. P., OELLERS, S. & MÜLLER, S. R. 2003. Occurrence and Fate of Carbamazepine, Clofibric Acid, Diclofenac, Ibuprofen, Ketoprofen, and Naproxen in Surface Waters. *Environmental Science & Technology*, 37, 1061-1068.
- TRAAS, T. P., JANSE, J. H., ALDENBERG, T. & BROCK, T. C. M. 1998. A food web model for fate and direct and indirect effects of Dursban® 4E (active ingredient chlorpyrifos) in freshwater microcosms. *Aquatic Ecology*, 32, 179-190.
- TRAN, N. H., HU, J., LI, J. & ONG, S. L. 2014. Suitability of artificial sweeteners as indicators of raw wastewater contamination in surface water and groundwater. *Water Research*, 48, 443-456.
- TRICHOPOULOS, D., YEN, S., BROWN, J., COLE, P. & MACMAHON, B. 1984. The effect of westernization on urine estrogens, frequency of ovulation, and breast cancer risk. A study of ethnic chinese women in the orient and the USA. *Cancer*, 53, 187-192.
- TUKEY, J. 1977. *Exploratory Data Analysis*, Pearson.
- TURNER, E., NETHERLAND, M. & GETSINGER, K. 1991. Submersed plants and algae as factors in the loss of Rhodamine WT dye. *Journal of Aquatic Plant Management*, 29, 113-115.
- TYLER, C. R. & JOBLING, S. 2008. Roach, Sex, and Gender-Bending Chemicals: The Feminization of Wild Fish in English Rivers. *BioScience*, 58, 1051-1059.
- US EPA 1995. SMPTOX version 4.0 (SMPTOX4) - User's Manual. Athens, Georgia: US EPA.
- US EPA 2002. Method 1002.0: Daphnid, *Ceriodaphnia dubia*, Survival and Reproduction Test; Chronic Toxicity. United States Environmental Protection Agency.
- US EPA 2011. Estimation Program Interface (EPI) Suite. Ver. 4.1.
- VAN DEN BRINK, P. J. 2008. Ecological Risk Assessment: From Book-Keeping to Chemical Stress Ecology. *Environmental Science & Technology*, 42, 8999-9004.
- VAN DEN BRINK, P. J., BAVECO, J. M., VERBOOM, J. & HEIMBACH, F. 2007. An individual-based approach to model spatial population dynamics of invertebrates in aquatic ecosystems after pesticide contamination. *Environmental Toxicology and Chemistry*, 26, 2226-2236.
- VAN LEEUWEN, S. P. J., KÄRRMAN, A., VAN BAVEL, B., DE BOER, J. & LINDSTRÖM, G. 2006. Struggle for quality in determination of perfluorinated contaminants in environmental and human samples. *Environmental Science and Technology*, 40, 7854-7860.
- VAN STEMPOORT, D. R., ROY, J. W., GRABUSKI, J., BROWN, S. J., BICKERTON, G. & SVERKO, E. 2013. An artificial sweetener and pharmaceutical compounds as co-tracers of urban wastewater in groundwater. *Science of The Total Environment*, 461-462, 348-359.
- VELDHOEN, N., SKIRROW, R. C., OSACHOFF, H., WIGMORE, H., CLAPSON, D. J., GUNDERSON, M. P., VAN AGGELEN, G. & HELBING, C. C. 2006. The bactericidal agent triclosan modulates thyroid hormone-associated gene expression and disrupts postembryonic anuran development. *Aquatic Toxicology*, 80, 217-227.
- VIENO, N. M., TUHKANEN, T. & KRONBERG, L. 2005. Seasonal Variation in the Occurrence of Pharmaceuticals in Effluents from a Sewage Treatment Plant and in the Recipient Water. *Environmental Science & Technology*, 39, 8220-8226.
- VOGEL, R. & FENNESSEY, N. 1994. Flow Duration Curves. I: New Interpretation and Confidence Intervals. *Journal of Water Resources Planning and Management*, 120, 485-504.

- VON BERTALANFFY, L. 1968. *General Systems Theory*, New York, Braziller.
- VON DER OHE, P. C., SCHMITT-JANSEN, M., SLOBODNIK, J. & BRACK, W. 2012. Triclosan--the forgotten priority substance? *Environ Sci Pollut Res Int*, 19, 585-91.
- WAAGE, J. K., HASSELL, M. P. & GODFRAY, H. C. J. 1985. The Dynamics of Pest-Parasitoid-Insecticide Interactions. *Journal of Applied Ecology*, 22, 825-838.
- WAGNER, J.-O. & KOORMANN, F. 2011. *GREAT-ER Desktop Manual*, Osnabrück, Germany, Intevation GmbH
- WAINWRIGHT, J. & MULLIGAN, M. 2013. *Environmental Modelling: Finding Simplicity in Complexity*, Chichester, Wiley.
- WALTMAN, E. L., VENABLES, B. J. & WALLER, W. T. 2006. Triclosan in a North Texas wastewater treatment plant and the influent and effluent of an experimental constructed wetland. *Environmental toxicology and chemistry*, 25, 367-372.
- WANG, B. 2006. *The Asian Monsoon*, Springer.
- WANG, H., YAN, Z. G., LI, H., YANG, N. Y., LEUNG, K. M., WANG, Y. Z., YU, R. Z., ZHANG, L., WANG, W. H., JIAO, C. Y. & LIU, Z. T. 2012. Progress of environmental management and risk assessment of industrial chemicals in China. *Environ Pollut*, 165, 174-81.
- WANG, Z., DUAN, A. & WU, G. 2014. Time-lagged impact of spring sensible heat over the Tibetan Plateau on the summer rainfall anomaly in East China: case studies using the WRF model. *Climate Dynamics*, 42, 2885-2898.
- WARN, A. E. 1986. Planning investment for river quality using a catchment simulation model. *Water Quality Modelling in the Inland Natural Environment*. Cranfield, United Kingdom: BHRA, The Fluid Engineering Centre.
- WARN, A. E. & BREW, J. S. 1980. Mass balance. *Water Research*, 14, 1427-1434.
- WARN, T. 2010. *SIMCAT 11.5 A Guide and Reference for Users* [Online]. Available: [http://webarchive.nationalarchives.gov.uk/20121030220244/http://www.environment-agency.gov.uk/static/documents/Business/111\\_07\\_SD06.pdf](http://webarchive.nationalarchives.gov.uk/20121030220244/http://www.environment-agency.gov.uk/static/documents/Business/111_07_SD06.pdf) [Accessed 15/09/2017].
- WEBSTER, E., MACKAY, D., DI GUARDO, A., KANE, D. & WOODFINE, D. 2004. Regional differences in chemical fate model outcome. *Chemosphere*, 55, 1361-1376.
- WHELAN, M. J., GANDOLFI, C. & BISCHETTI, G. B. 1999. A simple stochastic model of point source solute transport in rivers based on gauging station data with implications for sampling requirements. *Water research*, 33, 3171-3181.
- WHELAN, M. J., HODGES, J. E. N., WILLIAMS, R. J., KELLER, V. D. J., PRICE, O. R. & LI, M. 2012. Estimating surface water concentrations of "down-the-drain" chemicals in China using a global model. *Environmental Pollution*, 165, 233-240.
- WHELAN, M. J., VAN EGMOND, R., GUYMER, I., LACOURSIERE, J. O., VOUGHT, L. M., FINNEGAN, C., FOX, K. K., SPARHAM, C., O'CONNOR, S., VAUGHAN, M. & PEARSON, J. M. 2007. The behaviour of linear alkyl benzene sulphonate under direct discharge conditions in Vientiane, Lao PDR. *Water Res*, 41, 4730-40.
- WHITMAN, W. 1923. A preliminary experimental confirmation of the two-film theory of gas absorption. *Chemical and Metallurgical Engineering*, 29, 146-148.
- WILLIAMS, R. J., CHURCHLEY, J. H., KANDA, R. & JOHNSON, A. C. 2012. Comparing predicted against measured steroid estrogen concentrations and the associated risk in two United Kingdom river catchments. *Environmental Toxicology and Chemistry*, 31, 892-898.
- WILLIAMS, R. J., JOHNSON, A. C., SMITH, J. J. L. & KANDA, R. 2003. Steroid Estrogens Profiles along River Stretches Arising from Sewage Treatment Works Discharges. *Environmental Science & Technology*, 37, 1744-1750.
- WILLIAMS, R. J., KELLER, V. D. J., JOHNSON, A. C., YOUNG, A. R., HOLMES, M. G. R., WELLS, C., GROSS-SOROKIN, M. & BENSTEAD, R. 2009. A national risk assessment for intersex in fish arising from steroid estrogens. *Environmental Toxicology and Chemistry*, 28, 220-230.

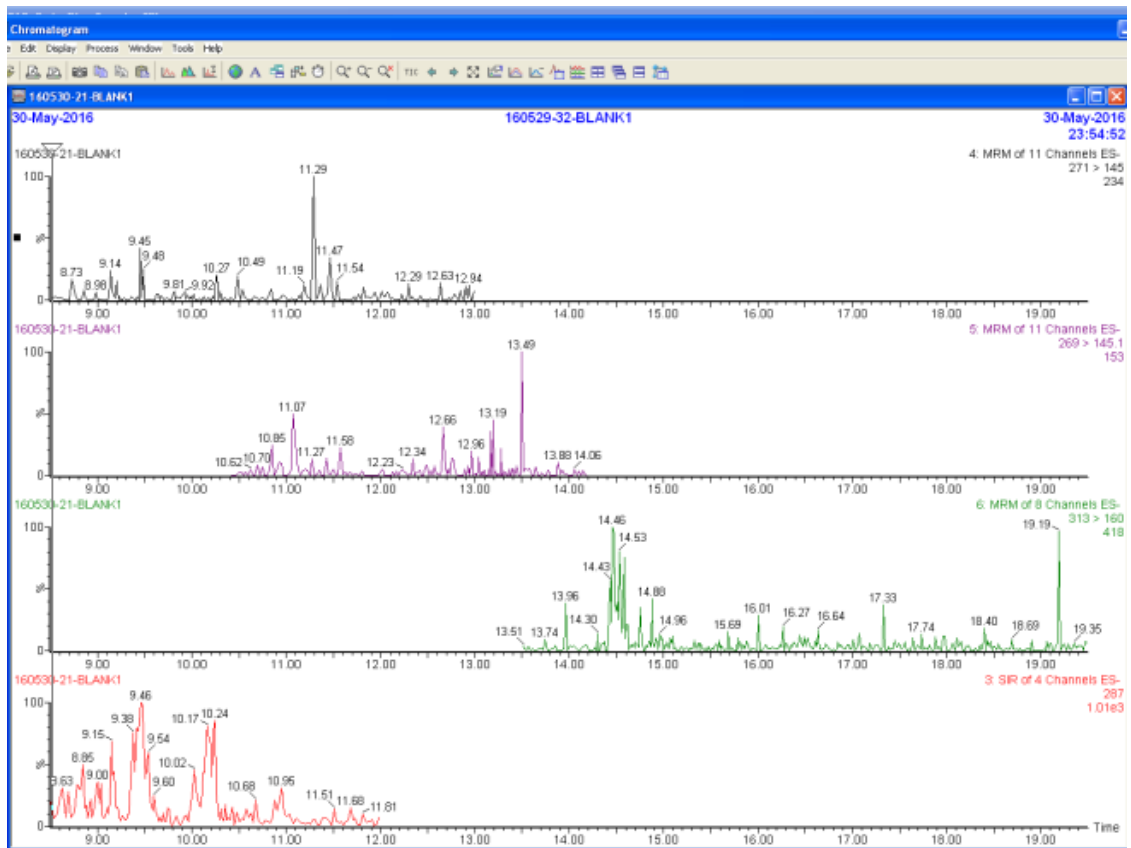
- WIND, T., WERNER, U., JACOB, M. & HAUKE, A. 2004. Environmental concentrations of boron, LAS, EDTA, NTA and Triclosan simulated with GREAT-ER in the river Itter. *Chemosphere*, 54, 1145-1154.
- WINKLER, G., THOMPSON, A., FISCHER, R., KREBS, P., GRIFFIN, P. & CARTMELL, E. 2007. Mass Flow Balances of Triclosan in Small Rural Wastewater Treatment Plants and the Impact of Biomass Parameters on the Removal. *Engineering in Life Sciences*, 7, 42-51.
- WOODFINE, D., MACLEOD, M. & MACKAY, D. 2002. A regionally segmented national scale multimedia contaminant fate model for Canada with GIS data input and display. *Environmental Pollution*, 119, 341-355.
- WORLD BANK. 2017. *World Bank Open Data* [Online]. Available: <https://data.worldbank.org/> [Accessed 27/10/2017].
- WRITER, J. H., RYAN, J. N., KEEFE, S. H. & BARBER, L. B. 2012. Fate of 4-nonylphenol and 17beta-estradiol in the Redwood River of Minnesota. *Environmental Science & Technology*, 46, 860-8.
- WU, C., SPONGBERG, A. L. & WITTER, J. D. 2009. Adsorption and Degradation of Triclosan and Triclocarban in Soils and Biosolids-Amended Soils. *Journal of Agricultural and Food Chemistry*, 57, 4900-4905.
- WU, G. & ZHANG, Y. 1998. Tibetan Plateau Forcing and the Timing of the Monsoon Onset over South Asia and the South China Sea. *Monthly Weather Review*, 126, 913-927.
- XIE, Y. & ZHOU, X. 2014. Income inequality in today's China. *Proceedings of the National Academy of Sciences*, 111, 6928-6933.
- XU, N., XU, Y.-F., XU, S., LI, J. & TAO, H.-C. 2012. Removal of estrogens in municipal wastewater treatment plants: A Chinese perspective. *Environmental Pollution*, 165, 215-224.
- YAN, Z., LU, G., LIU, J. & JIN, S. 2012. An integrated assessment of estrogenic contamination and feminization risk in fish in Taihu Lake, China. *Ecotoxicology and Environmental Safety*, 84, 334-340.
- YAO, Y. 2013. The Water Situation of the Future Mega City "Urumqi" (NW-China) – Resources, Risk, Conservation and Management. Heidelberg: Heidelberg University.
- YAZDANKHAH, S. P., SCHEIE, A. A., HØIBY, E. A., LUNESTAD, B.-T., HEIR, E., FOTLAND, T. Ø., NATERSTAD, K. & KRUSE, H. 2006. Triclosan and Antimicrobial Resistance in Bacteria: An Overview. *Microbial Drug Resistance*, 12, 83-90.
- YE, X., GUO, X., CUI, X., ZHANG, X., ZHANG, H., WANG, M. K., QIU, L. & CHEN, S. 2012. Occurrence and removal of endocrine-disrupting chemicals in wastewater treatment plants in the Three Gorges Reservoir area, Chongqing, China. *Journal of Environmental Monitoring*, 14, 2204-2211.
- YING, G.-G. & KOOKANA, R. S. 2007. Triclosan in wastewaters and biosolids from Australian wastewater treatment plants. *Environment International*, 33, 199-205.
- YOUNG, A., HUGHES, D. A. & DEMUTH, S. 2009. Estimating flows at ungauged sites. In: GUSTARD, A. & DEMUTH, S. (eds.) *Manual on Low-flow estimation and prediction*. Geneva: World meteorological organization.
- YOUNG, A. R. 2006. Stream flow simulation within UK ungauged catchments using a daily rainfall-runoff model. *Journal of Hydrology*, 320, 155-172.
- YOUNG, A. R., CROKER, K. M. & SEKULIN, A. E. 2000a. Novel techniques for characterizing complex water use patterns within a network based statistical hydrological model. *Science of The Total Environment*, 251–252, 277-291.
- YOUNG, A. R., GUSTARD, A., BULLOCK, A., SEKULIN, A. E. & CROKER, K. M. 2000b. A river network based hydrological model for predicting natural and influenced flow statistics at ungauged sites: Micro LOW FLOWS. *Science of The Total Environment*, 251–252, 293-304.

- YU, J. T., BOUWER, E. J. & COELHAN, M. 2006. Occurrence and biodegradability studies of selected pharmaceuticals and personal care products in sewage effluent. *Agricultural Water Management*, 86, 72-80.
- YU, X., GENG, Y., HECK, P. & XUE, B. 2015. A Review of China's Rural Water Management. *Sustainability*, 7, 5773.
- YU, Y., HUANG, Q., WANG, Z., ZHANG, K., TANG, C., CUI, J., FENG, J. & PENG, X. 2011. Occurrence and behavior of pharmaceuticals, steroid hormones, and endocrine-disrupting personal care products in wastewater and the recipient river water of the Pearl River Delta, South China. *Journal of Environmental Monitoring*, 13, 871-878.
- YU, Z., XIAO, B., HUANG, W. & PENG, P. A. 2004. Sorption of steroid estrogens to soils and sediments. *Environmental Toxicology and Chemistry*, 23, 531-539.
- ZEPP, R. G. & CLINE, D. M. 1977. Rates of direct photolysis in aquatic environment. *Environmental Science and Technology*, 11, 359-366.
- ZHANG, H. & DAVISON, W. 1995. Performance Characteristics of Diffusion Gradients in Thin Films for the in Situ Measurement of Trace Metals in Aqueous Solution. *Analytical Chemistry*, 67, 3391-3400.
- ZHANG, L., CAO, Y., HAO, X., ZHANG, Y. & LIU, J. 2015a. Application of the GREAT-ER model for environmental risk assessment of nonylphenol and nonylphenol ethoxylates in China. *Environmental Science and Pollution Research*, 22, 18531-18540.
- ZHANG, N.-S., LIU, Y.-S., VAN DEN BRINK, P. J., PRICE, O. R. & YING, G.-G. 2015b. Ecological risks of home and personal care products in the riverine environment of a rural region in South China without domestic wastewater treatment facilities. *Ecotoxicology and Environmental Safety*, 122, 417-425.
- ZHANG, X.-N., GUO, Q.-P., SHEN, X.-X., YU, S.-W. & QIU, G.-Y. 2015c. Water quality, agriculture and food safety in China: Current situation, trends, interdependencies, and management. *Journal of Integrative Agriculture*, 14, 2365-2379.
- ZHANG, Y., DUDGEON, D., CHENG, D., THOE, W., FOK, L., WANG, Z. & LEE, J. W. 2010. Impacts of land use and water quality on macroinvertebrate communities in the Pearl River drainage basin, China. *Hydrobiologia*, 652, 71-88.
- ZHANG, Z., FENG, Y., GAO, P., WANG, C. & REN, N. 2011. Occurrence and removal efficiencies of eight EDCs and estrogenicity in a STP. *Journal of Environmental Monitoring*, 13, 1366-1373.
- ZHAO, J.-L., YING, G.-G., LIU, Y.-S., CHEN, F., YANG, J.-F. & WANG, L. 2010. Occurrence and risks of triclosan and triclocarban in the Pearl River system, South China: From source to the receiving environment. *Journal of Hazardous Materials*, 179, 215-222.
- ZHENG, Y. 2014. *Contemporary China : a history since 1978*.
- ZHOU, Y., ZHA, J., XU, Y., LEI, B. & WANG, Z. 2012a. Occurrences of six steroid estrogens from different effluents in Beijing, China. *Environmental Monitoring and Assessment*, 184, 1719-29.
- ZHOU, Y., ZHANG, Q., LI, K. & CHEN, X. 2012b. Hydrological effects of water reservoirs on hydrological processes in the East River (China) basin: complexity evaluations based on the multi-scale entropy analysis. *Hydrological Processes*, 26, 3253-3262.
- ZHU, Y., PRICE, O. R., KILGALLON, J., RENDAL, C., TAO, S., JONES, K. C. & SWEETMAN, A. J. 2016. A Multimedia Fate Model to Support Chemical Management in China: A Case Study for Selected Trace Organics. *Environmental Science & Technology*, 50, 7001-7009.
- ZHU, Y., PRICE, O. R., TAO, S., JONES, K. C. & SWEETMAN, A. J. 2014. A new multimedia contaminant fate model for China: How important are environmental parameters in influencing chemical persistence and long-range transport potential? *Environment International*, 69, 18-27.

# Appendix

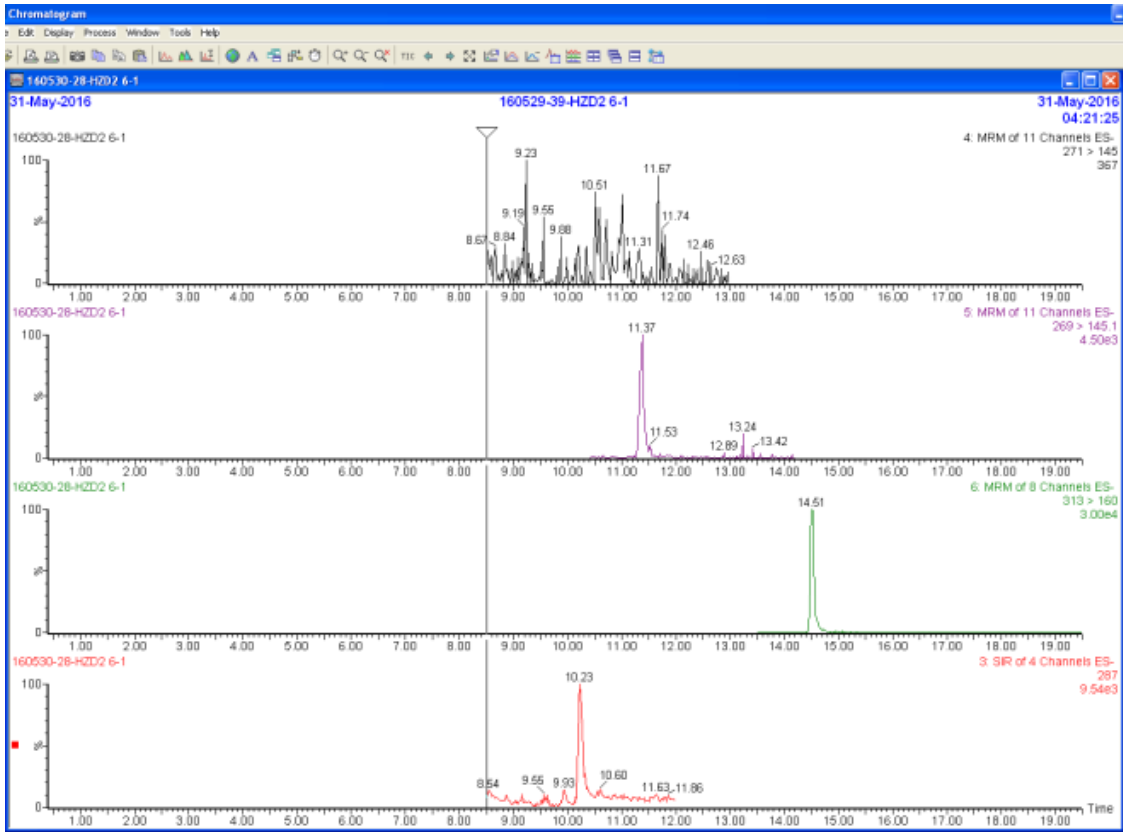


Appendix A-1 - Chromatograms for 100 µg/L internal standard. Chemicals in order from top to bottom: E2, E1, TCC, TCS.

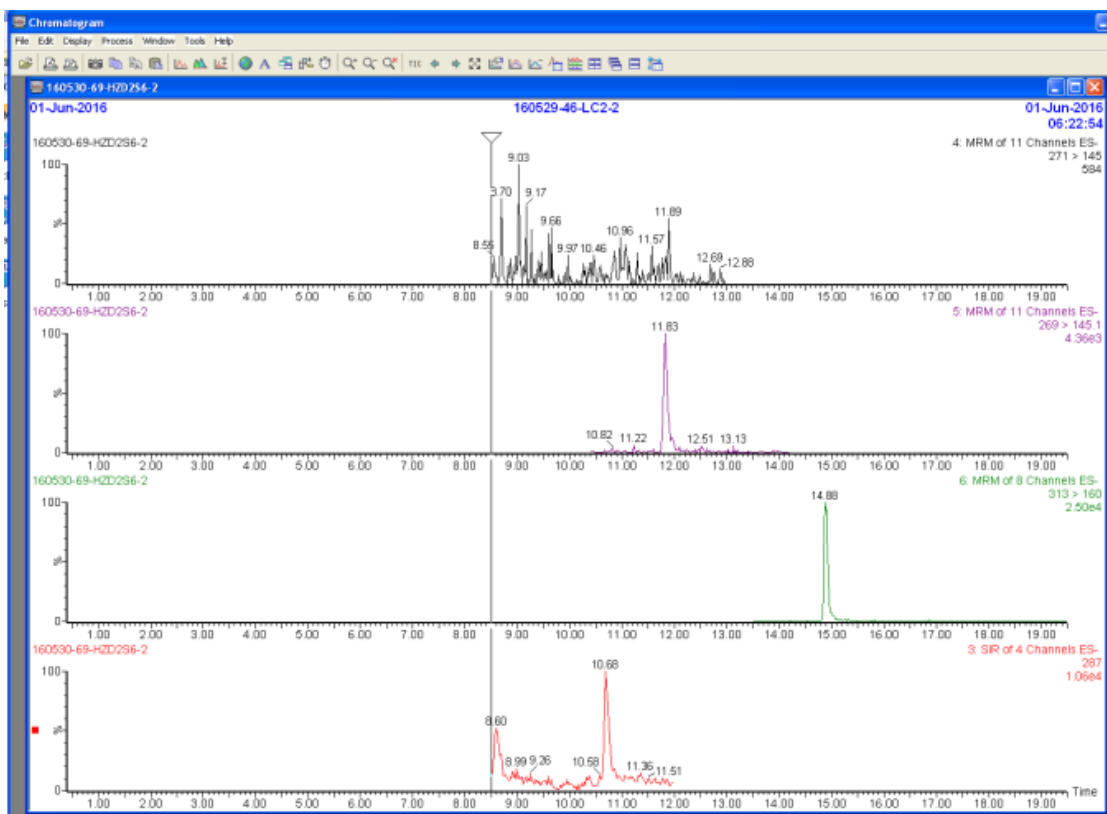


Appendix A-2 - Chromatograms for blank sample 1. Chemicals in order from top to bottom: E2, E1, TCC, TCS.

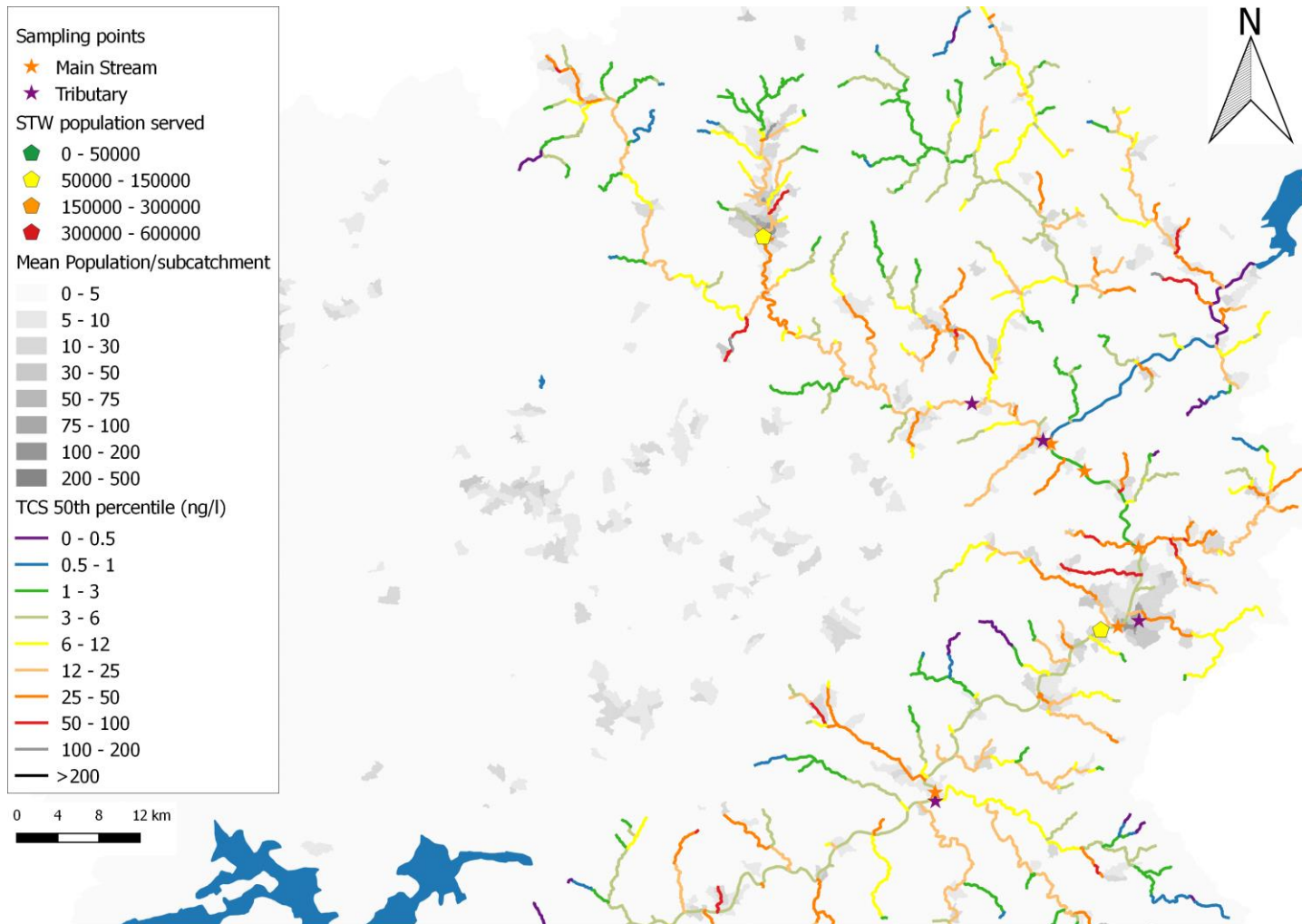




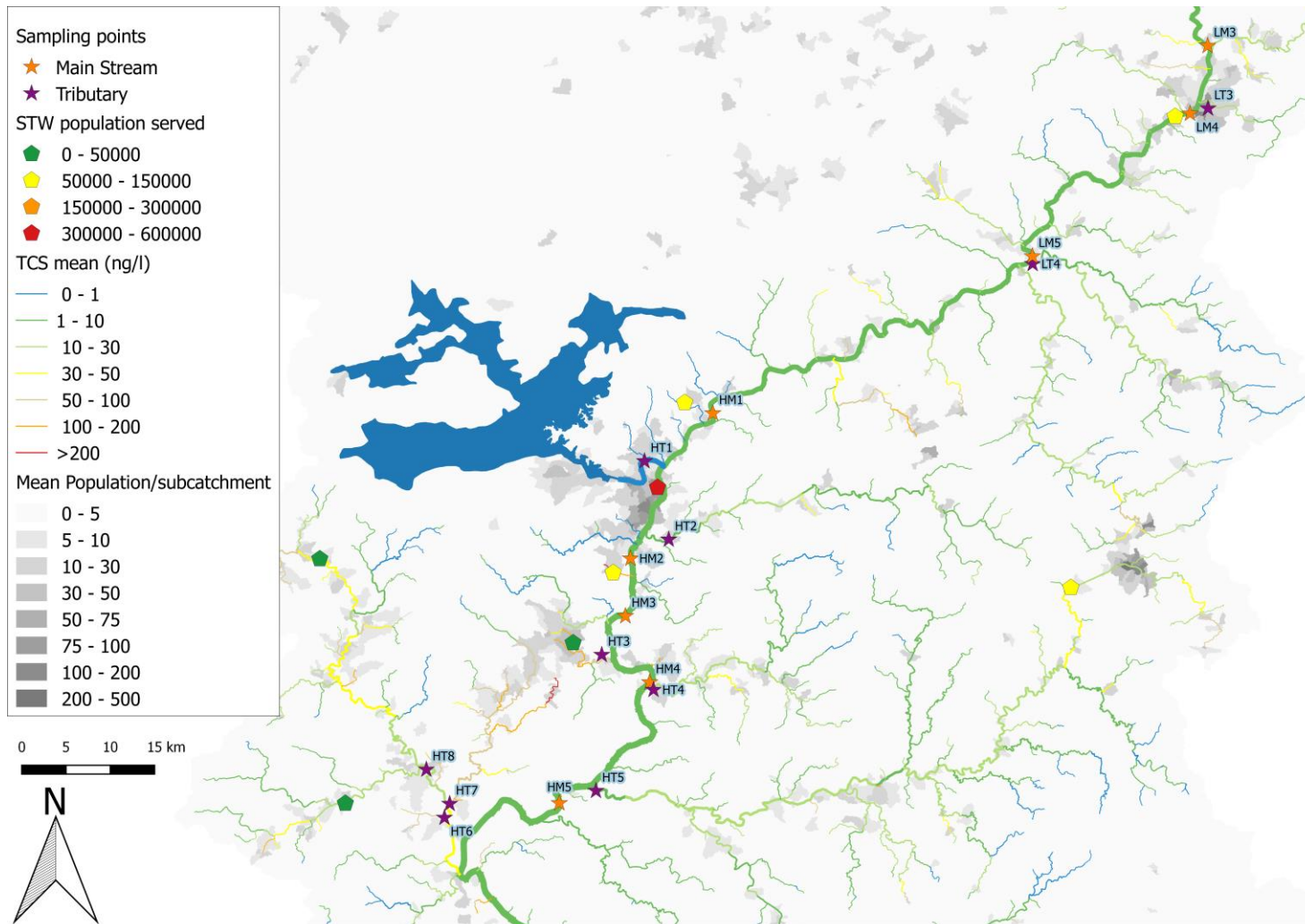
Appendix A-3 - Chromatograms for sample HA1-1. Chemicals in order from top to bottom: E2, E1, TCC, TCS.



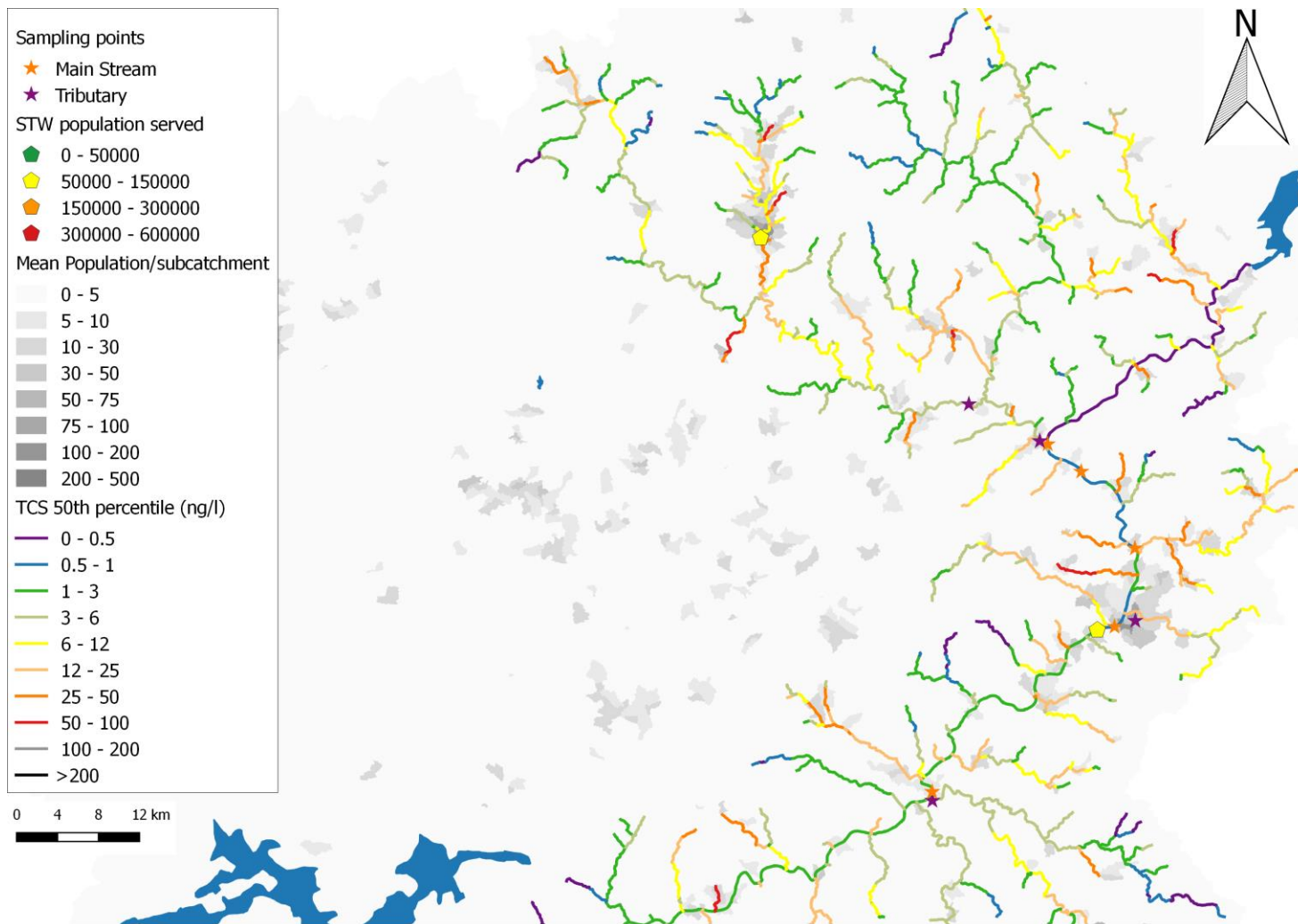
Appendix A-4 - Chromatograms for sample HA1-2. Chemicals in order from top to bottom: E2, E1, TCC, TCS.



Appendix B-1 - Mean simulated concentration of Triclosan A in 2016 in the Longchuan sampling zone (ng/l).

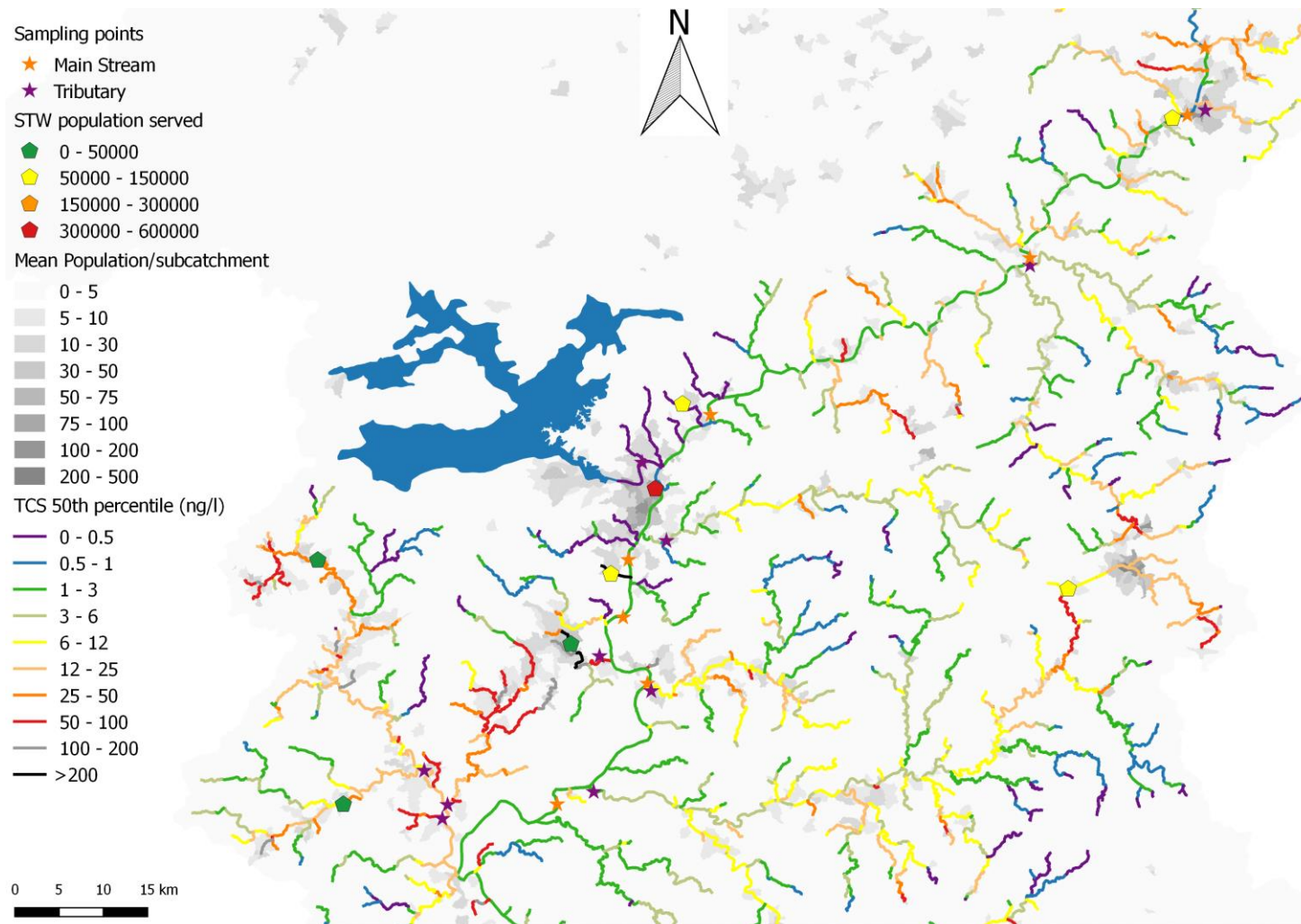


Appendix B-2 - Mean simulated concentration of Triclosan A in 2016 in the Heyuan sampling zone (ng/l).

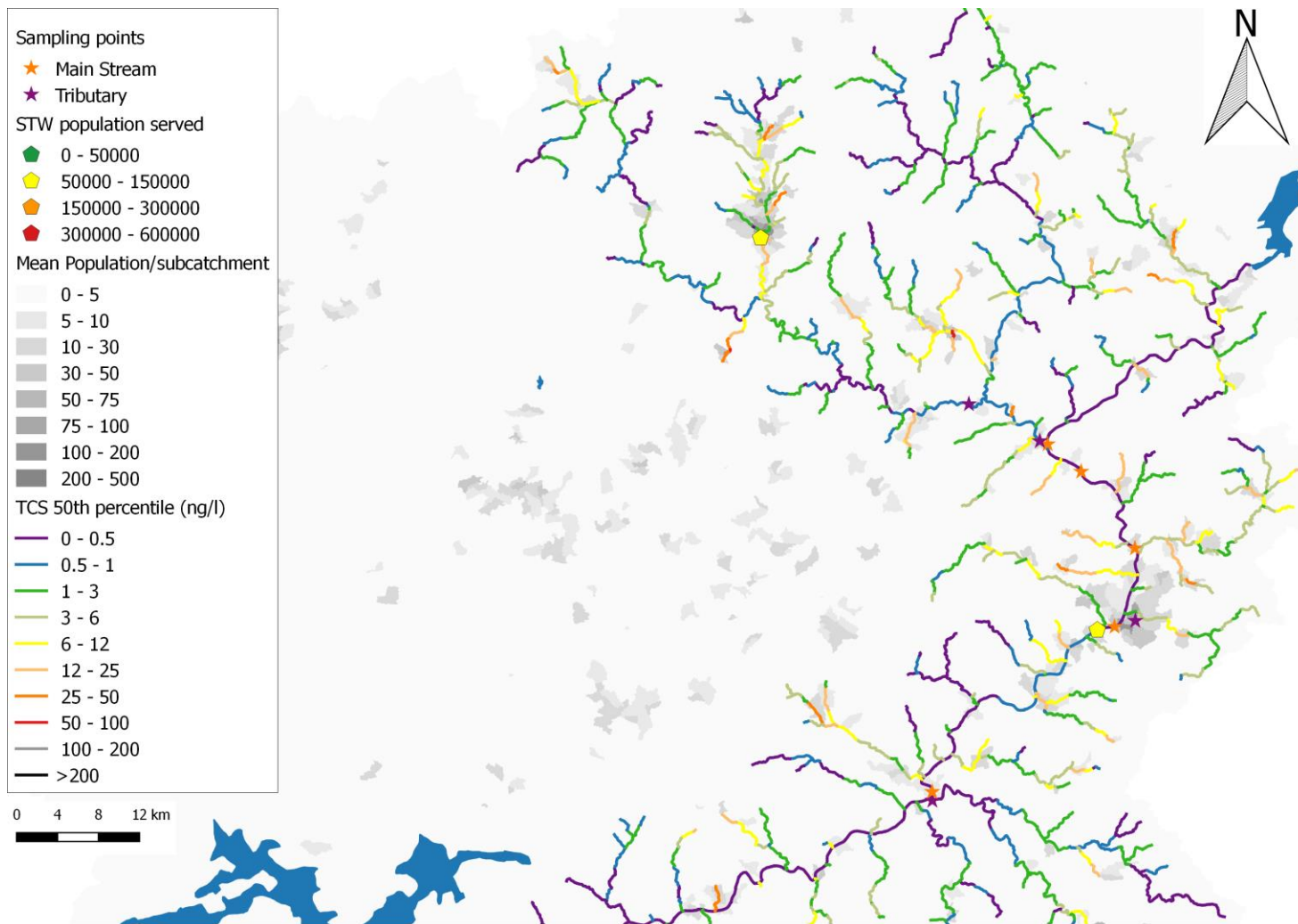


Appendix B-3 - Mean simulated concentration of Triclosan B in 2016 in the Longchuan sampling zone (ng/l).

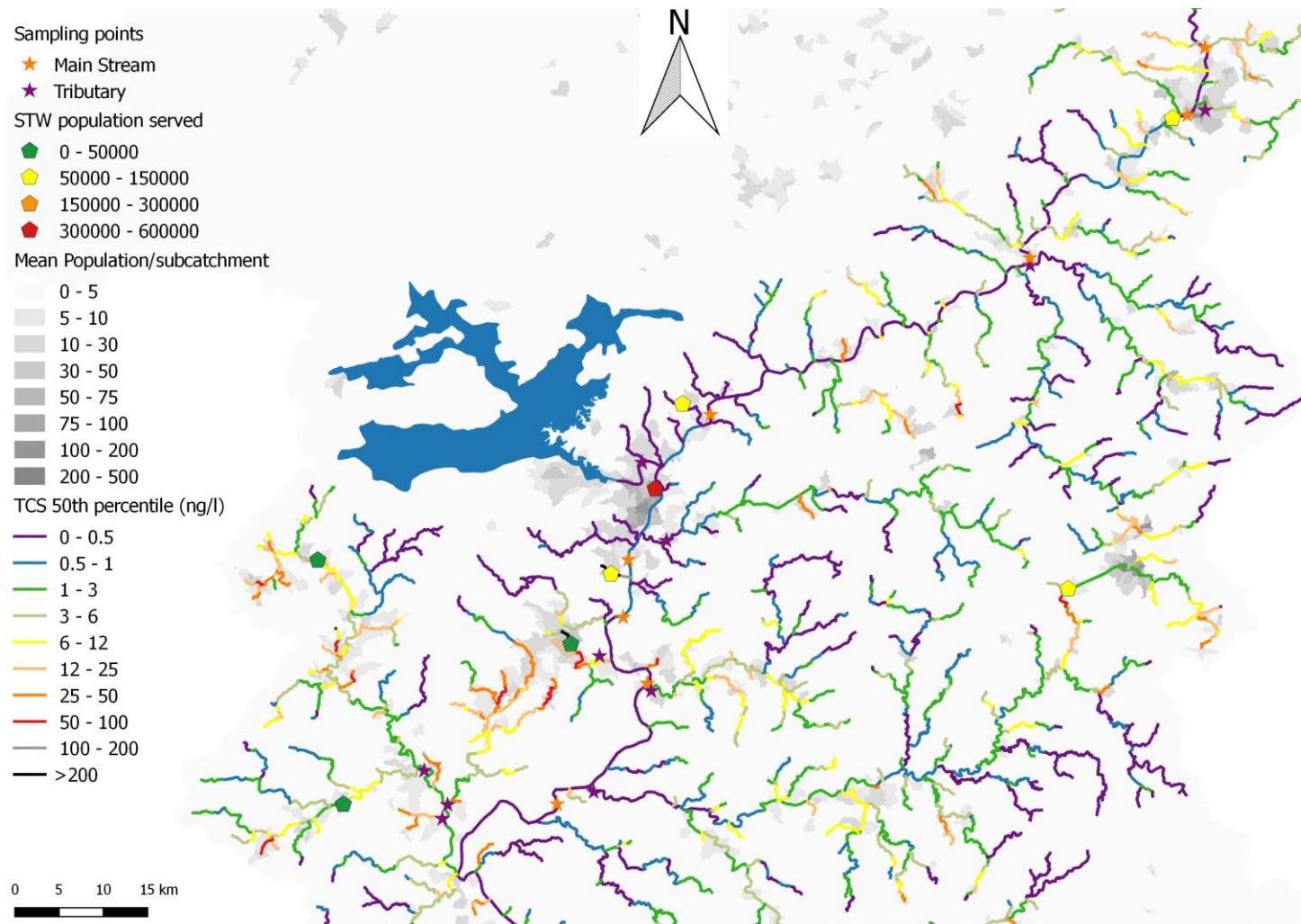




Appendix B-4 - Mean simulated concentration of Triclosan B in 2016 in the Heyuan sampling zone (ng/l).

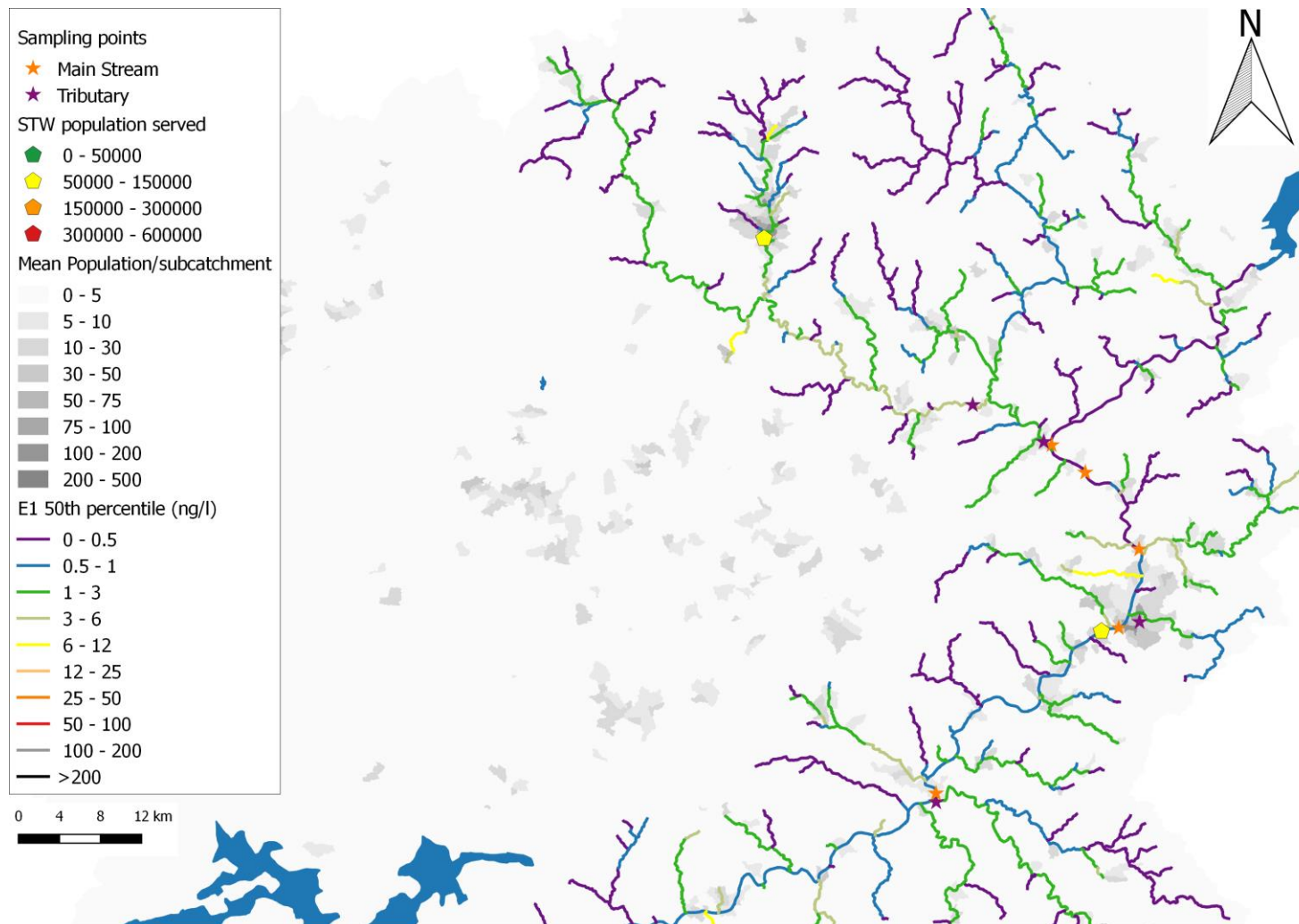


Appendix B-5 - Mean simulated concentration of Triclosan C in 2016 in the Longchuan sampling zone (ng/l).

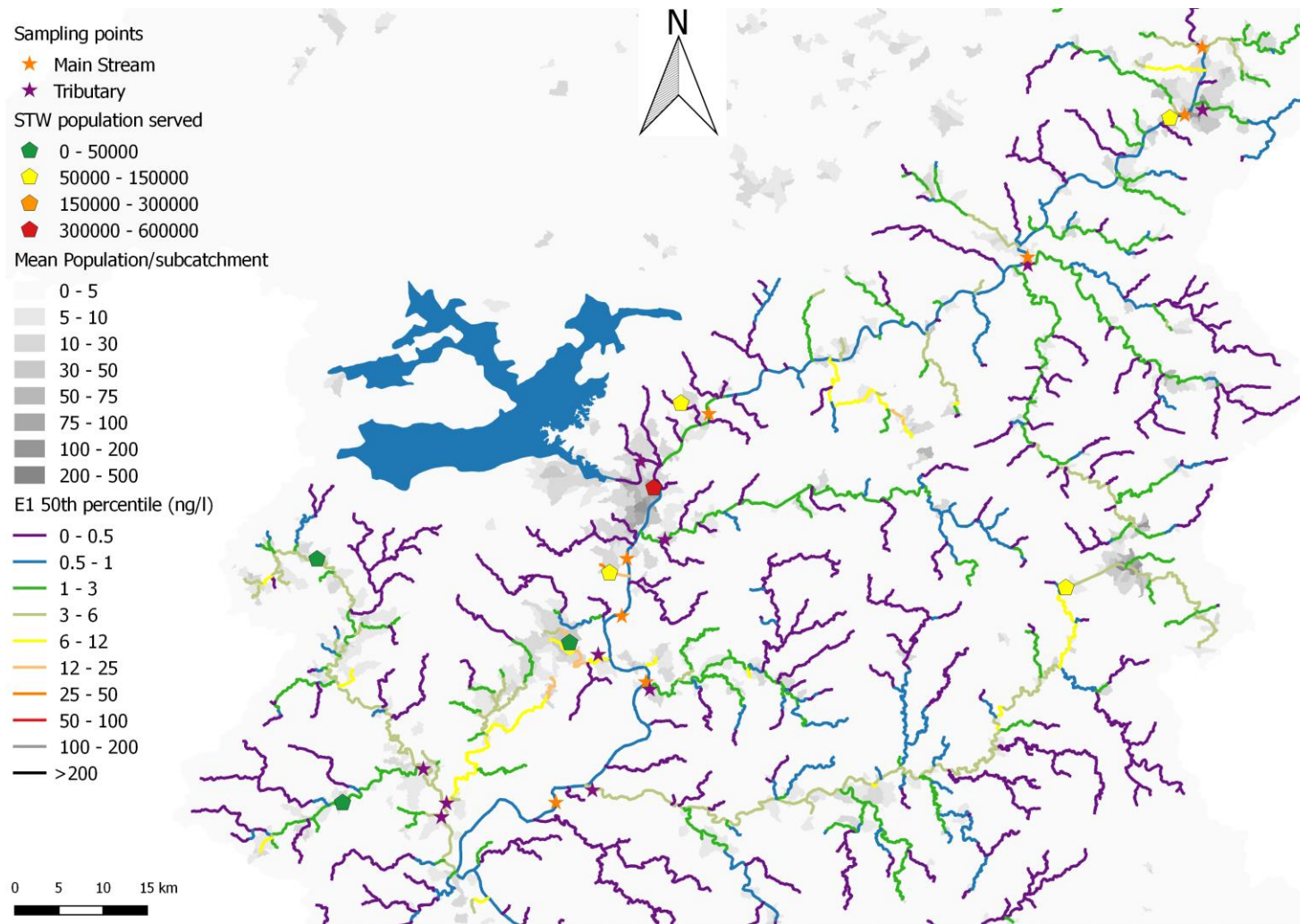


Appendix B-6 - Mean simulated concentration of Triclosan C in 2016 in the Heyuan sampling zone (ng/l).

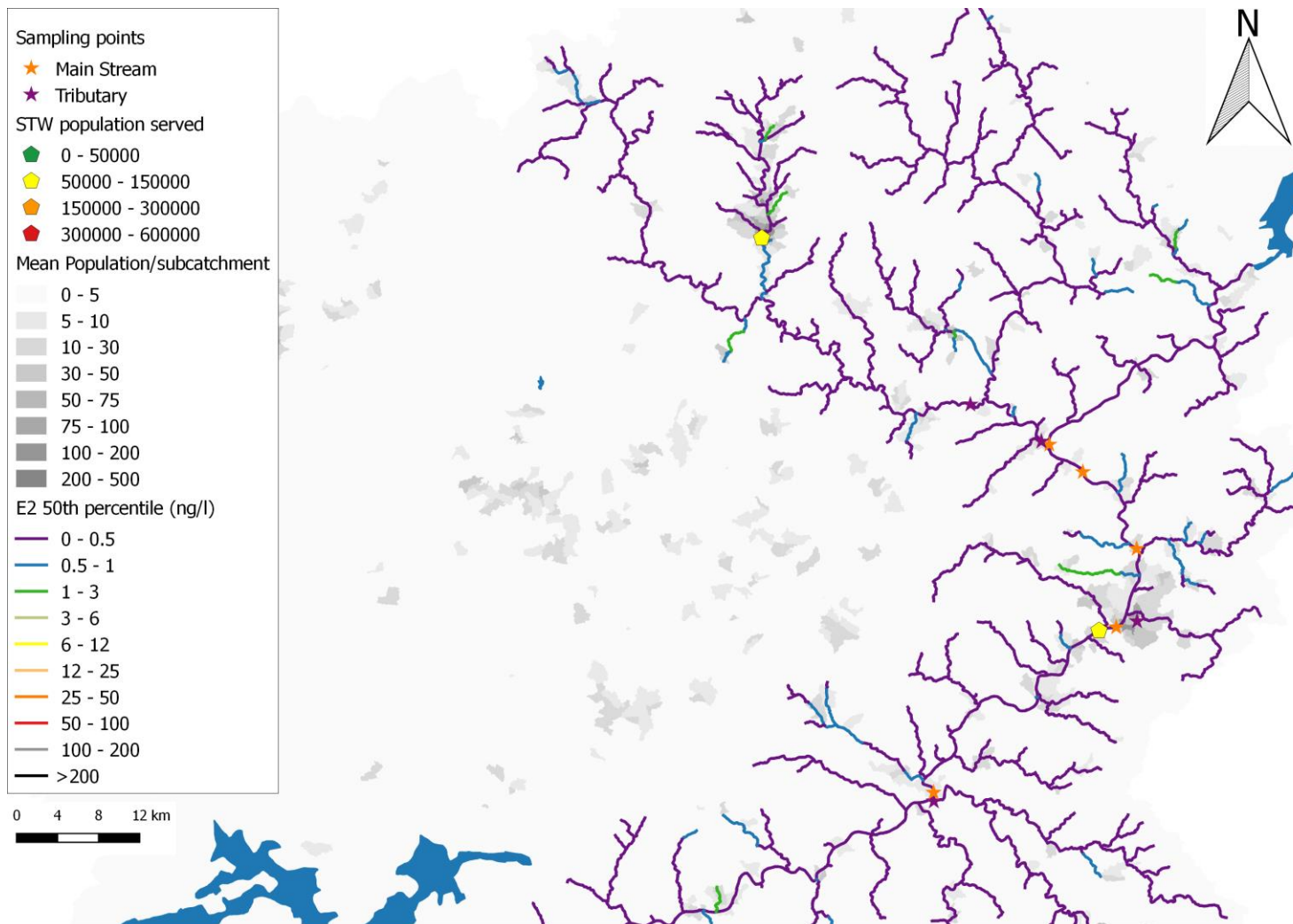




Appendix B-7 - Mean simulated concentration of Estrone in 2016 in the Longchuan sampling zone (ng/l).

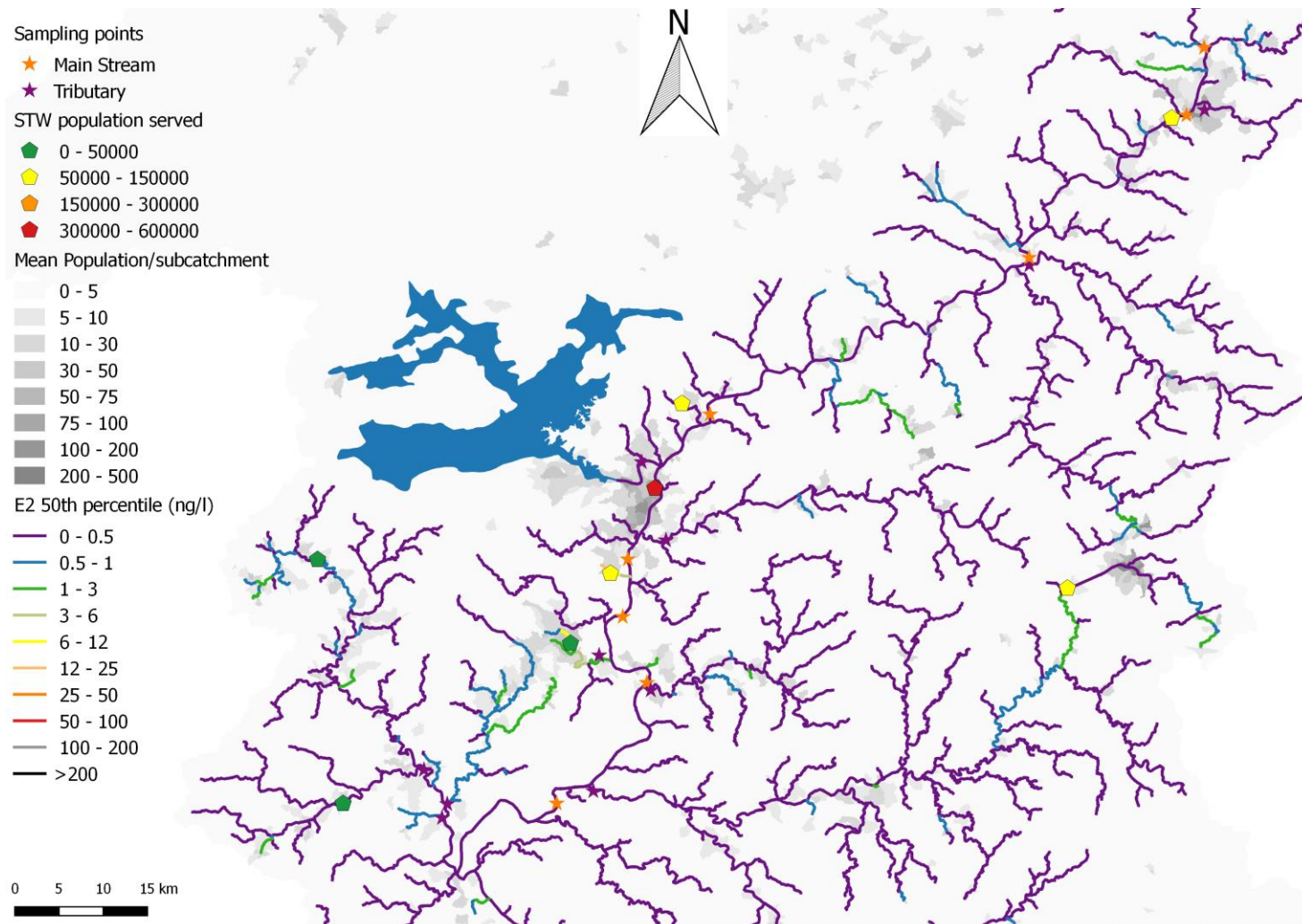


Appendix B-8 - Mean simulated concentration of Estrone in 2016 in the Heyuan sampling zone (ng/l).



Appendix B-9 - Mean simulated concentration of 17 $\beta$ -estradiol in 2016 in the Longchuan sampling zone (ng/l).





Appendix B-10 - Mean simulated concentration of 17β-Estradiol in 2016 in the Heyuan sampling zone (ng/l).